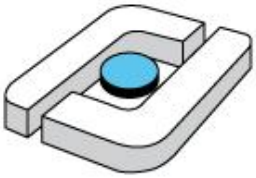

Hochschule Osnabrück
University of Applied Sciences

Fakultät Ingenieurwissenschaften und Informatik

Masterarbeit

über das Thema

Testing and Optimization of the performance of a Stirling engine.

vorgelegt durch

Aitziber Jiménez Abete

19 Juni 2013

HOCHSCHULE OSNABRÜCK
Fakultät Ingenieurwissenschaften und Informatik

Masterarbeit

Thema: Testing and optimization of the performance of a Stirling engine.

für
Aitziber Jiménez Abete

geboren am: 21/10/1989
in: Tudela (Spanien)

Erstprüfer: Prof. Dr. Matthias Reckzügel

Zweitprüfer: Prof. Dr. Ralf-Gunther Schmidt

Abgabe: 19/06/2013

_____ Erstprüfer

_____ Master

_____ Zwaitprüferx

Erklärung

Hiermit versichere ich, dass ich meine Masterarbeit selbständig verfasst und keine anderen als die angegebenen Quellen und Hilfsmittel benutzt habe.

Datum: 19.06.2013 .....
(Unterschrift)

ABSTRACT

This is a Master Thesis performed by one student of Industrial Engineering of the Public University of Navarra at the University of Applied Sciences of Osnabrück. The present Thesis is entitled "Testing and optimization of a Stirling engine". The first section describes the history of these engines, as well as its future prospects and its advantages and disadvantages.
The following chapter describes the various theoretical cycles of the engine. The third part deals with real Stirling engines: parts, possible configurations, different losses that can be found in them and the different working variables and their influence on performance.
In the fourth part of the thesis it is described in detail the system losses, both the combustion chamber and the engine losses. Furthermore, it is calculated an example of these losses.
In section 5 there is a deep study on the operation of the Stirling engine working with compund fluids.
The next chapter is a summary of the various parameters and conditions of the engine present at the "Labor für Kraftwerkstechnik" of the Hochschule Osnabrück.
Finally the last chapter is a depth development of numerous experiments with the engine, and a comparison of them with the theoretical cycles described above.

ZUSAMMENFASSUNG

Dies ist eine Masterarbeit eines Studentinn des Industrielles Ingenieurwessen von der Öffentlichen Universität von Navarra an der Hochschule Osnabrück. Die vorliegende Masterarbeit ist " Testing and optimization of a Stirling engine " berechtigt. Der erste Abschnitt beschreibt die Geschichte dieser Motoren, sowie ihre Zukunftsperspektiven und ihre Vor-und Nachteile.
Das folgende Kapitel beschreibt die verschiedenen theoretischen Zyklen des Motors. Der dritte Teil befasst sich mit realen Stirling Motoren: Teile, möglichen Konfigurationen, verschiedenen Verluste, die in ihnen gefunden werden und den verschiedenen Arbeitsgruppen Variablen und deren Einfluss auf die Leistung.
Im vierten Teil der Arbeit wird im Detail die Netzverluste, sowohl die Brennkammer und die Motor Verluste beschrieben. Ein Beispiel für diese Verluste wird berechnet.
Abschnitt 5 umfasst eine tiefe Studie über den Betrieb des Stirling-Motor arbeiten mit compund Flüssigkeiten.
Das nächste Kapitel ist eine Zusammenfassung der verschiedenen Parameter und Bedingungen des Motors auf der "Labor für Kraftwerkstechnik" der Hochschule Osnabrück.
Schließlich das letzte Kapitel ist eine eingehende Entwicklung der zahlreichen Experimenten mit dem Motor, und ein Vergleich von diesen Experimenten mit den theoretischen Zyklen oben beschrieben.

RESUMEN

Este es el Proyecto de Fin de Carrera realizado por una estudiante de Ingeniería Industrial de la Universidad Pública de Navarra en la Universidad de Ciencias Aplicadas de Osnabrück. El presente proyecto tiene por título “Testing and optimization of a Stirling engine”. En una primera parte, se describe la historia de dichos motores, así como sus perspectivas de futuro y sus ventajas e inconvenientes.
A continuación se describen los diversos ciclos teóricos del motor, comparándolos entre ellos.
La tercera parte trata sobre los motores Stirling reales: sus partes, posibles configuraciones, diferentes pérdidas que podemos encontrar en ellos y sobre las distintas variables de trabajo, así como su influencia en el rendimiento.
En la cuarta parte de la tesis se describen detalladamente las pérdidas del sistema, tanto de la cámara de combustión como del motor en sí. Además, se calcula un ejemplo de estas pérdidas.
En el apartado 5 se profundiza en el funcionamiento de los motores Stirling con fluidos de trabajo compuestos.
El siguiente capítulo es un resumen de los distintos parámetros y condiciones del motor presente en el “Labor für Kraftwerkstechnik” de la Hochschule Osnabrück.
Finalmente el último capítulo es un desarrollo a fondo de los numerosos experimentos realizados con el motor, así como la comparación de estos con los ciclos teóricos ya descritos.

AGRADECIMIENTOS

Al Prof. Dr. Matthias Reckzügel, a Fr. Birgit Tepe y a la Hochschule Osnabrück por darme esta valiosa oportunidad.

A todas las personas que me han apoyado durante esta etapa de mi vida, tanto mis amigos de Cortes, como mis compañeros de Pamplona y todos aquellos amigos con los que he compartido esta aventura en Osnabrück.

A mi familia, por todo.

A las tres estrellas que brillan por mí en el cielo: mi abuela Prudencia, mi padre José Luis y mi hermano Urko. Porque donde quiera que estén, me transmiten su calor y apoyo en cada momento.

Pero sobre todo, a mi madre, Loli Abete Segura, por ser un gran ejemplo de mujer fuerte, luchadora, hermosa y maravillosa. Por quererme incondicionalmente, apoyarme, y en definitiva, haber hecho todo lo posible porque siempre salga adelante. GRACIAS MAMÁ. TE QUIERO.

ACKNOWLEDGEMENTS

To Prof. Dr. Matthias Reckzügel, to Fr. Birgit Tepe and to the Hochschule Osnabrück for giving me this precious opportunity.

To all the people who have supported me during this stage of my life, friends from Cortes, colleagues from Pamplona and all that friends with whom I have shared this adventure in Osnabrück.

To my family, for everything.

To the three stars that shine for me in heaven: my grandmother Prudencia, my father Jose Luis and my brother Urko. Because wherever they are, they convey me warmth and support at all times.

But mostly, to my mother, Loli Abete Segura, for being a great example of strong, fighter, beautiful and amazing woman. For loving me unconditionally, supporting me, and ultimately, having done everything possible to make me always succeed. THANKS MOM. I LOVE YOU.

TABLE OF CONTENTS

LIST OF IMAGES

LIST OF CHARTS

1. HISTORY, PRESENT AND FUTURE OF THE STIRLING CYCLE ENGINES

1.1. DEFINITION AND NOMENCLATURE

A Stirling engine is a mechanism which operates in a regenerative thermodynamic cycle, with cyclic compression and expansion of the working fluid at different temperature levels. The flow is controlled by volume changes, and there is a net conversion of heat into work and vice versa.

This general definition covers a wide range of machines with different functions, characteristics and configurations. This includes machines capable of working as motor, heat pumps, refrigeration machines or pressure generators.
There are other machines that work through an open regenerative cycle, where the flow of working fluid is controlled by valves. For convenience in this development, we will refer to these machines as Ericsson engines. Unfortunately this distinction is not widespread, and in practice the name of "Stirling engine" is often used indiscriminately for all types of regenerative machines.

Stirling engines are often called by other names, such as hot air engines, or even other numerous designations reserved for specific machines such as Rankine-Napier. This creates a real lack of nomenclature. Therefore, the designation of "Stirling Cycle" will be reserved for a particularly idealized thermodynamic cycle, and the name of "Stirling Engine" for a particular machine. Anyway, we need to be clear with the distinction between machines in which the flow is controlled by volume changes (Stirling engine) or by a control valve (Ericsson engine), because they have radically different characteristics.

The use of the term "Stirling engine" as the general name for a regenerative thermal cycle engine is relatively recent. It is believed to have been originated in the "Research Laboratories of Philips" in Eindhoven in 1954. Before it, it was common to refer to it as "hot air engine".
The working fluid change from air to helium or hydrogen at Phillips in the mid-50es made the term "hot air engines" inappropriate. Alternative name "Philips Stirling engine" was showed even more inappropriate than "Stirling Engine" or "Stirling Cycle Engine (SCE)" and because of that, this name started to be widespread used.

1.2. EARLY HISTORY

Stirling and Ericsson engines have a long history, which has been well studied by many authors as Finkelstein (1959), Zarinchang (1972), Ross (1977),...

The first recognized air engine was the "Wheel of Fire" of Amontons (France, 1699), rudimentary artifact which took advantage of the expansion of hot air to turn a wheel, just a year after that Savery fabricated the first steam engine to pump water. In fact, the Stirling engine development has always happened parallel to the steam engine.

Another of the earliest was the air engine of H. Wood (1759) who used a modified atmospheric steam engine of Newcomen. After that, Glazebrook described several machines working with cycles of hot gas and in 1801 introduced the original use of a closed cycle with repeated use of the same working fluid.

In 1807 George Cayley designed a hot air engine, wtih open cycle and internal combustion, which was probably the first engine of this type that worked.

Robert Stirling, a minister of the Church of Scotland and creator of the regenerative heat exchanger, invented the regenerative closed cycle engine in 1816 and remained active, along with his brother James in its development for several years. Like all engineering developments, was limited by the materials available at that time.

This Stirling's patent was the end of a number of attempts to simplify steam engines. Stirling considered too complicated to heat water in a boiler, produce steam, expand it in an engine, condensate it and through a pump re-enter the water in the boiler. Another reason to develop a new system was the fatal accidents often caused by steam engines, because the steel had not been yet invented and the boilers easily exploded because of both poor materials used and the imperfect techniques of their gaskets.

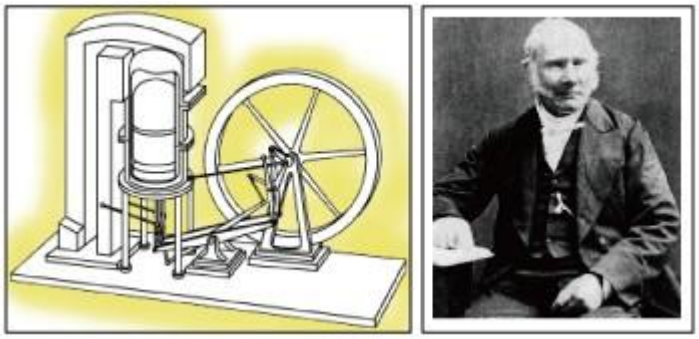

Image 1 - Robert Stirling and his original patent (1816).

At the same time that Stirling, the Swedish inventor John Ericsson, working in England, introduced the air engine with regenerative open cycle in a variety of ways. The family of machines whose flow was controlled by valves was known as Ericsson engines.

During the nineteenth century thousands of hot air engines were manufactured and used in a variety of sizes and shapes both in Britain, the USA and elsewhere. They were reliable and reasonably efficient. In a very important way, they were compared with the facilities of alternating steam machines of the era and their associated boilers.

Image 2 - Stirling boilers (Philadelphia and Columbia).

The Stirling engine performed the same processes of heating and cooling of a gas, but all within the engine, and in addition the gas was air instead of steam, therefore it was not required boiler. Physical theory, Carnot process, was defined 40 years later.

Lots of hot air engines were built small and with low power, from about 100 W to 4 kW, although there were also some more powerful machines. The most notable machine among these was undoubtedly the great engine of vessel that built Ericsson in 1853, which had 4 cylinders of 4,2 m of diameter and a stroke of 1,5 m, worked at 9 rpm and produced approximately 220 kW of power at the crankshaft. The engine was designed for 330 kW and its performance was disappointing when it was installed in the ship called "The Ericsson".

The internal combustion engine (ICE), was invented in the mid nineteenth century. Later it was developed as both gasoline spark ignition and compression ignition. Later, at the end of the century, the electric motor was invented and developed. Together, ICE and electric were gradually displacing both the steam engine and the Stirling.

As can be seen, the SCE were used in a wide range of utilities until the beginning of the First World War. The most important feature in those days was the inherent simplicity of the machine, its ease of maintenance and safety. Security was an important aspect, since the first steam engines could compete favorably in most other areas, but as boilers were unreliable and had an alarming tendency to explode occasionally.

Efficiency was an aspect that was also considered. The coal, the main source of energy, was increasing its price since the beginning of the Industrial Revolution. Usually, it was possible to get an overall efficiency of 7% with a Stirling engine and this was considered fully competitive;

in fact, even today, this can be a good value in many applications. In the table below we can see the performance of some of the early Stirling engines.

Air Engine	Bore (mm)	Stroke (mm)	Speed (rpm)	Indic. Power (kW)	Brake power (kW)	Cons. of coal per hour (kg)	Mech. efficiency (%)	Overall efficiency (%)
Buckett	610	406	61	15,06	10,73	16,59	71	7
Bailey	373	175	106	1,77	0,98	4,52	55	2
Bénier	340	350	117,6	4,36	3	5,59	69	5
Stirling	406	1219	-	30,00	-	45,40	-	7
Ericsson	4300	-	-	239,00	-	262,30	-	10

Chart 1 - Tests with air engines (Donkin 1896).

In 1876 Otto presented his Otto Cycle engine, which was safe, reliable and had some excellent specific power ratios that allowed it to be easily incorporated as motor in transport. To overcome the Stirling engine even further, Otto's engine was cheap to operate because of their high efficiencies and cheaper fuels. Broadly, Otto cycle efficiency depends on the compression ratio, while the Stirling cycle is dependent on the temperature ratio. Due to the limitations of materials at that time, the first Stirling engine could not operate at the high temperatures needed to ensure good efficiency.

Furthermore, those first SCE did not use preheaters, so the exhaust gas temperatures were unnecessarily high, resulting in a reduction of the overall efficiency. On the other hand, it was a simple task to design an Otto design which would work with a compression ratio with good efficiency. Thus, the growing success of the first gasoline engines and the introduction of boilers which made safe the steam engines soon exceeded the Stirling engine technology. Even in these circumstances, in areas of the world was the Stirling engine successful. In these areas, the ability of Stirling engines of using almost any fuel helped to the survival of these engines.

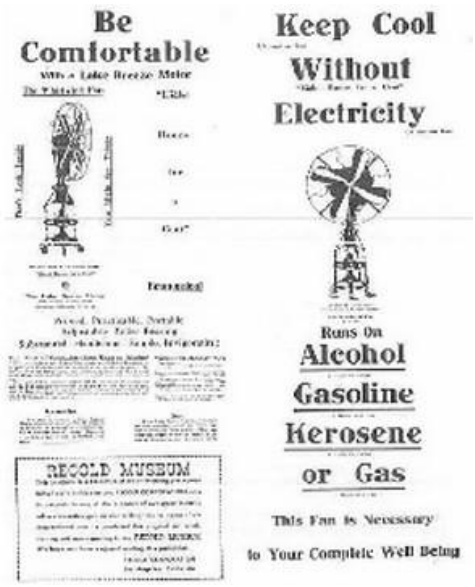

Image 3 - Propaganda of ventilation with SCE (1900).

However, at the time of the First World War, hot air engines were not commercially available in large quantities, although the production of special purpose machinery continued for many years.
One of the most common uses for hot air engines in small sizes was to move fans and water pumps.

1.3. LATE HISTORY

The revival in the interest of Stirling engines was due almost entirely to the workers of the "Philips Research Laboratory" in Eindhoven. The work with small Stirling engines began here in the mid 30s. The goal was to get a small electric generator, silent and thermally active for areas of the world without regular power supply. Modern materials and technology of its time raised the efficiency of hot air engines to values that never could have been imagined in older engines.

The SCE development continued during the Second World War. It was a brilliant research, and the results showed that a small generator was much better than any of the old hot air engines. Anyway, in the early 50s the invention of the transistor and improvements in dry batteries involved progress in these engines. Philips engineers worked for getting major powers, and the invention of the rhombic drive helped them to develop a family of one or more cylinder engines operating in hundreds of horse power. This work was collected periodically by Meller (1969) in a large number of documents and more recently by Van Beukering and Fokker (1973).

In 1958, General Motors made a legal agreement with Phillips, which continued until 1970. Their concern was the SCE for spacecraft propulsion, submarines, ships and to produce static power.

In the early 70s, the uncertainty in energy costs and supply, as well as increasing public concern because of increased pollution, became an important topic the research of engines that were an alternative for the known ones. The major requirement of these devices was that they should be efficient, clean, reliable, and economically and socially acceptable.

After breaking the legal agreement with Philips by General Motors, was Ford who started their agreements in 1971 and after a few preliminary work and its evaluation, embarked in 1977 on a multimillion dollar agreement, during seven years, for the development of Stirling engines for cars; the deal was managed by the Department of Energy of United States.

Other agreements were signed by Philips with the United Stirling AB of Malmo, a consortium formed by the great Swedish shipbuilder Kockums, Malmo and FFW (1968) and a consortium of German companies formed by two diesel engine companies, MAN and MWM (1967). In the early 70s there were important cooperative efforts between Philips and European consortia for the development of engines for vehicles, marine transport and submarines. After that, the Europeans decided to follow in a more independent way.

The Swedish group United Stirling, worried in the beginning by the engines for heavy vehicles, expanded its interests in the area of passenger cars. They performed several works in cooperation with Ford, and in 1978 began a second program for Stirling engines for cars with the Department of Energy of the United States, which involved in it two U.S. companies: Mechanical Technology Inc. of Latham (New York) and American Motor Corp. (Detroit).

To manage these two automotive programs, it was established the Stirling Engine Project Office in the "National Aeronautics and Space Administration (NASA) Lewis Research Centre" (Cleveland, Ohio) and to develop skills in this field, an independent program of research and development began at NASA Lewis in 1975.

The External Combustion Engine Project was initiated by the Department of Energy of the United States in 1977 to study the use of Stirling engines from 370-1480 kW burning coal and other alternative fuels with high efficiency, including industrial, agricultural and municipal waste. The direction of this program was responsibility of the Agronne National Laboratory (Illinois).

In the early 60s, William Beale, a professor at the University of Ohio, invented the "free-piston Stirling engine". Beale's company, Sunpower Inc. in association with MTl Latham, N.Y. began with the production of free-piston Stirling engines for various applications, particularly for energy production with nuclear energy for space missions and electric generators powered by solar energy.

Important works in miniature motors for artificial hearts were funded for more than a decade by the U.S. National Institute. Several laboratories have studied this type of engine. Another program of Stirling engine development for artificial hearts was carried out jointly by Westinghouse and Philips.

After this time there have been considerable researches on Stirling engines, for electricity, power source in space or underwater media.

Different free piston Stirling engines were developed for vehicles, as an aid to navigation systems, or for generating electricity for places in need of little electrical power.

Since even before 1980, interest in the SCE increased due to public concerns about noise, air pollution and energy conservation. This may be reflected in a multitude of documents published annually by the "Intersociety Energy Conversion Engineering Conference". Many original and innovative developments in the practice and theory of Stirling engines were made, much research by companies, universities and governments worldwide. William Martini (1978) developed a directory of all hitherto known activities on Stirling engines.

Also we can find multiple uses for this type of machine operating as coolers or heat pumps. Due to its design and thermodynamic cycle, this machine is capable of operating in four modes. As an engine from a cold source or a warm one and from applied mechanical work, it can work as a heat pump or refrigerator.

The ability to work as a refrigerator was discovered in 1834 by John Herschel, and in 1876 Alexander Kirk described a refrigerating machine that was in use for 10 years.

However, it was not until the late 40s when he made a serious effort to develop a Stirling-cycle cooling machine. Again, this study was undertaken by the company Philips in Eindhoven. The first machine, an air condenser, was introduced in 1953.

Since then, considerable research has resulted in the development of different cryogenic refrigeration machines, covering a wide range of cooling capacities, and have led to the manufacture of equipment associated cryogenic research and industrial applications. Shortly afterwards, it was demonstrated that the Stirling cycle machines were more suitable for cryogenic ranges (extremely low temperature) than for higher temperature ranges, (domestic or industrial interest, which are currently dominated by cooling machines of vapor or gas compression cycles).

It was also conducted research of miniature cooling machines for several companies, some of them specialized in miniature cryogenic refrigerators as the North American Phillips Inc. Their main interest was the provision of small refrigerators for electronic applications, primarily for equipment for infrared detection for various military and civilian purposes.

1.4. PRESENT AND FUTURE OF STIRLING CYCLE ENGINE

In 1980, with the oil crisis, Stirling engines have become a viable option due to the last advances in the technology of materials.

Against the imminent inability of supplying everybody with energy from traditional energy sources, alternative energy sources are becoming more important and bring up a new way of coexisting with the environment. The renewable energy sources bring with them great advantages, such as: its inexhaustible nature, the care for the environment and the possibility of decentralized and independent production.

After checking the good features of the Stirling Cycle engine and its throughout the history, one wonders why then the use of the Stirling engines has not been more important, if their efficiency is high, do not produce exhaust gases and can operate with clean energy sources. The impediments to the replacement of existing engines (Diesel and Otto) are various, among which the fact that these are produced on a large scale, reason why their production is cheaper. A change in the industry to produce another kind of engine is a great investment and therefore a high price for the same, at least at the beginning.

On the other hand, electric motors have been seen as a good alternative to replace the internal combustion engine. One advantage is that they can produce any power at a high efficiency (over 90%), and it is also possible to use them in automobiles and for many industrial applications.

Another aspect to consider is that of energy sources. Replacing fossil fuels with clean sources is complicated because of both the economic interests of companies and countries that produce and distribute, and the fact that technological advances in alternative energy such as solar, are insufficient to use widely. However, the idea of developing engines as the Stirling ones is gathering strength, engines that can run on with either fossil fuels or clean energy sources, so that gradually the fossil fuels are replaced by those sources. The environmental benefits of this change would be enormous.

The recent interest in the theoretical high-efficiency of Stirling engines has been encouraged by the instability in the supply of current primary energy sources.

Many governments and organizations are making significant efforts in research for the development of practical Stirling engines. As already said, the most significant advantages of the Stirling engine is that it is capable of being fed by many fuels; it is quiet, with high efficiencies at low and medium power levels and produce low emissions.

Thus, the challenges regarding to energy are making better use of non-polluting sources while producing more efficient engines. The invention of Robert Stirling could be the key and become what he envisioned: the engine of the future.

Currently, the most fruitful use of Stirling engines, apart from major space programs, in which is used power generated from atomic energy, we can say that it is electricity production.
Today the engine is already very mature in its design (approximate lifetime of 100.000 hours), but there are still few commercial applications and research projects.

The units based on Stirling engines are considered the most efficient units in thermal solar conversion of low power.

Seeing all these aspects of the SCE we describe a summary table in which we see reflected the different needs and trends in power units and some attractive properties of Stirling engines associated with them.

NEEDS AND TRENDS	ATTRACTIVE PROPERTIES OF SCE
Reduction of conventional fuels	Capability of working with many different fuels Low fuel consumption
Rise of fuel prices	High efficiency Use of alternative fuels
Use of alternative fuels	Use of alternative fuels Use of many different fuels
Demand of low sound level and less contaminant engines	Clean combustion (depending on energy source without combustion) Low sound level
Utilization of residual heat	Low working temperature

Chart 2 - Needs and trends of our society, and related properties of SCE.

Following, we will deal with the various current applications of this engine and will be displayed the current technological status and future prospects of the SCE.

1.4.1. MICRO-COGENERATION

An application that profits from those features is the field of micro-cogeneration. Micro-cogeneration systems generate electrical power on-site, meeting the demands of heat, using the excess of heat generated. Silent operation and long life are important requirements. In the

figure we can see the prototype of a free-piston Stirling engine of1 kW, developed specifically for this application.

Image 4 - Free piston Stirling engine for micro-cogeneration.

The following diagram shows the ecological advantages found in heat generation with Stirling engine cogeneration.

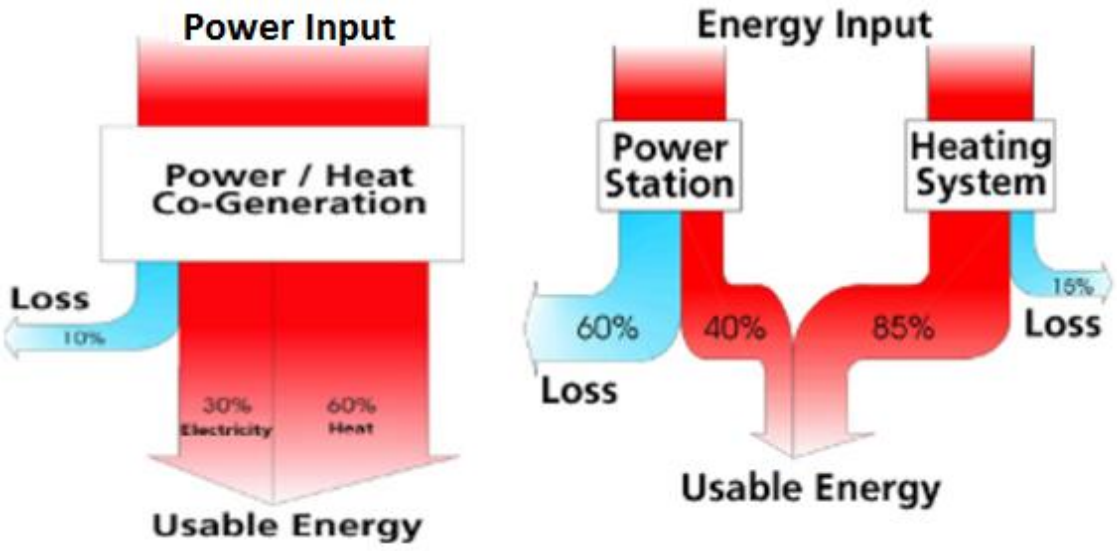

Image 5 - Sankey diagram for Stirling engines in micro-cogeneration.

The decentralized production of electricity and heat in cogeneration is one very effective way to reduce CO_2 emissions. Currently there are many developments of this type of decentralized generation units, with a great potential, especially those small units with power ranges between 5-10 kW electric.

The idea of combined heat and power (CHP) is not new. The first power plant of Thomas Edison was a combined one.
However, the concept of generating both electricity and heat in a combined way is not only economic but also silent enough to use in the home, as demonstrated in recent developments. CHP at industrial scale is commonly used.

Image 6 . Microcogeneration unit Stirling SOLO 161.

A micro-CHP unit fueled by natural gas has the potential to save money by using the same fuel more efficiently to generate heat and electricity. Micro-CHP systems respond primarily to the heat demand, providing electricity as a byproduct. This technology is the simultaneous production of heat and electricity in houses.

CHP effectively replaces the traditional gas boiler providing not only heat and hot water, but additionally most of the electricity required in the home. Although small units produce, by definition, small amounts of electricity, the importance of micro CHP lies in the great potential of a large number of systems installed in homes across Europe where natural gas is currently the dominant fuel in the heating of homes. A large percentage of the electricity consumed in those countries could be produced by this means.
Those units consist of two parts, one that acts as a generator and another that basically acts as a boiler or a heat pump providing heating and other similar domestic services.

In the present time micro-CHPs are already used in approximately 30.000 homes in Japan. The system has been very well received by users. Although the initial cost is more than double than a conventional boiler, micro-CHPs can save users up to 700 dollars per year in electricity bills, according to Guyer. Some devices have even a device for auxiliary power supply in case of power failure.

These machines also have the advantage of being far superior in terms of energy conservation than the traditional systems. The basic strategy is that the fuel used in a conventional system to keep warm a house, is in a micro-CHP used to generate electricity.
The company Guyer Climate Energy has been running free demonstrations of their micro-CHP unit, in order to expand market. Many people were surprised at how silent is the generator and its remarkable production of useful heat for heating.

On the market, this type of machines with Stirling engines and biomass boilers can be easily found, causing important economic savings, and even income. This income is caused by an excess of electricity supplied by the system that can be sold to the grid. Besides this a

reduction in pollutant emissions and dependence on fossil fuels that the use of biomass accounts can be achieved.

We find the following advantages in the micro-cogeneration:

- Significant saving in CO_2 emissions.
- Economic savings to the owners through the production of their own electricity.
- Economic benefits by helping to support electricity when the network is overloaded.
- Reduction of the need of large power plants and associated distribution networks.
- Creation of opportunities for the integration of fuels such as biomass and sale of electricity created by small producers.

1.4.2. REFRIGERATION

As already mentioned, Stirling machines can work as a refrigerator, heat pump and as engine; as refrigerator, if the machine is designed properly, can be achieved extremely low temperatures. In fact, Stirling coolers have achieved temperatures below 10 Kelvin.
Clearly, this facility to work as coolers is a great benefit in warm climates. However, it is also beneficial in the field of cryogenic technology to the point of solving the requirements of liquefaction of methane.

European companies, together with German universities have developed as a Stirling engine cooler, achieving temperatures below -200 ° C. These temperatures are used in low-temperature technology, such as liquefaction of methane in the medical industry, food processing industry or superconducting.
With variations in the speed and pressure of the gas during the process, the output can be controlled within a wide range.

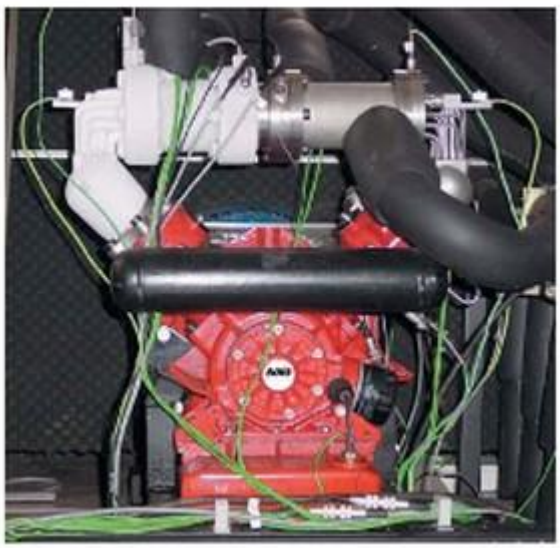

Image 7 - Stirling refrigerator (SOLO Stirling GmbH).

Aspects of the refrigeration:

- Any temperature can be selected for the cooling process and for the cooling water.
- Excellent characteristics of load in each one of the components.
- Excellent control.
- Maximum values in cooling output: aprox. 4 kW at -120 ºC / aprox. 8 kW at -40 ºC.

1.4.3. IMPULSION OF SUBMARINES

Recently, there has been a growing demand of submarines with the capability of staying submerged longer, which generated a growing interest in technologies of air-independent propulsion (AIP).
Currently, the propulsion system developers are actively working on the following generic lines propulsion equipment:

- Diesel equipment using stored liquid oxygen (LOX)
- Steam turbines closed cycle.
- Stirling external combustion equipment.
- Hydrogen Fuel Cells-oxygen. Closed Cycle Diesel Equipment
- Stirling-cycle machinery.

In the Stirling cycle machines, the heat generated by an external source is transferred to a closed quantity of working fluid, generally an inert gas, and the same is guided through a repeated sequence of thermodynamic changes.

Through the expansion of the gas against a piston and leading it then to a separate heat exchanger for the subsequent compression, heat from external combustion can be transformed into mechanical and then into electricity. This motor has advantages over internal combustion systems. Stirling systems provide significant advantages in the administration of the exhaust gases and sound radiation control.

Stirling Cycle Engines forms the basis of the first AIP system which entered service in the Swedish Navy. The Swedish builder Kockums Naval Systems is a company which tested a prototype plant in 1989. Today, three Swedish submarines are equipped with two 75 kW Stirling engines. Those auxiliary engines burn liquid oxygen and diesel to generate electricity to move the submarine or charge its batteries, everything within an approach that retains conventional diesel electric plant as the main engine of the submarine apparatus. The Swedish Navy reports that while these can remain submerged submarines from 1500 tons at a speed of 5 knots, is 14 days. It is possible to achieve a considerable speed immersion when the batteries are fully laden.

Image 8 - Submarine with AIP Stirling system.

1.4.4. AUTOMOTION

As seen before, they have made significant efforts in developing this type of engines for automotive applications, which, as can be seen today, have not had good results, or have not been so taken into account as expected. Following, we enumerate the advantages and disadvantages of these engines compared to the ones currently used in automotive: diesel and petrol.

The main advantages are:

- Its high performance, as the Stirling engine can potentially achieve ideal performance of Carnot.
- It has a low number of moving parts, especially in comparison with internal combustion engines, which allows very low friction losses.
- The fact that the cycle is closed makes potentially able to obtain very low levels of emissions.
- Since it is an external combustion engine, combustion process can be controlled very well, thus reducing emissions.
- As exchanges heat with the outside, we can use a lot of heat sources, such as nuclear energy, solar energy and fossil fuels, among others.
- The low noise and vibration-free operation with which it operates.

Its main disadvantages are:

- Low power density due to the external combustion, which determines its size.
- Difficulty in engine construction to seal the working fluid throughout life, which raises the cost.
- Lack of experience in the construction of this engine in the automotive field.
- As the working fluid is a gas, this leads to operational difficulties; viable fluids because of their good thermodynamic properties are helium and hydrogen.
- Slow response time.
- Require large heat exchange surfaces, which increases disproportionately its size in comparison with internal combustion engines.
- Long time for starting and stopping.

One of the major difficulties in using Stirling engines in hybrid vehicles is that it is very difficult to build one of these engines that achieve instant starting-up.

Despite these limitations, Ford, General Motors and American Motors Corporation spent millions of dollars developing Stirling engines for cars before the 70s. Ford also built a Stirling which could run (with a relatively low power) 20 seconds after starting.

Many prototypes were built and tested. After that, oil prices collapsed in the 80s and people started buying big cars, without worrying about their performance. Despite this, apparently there is no any good reason to build a motor which is substantially more efficient than the internal combustion engine, but do not start instantly.

Here is the photo of an AMC Spirit car (1979), which was equipped with a Stirling engine pilot plant called "P-40". This car was capable of burning gasoline, oil or a gas type formed by a mixture of gasoline and alcohol (gashol). The Stirling engine P-40 promised a low, contamination, a 30% improvement in efficiency, and performance equal to the standard internal combustion engine.

Image 9 - AMC Spirit (1979).

Given the characteristics of the Stirling engine, much research is being developed in the world to analyze the appropriateness of use them as engine in hybrid vehicles (HEV).
The U.S. giant GM (General Motors) is currently building and developing Stirling engines to develop a hybrid powertrain for its vehicles in the future. The GM developed in 1998 a concept car called Gen2 Stirling HEV, whose picture is shown below.

Image 10 - Gen2 Stirling HEV.

The Stirling engine developed by GM uses hydrogen as working fluid and has several peculiarities. The main one is a rotating disc mounted at an angle and attached to the piston (swash plate) that replaces the traditional rod.
Stirling engines are quiet, smooth and, as turbines, are continuous combustion engines, so they should produce very low emissions. The swash plate was developed to get a better control of the output power and thus give the engine a faster response.

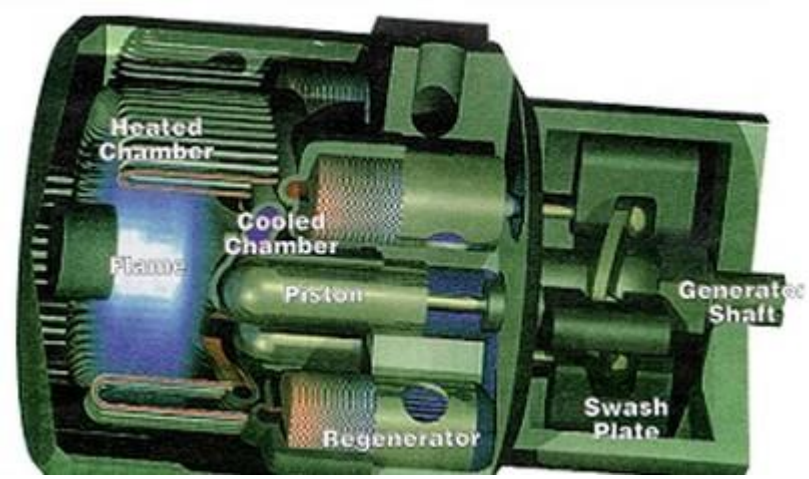

Image 11 - Stirling engine with swash plate mechanism.

1.4.5. ELECTRICITY GENERATION

Stirling dish technology is one of the oldest solar technologies. In the late 70's and early 80's a modern disk technology was developed by Adamo Stirling Corporation, United Stirling AB, McDonnell Douglas Aerospace Corporation (MDA), the Department of Energy of the United States (DOE) and the Jet Propulsion Laboratory of NASA.
The parabolic dishes have evolved in the U.S. and in Europe towards building autonomous units connected to Stirling engines located at the focus. The dish/Stirling systems have demonstrated the highest efficiency of conversion of solar radiation into electrical energy with maximum values of 30% and to 25%. Due to the curvature of the parabolic concentrator and low ratio focal distance/diameter, we can achieve high concentration ratios. This allows to

reach very high operating temperatures (between 650 and 800 °C), resulting in the Stirling engine efficiencies of around 30 to 40%.

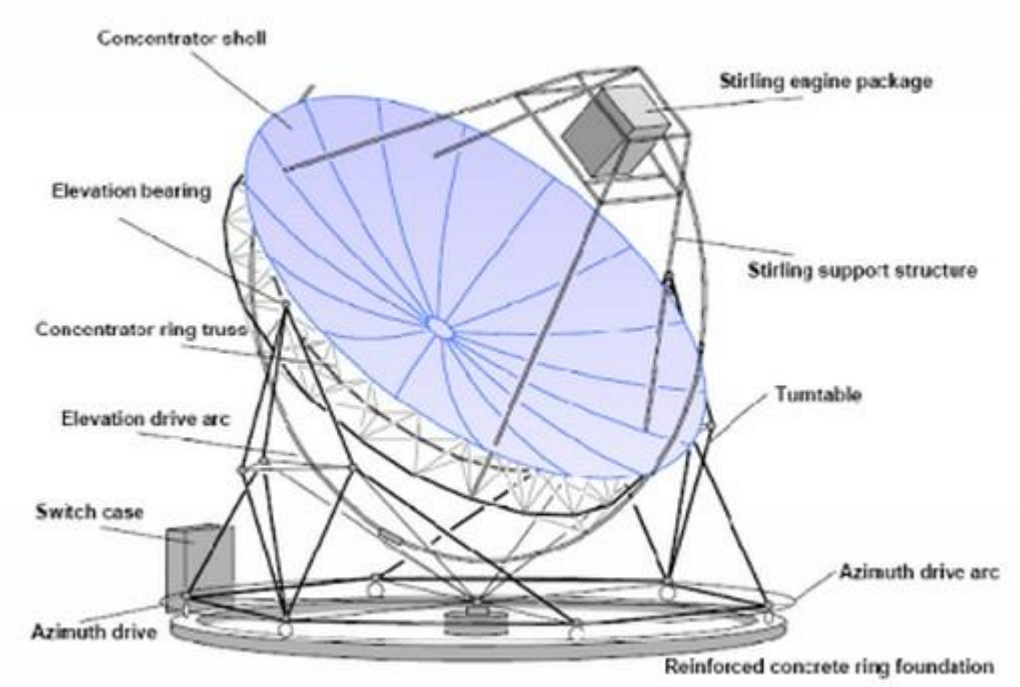

Image 12 - Stirling solar dish.

Typically, two methods are used for transfer of solar radiation to the working gas. The first one is that one where panels are illuminated directly; inside these panels there are tubes wherein the gas flows (usually helium, hydrogen or air). In the second method, we use the concept of heat pipe, vaporizing a liquid metal (typically sodium) which condenses on the surface of the tubes inside which the working gas flows.

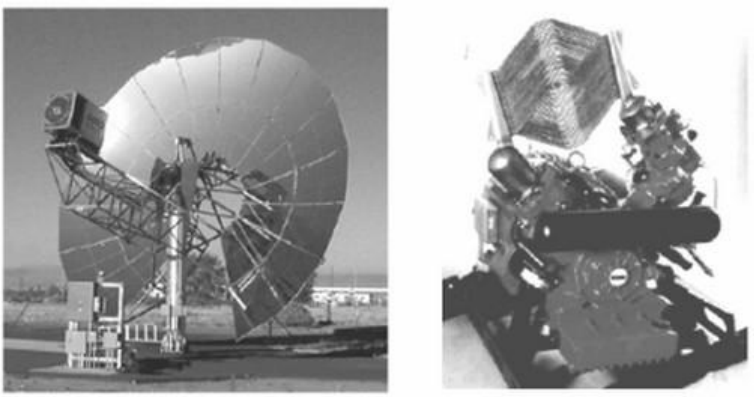

Image 13 - Stirling dish system (left). It is shown the dish of WGAssociates of 10 kW with possibility of hybridation with natural gas. In the spotlight there is a receptor, which has an absorber and a Stirling engine with pistons set in V (SOLO Kleinmotoren).

Operational experience with dish-Stirling systems was limited to a few units tested primarily in the U.S. and Europe, more specifically in the Plataforma Solar de Almeria (Spain).

The "Vanguard" disc was operated in Rancho Mirage (California) in the Mojave Desert for a period of 18 months (February 1984 to July 1985). This dish was 10,7 meters of diameter, a surface area of 86,7 m and had a motor/generator of 25 kWe of United Stirling AB (USAB), 4-95 Mark II model. This engine has four cylinders with a displacement of 95 cm per cylinder. The cylinders are arranged in parallel and mounted on a square. Are interconnected with the regenerator, cooler, and use double acting pistons. The working gas was hydrogen at a maximum pressure of 20 MPa and a temperature of 720 °C. Engine power is controlled by the gas pressure. With more than 30% of net conversion (including auxiliary consumption), this world record was not surpassed until February 2008.

It should be noted other developments in the U.S. involving companies like LaJet, Solar Kinetics, SAIC, Acurex and WG. In Europe, the main developments have been carried out by German companies like Steinmüller and Schlaich, Bergermann und Partner (SBP), and the company Solo Kleinmotoren in regard to supply solarized Stirling engine.
After 20 years of development, solar thermal technology is very important.

Image 14 - Stirling dishes plant (California).

1.4.6. OTHER APPLICATIONS

We can find some projects that use Stirling engines as its technology base. For example, we can find a design for cooling computer motherboards without additional energy consumption, using the heat from the processor.

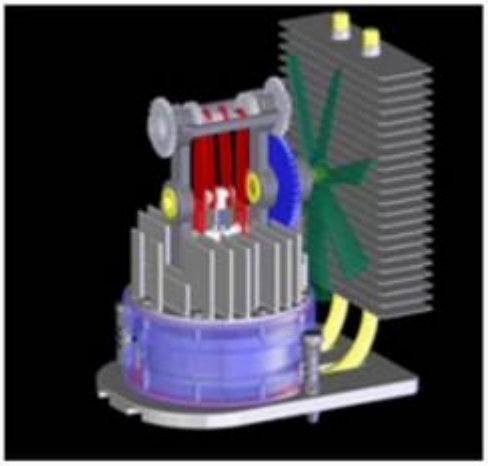

Image 15 - Cooling of computer motherboards without additional energy consumption.

NASA itself is very interested in this type of converters and has devoted significant energy and economic efforts in the development of applications that incorporate different engine models. One is to use different configurations of this engine as power generator for its satellites and spacecraft, and is currently working with a lot of interest in thermoacoustic Stirling engine.

At distances larger than the orbit of Jupiter, the solar panels are virtually useless, it is from here that the probes trust their electric power supply, which should feed both scientific instruments, electronics in general and radio transmitters, ensuring contact with Earth. All ships without exception which have exceeded the asteroid belt have used Radioisotope Thermoelectric Generators (RTG) to convert the heat generated by the decay of a radioactive element, plutonium normally. The efficiency of such devices is very low but now a new device to generate more power or reduce radioactive contamination in future missions to the outer solar system. A scientist at the University of California, who works at the "Los Alamos National Laboratory" and other Northrop Grumman researchers have devised a new method to generate useful electricity for deep space probes. This generator uses a new way to convert heat from plutonium into electricity. And has an efficiency of 18% compared to 7% of current thermoelectric generators.

The traveling-wave engine is a modern adaptation of the Stirling engine. Instead of high pressure steam, it exploits the temperature difference that drives the engine with impressive efficiency.

The propagating waves engine works by sending helium gas through a series of stainless steel wire mesh discs. This regenerator is connected to a heat source and a heat sink that makes the helium expand and contract.

This expansion and contraction creates powerful sound waves, in the same way that a lightning in the atmosphere that produces thunder due to thermal expansion. These oscillating sound waves in the wave propagation engine activate a linear alternator piston that generates electricity.

The use of traveling-wave allows typical parts of an engine, such as the crankshaft and pistons, to be replaced by the action created by the waves (a design sometimes called "Stirling engine without pistons").

The SCE have demonstrated their ability to operate with multiple fuels such as liquid, solid or gaseous fuels with a wide range of temperature. This is a very important feature of these engines that can use abundant sources of heat from solar radiation, waste heat from industry, heat produced from agricultural waste and many other low-temperature sources. This particular engine characteristic placed Stirling cycle engines in the crosshairs of many designs for the development of more efficient systems where you can find a powerful engine of this type.

1.5. ADVANTAGES AND DISADVANTAGES

1.5.1. ADVANTAGES

The Stirling cycle machines, which can operate both as motors and heat pumps have attracted much attention due to its many favorable characteristics, among which we can include:

- High efficiency, as the Stirling engine can potentially achieve ideal performance of Carnot, which has the maximum obtainable efficiency or COP for any engine working between the same differences of temperatures.
- Minimal contamination. For our engine, the exhaust gases are relatively clean and cool. We can get a fine combustion control (if the chosen fuel require it), which occurs near at atmospheric pressure and therefore does not generate nitrogen oxides and other highly toxic compounds.
- Quiet and almost vibration-free in any of its configurations.
- Ability to be powered by different fuels. The energy source can be almost any, while we get the high temperature required. Stirling engines can run with solar power and a wide variety of gas, liquid and solid fuels.
- Maintains its interior sealed, and contains no inlet or exhaust valves, so it is kept clean, lubricated and with minimum wear of its parts.
- The reversible operation allowed in some devices can be used for wide temperature ranges as refrigerator or heat pump. This feature also introduces the possibility of regenerative braking.
- Waste heat is relatively easy to recover (compared with the waste heat of an ICE) which makes these engines very useful for working as hybrid heat pumps or power generators.
- Reasonable specific power.
- Appropriate torque characteristics for transport applications.
- It has the highest specific work of any closed cycle.
- For not being an internal combustion engine, we highlight their silence, its power delivery is more linear, so it requires smaller flywheel, and no parts are impacted so it lasts longer.
- It has a low number of moving parts, especially in comparison with internal combustion engines, which enables very low friction losses.
- The working fluid tends to keep an internal pressure near the design pressure; in this way for a properly designed system the risk of explosion is minimal.
- In many cases, low operating pressure allows us to use lightweight cylinders.
- They can be built to work silently and without air supply, so it can be used in applications such as underwater or in space propulsion.
- Start-up easily (although slowly) and work very efficiently with cold weather, compared with internal combustion engines, which start quickly in hot weather, but not cold.

1.5.2. DISADVANTAGES

We can also name some defects; the most outstanding are:

- **Aspects of size and cost**

- The design of the Stirling engine requires heat exchangers for the input and output heat, and these must be at the pressure of the working fluid, and the pressure is proportional to the output power of the motor. Additionally, the expansion zone is usually at a very high temperature, so the materials must withstand the destructive effects of the heat source, and possess little deformation due to the temperature. Typically these materials requirements increase the cost of the engine. The materials and assembly costs for a heat exchanger working at high temperature generally are the 40% of the total cost of the engine.
- Large heat exchange surfaces are required, which causes a great increase of the size of the engine in comparison with the ICE.
- Every thermodynamic cycle needs a large temperature difference for an efficient operation. In external combustion, the heater temperature is always equal to or greater than the expansion temperature. This means that the metallurgical requirements for the heater material are very demanding. Something similar happens with the gas turbine, but in the internal combustion engine the expansion temperature can far exceed the metallurgical limit of the materials of the engine as the heat source is not directed through the engine; because of this, the engine materials work near the average temperature of the working fluid.
- Heat dissipation is particularly complicated because the coolant temperature should be kept as low as possible to maximize thermal efficiency. This increases the size of the radiators, which may complicate the coating. Along with materials cost, this has been one of the limiting factors to the development of the Stirling engines as automotive propulsion. For other applications we do not need high power density, such as propulsion, or stationary microgeneration systems that combine heat and power pumps.
- Difficulty in engine construction to seal the working fluid throughout its lifetime, and its manufacture requires a lot of precision, although less than the manufacture of other engines.

- **Aspects of power and torque**

- The SCE, especially those working with small temperature difference, are quite large in proportion to the amount of power they produce. That means that they have little specific power. This is mainly due to the low heat transfer coefficient of gas convection, which limits the flow of heat that can be found in a heat exchanger. This makes it very challenging for the engine designer to achieve heat transfer to and from the working gas. Increasing the pressure and/or temperature of the engine enables Stirling engines produce more power, assuming that the heat exchangers are designed to increase of heat load, and can deliver the required heat flow.
- A Stirling engine cannot be started-up instantly, it needs pre-heating. This is true for every external combustion engines, but the warm up time is lower for Stirling engines

than for other steam engines. The best uses of the Stirling engine are as constant speed motor.

- The power output of these engines tends to be constant, and to vary it we require a special design and additional mechanisms. Generally, the output changes are typically obtained with changes in engine displacement (typically a transmission by using a rotating disc) or modifying the amount of the working fluid, by changing the phase angle of the displacer or the power piston, or in other cases simply modifying engine load. This property is less important if we consider hybrid electric propulsion or base load generation, where constant power delivery is desirable.
- The speed control is difficult.

- **Aspects of gas choice**

- The working fluid is gaseous, which causes operational difficulties, thereby truly viable fluids due to good thermodynamic properties are helium and hydrogen.
- Hydrogen's low viscosity, high thermal conductivity and high specific heat make this gas the most efficient to be used in a SCE in terms of thermodynamics and fluid dynamics.
- The most technically advanced SCE use helium as working gas. But helium is quite expensive and must be fed by a gas bottle.
- Some engines use air or nitrogen as working fluid, but the use of compressed air in contact with flammable materials or substances has a risk of explosion because compressed air contains high oxygen partial pressure.

1.6. LOW TEMPERATURE DIFFERENCE (LTD) STIRLING ENGINES

1.6.1. INTRODUCTION

Stirling engines with low temperature difference (LTD engines) are engines with a configuration exactly like other Stirling engines, but in working operation with low temperature differences between hot and cold areas.

Obviously, these engines have lower performance than those operating with large temperature differences, but the interesting thing about them is not the performance they offer, but the ease with which you have to get these low temperatures. There are many sources of low temperature heat, and including renewable energies, like solar and biomass.
Therein lays the great interest in these engines: instead of being powered by combustion, can be heated with renewable sources, obtaining a 100% clean energy (because if there is no combustion, Stirling engines do not emit greenhouse gases). LTD Stirling engines thus represent a way to convert solar energy directly into mechanical work.

There are two typical configurations for LTD Stirling engines:

- Ringbom engine: in this configuration, only the working piston is connected to the flywheel.
- Kinematic engine: in this configuration, the two pistons are connected to the flywheel with a typical lag of 90º and Gamma configuration. This is the configuration of the engine in the laboratory.

A calculation using the Carnot cycle formula shows that an engine operating with a source temperature of 100 °C and a sink temperature of 35 °C gives a maximum thermal efficiency of about 17.42%. If an engine could be built for achieving 50% of the maximum thermal efficiency, it would have about 8.71% overall Carnot efficiency. Even the calculated thermal efficiency seems rather low, but LTD Stirling engines could be used with free or cheap low temperature sources. This engine should be selected when the low cost engines are put into consideration. Although the specific power developed by LTD Stirling engines is low, lightweight and cheap materials such as plastics can be used as engine parts.

Currently most of the available LTD Stirling engines are smaller model sized engines. These are usually purchased for demonstration in an educational setting.

1.6.2. COMPONENTS AND OPERATION OF LTD STIRLING ENGINES

The basic elements of an LTD engine are the same as any other conventional Stirling engines. The most common LTD engine configuration is a Gamma type Stirling. These are the most important components:

- Piston
- Displacer
- Cylinder
- Connecting rods and linkages
- Flywheel
- Hot side plate (heat exchanger)
- Cold side plate (heat exchanger)

The arrangement of elements in a LTD engine is not exactly equal than in Stirling engines with higher temperature differences. In the LTD, the shape has requirements that must be met, as they are limited. These engines have a relatively large volume of working fluid and displacer to compensate the small amounts of energy available when running on such small heat differences.

In Stirling engines, the working fluid must be sufficiently heated to expand and push the piston outward the appropriate distance for the engine to operate.
In the case of a high temperature differential Stirling a relatively small amount of gas is heated. An LTD Stirling engine aims to do the opposite. To offset the small heat difference it heats a relatively large amount of gas.
This leads to LTD Stirling engine designs that have a relatively large surface area for the heating and cooling plates. These plates allow a larger volume of gas to be affected.
It is also necessary to have a displacer that has nearly the same surface area as the heating and cooling plates. The displacer is almost always light weight and has high insulation properties.

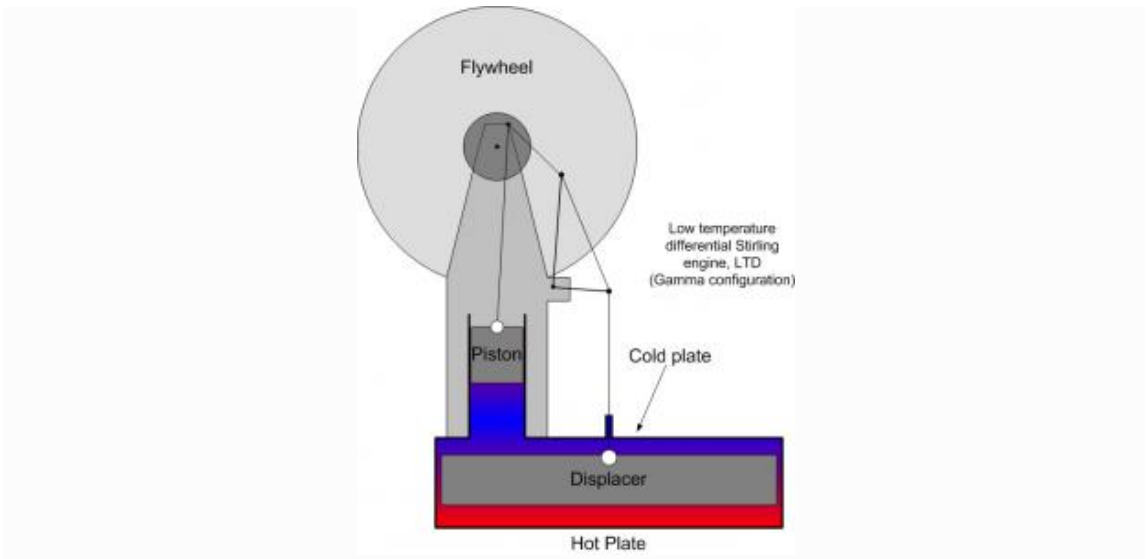

Image 16 - LTD Stirling engine.

Because the temperature difference required to operate a motor LTD is so small, a large number of energy sources may be used. Some possible sources are:

- Solar energy
- Geothermal energy
- Landfill heat energy
- Captured heat from homes
- Waste heat from industrial processes
- Automobile engine waste heat

2. THEORETICAL STUDY OF THE STIRLING CYCLE ENGINE

2.1. INTRODUCTION

This part of the project aims to present a review of the literature on technological development of Stirling engines. For that purpose many researches on SCE have been read and will be commented in that section.

A Stirling cycle engine is a mechanism which operates in a regenerative thermodynamic cycle, with cyclic compressions and expansions of a working fluid at different temperature levels. The flow is controlled by volume changes and as a result there is a net conversion of heat into work and vice versa.

They have been developed many different analysis, with different degrees of sophistication.
First, we find the ideal Stirling cycle analysis, whose thermodynamics is based on two isothermal processes and two isochoric processes, both regenerative. This analysis is overly idealized, and only serves to make estimations.

Following we find the isothermal analysis, studied by Gustav Schmidt (1871), this analysis is the most used historically as it gives a more realistic result. However, the actual efficiency of the engine never exceeds 60% of that estimated by the analysis. This is due, basically, to the Schmidt process assumes that the compression and expansion processes are isothermal, which does not happen in reality, since these processes are closer to being adiabatic than isothermal.
Next place we find the adiabatic cycle, mainly developed by Finkelstein (1960).
Below are explained in detail each of the analyzes.

2.2. CARNOT AND STIRLING THERMODYNAMICAL CYCLES

The maximum possible theoretical efficiency in a thermodynamic cycle is given by the Carnot cycle. Thus, three theoretical advantages of the ideal Stirling cycle can be found on the Carnot cycle.

The thermal efficiency of ideal regeneration cycle is similar to the Carnot cycle. During the heat transference, the regenerator, that is a temporal energy "depot", absorbs and gives heat quickly to the fluid which goes through it. Therefore, the amount of heat taken from the external hot source is low, which provokes an increase in the thermal efficiency of the cycle.
Stirling cycle obtained from Carnot one simply requires replacing two isentropic processes by two processes at constant volume. This causes an increase in the area of the p-V diagram. Therefore, it is obtained a substantial amount of work from the Stirling cycle without using very high pressures and large swept volumes, as the Carnot cycle. Stirling cycle, compared with Carnot, between the same limits of pressure, volume and temperature, can be seen in the following figure.

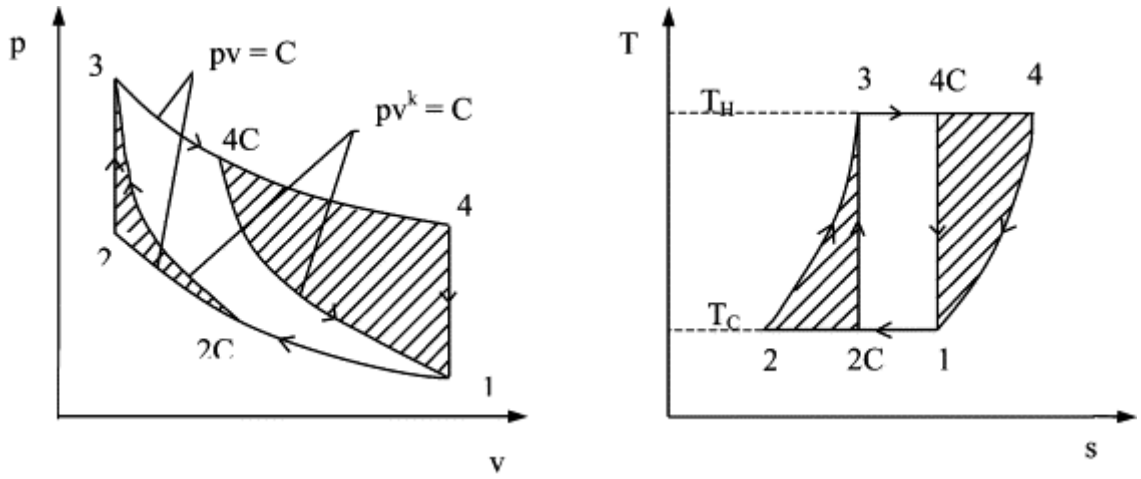

Image 17 - Stirling and Carnot cycles.

Shaded areas 2C-2-3 and 1-4C-4 show the additional work available thanks to replace two isentropic processes by two processes at constant volume. Isotherms Carnot cycles (1-2C and 3-4C) are extended to the processes 1-2 and 3-4. The amount of removable work from the cycle increases in proportion to the heat applied to and extracted from the Stirling cycle.
Compared to all the hot alternating piston engines working with the same limits of temperature, volume ratios, the same mass of ideal working fluid, the same external pressure and mechanisms with the same overall efficiency, ideal Stirling engine has the maximum efficiency mechanically possible.

2.3. THERMODYNAMICS OF THE IDEAL STIRLING CYCLE ENGINE

Robert Stirling built an engine which worked with a closed thermodynamic cycle. We can see the cycle of the engine invented by Robert Stirling represented in p-V and T-S diagrams below.

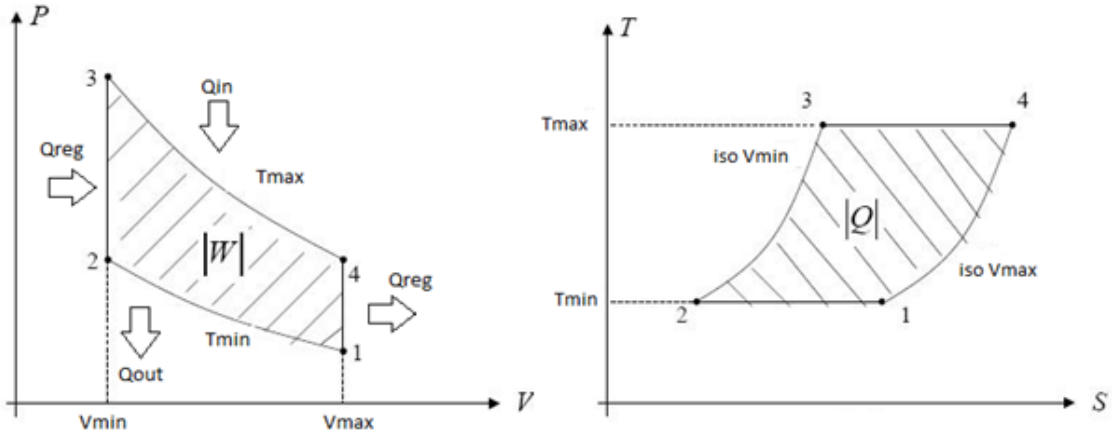

Image 18 – p-V and T-S Stirling engine diagrams.

The cycle has four processes, called isothermal compression (1-2) and expansion (3-4), and heating (2-3) and cooling (4-1) at constant volume (isochoric). Let us consider a cylinder which contains two opposing pistons with a regenerator between them. The regenerator is like a thermal sponge which absorbs and transfers heat alternately, and consists of a metal wire matrix. The volume between the regenerator and the piston on the right is the compression volume and the one located between the regenerator and the piston on the left is called the expansion volume. The expansion volume is maintained at high temperature, while the compression volume is at low temperature. The temperature gradient ($T_{max} - T_{min}$) between the ends of the regenerator will also remain constant.

2.3.1. CYCLE OF THE ENGINE

First of all, we will assume that the piston of the compression space is in the external death point (right end), and the expansion space piston is beside the regenerator. In this case, all the fluid is in the cold area of the compression space, and the compression volume is maximal and the pressure and temperature are in their minimum values; this moment is represented by the point 1 in the diagrams. From here, we will define the 4 processes of the thermodynamical cycle.

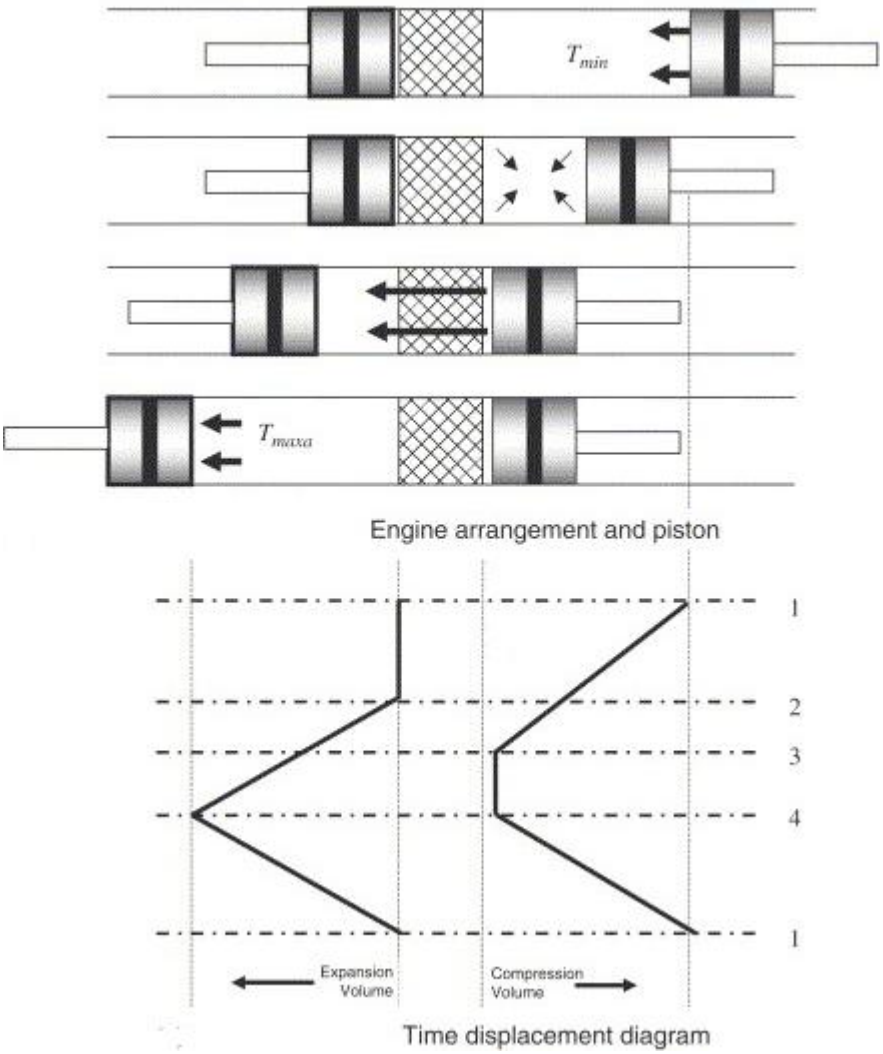

Image 19 - Stirling engine cycle. Pistons arrangement and displacement diagram.

- Process 1-2, isothermal compression. During the compression process from 1 to 2, the compression piston moves towards the regenerator, while the expansion piston remains stationary. The working fluid is compressed in the compression space, and:
  - Pressure increases from p_1 to p_2.
  - Temperature remains constant because of the heat flow from the cold space to the surroundings, $T = ct$.
  - Work is performed on the fluid in the same magnitude as the heat extracted from the cycle, $W = Q$.
  - There is no change in the internal energy, $U = ct$.
  - Decrease in the entropy.
  - The isothermal compression of the working fluid carries a heat transfer from the fluid to a external sink at Tmin.

$$p_2 = \frac{p_1 V_1}{V_2} = p_1 r_v$$
$$T_1 = T_2 = T_{min}$$

$$Q(heat\ transferred) = W(work\ done)$$
$$Q = W = p_1 V_1 \ln\left(\frac{1}{r_v}\right) = mRT_1 \ln\left(\frac{1}{r_v}\right) \qquad [Ec.1]$$
$$s_2 - s_1 = R \ln\left(\frac{1}{r_v}\right) \qquad [Ec.2]$$

- Process 2-3, regenerative heat transfer at constant volume. During this process, both pistons move simultaneously, i.e., the compression piston towards the regenerator and the expansion one moving away from it, and that is why the volume between them remains constant. The working fluid is transferred from the compression to the expansion space through the porous mesh of the regenerator.
    - The temperature of the working fluid increases from T_{min} to T_{max}, because of the heat transfer from the regenerator to the fluid.
    - This gradual increase of the working fluid temperature while goes through the regenerator provokes an increase in the pressure from p_2 to p_3.
    - In this process no work is performed, $W = 0$.
    - The entropy and internal energy increase.
    - So we have an isochoric heat transfer from the regenerator matrix to the working fluid.

$$p_3 = \frac{p_2 T_3}{T_2} = \frac{p_2}{\tau}, \qquad \tau = \frac{T_2}{T_3}$$
$$V_2 = V_3$$
$$Q(heat\ transferred) = C_v(T_3 - T_2) \qquad [Ec.3]$$
$$W(work\ done) = 0$$
$$s_3 - s_2 = C_v \ln\left(\frac{1}{\tau}\right) \qquad [Ec.4]$$

- Process 3-4, isothermal expansion. During this process, the expansion piston keep on moving away from the regenerator to the external dead point, while the compression piston stays stationary in the internal dead point, beside the regenerator.
    - During the expansion, pressure decreases from p_3 to p_4.
    - Volume increases from V_3 to V_4.
    - Temperature keeps constant thanks to the heat addition from an external sink at T_{max}, $T_3 = T_4 = T_{max}$
    - Work is performed by the working fluid on the piston in the same magnitude as the applied heat, $Q = W$.
    - There is no change in the internal energy, $U = ct$.
    - There is an increase in the working fluid entropy.

$$p_4 = \frac{p_3 V_3}{V_4} = p_3 \frac{1}{r_v}$$
$$T_3 = T_4 = T_{max}$$
$$Q(heat\ transferred) = W(work\ done)$$
$$Q = W = P_3 V_3 \ln(r_v) = mRT_3 \ln(r_v) \qquad [Ec.5]$$
$$s_3 - s_4 = R \ln(r_v) \qquad [Ec.6]$$

- Process 4-1, regenerative heat transfer at constant volume. In this process, both pistons move simultaneously, to transfer the working fluid from the expansion space to the compression one through the regenerator at constant volume.
    - During the working fluid flow through the regenerator, the heat transferred from the fluid to the matrix provokes a reduction in the working fluid temperature to T_{min}.
    - No work performed, $W = 0$.
    - Decrease in internal energy and in entropy.

$$p_1 = \frac{p_4 T_1}{T_4} = p_4 \tau, \qquad \tau = \frac{T_2}{T_3}$$

$$V_4 = V_1$$

$$Q(heat\ transferred) = C_v(T_1 - T_4) \qquad [Ec.7]$$

$$W(work\ done) = 0$$

$$s_1 - s_4 = C_v \ln(\tau) \qquad [Ec.8]$$

This evolution of the processes can be seen summarized in the following figure, which evidences where the fluid in the different chambers of the mechanism is. Thereby, there are symmetries in the location and evolution of the fluid, that make the fluid to be totally confined in the hot chamber during the expansion and in the cold one during the isothermal compression, while during the isochoric transfers, it goes from one chamber to another one absorbing or giving heat to the regenerator.

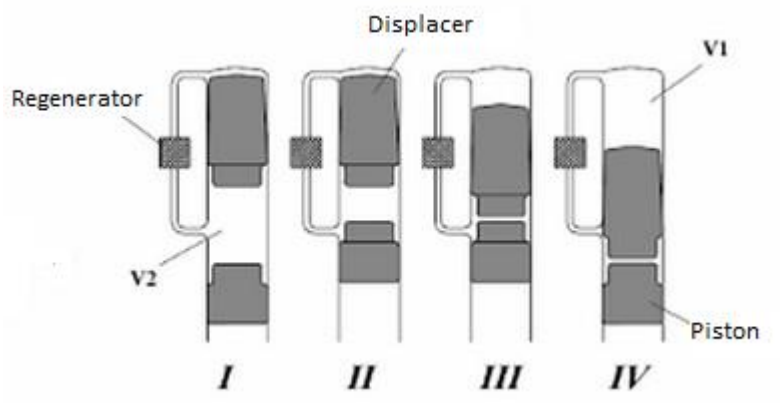

Image 20 - Stirling engine cycle. Chambers arrangement.

The difficulty of performing the theoretical cycle is because of displacement requirements of the pistons, as seen in the following figure, the evolution 4-1 and 3-4 on the hot and cold chamber, respectively, have no time be performed to maintain synchronization of position between the two chambers. This problem motivates the practical realization of this engine forced to give up the correct realization of one of the forms of the cycle to adapt to the mechanism.

One possible implementation of the engine may be by the known rod-crank mechanism which characterizes alternating engines. The mechanism subjects the fluid to a cycle that if the result of the "overlapping" of processes 4-1 with the expansion in 3-4 and compression in 1-2.
The evolution of the mechanism and performance of the cycle, as can be seen in the figure above, is summarized as follows:

I. The piston is at the bottom dead point, and the displacer on the upper, so that all fluid is in the cold area.
II. The displacer remains in the top dead point and the piston compresses the fluid at low temperature. The fluid gets the minimum volume.
III. The piston is held at that point and the displacer lets the fluid going into the hot chamber, moving to its bottom dead point. This transfer is performed through the regenerator. The fluid volume is still minimal.
IV. The fluid is heated while it goes through the regenerator and thus creates high pressure on the displacer; this pressure motivates the stroke of the displacer, which reaches its bottom dead point with the piston. Then the displacer is moved to its upper dead point letting expanded fluid pass to the cold chamber through the regenerator. When the displacer reaches its top dead point, we again have the structure in position I.

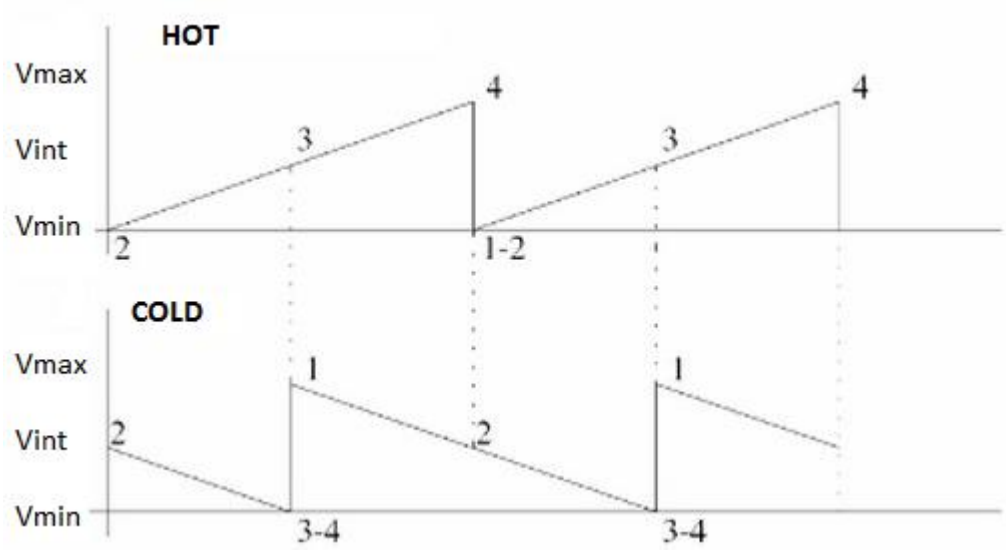

Image 21 - Evolution of the volume of the hot and cold chambers during the cycle.

If we consider the volume ratio, $r_v = \frac{V_4}{V_3} = \frac{V_1}{V_2}$
Express the heat applied like $Q = mRT_3 \ln r_v$
And the heat extracted $Q = mrT_1 \ln\left(\frac{1}{r_v}\right)$

The efficiency can be written like:

$$\eta = \frac{W_{output}}{Q_{input}} = \frac{W_{1-2} + W_{3-4}}{Q_{3-4}} = \frac{mRT_3 \ln r_v + mrT_1 \ln\left(\frac{1}{r_v}\right)}{mRT_3 \ln r_v} = \frac{mRT_3 \ln r_v - mrT_1 \ln(r_v)}{mRT_3 \ln r_v}$$

$$\eta = 1 - \frac{T_1}{T_3} = 1 - \frac{T_{min}}{T_{max}} = 1 - \tau \qquad [Ec.9]$$

This is all for a highly idealized cycle, which is composed of two isothermal processes, two processes at constant volume and also is considered a reversible thermodynamic cycle. These assumptions have several implications, which are impossible to achieve in a real engine:

- Isothermal processes: means that heat exchanges should be perfectly effective and this requires an infinite ratio of heat transfer between the cylinder walls and the working fluid.
- Constant volume processes (isochors): assumes that there is no heat transfer between the walls and the working fluid.

2.3.2. ISOTHERMAL ANALYSIS

To achieve effective heat transfer, the ideal engine will be modeled as a system consisting of a five-component connected in series, as shown in the figure, which will be compression space C, cooler K, regenerator R, heater H and expansion space E. The pipes that connect these spaces are added in the appropriate volumes for simplicity. The engine analysis was performed for evaluating the heat transfer to the working fluid by evaluating the area enclosed in the p-V diagram.

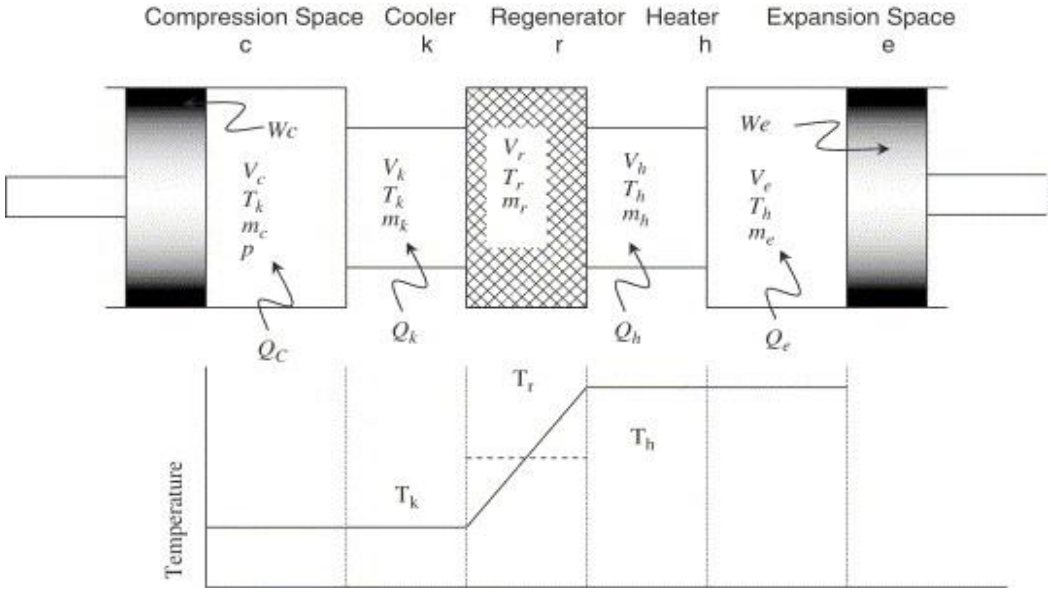

Image 22 - Model of ideal engine and temperatures for the isothermal analysis.

The analysis starts considering the mass of the working fluid as constant:

$$M = m_c + m_k + m_r + m_h + m_e = ct$$

Pressure along the motor is considerate also constant: $p = ct$.
Temperature in compression space and cooler is constant: $T_c = T_k$

Temperature in expansion space and heater is constant: $T_e = T_h$

Applying the ideal gas equation, $pV = mRT$ $[Ec.10]$, we get:

$$M = \frac{p}{R}\left(\frac{V_c}{T_k} + \frac{V_k}{T_k} + \frac{V_r}{T_r} + \frac{V_h}{T_h} + \frac{V_e}{T_h}\right) \qquad [Ec.11]$$

For evaluating properly the gas mass in the regenerator, we should know the temperature distribution along it. We will assume that an ideal regenerator has a lineal temperature distribution between the cold and the hot temperatures, as shown:

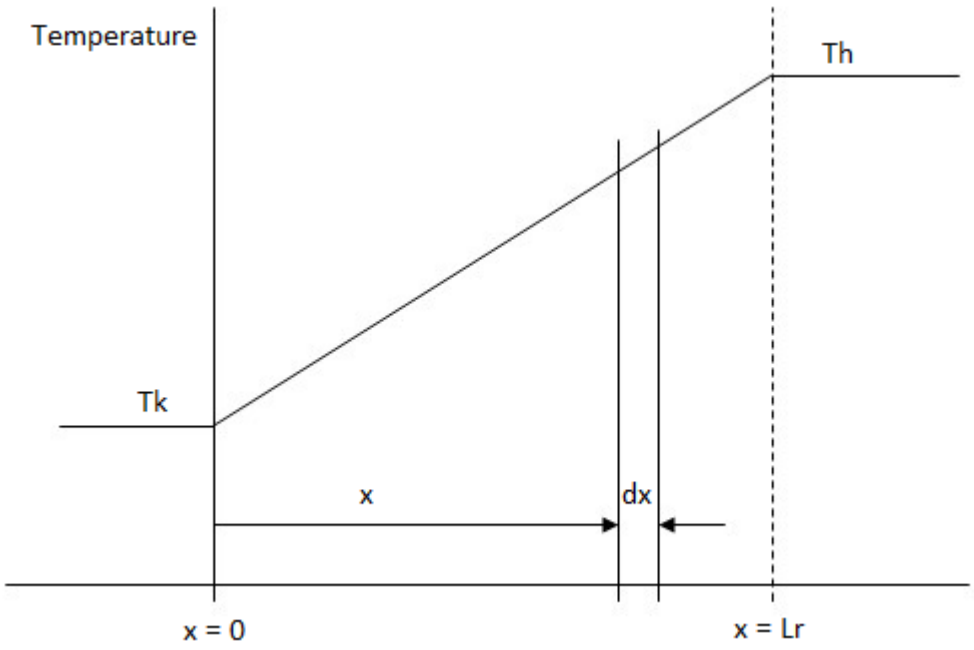

Image 23 - Linear temperature distribution in the regenerator.

The temperature distribution in the regenerator can be described by:

$$T(x) = (T_h - T_k)\frac{x}{L_r} + T_k \qquad [Ec.12]$$

Where

$L_r = length\ of\ regenerator$

Total mass of gas, m_r, inside the volume of the regenerator, V_r:

$$m_r = \int_0^{V_r} \rho dV_r$$

With the state equation for ideal gases, and for a constant flow area, A_r, we have:

$$p = \rho RT$$
$$dV_r = A_r dx$$
$$V_r = A_r L_r$$

Applying these equations to the previous expression, and simplifying:

$$m_r = \frac{V_r p}{R} \int_0^{L_r} \frac{1}{(T_h - T_k) \cdot x + T_k \cdot L_r} dx$$

And if we integrate and simplify, we get:

$$m_r = \frac{V_r \cdot p}{R} \cdot \frac{\ln\left({}^{T_h}/_{T_k}\right)}{(T_h - T_k)} \qquad [Ec.13]$$

And so, we define from this expression the effective mean temperature, T_r, of the gas in the regenerator, in terms of the state gas equation:

$$m_r = \frac{V_r p}{R T_r}$$

Comparing both expressions we get the effective mean temperature of the gas in the regenerator as a function of the hot and cold temperatures:

$$T_r = \frac{T_h - T_k}{\ln {}^{T_h}/_{T_k}} \qquad [Ec.14]$$

Clearing the previous equations, we can express the pressure of the cycle as:

$$p = M \cdot R \cdot \left(\frac{V_c}{T_k} + \frac{V_k}{T_k} + \frac{V_r \ln\left({}^{T_h}/_{T_k}\right)}{(T_h - T_k)} + \frac{V_h}{T_h} + \frac{V_e}{T_h} \right)^{-1} \qquad [Ec.15]$$

So we have obtained an equation for the pressure of the working gas, which is function of the variation in volumes in expansion and compression areas, V_c and V_e.
In a complete cycle, the total performed work is the algebraic addition of the work performed by the compression and expansion spaces.

$$W = W_c + W_e$$

$$W = \oint p dV_c + \oint p dV_e$$

$$W = \oint p \left(\frac{dV_c}{d\theta} + \frac{dV_e}{d\theta} \right) d\theta\,, \qquad where\ \theta = crank\ angle \qquad [Ec.16]$$

2.3.3. HEAT TRANSFERRED IN THE ISOTHERMAL MODEL

To study the heat transfer in the heater and cooler we have to considerate the energy equation of the working fluid. For this study, we will use the cell of working spaces, modeled

by Rallis (represented in the figure), which can be considerate as the working space o as the cell of a heat exchanger. Enthalpy is transferred into the cell through the mass flow m, at a temperature T, and comes out at m_0 and T_0.

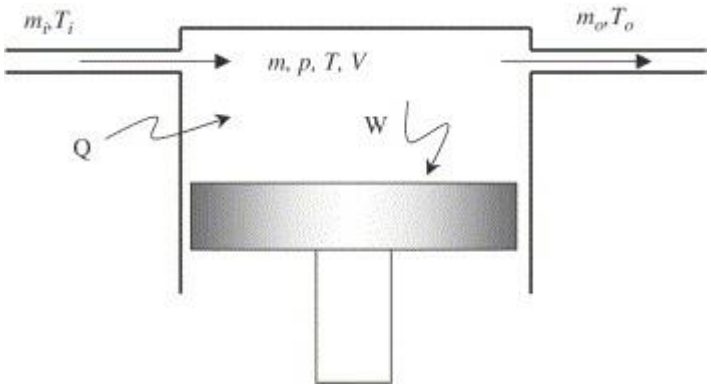

Image 24 - Generalized cell for a working space, modeled by C. J. Rallis.

The equation of energy for the working fluid inside the cell can be written like:

$$\begin{bmatrix} Heat\ rate \\ transferred \\ to\ the\ cell \end{bmatrix} + \begin{bmatrix} Enthalpy \\ net\ conversion \\ inside\ the\ cell \end{bmatrix} = \begin{bmatrix} Work\ rate \\ performed \\ over\ the\ environment \end{bmatrix} + \begin{bmatrix} Increase\ of \\ internal\ energy \\ inside\ the\ cell \end{bmatrix}$$

Mathematically, we can express it like:

$$\frac{dQ}{d\theta} + \left(C_p T_i m_i' - C_p T_o m_o'\right) = \frac{dW_d}{d\theta} + C_v \frac{d(mT)}{d\theta} \qquad [Ec.\,17]$$

$$C_p, C_v: specific\ heat\ of\ the\ gas\ a\ constant\ pressure\ and\ volume, respectively.$$

This expression is the classic form of the equation of energy for discontinuous flow, dismissing terms of kinetic and potential energies.

For the isotherm model that we are studying, both expansion and compression spaces, and heater and cooler can be considerate like T_i=T_o=T. So:

$$\frac{dQ}{d\theta} + C_p T(m_i' - m_o') = \frac{dW_d}{d\theta} + C_v \frac{d(mT)}{d\theta}$$

$$\frac{dQ}{d\theta} = C_p T(m_o' - m_i') + \frac{dW_d}{d\theta} + C_v \frac{d(mT)}{d\theta}$$

Keeping in mind the considerations of mass conservation, the difference of mass flow $m_o' - m_i'$ is simply the variation of mass inside the cell, and for the working fluid, $R = C_p - C_v$. With these considerations, the equation is simplified:

$$\frac{dQ}{d\theta} = (C_p - C_v) \cdot T \frac{dm}{d\theta} + \frac{dW_d}{d\theta}$$

$$\frac{dQ}{d\theta} = RT \frac{dm}{d\theta} + \frac{dW_d}{d\theta}$$

We can obtain the net heat transferred to the working gas during the cycle by integrating the previous equation in one cycle:

$$Q = \oint \frac{dQ}{d\theta} = RT \oint \frac{dm}{d\theta} + \oint \frac{dW_d}{d\theta} \qquad [Ec. 18]$$

However, the implicit assumption that the stationary state cycle can be achieved implies that the cyclic change of the mass of the working fluid is zero for each of the cells. So, applying equation 18 to each of the isotherm cells and integrating for the entire cycle, we obtain for the workspaces:

$$Q_c = W_c$$
$$Q_e = W_e$$

And in a similar way for the heat exchangers, where no work is made:

$$Q_k = 0$$
$$Q_h = 0$$

And of course, for an ideal regenerator, $Q_r = 0$. This is caused because the heat exchanges between the matrix of the regenerator and the working fluid are internal, i.e. there are no heat exchange between the regenerator and the outside.

This result is astonishing, since it implies that the heat exchangers are redundant, all heat exchanges with the outside necessary take place around the workspaces. This apparent paradox is a direct result of the isothermal model, in which the compression and expansion spaces are maintained at the respective temperatures of the heater and cooler. Obviously, this cannot be correct because the cylinder walls are not designed to transfer heat.

2.3.4. SCHMIDT ANALYSIS

The apparent conceptual simplicity of the Stirling engine conceals its complicated mathematical analysis. The difficulty to describe even idealized models of the engine in terms of simple and closed equations is one of the main reasons for the widespread skepticism and lack of understanding that exists even today. 55 years after the invention of the Stirling cycle engine, Schmidt made an analysis of the cycle in 1871, which is known as classical analysis. This analysis was performed for 3 different types of practice settings: alpha, beta and gamma.

Schmidt got a theory close to the known, which showed sinusoidal variations of the workspace volume in alternating engines. The theory keeps the most important assumptions of the compression and expansion isotherms and perfect regeneration. Hence we see that the cycle still being highly idealized, but despite this is far more realistic than the ideal Stirling cycle. The configurations considered in the SCE classical analysis are shown in the following figures:

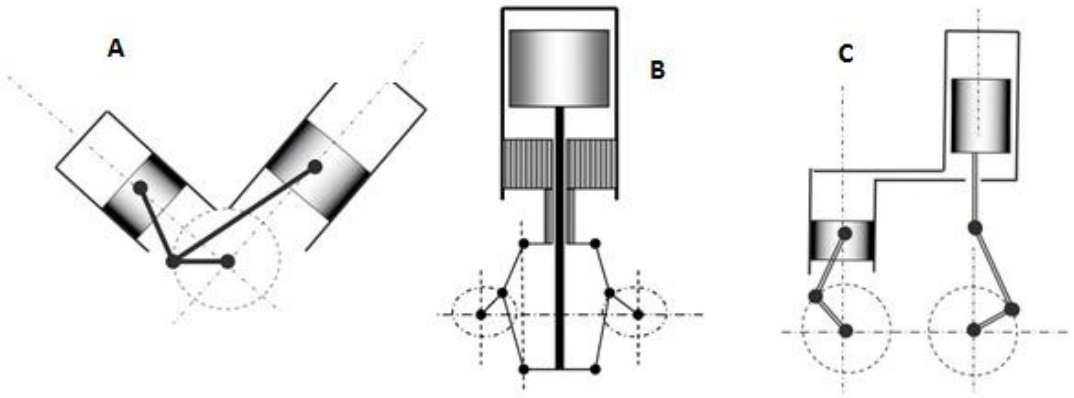

Image 25 - SCE Configurations. A) Alpha. B) Beta. C) Gamma.

Principal assumptions of the analysis of Schmidt for SCE:

1. All processes are reversible.
2. Regeneration is a perfect process.
3. The working fluid follows the perfect gas law: pV = mRT
4. The mass of air in the system remains constant, no leakage in the system.
5. Volume changes in the workspace are sinusoidal.
6. There is no temperature gradient in the heat exchanger.
7. The temperatures of the piston and cylinder wall are constants.
8. The machine speed is constant.
9. Terms of continuity established.
10. No flow losses and therefore no loss of pressure.
11. No leakage of the working gas.
12. Temperature in the heater and the expansion space is isothermal, T_h.
13. Temperature in cooler and the compression space is isothermal, T_k.
14. Temperature in the dead zone and therefore the regenerator space is constant, T_r.

But actually, no drive mechanism that is capable of producing sinusoidal motion. Schmidt supposed a mechanism with an infinitely long push rod, with which he could get the actual sinusoidal motion of displacer and power piston.

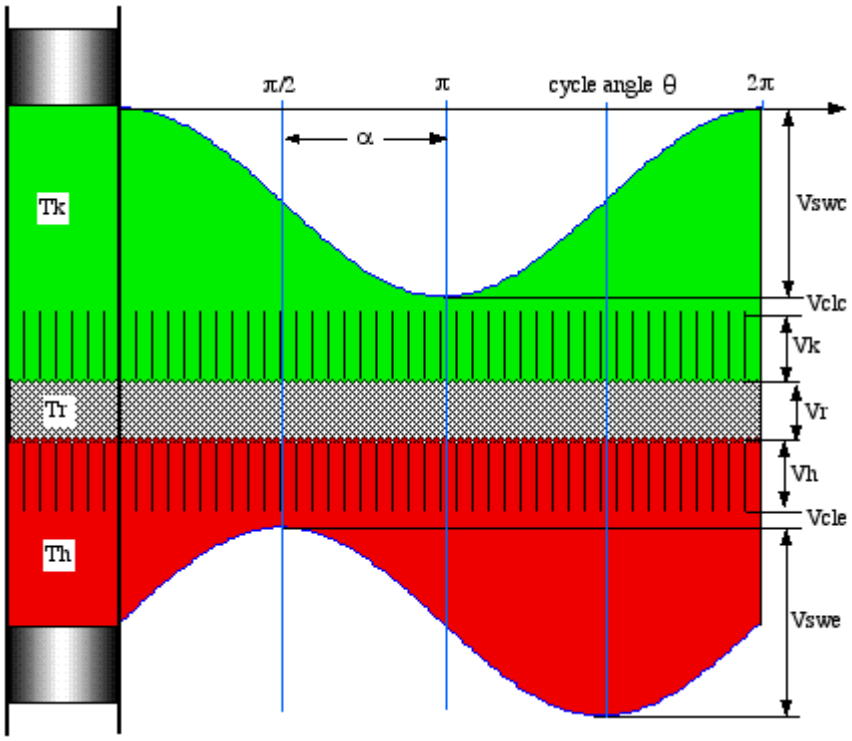

Image 26 - variations in expansion and compression spaces.

In the figure above, we can find:
V_{swc}, V_{swe}: *swept volumes in compression and expansion spaces*
V_{clc}, V_{cle}: *clearance (death)volumes in compression and expansion spaces*
V_k, V_r, V_h: *volumes of heater, regenerator, cooler*
α: *phase angle between pistons (and between compression and expansion spaces)*

Keeping in mind the previous figure of volume variations in compression (V_c) and expansion (V_e), and the phase angle α, we have:

$$V_c = V_{clc} + \frac{V_{swc}}{2}(1 + \cos\theta) \qquad [Ec.19]$$

$$V_e = V_{cle} + \frac{V_{swe}}{2}(1 + \cos(\theta + \alpha)) \qquad [Ec.20]$$

Replacing these equations in **[Ec. 15]** and simplifying:

$$p = M \cdot R \cdot \left(s + \left(\frac{V_{swe} \cdot \cos\alpha}{2T_h} + \frac{V_{swc}}{2T_k}\right)\cos\theta - \left(\frac{V_{swe}}{2T_h}\sin\alpha\right)\sin\theta\right)^{-1} \qquad [Ec.21]$$

Where

$$s = \left(\frac{V_{swc}}{2T_k} + \frac{V_{clc}}{T_k} + \frac{V_k}{T_k} + \frac{V_r \ln\left(\frac{T_h}{T_k}\right)}{(T_h - T_k)} + \frac{V_h}{T_h} + \frac{V_{cle}}{T_h} + \frac{V_{swe}}{2T_h} \right)$$

In order to simplify the pressure equation, we consider a trigonometric substitution of β and c as defined by the following right-angled triangle:

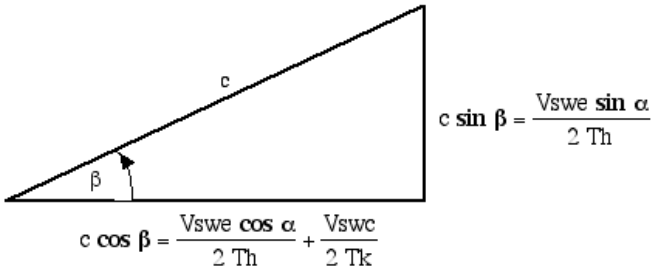

Image 27 - Schmidt analysis triangle.

Where

$$\beta = \tan^{-1}\left(\frac{\frac{V_{swe}\sin\alpha}{T_h}}{\frac{V_{swe}\cos\alpha}{T_h} + \frac{V_{swc}}{T_k}} \right)$$

$$c = \frac{1}{2}\left[\left(\frac{V_{swe}}{T_h}\right)^2 + 2\left(\frac{V_{swe}}{T_h}\right)\left(\frac{V_{swc}}{T_k}\right)\cos\alpha + \left(\frac{V_{swc}}{T_k}\right)^2 \right]^{1/2}$$

Using these expressions in **[Ec. 21]** and simplifying, we obtain:

$$p = \frac{MR}{s(1 + b\cos\phi)}$$

Where

$$\phi = \theta + \beta, \quad b = {}^{c}/_{s}$$

If we evaluate that equation for maximum and minimum values of $\cos\phi$, we can get the maximum and minimum pressure of the cycle:

$$p_{max} = \frac{MR}{s(1 - b)} \qquad [Ec.\,22]$$

$$p_{min} = \frac{MR}{s(1+b)} \qquad [Ec.23]$$

The global mean pressure for the cycle is given by:

$$p_{mean} = \frac{1}{2\pi}\int_0^{2\pi} p d\phi = \frac{MR}{2\pi}\int_0^{2\pi} \frac{1}{s(1+b\cos\phi)} d\phi$$

And solving:

$$p_{mean} = \frac{MR}{s\sqrt{(1-b^2)}} \qquad [Ec.24]$$

This equation is one of the most convenient relations to relate the total mass of the working gas with average pressure operation.

The work done by the engine to the environment is due to variations in the volumes of work spaces V_c and V_e The total work done by the engine during a cycle is the algebraic sum of the work done by spaces expansion and compression.

Thus along a cycle:

$$W_c = \oint p dV_c = \int_0^{2\pi} p \frac{dV_c}{d\theta} d\theta$$

$$W_e = \oint p dV_e = \int_0^{2\pi} p \frac{dV_e}{d\theta} d\theta$$

$$W = W_c + W_e$$

We get the derivatives of the volumes from the **equations 19 and 20:**

$$\frac{dV_c}{d\theta} = -\frac{1}{2} V_{swc} \sin\theta$$

$$\frac{dV_e}{d\theta} = -\frac{1}{2} V_{swe} \sin(\theta+\alpha)$$

And replacing:

$$W_c = -\frac{V_{swc} MR}{2s}\int_0^{2\pi} \frac{\sin\theta}{1+b\cos(\beta+\theta)} d\theta$$

$$W_e = -\frac{V_{swe} MR}{2s}\int_0^{2\pi} \frac{\sin(\theta+\alpha)}{1+b\cos(\beta+\theta)} d\theta$$

Applying the analitic development of these equations, with Fourier series and appropiate integrals, we obtain the following expressions:

$$W_c = \pi V_{swc} p_{mean} \sin\beta \frac{\left(\sqrt{1-b^2}-1\right)}{b} \qquad [Ec.25]$$

$$W_e = \pi V_{swe} p_{mean} \sin(\beta-\alpha) \frac{\left(\sqrt{1-b^2}-1\right)}{b} \qquad [Ec.26]$$

These equations are essentially the same result that obtained Schmidt, and constitute the main analytical result of this analysis.

Now, as Schmidt's analysis is based on an ideal isothermal model, the thermal efficiency should be reduced to the Carnot efficiency. The thermal efficiency is defined as the ratio of work done by the engine and heat applied externally to the motor. It has already been shown that the externally supplied heat is equal to work performed by the expansion space, so that:

$$\eta = \frac{W}{W_e} = \frac{W_e + W_c}{W_e}$$

And applying in this expression the work expressions before founded:

$$\eta = 1 + \frac{V_{swc} \sin\beta}{V_{swe} \sin(\beta-\alpha)}]$$

Simplifying:

$$\eta = 1 - \frac{V_{swc}}{V_{swe}} \left(\frac{\tan\beta}{\sin\alpha - \tan\beta \cos\alpha} \right)$$

Using the value of β, we get the expression:

$$\eta = 1 - \frac{T_k}{T_h} \qquad [Ec.27]$$

Which, as we can see, is the Carnot efficiency.

2.3.5. IDEAL ADIABATIC ANALYSIS

In the previous section has been considered an ideal Stirling engine model, in which the compression and expansion spaces were kept at the respective temperatures of the cooler and heater. In an ideal isothermal model Stirling cycle, both the compression space and the expansion are maintained under isothermal conditions. Different studies show that neither heating nor cooling is performed exactly at constant volume or temperature. What leads to the paradoxical situation that neither the heater nor cooler contribute to the net heat transfer over the cycle, which can be considered that they are not necessary. All required heat transfer occurs through the border of the isothermal workspace. However, the practical requirements

for effective heat exchange conflict with the workspace designed to compress and expand the working gas. So, in the actual machines, working space more often tends to be adiabatic better than isothermal. This implies that the net transfer of heat to the cycle must be provided by heat exchangers.

Stirling cycle machines with non-isothermal working spaces were analyzed for the first time in 1960 by Finkelstein, and his analysis represents the most significant development of the century in terms of SCE. His model assumes finite heat transfers in the working space through the heat transfer coefficient.

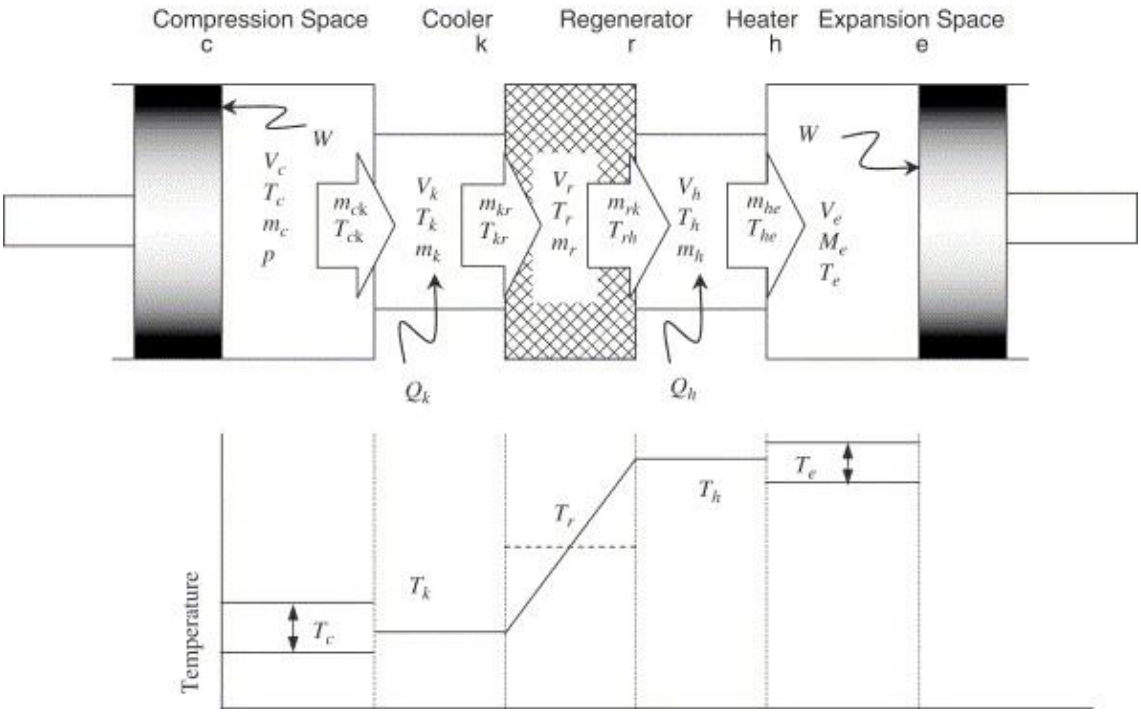

Image 28 - Ideal adiabatic model.

This theory, presented by Finkelstein, was heavily explored by Walker and Kahn in 1965, with special emphasis on the limiting case of adiabatic compression and expansion. They made a study of the effect of four important design parameters, such as:

- Temperature difference.
- Phase angle.
- Swept volume ratio.
- Dead volume ratio.

More recently, the adiabatic analysis was considered by Berchowitz.

To the development that regards to this thesis, we will take the adiabatic model developed by Urieli. The engine is modeled as having five components, as had been done before, considering regenerator and heat exchangers as perfect. Thus, the gas in the cooler and the heater is maintained under isothermal conditions at temperatures T_k and T_h respectively. Both the matrix of the regenerator and the gas inside it will have a linear distribution of temperature: gas flow through the interface between the regenerator and the cooler will be at the latter

temperature, T_k, while the flow located between the regenerator and the heater is at temperature of this, T_h.

Workspaces, both compression and expansion, are assumed adiabatic, therefore T_c and T_e temperatures will be above cycle according to the adiabatic nature of these processes. Parameters and workspaces are represented as in the previous development with suffixes *c, k, r, h, e,* and the parameters with double subscript, *ck, kr, rh, he*, represent the four interfaces between the above spaces. Enthalpy is transported through the interface in terms of a mass flow, *m'*. The arrows in the diagram represent the positive direction of flow, arbitrarily determined from the compression space to the expansion one.

Notably, the temperature distribution diagram in the compression and expansion space is not constant, but varies throughout the cycle according to the adiabatic compression and expansion occurring in the workspaces. Thus, the enthalpies that flow through the interfaces *ck* and *he* transport the same temperature of the previous cell from which they came, whereupon T_{ck} and T_{he} temperatures are influenced by the direction of flow, and can be defined algebraically as:

$$if\ m'_{ck} > 0 \rightarrow T_{ck} = T_c \quad else \rightarrow T_{ck} = T_k$$
$$if\ m'_{he} > 0 \rightarrow T_{he} = T_h \quad else \rightarrow T_{he} = T_e$$

In the ideal model there are no fluid leaks, the total gas mass M is kept constant within the system and there is no pressure loss; therefore p has no subscript, and represents the instantaneous pressure in the system.

The work W is done by volume variations in workspaces, V_c and V_e, and Q_k and Q_h are the heats transferred from the outside to the working gas in the cells of the cooler and heater respectively. The regenerator is adiabatic outward, and Q_r heat is transferred internally from the matrix of the regenerator to the gas through the dead volume occupied by the fluid, V_r.

2.3.6. ANALYTICAL DEPELOPMENT OF THE ADIABATIC ANALYSIS

More general approximation made to define an appropriate mathematical model starts applying the energy and state equations to each of the cells defined. The resulting equations are joined by applying the equation of continuity along the entire system. We will consider, at first, the equation of energy applied to a cell which can generally be reduced to either a cell of workspace or a cell of heat exchanger. Enthalpy is introduced into the cell by a mass flow m_i' at the temperature T_i, and removed from it through the mass flow m_o' at temperature T_o.
We will write the energy equation for the working fluid inside the cell generalized as:

$$\begin{bmatrix} Heat\ rate \\ transferred \\ to\ the\ cell \end{bmatrix} + \begin{bmatrix} Enthalpy \\ net\ conversion \\ inside\ the\ cell \end{bmatrix} = \begin{bmatrix} Work\ rate \\ performed \\ over\ the\ environment \end{bmatrix} + \begin{bmatrix} Increase\ of \\ internal\ energy \\ inside\ the\ cell \end{bmatrix}$$

Mathematically, we can express it like:

$$\frac{dQ}{d\theta} + \left(C_p T_i m_i' - C_p T_o m_o'\right) = \frac{dW_d}{d\theta} + C_v \frac{d(mT)}{d\theta} \qquad [Ec.17]$$

$$C_p, C_v: specific\ heat\ of\ the\ gas\ a\ constant\ pressure\ and\ volume, respectively.$$

This expression is the classic form of the equation of energy for discontinuous flow, dismissing terms of kinetic and potential energies.

We consider working gas as an ideal gas; this is a reasonable approximation for Stirling engines, because the processes to which the gas undergoes are far from the critical point of the gas.

$$Ideal\ gas\ equation: pV = mRT \qquad [Ec.10]$$

$$R = C_p - C_v$$

We also can see

$$C_p = \frac{\gamma R}{\gamma - 1}; \quad C_v = \frac{R}{\gamma - 1}; \quad where\ \gamma = {C_p}/{C_v} \qquad [Ec.28]$$

Taking logarithms in both terms of the equation and taking derivatives, we obtain the differential equation for ideal gases:

$$\frac{dp}{pd\theta} + \frac{dV}{Vd\theta} = \frac{dm}{md\theta} + \frac{dT}{Td\theta}$$

Total mass of working fluid keeps constant: $M = m_c + m_k + m_r + m_h + m_e$
Deriving this equation:

$$\frac{dm_c}{d\theta} + \frac{dm_k}{d\theta} + \frac{dm_r}{d\theta} + \frac{dm_h}{d\theta} + \frac{dm_e}{d\theta} = 0$$

We have the pressure of the cycle, which was obtained from the ideal gas equation:

$$p = M \cdot R \cdot \left(\frac{V_c}{T_k} + \frac{V_k}{T_k} + \frac{V_r \ln\left({T_h}/{T_k}\right)}{(T_h - T_k)} + \frac{V_h}{T_h} + \frac{V_e}{T_h} \right)^{-1} \qquad [Ec.15]$$

If we considerate the areas of heat exchanging, where as supposed, volumes and temperatures are constant, we can express their state equation as:

$$\frac{dp}{pd\theta} = \frac{dm}{md\theta}$$

And applying this equation for the exchanging spaces and replacing in the mass conservation equation:

$$\frac{dm_c}{d\theta}+\frac{dm_e}{d\theta}+\frac{dP}{d\theta}\left(\frac{m_k}{p}+\frac{m_r}{p}+\frac{m_h}{p}\right)=0$$

If apply this expression to the ideal gas equation:

$$\frac{dm_c}{d\theta}+\frac{dm_e}{d\theta}+\frac{dp}{d\theta}\cdot\frac{1}{R}\left(\frac{V_k}{T_k}+\frac{V_r}{T_r}+\frac{V_h}{T_h}\right)=0$$

Following, we will try to eliminate terms $\frac{dm_c}{d\theta}$ and $\frac{dm_e}{d\theta}$, because we want to get an explicit equation in $\frac{dp}{d\theta}$. Keeping in mind that in both compression and expansion spaces $\frac{dQ_c}{d\theta}=\frac{dQ_e}{d\theta}=0$. Applying the energy equation:

$$\frac{dQ_c}{d\theta}-\left(C_pT_{ck}m_{ck}{}'\right)=\frac{dW_c}{d\theta}+C_v\frac{d(m_cT_c)}{d\theta}\ \rightarrow\ -\left(C_pT_{ck}m_{ck}{}'\right)=\frac{dW_c}{d\theta}+C_v\frac{d(m_cT_c)}{d\theta}$$

$$\frac{dQ_e}{d\theta}+\left(C_pT_{he}m_{he}{}'\right)=\frac{dW_e}{d\theta}+C_v\frac{d(m_eT_e)}{d\theta}\ \rightarrow\ \left(C_pT_{he}m_{he}{}'\right)=\frac{dW_e}{d\theta}+C_v\frac{d(m_eT_e)}{d\theta}$$

We will take into account the following considerations:

Performed work can be written like: $\frac{dW}{d\theta}=p\frac{dV}{d\theta}$

Because of continuity considerations: ratio of accumulation of gas = input/output gas flow, ergo:

$$\frac{dm_c}{d\theta}=-m'_{ck}$$

$$\frac{dm_e}{d\theta}=m'_{he}$$

In this case, the previous equation will be reduced like:

$$C_pT_{ck}m_{ck}=p\frac{dV_c}{d\theta}+C_v\frac{d(m_cT_c)}{d\theta}$$

$$C_pT_{he}m_{he}=p\frac{dV_e}{d\theta}+C_v\frac{d(m_eT_e)}{d\theta}$$

Replacing the ideal gas state equation:

$$\frac{dm_c}{d\theta}=\left(p\cdot\frac{dV_c}{d\theta}+\frac{V_c}{\gamma}\cdot\frac{dp}{d\theta}\right)\cdot\frac{1}{RT_{ck}}\qquad[Ec.29]$$

$$\frac{dm_e}{d\theta}=\left(p\cdot\frac{dV_e}{d\theta}+\frac{V_e}{\gamma}\cdot\frac{dp}{d\theta}\right)\cdot\frac{1}{RT_{he}}\qquad[Ec.30]$$

Applying both expressions in the differential expression for the mass conservation in the system:

$$\frac{dp}{d\theta} = \frac{-p \cdot \gamma \cdot \left(\frac{1}{T_{ck}} \cdot \frac{dV_c}{d\theta} + \frac{1}{T_{he}} \cdot \frac{dV_e}{d\theta}\right)}{\frac{V_c}{T_{ck}} + \frac{V_e}{T_{he}} + \gamma \cdot \left(\frac{V_k}{T_k} + \frac{V_r}{T_r} + \frac{V_h}{T_h}\right)} \qquad [Ec.31]$$

Equations 29 and 31 are two simultaneous differential equations for the variables p and m_c (same with 30 and 31 to m_e) Once p and m_c are evaluated, the other variables must be obtained through the state equations and mass balances. Volume variables $\frac{dV_c}{d\theta}, \frac{dV_e}{d\theta}, V_c, V_e$, are possible to know analytically and all other parameters of the equations 29, 30 and 31 are constant except T_{ck} and T_{he}. These interface temperatures are conditioned by the mass flow direction; in order to evaluate the mass flow (and thus the direction) we consider the continuity equation given by:

$$\frac{dm}{d\theta} = m'_i - m'_o$$

The only thing that says this expression is that the rate of accumulation of mass in a cell is equal to the net flow of mass in the same cell. And applying this expression to all cells in image 28:

$$m'_{ck} = -\frac{dm_c}{d\theta}, \qquad m'_{kr} = m'_{ck} - \frac{dm_k}{d\theta}, \qquad m'_{rh} = m'_{kr} - \frac{dm_r}{d\theta}$$
$$m'_{he} = m'_{rh} - \frac{dm_h}{d\theta}, \qquad m'_{he} = \frac{dm_e}{d\theta} \qquad [Ec.32]$$

Total work performed by the motor will be the algebraic sum of work performed by both expansion and compression spaces:

$$\frac{dW}{d\theta} = p \cdot \frac{dV_c}{d\theta} + p \cdot \frac{dV_e}{d\theta} \qquad [Ec.33]$$

Considering the expression of the energy equation and replacing the previous values of dW/dθ and mT, we can get a more convenient simplification for the energy equation:

$$\frac{dQ}{d\theta} + \left(C_p T_i m'_i - C_p T_o m'_o\right) = \left(C_p \cdot p \frac{dV}{d\theta} + C_v \cdot V \frac{dp}{d\theta}\right) \cdot \frac{1}{R} \qquad [Ec.71]$$

As we have said, volumes in heat exchangers are constant, so no work is performed in these spaces. Therefore, applying this equation to each exchanger:

$$Cooler: \frac{dQ_k}{d\theta} = \left(\frac{C_v V_k}{R} \cdot \frac{dp}{d\theta}\right) - C_p(T_{ck} m'_{ck} - T_{kr} m'_{kr}) \qquad [Ec.34]$$

$$Regenerator: \frac{dQ_r}{d\theta} = \left(\frac{C_v V_r}{R} \cdot \frac{dp}{d\theta}\right) - C_p(T_{kr} m'_{kr} - T_{rh} m'_{rh}) \qquad [Ec.35]$$

$$Heater: \frac{dQ_h}{d\theta} = \left(\frac{C_v V_h}{R} \cdot \frac{dp}{d\theta}\right) - C_p(T_{rh} m'_{rh} - T_{he} m'_{he}) \qquad [Ec.36]$$

Other equation that will be important in the adiabatic study can be extracted from the differential state equation, getting:

$$\frac{dT_c}{d\theta} = T_c\left(\frac{dp}{d\theta}\cdot\frac{1}{p} + \frac{dV_c}{d\theta}\cdot\frac{1}{V_c} - \frac{dm_c}{d\theta}\cdot\frac{1}{m_c}\right) \qquad [Ec.37]$$

$$\frac{dT_e}{d\theta} = T_e\left(\frac{dp}{d\theta}\cdot\frac{1}{p} + \frac{dV_e}{d\theta}\cdot\frac{1}{V_e} - \frac{dm_e}{d\theta}\cdot\frac{1}{m_e}\right) \qquad [Ec.38]$$

Note that since the exchangers have been considered as isothermal and the regenerator as ideal, we have by definition that $T_{kr} = T_k$, $T_{rh} = T_h$. Mahrkov used a computational method based on a fluid-dynamic approach to investigate the work process of the model of engine developed by Urleli. This method helps to have a close understanding of engine analysis. A computer program to simulate an engine system was carried out by Organ; Rallis also compared the ideal cycle regenerative with processes both isothermal and adiabatic in compression and expansion. The analysis shows that the thermal efficiency is a function of the regeneration efficiency and the volume ratio.

Finally, the work done in the compression and expansion cells is given by:

$$W = W_e + W_c$$

$$\frac{dW}{d\theta} = \frac{dW_e}{d\theta} + \frac{dW_c}{d\theta}$$

$$\frac{dW_e}{d\theta} = p\frac{dV_e}{d\theta} \qquad [Ec.39]$$

$$\frac{dW_c}{d\theta} = p\frac{dV_c}{d\theta} \qquad [Ec.40]$$

3. REAL STIRLING CYCLE ENGINE

3.1. INTRODUCTION

The ideal Stirling engine thermodynamics has been discussed in the previous block, but the practical reality, as internal heat exchanges, heat transfer in the cylinder walls and general situations were not taken into account. The effects of various practical factors which cause real engine deviates from the ideal case should be considered to be treated separately so we can highlight its influence. The basic cycle of four processes will be used as reference data to illustrate the effects of the practical factors. The working gas temperature along the engine will tend to be more influenced by adiabatic way than isotherm, which will influence the shape of the PV diagram. In fact the cylinder walls are not able to provide the heat transfer medium sufficient to ensure that the temperature of the gas in the cylinder is kept constant and even the use of tubular heat exchangers does not ensure isothermal conditions prevailing in the area inlet and outlet of the regenerator. Deviation from isothermal conditions is more pronounced on the hot side of the engine than on the cold side as can be seen illustrated in Fig.

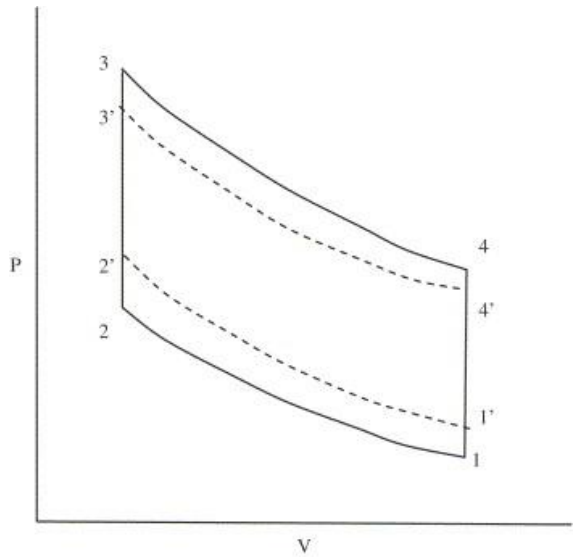

Image 29 – p-V diagram of a real Stirling engine.

Where the ideal cycle is reduced from 1-2-3-4 to 1'-2'-3'-4 'because of the effects on the heat transfer in the heater and cooler.

Kaushik and Kumar conducted an evaluation of the irreversible thermodynamic cycles Ericsson and Stirling, analysis for heat losses in the sump with the engine power output, based on an ideal gas and perfect regeneration. Shoureshi tried to optimize the cooler, regenerator and heater, based on the Mach number, the relationship of operating temperature and the percentage of heat exchanger in the dead volume.

3.2. HEAT TRANSFER IN STIRLING ENGINE

Stirling engine operation is caused by different heat exchanges.

Costea and Feidt observed that the heat transfer coefficient varies linearly with the local difference of temperatures of the engine hot components. The regenerator must be capable of working with a load of 4-5 times the heat load of the heater, and if it is not capable of it, an extra load will be imposed on the other exchangers. The regenerator must be as close as possible to perfect if we want to achieve good engine efficiency values, and this means that the gas must be supplied from the regenerator to the cold side of the engine with the lower temperature and to the hot zone with the highest temperature . If this temperature does not prevail, the temperature and therefore the pressure of the cold gas will be too high while the pressure and temperature of the hot gas will be too low.

Because of the inefficiencies of the regenerator the gas will enter the compression phase of the cycle in state 1' instead of 1 and in the expansion phase in the state 3' instead of 3. Chen and others developed a combined model to analyze the performance of the engine with heat losses and imperfect regeneration. The optimum operating temperature for the engine operating at maximum power is found as a result of the imperfection of the regenerator.

3.2.1. HEAT EXCHANGERS IN THE STIRLING ENGINE

The heat exchangers are crucial components in a Stirling engine. There should be about three or four exchangers in SCE system. They are engine parts, that despite having to perform functions as mechanical support and driving the fluid pressure, their primary function is thermal, and is to transmit heat from one medium to another.
We can see them illustrated in image 30, which includes the heater, cooler, regenerator and pre-heater (which may be optional).

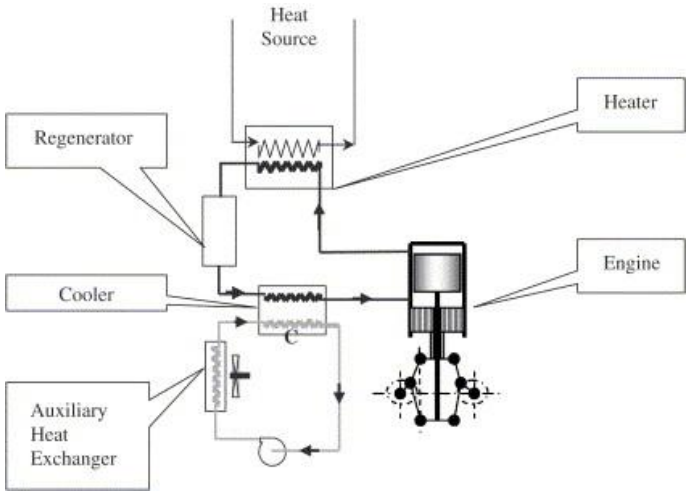

Image 30 - Heat exchangers in a SCE.

- Heater: transfers heat from an external source to the working fluid of the engine. Is the output of the expansion chamber.
- Cooler: exactly the opposite, it absorbs heat from the working fluid and rejects it to the atmosphere through the condenser. Is the output of the compression chamber.
- Regenerator: acts as a thermal sponge, alternately accepting heat from the working fluid and ceding it.
- Preheater: in engines heated by combustion, it heats with air with combustion fumes. In the case of our engine, it does not have a preheater.

Sankey representation of heat flow was first introduced in 1971 by Zacharias and more intensive work was carried out by Pertescu, which showed how the heat exchanger configuration is strongly affected by the amount of losses in the pumps.
The above enumeration defines the heat exchangers often provided in a Stirling engine. Top three: heater, cooler and regenerator act on the working fluid and their presence is required. Some small machines seem not to have these items, but they have them, but are reduced to a minimum.

The last one, the preheater, acts on the fluid that transfers heat to the outside of the heater, and therefore, it is not strictly necessary for engine operation. The reason for their use is to improve the overall performance of the machine.
The design of the heat exchangers must meet three basic points:

- Provide the minimum possible dead volume. If this volume increases, the thermodynamic cycle is shifted to the right in the PV diagram, and the area reduced, providing less power.
- Make the most of the dead space used, making heat exchange per unit volume as large as possible.
- Avoid excessive friction during the passage of the working fluid.

Before coming back to the study of the exchangers one by one, it is necessary to understand the internal dynamics of Stirling regarding energy flows and working fluid. As will be seen, their actual behavior deviates from the cycles used to explain its operation.
The search for energy efficient requires maximum and minimum temperatures between working the engine to be as distant as possible. As generally, T_{min} is the room temperature, so T_{max} must be as high as possible, but has a limit given by the resistance of materials, typically metals, which are good thermal conductors.

ENERGY FLOW

While in an alternating internal combustion engine the energy flow tends to be distributed so that one third of the combustion energy becomes useful work, one third is lost through leakage and the last third is discharged by the cooling system, a combustion Stirling engine has different distribution. Also a third (32%) of the energy is converted into work, but the escape only takes 14% and cooling, however, 46%. So it has 8% of losses.
Therefore, for equal power, Stirling engines require a better cooling capacity than the internal combustion engine. This disadvantage is compensated by the fact that, if the engine is

equipped with preheater, the exhaust gases come out at a lower temperature, since it has taken part of the heat energy that they have when leaving the motor.

The following figure shows the energy flow diagram for a carefully designed Stirling engine (high performance), heated by combustion and with preheater. From this diagram it should be noted the high heat flow through the regenerator, which is more than three times the one provided by the fuel, which determines the dependence of the correction viability of the regeneration process.

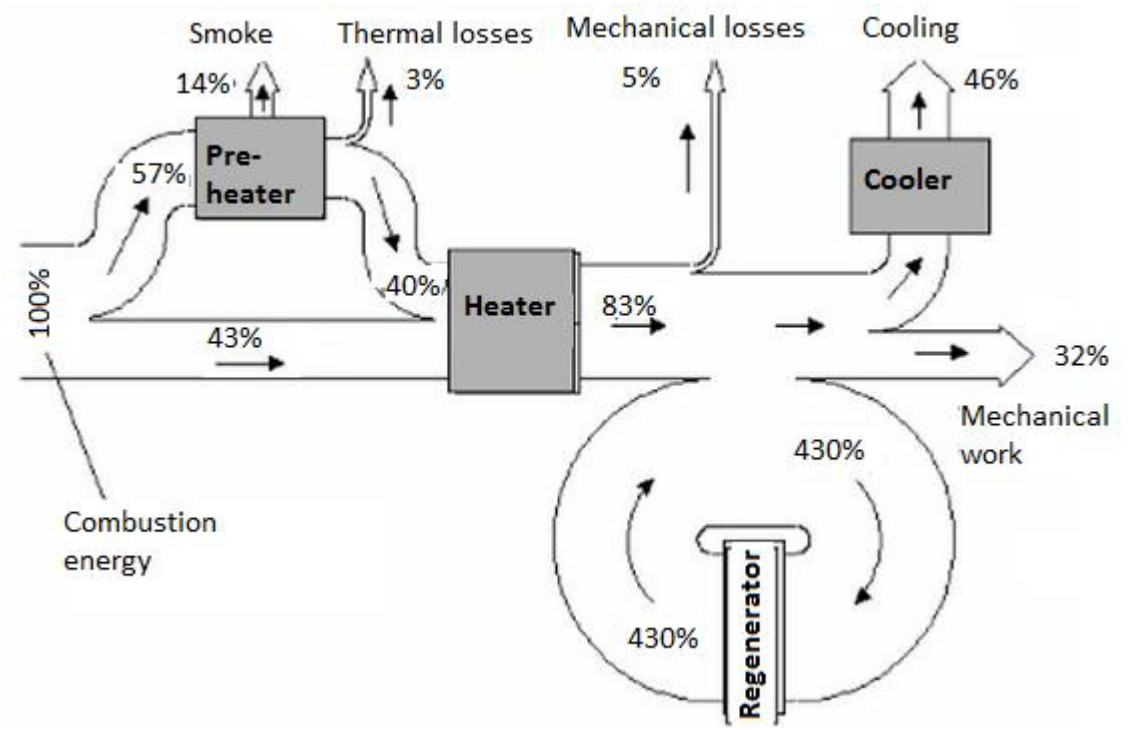

Image 31 - Energy flow for a high performance Stirling engine, with preheater and warmed up with combustion (regenerator flow is not well scaled).

MASS FLOW

The working fluid is moved through the interior of the engine thanks to the pistons. If these would move very slowly, following a continuous motion law in sequence, the ideal cycle predicted by Rallis would be the reality, and the design of the heating elements of the motor would be relatively simple. But the reality is this: the practical needs require high speeds and movements approximately sinusoidal. The impact that this represents on the mass flow are the following:

- Most of the working fluid particles do not complete the course of the cycle. In fact, when the speeds are very high, no particle complete this journey.
- There is net flow through the set regenerator-cooler-heater in less than half of the time of the cycle. The rest of the time the flow is entering or exiting from both ends at once.

- Because of the inertia and friction of the fluid, the net flow through the regenerator is much less than the flow into or out of the expansion and compression chambers.
- The flow inside the heat exchanger is highly variable, both in pressure, density, temperature and speed. This fact complicates the design of these elements.

3.2.1.1. HEATER

The mission of the heater in a Stirling engine is to transmit heat from a hot outside environment to the working fluid, and also to lead this fluid in its path inside the device. It is always positioned at the exit of the expansion chamber, although often it is part of the heater chamber. The heat transfer process involved in the heating are three, and each one make conditional to the design of this element:

- Heat transfer by convection and radiation: from a heater environment to the walls of the heater tube or flaps. This is critical in the design process of heaters.
- Heat transfer by conduction, from the tube outer surface to the inner surface. For a good conduction, heater usually is metallic, specifically a temperature-resistant steel (containing a high amount of nickel). Sometimes ceramic grafts are also used especially in hot points. The wall thickness must meet a balance between good thermal conductivity and resistance to fatigue at high temperature (because the inner pressure swings).
- Heat transfer by convection, in this case from the cylinder inner wall to the working fluid. This fluid is compressed and moves at high speed, which facilitates heat transfer. Therefore a small temperature difference will be sufficient. This transfer process is not usually problematic.

Heat transferred in this case will be:

$$Q_h = h_h A_h \Delta T_h \qquad [Ec.41]$$
$$A_h = n_h \pi d_h l_h$$

$$h_h: convection\ coefficient\ of\ material\ of\ heater\ cylinder$$
$$n_h: number\ of\ pipes\ in\ heater$$
$$d_h: \emptyset\ of\ each\ pipe$$
$$l_h: length\ of\ pipe$$

In the relatively simple case of continuous turbulent flow, analytical techniques are not suitable. In this case the heat transfer coefficient should be determined using the well known method of Reynolds similarity in their original form or modified. This similarity relates the heat transfer with fluid friction using the standard dimensionless parameters, the Prandtl number (Pr), which is typical of the working fluid, and the Reynolds number (Re) of the flow itself.
The Nusselt number relates heat transfer coefficient (h), the length of the heater tube and the thermal conductivity of fluid:

$$Nu = \frac{h \cdot l}{k}, \quad and\ for\ a\ cylinder\ of\ diameter\ D: Nu = \frac{h \cdot D}{k} \qquad [Ec.42]$$

Correlations between Nusselt, Reynolds and Prandtl are: $Nu = f(Pr, Re)$.
The heater is difficult to design, due to the requirements of the inner tube and the outside. The design also depends on the selected heat source.

- The outer tube surface typically must withstand an environment of high temperature, low pressure and continuous flow.
- The inner surface of the pipe shall withstand an environment with high temperature, high pressure and flow very discontinuous.
- The heat transfer coefficients are significantly different between the inside and the outside; therefore, the surface area requirements cannot be compared with each other.

In addition we find two strong restrictions:

- The ratio of diameters between the interior and the exterior is determined by both temperature and pressure load.
- The optimal ratio between the diameters may not be in harmony with the needs of area.

All these factors may also be unbalanced with the resistance to fluid friction and dead space requirements required as well, two other properties which should be taken into account when designing a heater.

The two main parameters which are important for the internal surfaces of the heater are the coefficient of heat transfer and the friction factor. With the knowledge of these two factors, heater performance can be calculated and the optimal size of a proposed design can be formulated by taking the necessary thermodynamic specifications. The ratio of heat transfer which is capable of supporting the heater through the inner walls of the cylinder to the working fluid film coefficient depends on the inner tube to heat transfer, mass flow and gas specific heat.

Depending on the location of the heater, we can distinguish three cases:

- The heater is the same expansion cylinder
- The heater comprises the expansion cylinder and an auxiliary heater.
- The heater is only an auxiliary heater.

The first option is only present in small engines for demonstration, in which performance is not important; the cylinder offers little surface contact with the gas, which makes it very difficult to transfer heat. This option is the one in our engine in the laboratory. The second option is the most used; in this case the auxiliary heat exchange takes majority of heat, while the cylinder, too hot, completes the transmission. It is the solution that provides better thermal performance. Finally, the third case is used when you want to reduce the cost of the steel used in the cylinder; the auxiliary heater makes the whole exchange while maintaining the cylinder water cooled. Its thermal performance is not as good.

We can find flips or tubular heaters; in the case of our engine, we have a tubular heater, as shown in the picture:

Image 32 - Tubular heater of the Stirling engine of this thesis.

3.2.1.2. COOLER

The refrigerator of a Stirling engine has to evacuate heat from the working fluid to a colder outside environment, while driving the fluid in its path inside the device.
It is formed by the compression chamber itself and often also by a heat exchanger at the outside.

In principle, the SCE can be cooled by air or water like ICE. To reduce the temperature of the working fluid of the engine, the cooling system will need to handle a cooling load almost double than the cooling load of a conventional internal combustion engine. As the coolant temperature increases there is a substantial drop in thermal efficiency so that it will be desirable to have the coolant temperature to a minimum.

Despite being an element of low cost and relatively simple design, the refrigerator is as important as the Stirling engine heater, especially if you consider to evacuate nearly 50% of the energy that the engine receives, and to achieve the lowest possible temperature, since as mentioned, at lower temperature, better thermal performance is obtained, and less will deteriorate rubbers and joints of the motor.

The flow conditions are similar to those of the heater but with a lower temperature. Convection of working fluid with the metal wall is an easy process due to the characteristics of speed and density of this fluid. Conduction inside the metal also has no problem, since the low

temperature allows the wall thicknesses to be less than the heater, to withstand the same pressure.

Finally, the convection to the outside environment, if the cooling fluid is water, also has a very good heat transfer. The air cooling requires more heat jump.

While the temperature of the external environment is usually atmospheric, the working fluid goes outside the cooler 50 °C hotter, what is a very small temperature increase for the amount of heat transmitted, due to the fact of the ease of transmission.

The compression cylinder and auxiliary refrigerator, attached to it, form the set of the refrigerator and its shape depends on the type of cooling done:

a) Water cooling: if we have an inexhaustible source of water at room temperature (river, lake, public, ...), we just need to pump it inside the refrigerator, and this is the most efficient solution, but only usable in stationary engines. In the case of the laboratory engine, object of this thesis, cooling is by water.
b) Air cooling: in most cases continuous water cooling is not possible, either because the motor is not stationary, or because of the absence of a viable source.

Cooler outer tubes experience the same flow conditions as in a conventional engine.
The following expressions are satisfactory for the analysis of the cooler, where h_t is the total heat transfer coefficient and h_w is the heat transfer coefficient of the water film.

$$h_t = \frac{h_w}{(1 + 0{,}882 h_w)} \qquad [Ec. 43]$$

$$h_w = 0{,}35 Re^{0{,}55} Pr^{0{,}33} k_w d_o \qquad [Ec. 44]$$

$$d_o: external\ diameter\ of\ water\ pipes$$

3.2.1.3. REGENERATOR

Part of the heat applied by the external source to the working fluid is converted into useful work, and while the expanded gases leave the expansion space to the refrigerator, the remaining heat is stored in the regenerator. After cooling and compression in the compression zone the gases pass back to the expansion zone through the regenerator. The stored heat is returned to the working fluid as it flows back into the expansion space. This process is what we will call as regeneration. Stirling engine efficiency depends on the efficiency of the regenerator.

The ideal regeneration occurs when the flow into and out of the matrix of the regenerator makes it at two constant temperatures: T_e in the end of the expansion zone of the regenerator and T_c in the compression one. This is possible only if the operation is performed infinitely

slowly or the heat transfer coefficient or heat exchange area is infinite. This is also possible if the heat transfer capacity of the matrix is infinite.

Regenerator fundamental requirements are defined by the thermodynamic process of the ideal cycle. For maximum efficiency the heat extracted during the isochoric process 4-1 must be returned to the gas in the also isochoric process 2-3. Ideally, the heat transfer is carried out reversibly inside the regenerator. A linear temperature gradient from T_{max} to T_{min} is maintained throughout the regenerator.

The working fluid enters the regenerator on the thermodynamic state 4 and begins transferring its heat to the material of the regenerator and leaves the regenerator in state 1. During this process, the temperature of each element of the refrigerator is high. After compressing, the working fluid enters the regenerator in state 2 (minimum temperature of the cycle) and the flow returns through the regenerator receiving the heat stored in it and increasing the temperature from T_2 to T_3.

Regenerator in a real engine operates away from these assumed conditions for the ideal case. The temperature of the working fluid entering the regenerator is not constant because the pressure, density and flow velocity vary over a wide range. The effectiveness of the regeneration process also depends largely on the thermal capacity of the material used to manufacture the regenerator.

3.2.2. ANALYSIS OF THE REGENERATOR

We can find various kinds of materials that can be used in the matrix of the regenerator, as for example: steel wool, steel filters, wire mesh, metal balls, metal flakes, steel cotton, parallel fins…

To improve the heat transfer coefficient and setting the minimum temperature difference between the matrix and the fluid is necessary to expose the maximum possible area of the matrix, so the matrix should be finely divided.
Here we can see the features desirable for the matrix of the regenerator:

- Maximum heat capacity: big and solid matrix.
- Minimum flow losses: small and highly porous matrix.
- Minimum dead space: small dense matrix.
- Maximum heat transfer: large and finely divided matrix.
- Low pollution: unobstructed matrix.

Therefore, the design of the regenerator is a problem of optimizing its volume in order to get the best values for the previous parameter.

3.2.2.1. HEAT TRANSFER AND FLUID FRICTION IN THE REGENERATION

To simplify the analysis of the regenerator we will make the following assumptions:

- The thermal conductivity of the matrix material is constant.
- Specific heats of the fluid and the matrix do not change with temperature.
- The fluid flow and temperature are constant in the flow section.
- Heat transfer coefficients and the flow velocities are constant in time and space.
- The ratio of the mass flow is constant.
- The pressure drop along the length of the regenerator is negligible.
- Gas flow in the duct is one-dimensional.
- The working gas is considered ideal gas.

The heat transfer process is carried out reversibly. The temperature differential between the working fluid and the regenerator must be infinitesimal. And to meet these requirements above, certain conditions must be achieved.

That the process is reversible can only be ensured if the process is in thermodynamic equilibrium, i.e. regeneration system passes through a series of equilibrium states.
But really, this cannot be achieved in practice, so all efforts should be made to satisfy the other conditions, which can be easily identified by the fundamental equation for the dynamic behavior of the regenerator.

Thus, the heat transfer to / from the working fluid from / to the matrix in the flow passage through the regenerator is given by:

$$h_{bulk} \cdot A \cdot (T_M - T_F) = m_f \cdot C_{PF} \cdot L_R \cdot \frac{dT_f}{dx} + M_{FR} \cdot C_P \cdot \frac{dT_f}{dt} \qquad [Ec. 45]$$

Left part of the equation refers to the calorific energy available in the working fluid. To transfer the maximum calorific energy from the working fluid to the regenerator, the difference of temperatures of the fluid in the matrix ($T_M - T_F$) must be infinitesimal. Therefore, the heat transfer coefficient of the matrix, h_{bulk}, must be infinite to compensate the small difference of temperatures. Once again, this condition is impossible to get in reality.

The only parameter we have is the heat transfer area, A, and it will have to be infinite to be close to the ideal conditions. Therefore, we need to have as maximum area as possible.
The following equation (Nusselt-Hausen) describes the storage capacity of the regenerator:

$$h_{bulk} \cdot A \cdot (T_M - T_F) = M_M \cdot C_{PM} \cdot \frac{dT_M}{dt}$$

Calorific capacity of the regenerator, C_R, is expressed by $M_M \cdot C_{PM}$.

If we combine these two equations, we can find out that the temperature of the matrix of the regenerator can be expressed like:

$$\Delta T_M \approx \frac{m_f \cdot C_{PF} \cdot \Delta T_F}{C_R} \qquad [Ec. 46]$$

A good approximation to get the efficiency of the regenerator is:

$$\varepsilon_R = \frac{Real\ heat\ transferred}{Available\ heat\ for\ transference} = \frac{T_2 - T_1}{T_3 - T_1} \qquad [Ec. 47]$$

3.3. ENGINE CONFIGURATION

The mechanical solutions of Stirling engines are diverse and accomplish one genera schema. The elements of a Stirling engine include 2 volumes at different temperature, connected through a regenerator, and auxiliary heat exchangers. To satisfy the thermodynamic, dynamic (of the gas) and heat transfer requirements, these volumes must change periodically thanks to the alternating movement of two pistons. In the following figure we can see a possible configuration of the engine with the basic elements:

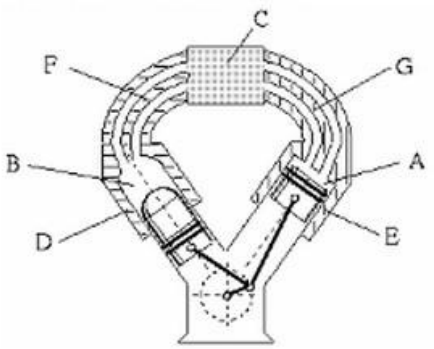

Image 33 - engine configuration. A) Compression chamber. B) Expansion chamber. C) Regenerator. D) Expansion space. E) Compression space. F) Heater. E) Cooler.

The main function of the conducting mechanism will be to reproduce these volumetric changes as exactly as possible. The elements of the mechanism can be combined to satisfy the previous requirements in a wide range of mechanical adaptations. The conducting mechanism must be considerate at the time of selecting the engine configuration, because no every mechanism is compatible with every SCE configurations.

In mechanic engineering there is a parameter, called Beale number, which characterizes the efficiency of Stirling engines. It is usually used to estimate the output power of the design of the Stirling engine. For example, for engines working with a high temperature difference, a typical range for Beale number use to be 0,11-0,15 (higher number means higher efficiency).
There are basic parameters of the motor that also are important to understand the Beale number. These parameters are engine speed, pressure and displacement.

Gary Wood listed the following parameters, which are necessary to get an appropriate configuration of the engine, i.e., the optimum geometry of the engine will be based in the following parameters:

- Cylinder design
- Mechanism of the engine
- Heater type
- Construction of displacer and piston
- Type and size of regenerator
- Construction of the crankshaft “room”

3.3.1. TYPES OF ENGINES

The cylinder is the materialization of the variable volume chamber. One side is open to the heat exchangers and the another is closed by the piston, whose movement determines the volume variations. We find two different pistons:

- Working piston: this piston has to resist a high difference of pressure between its both sides, but doesn't have to resist any thermal jump between the working fluid and the environment. Thermal conduction losses are not a problem, because they are minimal.
- Displacer: it works with similar pressures in both sides, but it must afford a high thermal gradient. Its resistance is not critical, but it is the thermal isolation.

Depending on the distribution of cylinders, pistons and displacers, Stirling engines can be classified as followed.

3.3.2. STIRLING ENGINE ARCHITECTURE

Stirling engines may generally be classified into two categories, single or double acting. The terms single or double in SCE technology is used to describe the mode of operation of a particular engine.

3.3.2.1. SINGLE ACTING PISTONS

The first engine of this type was the one invented by R. Stirling in 1816. There are three categories within architectures of pistons of simple action:

- Double piston.
- Piston-displacer.
- Liquid Piston.

DOUBLE PISTON

Double piston architecture, also called ALPHA, is characterized by a plunger which is a piston and the other one is a piston / displacer that move in two different cylinders. These two cylinders are connected in series by the heater, regenerator and cooler. Configuration is more intuitive, but it is applied only in large motors, in which the weight is not an important factor. The arrangement is conceptually the simplest, but suffers the disadvantage that both pistons need to be sealed to contain the working gas.

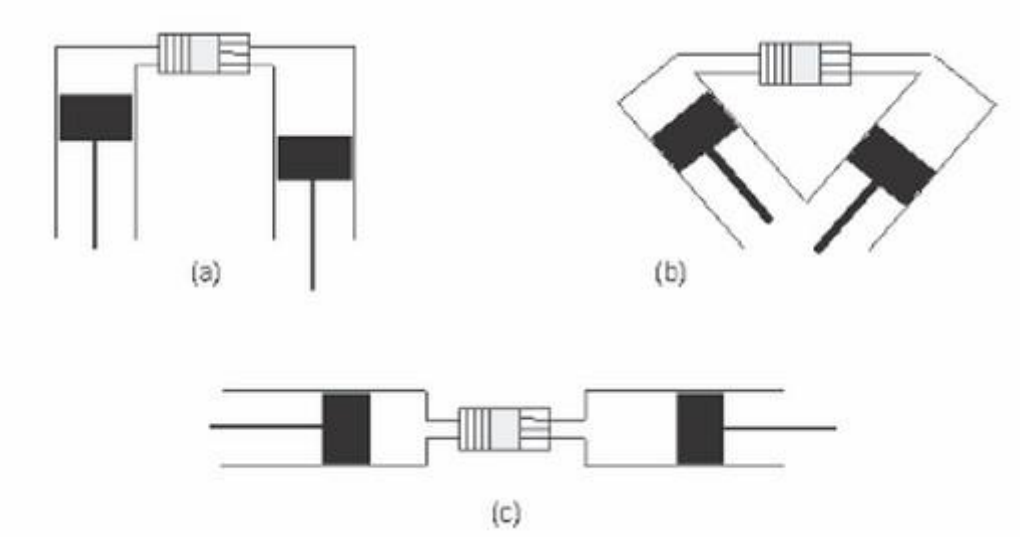

Image 34 - Simple acting and double piston (Alpha) Stirling engines. A) Parallel cylinders (Ryder). B) Cylinders in V. C) Opposite cylinders.

PISTON DISPLACER

In the configuration of piston-displacer, one of the pistons is a piston and the other is a displacer. With this configuration, fluid pressure is supported only by a piston, which works well at low temperature, which greatly reduces the problem of leakage. Being also the displacer lighter than a piston, it is lower the oscillating mass and vibration, thus reducing the dimensions of bearings, connecting rods,...

This is the most used configuration in low power engines, but also in higher. In this configuration, we can find 2 alternatives:

- Single cylinder: configuration BETA.
- Double cylinder: configuration GAMMA. The engine in our laboratory is a Gamma engine.

The single cylinder configuration (BETA) reduces dead space to a minimum and gives the engine maximum compactness. It is the original Stirling engine. It consists of a cylinder with a hot and a cold zone. In the engine construction can be seen as both the displacer and the piston are accommodated in the same cylinder. In this model the compression space is swept between the bottom of the displacer and the top of the power piston. The displacer and piston may or may not physically touching, but they are connected to the crank by separate links to maintain the required phase angle.

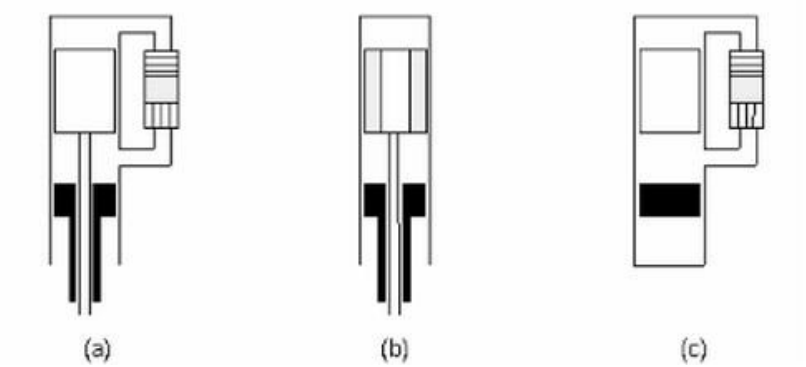

Image 35 - Beta Stirling engines. A) External regenerator (Rankine-Napier). B) Regenerative displacer (Stirling). C) Free pistons (Beale).

Double cylinder arrangement (GAMMA) is derived from the beta, but simpler to construct; it uses, as beta, piston-displacer, but in this case they are located on different cylinders. In these machines the compression space is divided between the two rolls with intermediate connection. It provides much greater freedom in designing the transmission to a rotary shaft and facilitates construction and assembly.

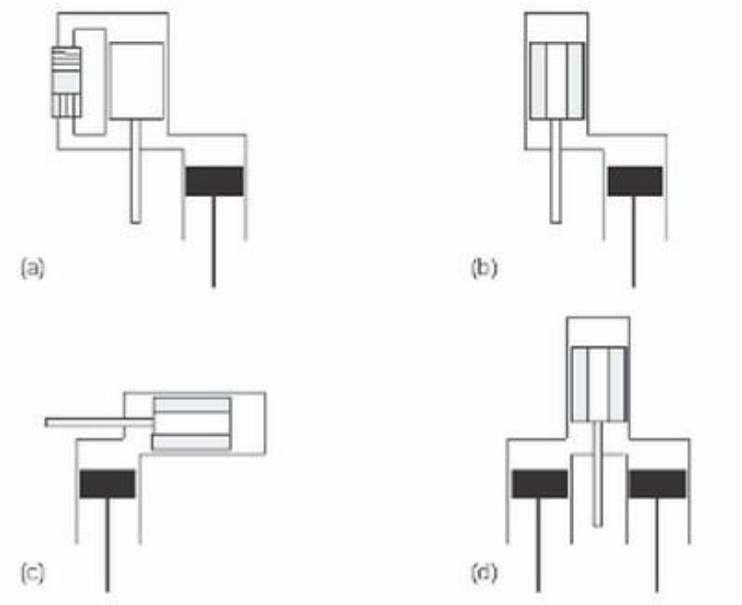

Image 36 - Gamma Stirling engines. A) External regenerator. B) Regenerative displacer. C) Regenerative displacer and cylinders at 90°. D) Double expansion cylinder (Rainbow).

LIQUID PISTON

In the liquid piston Stirling engines the pistons are free surfaces of a liquid. The working gas is pushed and compressed by the movement of the liquid column over the cylinders. There are many design variations, but most follow the basic scheme shown, consisting of two columns in U, one acting as displacer and the other as piston.

It has the advantage of being very simple and cheap, but presents problems of evaporation of liquid and friction head losses.

3.3.2.2. DOUBLE ACTING PISTONS

These engines were developed by Babcock in 1885. They use both sides of the piston to move fluid from one space to another. The most developed and manufactured of these engines has been P'de United Stirling series, developed by Bratt. It is a double acting engine, with 4 cylinders and 40kW. The initial objective of this engine has been the development of new components, and experiments were performed with various different working gases and heater temperatures.

In these engines the reciprocating element is a piston / displacer that works on two sides: one compresses the gas of a cycle while the other expands the gas in the another cycle, or vice versa. At first it was thought that its construction would be too complex due to the pipes necessary to connect the workspaces with the regenerator.

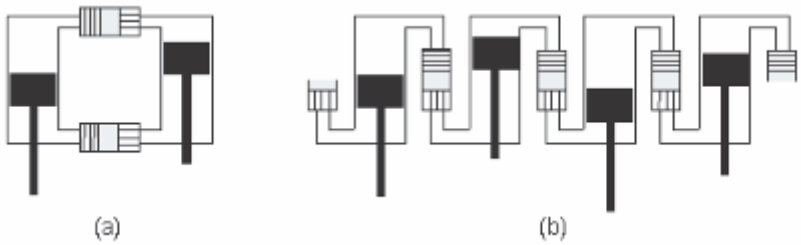

Image 37 - Double-acting Stirling engines. A) Double cylinder. B) Multicylinder (Siemenes).

As a consequence of this configuration, the number of thermodynamic cycles is the same that the number of cylinders and pistons, and it is always equal or greater than 2.
These engines have the advantage of having a half of moving parts than the simple-acting engines, which makes it easier the sealing and cheaper the engine. Their advantage is that they are not flexible in their design. These engines are used for powers higher than 20 kW.

3.3.3. CHARACTERISTICS OF MECHANICAL ELEMENTS

One of the most important advantages of Stirling engines versus explosion engines is the smoothness in operation, and the low compression ratio (about 2) that are needed. Because of this, mechanical components in a Stirling engine bead relatively low load: crankshaft, connecting rods, bearings, pistons, crankcase, cylinder,... have lower weight and dimensions than in other engines, and a longer working life. The only one enemy of the mechanics in Stirling engines is the high temperature that some of the pieces achieve (for example the ones around the expansion chamber). The election of the material and design of these elements must be very careful, keeping in mind their thermal and mechanical fatigue.

3.4. WORKING FLUIDS IN STIRLING ENGINES

Any working fluid with high specific heat can be used in a Stirling cycle. Many engines in nineteenth century used air as working fluid. Most of them worked at pressures near to the atmospheric. Air is cheap and quickly available, big advantages.

In twentieth century, the company Philips started to use pressured air to get higher power, and in 1954 incorporated new gases as hydrogen and helium for engines, after seeing the exit of them working in coolers.

Since then, hydrogen and helium have consolidated as the most used working fluids in Stirling engines. Air, argon and other fluids are only in small experimental or demonstrative engines. But there are more possibilities.

In the following chart we enumerate exhaustively the kind of fluids that can be used in Stirling engines. Some of them have been experimented; some of them are only theoretical.

Mono-component	Mono-phase	Gas	H, He, Ar, CO_2, $H_2O_{(V)}$
		Liquid	H_2O, oils, alcohols, $CO_{2(L)}$, gasoline,…
	Multi-phase	Condensing fluid	$H_2O_{(V+L)}$
Multi-component	Mono-phase	Gas mix	Air
		Liquid multi-component	H_2O + solutes, liquid mix
		(carrier gas) + dissociating gas	Never studied
	Multi-phase	Carrier gas + condensing fluid	Air + $H_2O_{(V)}$ + $H_2O_{(L)}$

Chart 3 - Possible working fluids in Stirling engines.

The ones shadowed are the ones studied and experimented in this thesis in the laboratory.
The working fluid of a Stirling cycle must have the following thermodynamic, heat transfer and dynamic properties:

- High thermal conductivity.
- High heat capacity.
- Low viscosity.
- Low density.

For best system performance in addition to these features we must consider the availability, cost, operational safety and storage requirements as other important aspects of the fluid. The

capacity of a working fluid in terms of specific heat, thermal conductivity and density is defined by Martini, in what may be a good approximation for preliminary working fluid:

$$Capacity\ factor = \frac{Thermal\ conductivity}{Specific\ heat \cdot density} \qquad [Ec. 48]$$

To determine the best working fluid performance, the entire system can be analyzed for various working fluids. Experimental research to see which one is more apt it is difficult and expensive. The empirical equations developed by Beale do not exist for the assessment of the working fluid, probably because of the scarcity of experimental data to allow a significant correlation form. A simple approach suggested by Walker based on steady-flow analysis is useful for the choice of fluid.

Using the Reynolds analogy we find a relation between the heat transfer and frictional resistance through a conduit in terms of the ratio of heat transfer and temperature limits:

$$Q_{wf} \propto \left(\rho^2 {C_p}^2\right)^{0,5}$$

This expression is required to simulate the operation of the engine with different working fluids with the available equations for selecting the best working fluid.

To improve engine thermal efficiency, Gu and company proposed the use of a composed working fluid and devised a criterion to select the ideal working fluid.

3.4.1. GASEOUS WORKING FLUIDS

Gaseous working fluids, formed by one or more chemically not-reactive components, are with no doubt the more studied and used fluids in Stirling engines. Hydrogen, helium and air are the best ones, with the main advantages, and therefore, the most used ones.

Meijer presented in 1970 a numerical study based in the simulation software of Philips. He compared hydrogen, helium and air with pre-set conditions:

$$T_{max} = 700\ ºC$$
$$T_{min} = 25\ ºC$$
$$p_{max} = 110\,\frac{kg}{cm^2} = 107{,}87\ bar$$

With this data, he got the following graph. With engine global efficiency in Y axis and specific power (kW/L swept volume) in X axis, for each gas we have a curve formed by points get at different speed.

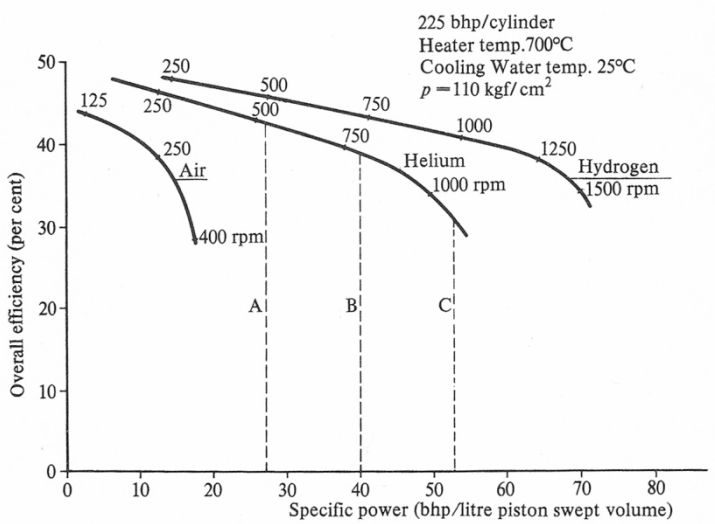

Image 38 - Meijer's theoretical comparison (1970) between hydrogen, helium and air.

From the above graph we can deduce:

- By increasing speed, performance decreases almost linearly up to a limit of rpm in which it plummets. Air reaches this limit before helium and this before hydrogen. For equal speeds, we have: $\eta_{air} < \eta_{helium} < \eta_{hydrogen}$. The difference increases when increasing the speed.
- By increasing speed, specific power increases almost linearly up to a limit, which depends on the gas and which cannot be exceeded even with higher speed. Air has a lower specific power limit, while hydrogen has the higher. For identical speeds we have: $P_{esp(air)} < P_{esp(helium)} < P_{esp(hydrogen)}$. That is, hydrogen has less volume needs to offer the same power (engine more compact and lightweight).
- As a result of the above relationships, an increase specific power implies a decrease in performance for any of the gases.

A variation in pressure and temperature conditions modifies the curves:

- An increase in T_{max} causes a rise in the whole performance curve.
- An increase in p_{max} makes the curve flatter, that is, increases the efficiency at high specific power, but leaves it equal at lower specific power.

In 1976 Michels made the same study using T_{max} and T_{min} constants, but taking the p_{max} to give the best performance in each case. He compared nitrogen, helium and hydrogen by the same curves used by Meijer. Michels deduced that the maximum achievable yield between two temperatures T_{max} and T_{min} does not depend on the working fluid; however, the hydrogen obtained the best performance at a specific power, larger than helium and especially nitrogen. The behavior of nitrogen is extrapolated into the air. There have been other comparative studies, such as Hall (steady flow analysis) that classifies gases as good (hydrogen), medium (helium and water vapor) and bad (air and carbon dioxide). There have also been experimental studies, but all arrive at similar conclusions.

3.4.2. LIQUID WORKING FLUIDS

Liquids, such as fluids that are, can be compressed despite requiring high pressures to do so, and volume variations are small compared with the gases. John Malone, in 1931, with two prototypes showed that it was possible to use liquid as the working fluid in a Stirling engine. He got a yield of 27% rotating at 250 rpm on an engine with pistons filled with water. The pressure ranged from 207 to 820 bar, always above the critical point, and the maximum temperature was next to the critical, so that the liquid behaved like a high-density gas.

The advantages of using liquid working fluid, compared to gas, are:

- Heat transfer favored by the high thermal conductivity of the liquid and its large heat capacity.
- The sealing can be solved better.
- The liquid lubricates in the movement of the pistons.
- The system pressurizes itself, because at cold temperatures can be filled at atmospheric pressure, but when it warms up, the pressure rises quickly.

But the use of liquids imposes restrictions on Stirling engines:

- The high pressures require thicker walls, which make heavier the engine.
- To prevent heat loss along these walls, it is necessary to make the cylinders and pistons very long and with small diameter.
- Density and inertia of the liquid is not allowed for high speeds.

Stirling engines have been tested with several liquid: mercury, oil, gasoline, alcohols, liquid carbon dioxide, sulfur dioxide, etc...; but water has always worked best. It is left to study potential effects of solutes in liquids or mixtures thereof.

3.4.3. COMPOUND WORKING FLUIDS

One of the possible working fluids in Stirling engines is a compound working fluid. This kind of fluids, also named TPTC (two-phase two-component), consist basically in the incorporation of a phase-changing component in the normal working fluid, to enhance the power density of the engine.

In the TPTC working fluids, the carrier component remains gaseous during the whole cycle, while the another component changes its phase from liquid to vapor in moving from the cold space to the hot space through the regenerator (absorbing heat from the regenerator), and vice versa, it condensates when going again from the hot to the cold space (giving back the heat to the regenerator).

This kind of working fluids are further explained in chapter 5.

3.5. PERMORMANCE AND CHARACTERISTICS OF A STIRLING ENGINE

3.5.1. CHARACTERISTIC CURVES

A first approximation to the power value that can be performed by a Stirling engine is given by the Beale formula. Constants given in the following chart are a mean obtained from many real engines.

$$P = B_N \cdot p_{mean} \cdot N \cdot V_{swe} \qquad [Ec. 49]$$

Where

$P = engine\ power\ [W]$
$p_{mean} = mean\ pressure\ of\ the\ cycle\ [bar]$
$N = cycle\ frequency\ [Hz]$
$V_{swe} = swept\ volume\ in\ expansion\ space\ [cm^3]$
$B_N = Beale\ number$

Heater Temp.	600 K	800 K	1000 K	1200 K
Beale number (well-designed engine)	0,008	0,017	0,025	0,030
Beale number (not optimized engine)	0,002	0,006	0,009	0,010

Chart 4 - Beale number depending on heater temperature.

This relationship is very useful for preliminary calculations and viability studies. It is also very interesting to know the range of efficiency of real Stirling engines:

$$\eta_{STIRLING} \approx 0{,}5 \cdot \eta_{CARNOT} = 0{,}5 \cdot \left(1 - \frac{T_{min}}{T_{max}}\right) \qquad [Ec. 50]$$

This means that, for example, a well-designed and adjusted Stirling engine, which works between T_{max} = 600 ºC (usual metallurgical limit) and T_{min} = 20 ºC (running water temperature), would get 33% of efficiency. Anyway, first prototypes of any model, not optimized yet, use to give the half of this value.

The utility of a thermal engine is to convert calorific energy in mechanical work. Therefore, to know its benefits means to know how much energy it consumes and how much work it generates per unit time, which means: to know the mechanical power (P) and efficiency (η).
Power and efficiency of an engine are function of working conditions. These conditions are named the **working variables**.

3.5.1.1. WORKING VARIABLES

SPEED (n)

Increment of speed (cycle repetition frequency) should cause proportional increments in power; this is true at low revolutions, but at high speed, losses increase and P_i starts to fall. Efficiency should not be affected by speed, but also engine losses make the efficiency curve to be convex. There is a n for P_{max} and a n for η_{max}, between it is convenient to work, and $n[\eta_{max}] > n[P_{max}]$.

MEAN CYCLE PRESSURE (p_{mean})

The output power of the SCE is proportional to the mean pressure of the cycle. Berrin Erbay showed that for getting high values of power and density are needed pressures of 100-200 bar. This elevated pressure presents particular problems related with pollution of the working fluid, heat exchangers stress and loads in mechanism.

The SCE can achieve efficiencies of 65-70% of the Carnot cycle efficiency with current technology. Kongtragool and Wongwises engine, which worked at low temperature shows that the engine efficiency is relatively insensitive to the speed elected if the temperature of the heater tubes is maintained at a fixed value throughout the operating range of the engine and not allowing the temperature of the refrigerator rises.

The heater temperature should be kept as high as possible to achieve high pressure.
The effect of the working fluid pressure on the power and performance is almost the same as the speed. Ideally P_i should be proportional to the pressure, and η independent, but the losses caused by the increased pressure change these relationships as the speed does. There will be a pressure for P_{max} and another one for η_{max} between, as the speed, is convenient to work: $p[\eta_{max}] > p[P_{max}]$.

HEATER TEMPERATURE (T_{max})

Obviously, the higher temperature the more heat exchange, and hence more power will be generated. It is also clear that increasing the temperature rises ideal Carnot efficiency, and consequently also the efficiency of the engine grows.

COOLER TEMPERATURE (T_{min})

For the same reason, an increase in temperature of the refrigerator causes a decrease in both the power and performance.

The effects of all these parameters and also of the following have been analyzed keeping all others constant. Benefits of P and η are also based on the parameters that define the configuration of the motor. These are the **design variables**.

3.5.1.2. DESIGN VARIABLES

CUBIC CAPACITY

In the Stirling engine, the cubic capacity or displacement is the difference between minimum and maximum volumes which the working fluid is submitted to at each cycle. The ratio of the cubic capacity with the power output is linear (but not proportional). The performance should not be affected by this parameter, but experience shows that small demonstration engines do not give as good results as its larger counterparts.

SWEPT VOLUME RATIO (k)

It is the ratio of the volume swept by the compression and expansion pistons. There is a maximum power for values of k between 0,8 and 1, depending on other parameters.

RATIO STROKE / DIAMETER (s/D)

Usually found around 0,5 for both the expansion and compression chambers. It is a constitution that favors the thermal exchange and reduces the dimensions of a possible crankshaft, although it is usually difficult to design.

DEAD VOLUME RATIO (x)

In SCE, dead volumes are the volumes not swept by the pistons, they should theoretically be zero, but in practice are even over 50% of the total internal volume of the gas. Wu Feng has developed a criterion for the optimization of this dead volume, this amount of dead volume is needed to allow necessary heat exchanges and facilitate heat transfer surfaces. Dead spaces reduce engine power output but have opposite effects on the efficiency, depending on the location of the dead space. These spaces can be modified during operation so as to achieve some control of the output power.

Increasing the volume swept get increased power output of the engine if the pressure and temperature levels are kept constant. There is an empirical correlation for relating the dead volume existing with output power.

x is the ratio of the dead volume and the volume of the expansion chamber. The increase in the interior space of the regenerator and auxiliary heat exchangers, which causes an increase in x, affects adversely the power. It will therefore be necessary to design the engine with an x as low as possible.

PHASE ANGLE (α)

Both pistons in a Stirling engine move sinusoidal, with the same frequency, but with a phase α. Power is maximal for α between 60º and 120º, depending on the engine.

The following figure shows some of these effects on the power, shaped like invariant graphics. These are not enough when a fine design is needed. Because of this, there are design charts which allow working with some variables at the same time. Anyway, a rigorous development demands a personalized study of each engine, with the help of computer tools.

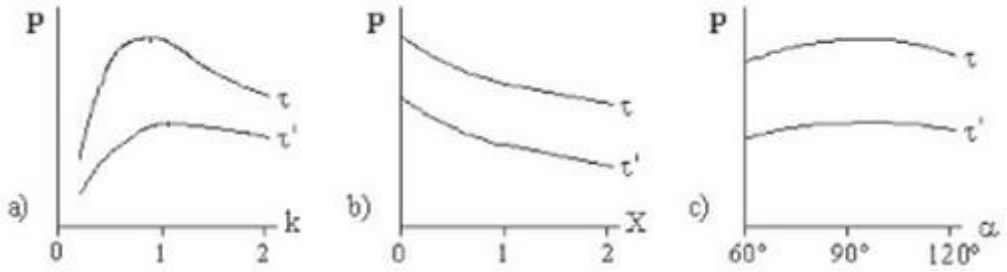

Image 39 - Influence of some design parameters in engine power, at fixed pressure and speed, and at two different temperature ratio, τ=0,25 and τ=0,5. A) Effect of swept volume ratio. B) Effect of dead volume ratio. C) Effect of phase angle.

Most of thermal engines transmit mechanical power through a rotary shaft. Because of this, the value of the output torque is very interesting.

Comparing internal combustion engines with Stirling engines with identical power, it is observed that the torque developed by the second ones is quite superior. This is because the speed does usually not exceed 2500 rpm in Stirling, while the AICE can easily reach and exceed 5000 rpm.

Despite generate higher torque, Stirling engines require mechanical not as robust as the alternating internal combustion engine, as its torque is constant within each cycle.
This lack of abruptness in mechanical stress prevents fatigue of materials and makes the engine silent in the same way which makes it practically unnecessary the presence of a flywheel.

Representing the torque and performance, depending on the rotational speed and fluid pressure, set the **characteristic curves** which define very clearly the performance of the engine.

One of the attractions of the Stirling engine is its good behavior at partial loads, i.e., when operates at lower speeds or pressures than the ones for maximum power. This feature is evident in:

- Pairs very constant over a wide range of speeds and pressures, what is a highly valued feature in automotive. The thermal balance and performance vary little over a fairly wide range of speeds and pressures.
- As we can see, the levels of power and efficiency (as function of speed or engine pressure) are far from the ideal thermodynamic cycles. This means that power is not directly proportional to η or P, and efficiency is not constant regarding η or P. This deviation in working is because of losses that are impossible to avoid in real engines. We can see the effects of these losses, and how they affect to power and η in the following chart and graphic.

Kind of loss	Loss	Effect in power (P)	Effect in efficiency (η)
Losses of modified cycle	Dead volume: it reduces the amplitude of the pressure of the cycle.	Proportional	Null
	Fluid redistribution: the continuous (sinusoidal) movement of pistons and the fluid inertia make the distribution not ideal.	Proportional	Null
	Adiabaticity: the high speed with which the cycle is repeated does not allow isothermal heat exchanges.	Proportional	Constant
Thermal losses	Conduction: through and along the walls.	Constant	regressive
	Convection and radiation: to the environment.		
	Effect "pitcher": pistons moving absorb heat in the hot bottom of cylinders and lose it in the cold bottom.		
	Fumes: when heat source is combustion, part of the energy is lost in exhaust.	Proportional	Constant
	Thermal potential: because of the difference of temperature between the sides of the exchanger.		

Chart 5 - Reasons for power and efficiency losses in Stirling engines. Characterization of the effects in function of speed or environment pressure.

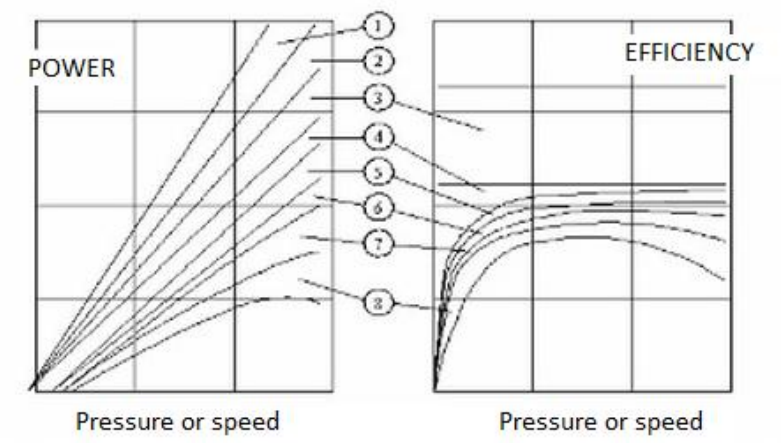

Image 40 - Effect of losses in power and efficiency, as a function of mean pressure or speed.

In the figure above we can see the following curves:

1. Effect of dead volume.
2. Loss because of working fluid redistribution.
3. Adiabatic effects.
4. Thermal losses in conduction, convection, radiation and “pitch” effect.
5. Thermal losses through exhaust fumes, thermal potential and imperfect regeneration.
6. Mechanical friction losses.
7. Aerodynamic friction losses.
8. Losses of auxiliary devices.

As engine speed increases, the heat losses described by Makhkamov become predominant factors since they are proportional to the square of speed, and there is a time when they are so large that they must be taken into account.
To reduce these losses we can use light molecular weight fluids as helium and hydrogen. However, these gases are difficult to contain due to their ability to diffuse with metallic materials.

Mechanical friction happens in the piston rings, rubber seals, bearings, oil pumps and other frictions that can be found in mobile elements. Compared with conventional motors friction is much lower, as we have less moving parts.
Unlike the internal combustion engine, the Stirling needs a heating period at the end of which can be started. Although there are systems to reduce this time, the implementation never is instantaneous. This represents a major obstacle to its use in tourism type vehicles and rapid response sets. Once heated, only the free-piston Stirling engines get to work spontaneously, others need the impetus of a starter motor or similar. Currently, the electronic control systems are responsible for commissioning by a scheduled process.
When desired a change of the power generated by the engine, we can increase or reduce the flow of fuel supplied, but this generates a slow change due to the thermal inertia of the Stirling. Other systems are needed to allow rapid changes in power and speed.

3.5.2. CONTAMINATION AND NOISE

The Stirling engine, belonging to the type of closed cycles engines, does not generate any polluting effect during its operation. Not even small leaks of working fluid (hydrogen, helium or air mainly) or renewals or lubricants (if treated correctly) can be considered harmful to health.
The main pollutant emission of the SCE comes from its heat source, especially if it is based on combustion. The good conditions in which this combustion develops (continuity and high temperatures) cause extremely low levels of unburnt hydrocarbons (UHCs) and carbon monoxide (CO), whereas the level of nitrogen oxides (N0x) increases significantly compared to internal combustion engines.

This happens especially when used fuels are fuel oil, diesel or gasoline. A commonly used solution is recirculating a third of smoke, which can reduce 30% $N0_x$ levels.

But thanks to the freedom of these engines in choosing a heat source, you can use much less polluting resources, such as solar radiation, combustion of natural gas or biomass, or waste heat utilization of other processes (CHP). This allows saying that the Stirling engine can be cleaner than internal combustion engines powered by fossil fuels.

Stirling engines make very little noise when running. This is another of its attractions, and is due to the lack of detonations in your cycle and relatively low operating speeds. If SCE are well balanced, vibration generated levels are insignificant.

In fact, the main noise source is not the Stirling engine itself, but the auxiliaries as the burner and the cooling fan. For example, a bus driven by a Stirling engine generates 10 dB to 15 dB less than a conventional one.

3.6. CONTROL SYSTEMS

As already seen in the previous chapter, the characteristic curves of the SCE have been defined as the evolution of torque generated, depending on the speed and pressure. When the motor is used to move a machine station, this presents a resistant torque curve as a function of speed and other parameters. The motor-receptor system always tends to a speed that matches the engine and resistant pair, and any changes in the curves of the engine or receiver produces a transient towards the new equilibrium speed.

Some applications such as power generation require constant speed operation, even versus sudden changes of load. These engines have a system that changes the torque curve as a function of changes according to the solicitation, to always maintain the same rate of equilibration. Step A to B in the figure represents the constant speed control. In many applications, such as in case of constant velocity and stationary fixed frequency generators, this is achieved by varying load conditions.

Instead, most applications need a control for both torque and speed. In automobiles, for example, a change from A to C could be possible when the vehicle confronts a ramp or change the transmission ratio.

Engines generally need to have a system that by varying the torque curve (or power curve) controls the speed according to a particular strategy, for example to maintain a constant frequency, either work always at maximum performance (minimum consumption) either at maximum power and maximum torque ... The system that seems more logical at first view is the variation of temperature of the heater by controlling the energy supplied by the heat source. Modifying this temperature, the curves of torque and power vary considerably.
This method has the advantage that only with one variable T_{max} the engine behavior is controlled. But it has two drawbacks important enough to make it totally inadvisable: the first is that the thermal inertia of the heater itself causes slow reactions, the second is that T_{max} also greatly influences the performance, and as most of the time working at partial loads, the average performance would be low.

Therefore, all existing control systems are designed as a combination of two: one that keeps the heater temperature, and other using other parameters to govern the torque curves. The two systems are:

- Torque (or power) is controlled by the torque control system, which can be of many types, but all with the same goals: to produce the desired changes as quickly and with minimal effect on performance.
- T_{max} heater temperature is maintained constant at its highest possible value (metallurgical limit), thanks to the temperature control, which adjusts the incoming heat flow to variations of power. In this manner always performances are kept as high as possible for each situation.

Most engines have, apart from these two, other control systems as security, for example speed limiter, maximum pressure, temperature probes at different points...

3.6.1. FLUID TEMPERATURE CONTROL

The control system takes care of the temperature automatic control of the heater temperature, keeping it constant at a value close to but below the metallurgical limit, i.e. below the temperature at which the heater material fail because of fatigue before the number of estimated working hours have been spent. Considering where the application in this case will have a heat source capable of providing the heat to maintain the temperature at such high levels. This safety margin between the temperature and the set temperature limit is necessary for the presence of hot spots in the heater tubes and also the inevitable oscillations of the regulation itself. The margin will be much smaller as more regular is the distribution of temperature on the tubes, and the more sensitive and faster is the regulator. In combustion engines heated by fuel, this margin may exceed 100 °C, while indirect heating with liquid metal circuit allows much smaller margins, i.e. higher yields.

The way of regulating T_{max} depends on the type of heat source used. All systems are equipped with one or more sounding lines to the heater temperature, the value of which is treated and amplified to suitably modify the heating power supplied to the motor. In the case of a burner, it is needed to modify the flow of the fuel-air mixture, in a solar concentrator is varied by the number of rays incident on the heater, in a nuclear reactor are introduced or extracted uranium rods of the sleeves graphite...

3.6.2. MEAN PRESSURE CONTROL

As has been demonstrated before, output power of a SCE is directly proportional to the mean pressure of the cycle of the working fluid. Curves torque-speed depend on the value of this pressure. The more pressure, the more torque, and vice versa.

The simplest method can be to unload the engine by taking air out, to get a reduction in power, and to load the engine to get more output power. But actually that variation needed of the mean pressure is not so easy to get. It is necessary to build storage and compressor for gas. Therefore, we can, when is necessary to increase the power, introduce working fluid in the engine, and extract it to the storage area when we want to reduce the power.

This system, conceptually so simple, is actually much more complicated, because both the time and the openness of valves must be carefully controlled and monitored.

3.6.3. VOID (DEAD) VOLUME VARIATIONS

An increase in the void volume (non-swept volume by pistons and displacers) in Stirling engines causes a decrease in the compression ratio and, therefore, a reduction in the output work per cycle. So, increasing the dead volume inside the SCE has as consequence a loss of power in the engine, but not necessary a loss of efficiency. Giving extra spaces, the void volume can be increased or reduced. Berrin Erbay analyzed the effect of dead volume variations in the efficiency, with the engine working in a thermodynamic cycle with polytrophic processes for displacer and piston, under conditions of maxim density of power.

A set of valves can communicate the cylinders with some chambers of different capacity and full of working fluid, that are incorporated in the same carter.

To each combination of open valves corresponds a particular added volume, such that with an appropriate valve opening sequence we can get a stepwise but regular evolution of dead volume.

This system has an extra advantage: the efficiency is less affected by the void volume variation than by the use of the short circuit. The reasons because of that their inventors (United Stirling) left this great system are surely the added volume and weight, and cost of the valve actuation system.

3.6.4. EFFECTIVE STROKE VARIATION

The SCE output power can be controlled also by changing the effective stroke length of the alternating components of the engine. This method is applicable for both engines of double and single acting, and also for free piston engines, but it is a difficult task to get a mechanical change in the effective stroke to adjust the power.

The decrease of the career of a displacer or piston leaves a certain volume of each cylinder unswept. The unswept volume becomes dead volume and increases the engine speed, which, as we have seen, greatly affects its torque and power.

This system has been successfully applied to engines driven by swash plate, wherein the modification of the angle of oscillation causes the variation of the stroke of the pistons. In all other mechanical transmissions system implementation is more difficult.

Now it is in the free-piston Stirling engines where this control method is commonly used. In these engines, the oscillation amplitude of the piston is regulated natural: the more load the smaller amplitude, and vice versa. But if there is a displacement limiting system, such as an adjustable pressurized gas spring, it can effectively control the torque generated by the motor.

3.6.5. PHASE ANGLE VARIATIONS

This is one of the best methods of controlling the power delivered by the engine. In the previous section has been discussed that the phase angle of the sinusoidal motion of the two pistons does not affect too much the mechanical power generated by a Stirling. This is true for angles in the range of angles between 60° and 120°, but when the lag interval extends from 0 to 360° power appears as a nearly sinusoidal function regarding the angle, as shown in Figure. With zero phase angle, the volumes of the compression and expansion area exactly in phase change, as if there were no cyclic flow of fluid through the system work.

The power control achieved by changing the phase angle is characterized by instantaneous response and is a very suitable method for a motor power control fast. It was the first system that adopted the General Motors for 8-cylinder engine in V. But this type of control is not applicable to double-acting engines.

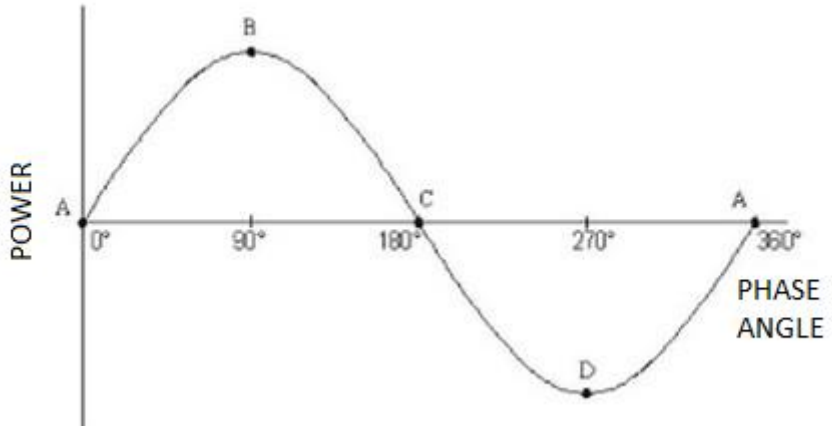

Image 41 - Effect of phase angle in power.

Points on the graph:

A. Maximum change in volume without generating power.
B. Maximum power generated.
C. Variation of void volume (not generating power).
D. Maximum power absorption (the motor acts as a brake, as a heat pump)

By varying the phase angle, not only can reduce the generated power (or torque) but can make negative, i.e., the motor can become a heat pump that acts as a brake, or if the resisting torque allows, you can reverse the direction of rotation.

This system is applicable only to single-acting engines, connecting the two pistons at two different axes, the movement of which is offset a planetary gear system.

Double-acting engines, however, have an invariable phase angle, always worth 360° divided by the number of cylinders, and thus cannot be controlled by this method.

3.7. FACTORS AFFECTING PERFORMANCE OF THE ENGINE

The ouput power of the engine can be calculated using the numbers of Beale and West:
Number of Beale:

$$B_N = \frac{P}{p_{mean} \cdot V_{swe} \cdot N} \qquad [Ec.51]$$

W. Beale noted that in practice, the maximum output power of an engine well developed is more or less proportional to the pressure, volume and speed. A very important factor that has not been taken into account in the correlation of Beale is the engine operating temperature. In the discussion made earlier on the simple analysis of the SCE has been said that the increase in the temperature of the heater will increase power for a fixed cooler temperature. Beale empirical relationship contains no temperature effects because most engines he analyzed had a heater temperature of above 650 °C. Above this temperature range the influence of increasing temperature is not significant.

Iwamoto showed that the number of Beale is about 0,15 for SCE with high temperature difference in which the temperature of wall of the heater is around 650 °C.
These effects themselves were considered by West, which defined another number that gives us an idea of the power that can deliver the SCE and can be expressed as:

$$W_S = \frac{P}{p_{mean} \cdot V_{swe} \cdot N \cdot \frac{(T_e - T_c)}{(T_e + T_c)}} \qquad [Ec.52]$$

It was showed that the number of West is 0,25 for engines of 5-150 kW and 0,35 for lower power engines. Patrescu discovered in 2002 a factor affecting engine performance based on the first law of thermodynamics. The method used for analysis is irreversible cycle and carries limited speed direct integration of equations based on the first law for processes. We can find several studies, as the one developed by Altman who wrote a very useful numerical program to determine engine performance.

3.7.1. EFFECTIVENESS OF REGENERATOR

Regenerator efficiency increases with increases in the reduced length and decreases in the reduced period. Regenerator design should be such that the heat transfer coefficient and the area of the matrix of the regenerator must be larger at the lowest possible rate while maintaining fluid flow. The flux in the regenerator changes in many rapid cycles, thus, it is likely that only a portion of the total charge of gas pass through the matrix and part of the fluid remains in the regenerator.

3.7.2. MATERIAL OF REGENERATOR

The choice of material for the matrix of the regenerator is an important issue because it affects engine performance considerably. Efficiency and engine power output is a function of engine speed for metal and ceramic regenerators.

Due to lower penetration rate of ceramic than metallic, it has been shown that the efficiency and power output of the engine with ceramics covered regenerator is greater than the metallic regenerator under all investigated speeds.

3.7.3. WORKING FLUID AND LOSSES

In a real engine, the existence of the working fluid losses is inevitable. The pressure inside the space is usually greater than the minimum pressure of the idealized cycle and this means that due to areas where there is loss of the gas tightness, the gas tends to escape from the system when the pressure is highest in the cycle, but tend to return to the system during the compression phase. Both effects reduce the output power. The effect of pressure loss due to friction, finite velocity and acceleration process in the regenerator of the engine is presented by Patrescu.

3.7.4. FLUID FRICTION

The fluid friction in the mesh of the regenerator is a very important issue in the SCE. Flow friction is primarily due to size, shape and density of the wire mesh and fluid properties such as density and viscosity. The flow friction consumes engine power; therefore the net power is reduced. Both the choice of regenerator material and the design of the system should try to get the lowest possible friction resistance.

It is shown that the friction factor of a wire mesh is simply a function of Reynolds number when the aperture size of the mesh is selected in the representative length scale. Also friction and Nusselt number of the porous medium are similar to those of the wire mesh simple storage. This result suggests that the friction factor decreases gradually with increases in Reynolds number.

4. LOSSES AND EFFICIENCIES

4.1. INTRODUCTION

Ss we have seen in previous chapters, Stirling engines, like all real machines, have no ideal operation for many reasons. The principal of them is the numerous heat losses that occur in the system, as we have seen in chapter 3.5.1.2, chart 5.

In the case of the engine in the laboratory, the whole system can be divided into two subsystems: Stirling engine and burning room. The performance of the operation will depend on both, and therefore, on their efficiencies.

In this chapter will be calculated the heat losses and efficiencies of each of the two systems, to see how influence both in the final output power.

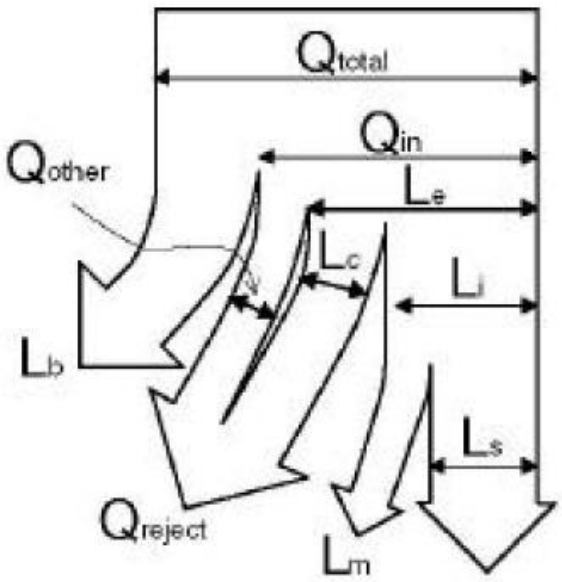

Image 42 - Sankey driagram for Stirling engines.

- Q_{total} = total heat input, supplied by the propane.
- L_b = heat losses in burning room.
- Q_{in} = overall heat that enters the engine, through the heater.
- Q_{reject} = rejected heat.
- L_c = compression space power.
- Q_{other} = other thermal losses.
- L_e = expansion space power.

- L_i = indicated power, provided by p-V diagram.
- L_m = mechanical losses.
- L_s = output power.

By the rough considerations, the burner efficiency is affected by the shape, materials, and fuel of the heat source, the indicated efficiency is affected by the heat flow in the engine, and the mechanical efficiency is affected by the mechanism and the operating conditions.

The efficiency of the complete system is:

$$\eta_{total} = \eta_b * \eta_i * \eta_m \qquad [Ec. 53]$$

Where

$\eta_b = {Q_{in}}/{Q_{total}}$ = burner efficiency.
$\eta_i = {L_i}/{Q_{in}}$ = indicated efficiency
$\eta_m = {L_s}/{L_i}$ = mechanical efficiency

That was the efficiency for the whole system; however, the burning room is an external device, not a part of the engine. Therefore, the efficiency of the engine is:

$$\eta_{engine} = \eta_i * \eta_m = \frac{L_i}{Q_{in}} * \frac{L_s}{L_i} = \frac{L_s}{Q_{in}}$$

L_s is the power output given by the engine, the one calculated with the break forze and frequency; Q_{in} depends on burning room efficiency:

$$Q_{in} = \eta_b * Q_{total} = \eta_b * \dot{m}_{propane} * LHV \qquad [Ec. 54]$$

Where LHV = Lower Heating Value = (for propane) = 11080 kcal/kg

Following, it will be made an analysis of losses and efficiencies for both the burning room and the engine; for that, it will be used the data of one of the experiments performed: the data got in the test of the engine of the 30th of May with a load pressure of 7 bars (Experiment 4, see chapter 7).

4.2. EFFICIENCY OF THE BURNING ROOM

As will be seen along this analysis, the highest losses of our engine happen in the burning room. While the propane gives a performance of almost 5 kW, the final power output of the engine can be, as maximum, up to 500 W, which supposes only a 10% of efficiency. But this efficiency is not the real efficiency of the engine, but the combined efficiency of both the engine and the burning room.

To figure out the real efficiency of our Stirling engine, is very important to know first which losses occurs in the burning room, because these losses are external to the engine and therefore, did not affect the efficiency of it, but the whole system as a group.

In the burning room there are many heat losses; some of them can be calculated easily with the equipment we have, some of them are harder to calculate exactly and will be only estimated. The most important are:

- Heat loss due to the conduction and convection through the walls, P_{cc}
- Heat loss due to the sensible heat of exhaust gases, P_{sh}
- Heat loss due to the latent heat of exhaust gases, P_{lh}
- Other heat losses (due to air excess, leakage, radiation, unburned fuel, etc.)

The efficiency of the burning room will depend on all of these losses, and of course, on the performance of propane combustion:

$$\varepsilon_{burning\ room} = \frac{useful\ heat}{total\ heat} = \frac{heat\ supplied\ by\ propane - heat\ losses}{heat\ supplied\ by\ propane}$$

Following, we will analyze each of the heat losses, calculating the ones which are possible to calculate.

We need to set a reference temperature (room temperature, T_∞). To make this analysis, I am going to use the data got in the test of the engine of the 30th of May with a load pressure of 7 bars (experiment 4, chapter 7). As we do not have any thermometer in the laboratory, the only way to see the room temperature is by taking the first test of that series of tests (Test 300513-4) and seeing the initial temperature in the outer surface of the burning room. This temperature is T_∞ = 21,9 ºC.

First of all, I will start with heat loss through the walls of the burning room (conduction and convection), because they are the most complicated to calculate due to the exhaust analysis that is necessary to do.

4.2.1. HEAT LOSS DUE TO THE CONDUCTION AND CONVECTION THROUGH THE WALLS, $P_{CC.}$

Inside the burning room we have the highest temperature at the engine performing. Therefore it is very important to estimate the heat losses through the wall of this chamber, because is only with a good isolation that we can reduce them, and thereby, a better efficiency of the system is achieved.

To calculate these losses, I proceed by calculating the heat losses through each "wall" of the chamber, which are represented in the following diagram:

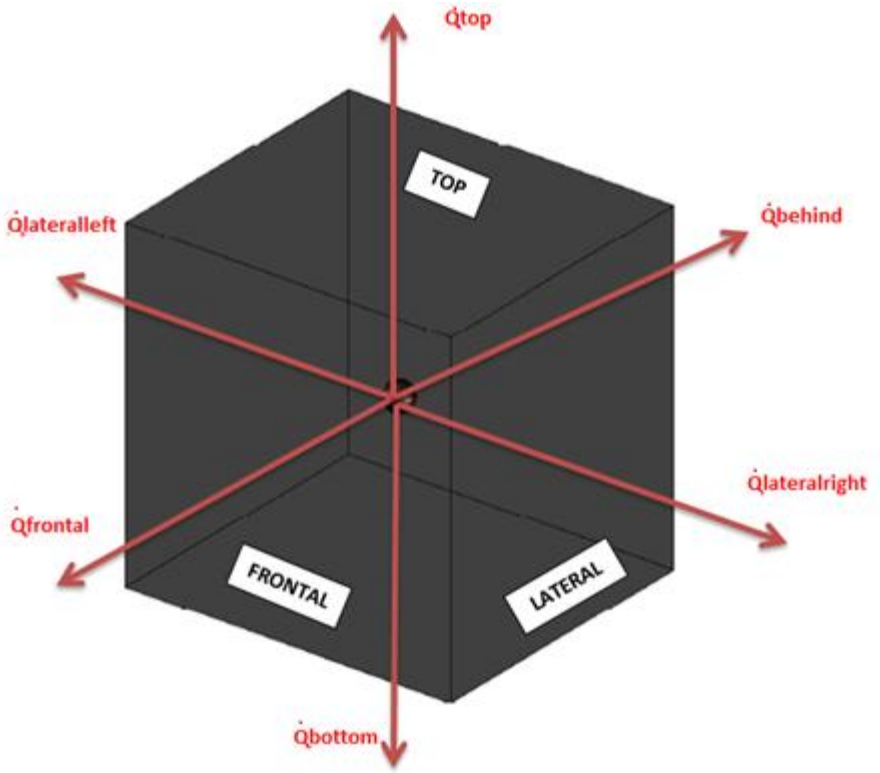

Image 43 - Heat losses in burning room.

The total amount of heat lost will be the sum of the heat lost through each one of the 6 "walls".

$$\dot{Q}total = \dot{Q}top + \dot{Q}bottom + \dot{Q}lateral,right + \dot{Q}lateral,left + \dot{Q}frontal + \dot{Q}behind$$

With DIADem I proceed to measure the Temperatures needed in this calculation:

$$Tint = Temperature\ in\ the\ central\ point\ inside\ the\ burning\ room$$
$$Ts = Temperature\ in\ the\ external\ surface\ of\ the\ chamber$$
$$T\infty = Temperature\ in\ the\ laboratory\ (ambient)$$

Each wall has the same structure: one layer of fire clay, another one of calcium silicate, and another one of steel:

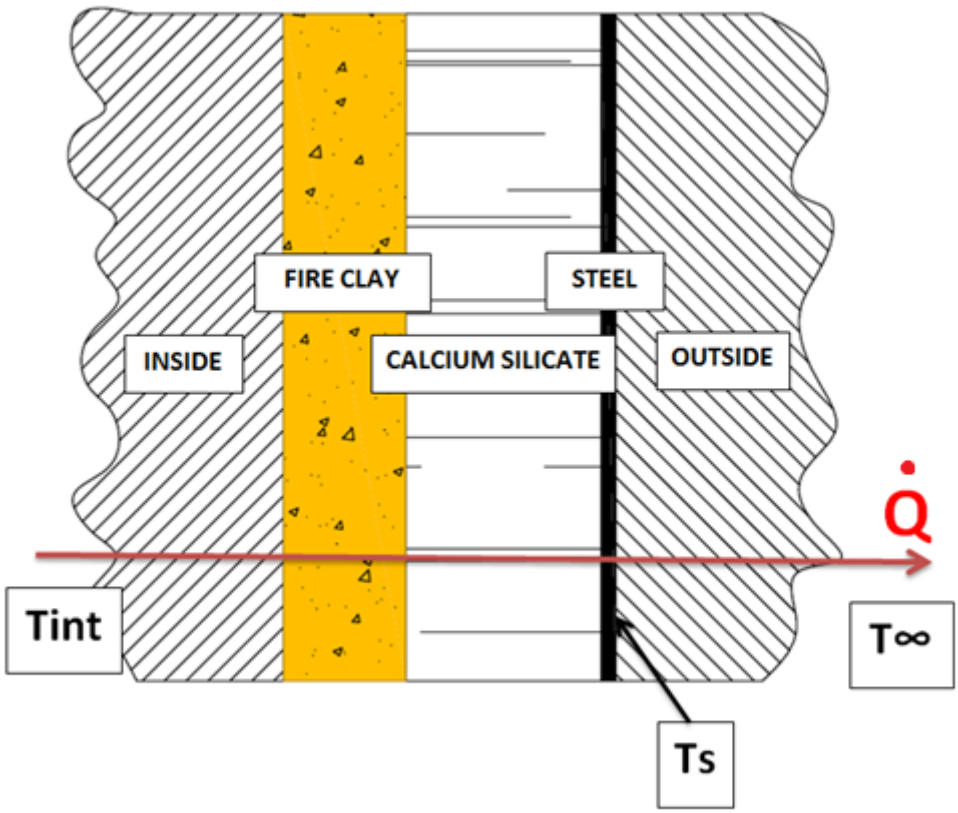

Image 44 - outline of a wall of the burning room.

Through the fire clay, calcium silicate and steel, the heat transfer method is conduction; from the central point of the chamber to the inner surface we have forced convection with air + combustible and from the external surface of the chamber to the environment, natural convection with air.

To calculate this heat lost through each “wall”, I use an electrical analogy, as followed:

Image 45 - electrical analogy for heat losses.

$$Rconv,i = \frac{1}{hi * Ai} \qquad [Ec.55]$$

$$Rfi.cl = \frac{L_{fi.cl}}{k_{fi.cl} * A_{fi.cl}} \qquad [Ec.56]$$

$$Rca.si = \frac{L_{ca.si}}{k_{ca.si} * A_{ca.si}} \qquad [Ec.57]$$

$$Rsteel = \frac{L_{steel}}{k_{steel} * A_{steel}} \qquad [Ec.58]$$

$$Rconv,e = \frac{1}{he * Ae} \qquad [Ec.59]$$

$$Tint - Text = Q * Rtot$$

$$Rtot = Rconv,i + Rfi.cl + Rca.si + Rsteel + Rconv,e$$

The estimation and working temperatures varies with the gas used in the combustion, so I will calculate the losses both for propane and natural gas.

In one of the multiple tests performed with the engine working with propane (Experiment 4, see chapter 7) the average temperatures measured are:

- $Tint = 574{,}5\ ºC$, temperature inside the burning room.
- $Ts = 63{,}7\ ºC$, temperature in the external surface of the burning room.
- $T\infty = 21{,}9\ ºC$, room temperature.

These are the temperatures I will use in all the following analysis.

4.2.1.1. FRONTAL AND BEHIND WALLS

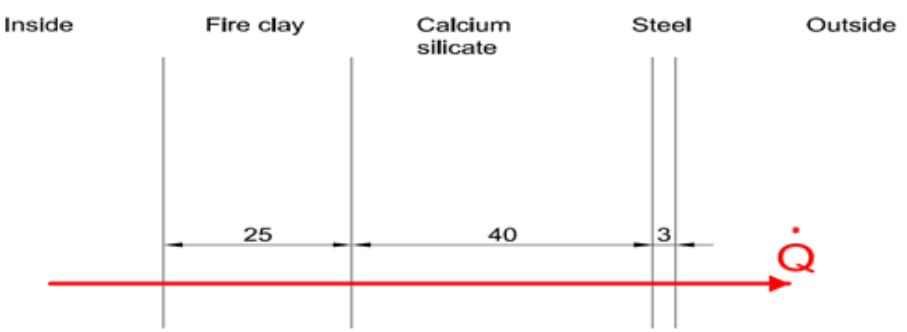

Image 46 - profile for frontal and behind walls.

For determinig the thermal properties in the convection, I use the characteristic length, Lc. For the frontal and behind walls, Lc is the largest length:

Internal convection: $Lc = inner\ height = 445 - 2 * 3 - 2 * 40 - 2 * 25 = 0{,}309\ m$
External convection: $Lc = exterior\ height = 0{,}445\ m$

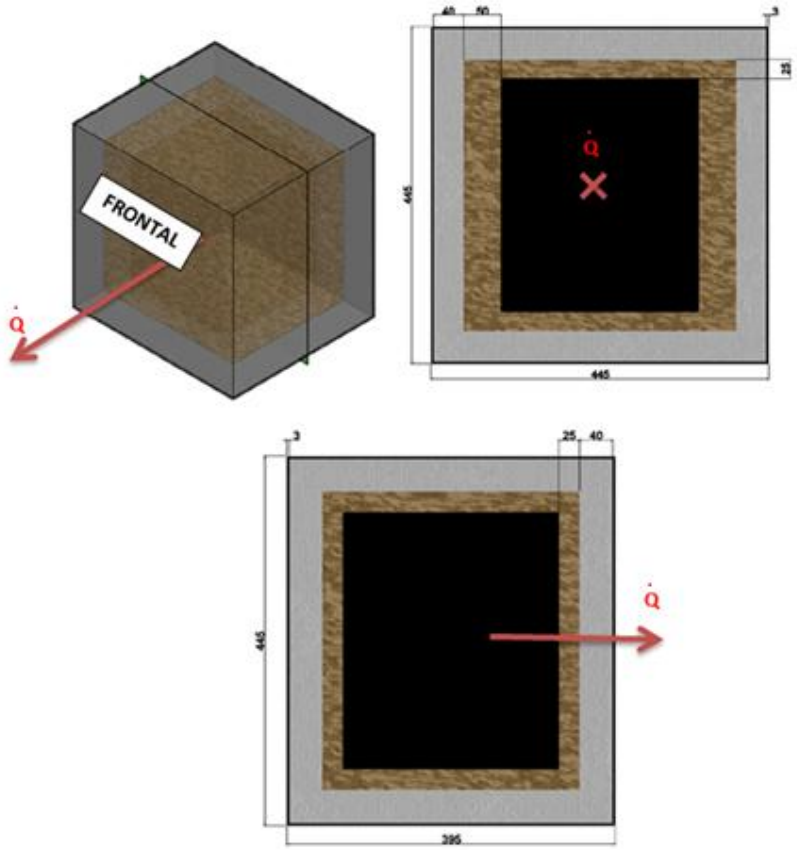

Image 47 - Sections for frontal and behind walls.

INTERNAL CONVECTION

$$Rconv, i = \frac{1}{hi * Ai} \qquad [Ec.55]$$

$$Ai = (445 - 2 * 3 - 2 * 40 - 2 * 50) * (445 - 2 * 3 - 2 * 40 - 2 * 25) = 0{,}080031\ m^2$$

Forced convection with air + propane in a flat plate. The equations depend on the flow regime (laminar or turbulent). I determine it with Reynolds. For calculating the convection coefficient, I relate it with Nusselt number:

$$Nu = f(Re, \mathrm{Pr}) = \frac{h * L_c}{k} \qquad [Ec.60]$$

So I have to determine, at first, the convection speed and characteristics of the gas mix.

Convection speed

$$Air\ enters\ at\ 21{,}2\ °C\ (chart\ A3.2\ in\ the\ annex) ==> \rho_{air} = 1{,}199\ g/L$$

$$M_{air} = 28{,}9\ g/mol$$

$$Air\ flow = 132{,}6\frac{L}{min} * 1{,}199\frac{g}{L} * \frac{1}{28{,}9}\frac{mol}{g} = 5{,}501\frac{mol}{min}$$

$$\rho_{propane} = 2{,}01\ g/L$$
$$M_{propane} = 44\ g/mol$$

$$Propane\ flow = 0{,}1\frac{g}{s} * \frac{60\ s}{1\ min} * \frac{1}{44}\frac{mol}{g} = 0{,}136\frac{mol}{min}$$

As seen in the propane combustion, we need 23,8 mol of air for each mol of propane; in this case, we have excess of air, because we have 5,5/0,14 = 39,3 mol of air for each mol of propane. In the combustion of the propane, it takes part 0,14*23,8 = 3,33 mol/min of air, and the excess of air will go directly to the exhaust gases, and the combustion is as follows.
In the annex 1 we can see the stoichiometric combustion of propane:

$$C_3H_8 + 5(O_2 + 3{,}76N_2) \rightarrow 3CO_2 + 4H_2O + 18{,}8N_2$$

For 0,14 mol/min of propane:

$$0{,}14*C_3H_8 + 0{,}7(O_2 + 3{,}76N_2) \rightarrow 0{,}42*CO_2 + 0{,}56*H_2O + 2{,}63*N_2$$

So we have 0,7*4,76 = 3,33 mol/min of air, which is correct; if we add the excess of air, finally we have:

$$0{,}14*C_3H_8 + \frac{5{,}5}{4{,}76}(O_2 + 3{,}76N_2) \rightarrow 0{,}42*CO_2 + 0{,}56*H_2O + 2{,}63*N_2 + \frac{5{,}5-3{,}33}{4{,}76}(O_2 + 3{,}76N_2)$$

$$0{,}14*C_3H_8 + 1{,}155*(O_2 + 3{,}76N_2) \rightarrow 0{,}42*CO_2 + 0{,}56*H_2O + 2{,}63*N_2 + 0{,}455*(O_2 + 3{,}76N_2)$$

So the leaving molar flow is 0,42 + 0,56 + 2,63 + 0,455*4,76 = 5,79 mol/min. With this escape gas flow I calculate the output speed, that will be the forced convection speed. I calculate it with the output flow and not with the input one, because I know the area of the output duct, but not the input duct (there are 2 input ducts, with different areas and speeds).

Densities of escape gases are calculated at 452 °C, using the data in the chart A3.1 of the annex.

Component	mol/min	g/mol	ρ (g/L)	$\frac{L}{min} = \frac{mol}{min} * \frac{g}{mol} * \frac{1}{\rho}$
CO_2	0,42	44	0,7432	24,86
H_2O	0,56	18	0,4598	21,92
N_2	2,63	28	0,3043	242
Air	2,166	28,9	0,489	128,01

Chart 6 – Gases inside burning room.

In total, come out $24{,}86 + 21{,}92 + 242 + 128{,}01 = 416{,}79 \frac{L}{min} = 6{,}947 * 10^{-3} \frac{m^3}{s}$ of escape gas.

Area of output duct = 0,0025 m^2 ➔ **output speed** = $6{,}934 * 10^{-3} \frac{m^3}{s} * \frac{1}{0{,}0025} \frac{1}{m^2} = \mathbf{2{,}77 \frac{m}{s}}$

So I have got a forced convection speed of 2,77 m/s inside of the burning room. I need to know if I have laminar or turbulent flow:

$$Re = \frac{\rho * v * L}{\mu} \qquad [Ec.61]$$

If Re ≥ 5e5 ➔ turbulent
If Re < 5e5 ➔ laminar

So I have to determine the density and viscosity of the gas mix air + propane and the Lc = 0,309 m.

Density

There is 40,45 L air for each L of propane.

	Air	Propane	Air + propane
V (m^3)	40,45	1	41,45
Density ρ (kg/m^3)	1,199	2,01	50,51/41,45 = 1,218
Kg (=V*ρ)	40,45*1,199=48,5	1*2,01 = 2,01	48,5 + 2,01 = 50,51

Chart 7 - Density calculation.

$$\rho_{air+propane} = 1{,}218\ kg/m3$$

Viscosity

For calculating the viscosity of the mix, I use the theory of Chapman Enskong:

$$\mu_{mix} = \sum_{i=1}^{n} \frac{X_i * \mu_i}{\sum_{j=1}^{n} X_j * \varphi_{ij}} \qquad [Ec.62]$$

$$\varphi_{ij} = \frac{1}{\sqrt{8}} * \left(1 + \frac{M_i}{M_j}\right)^{-\frac{1}{2}} * \left[1 + \left(\frac{\mu_i}{\mu_j}\right)^{1/2} * \left(\frac{M_j}{M_i}\right)^{1/4}\right]^2 ; \varphi_{ij} = 1 \; if \; i = j \qquad [Ec.63]$$

$Xi = molar\ fraction$
$\mu i = dynamic\ viscosity$
$Mi = molar\ mass$

The molar fractions are:

$$air: X_{air} = \frac{40{,}45}{40{,}45 + 1} = 0{,}9759$$

$$propane: X_{propane} = \frac{1}{40{,}45 + 1} = 0{,}0241$$

Component	Xi	Mi (g/mol)	μi (kg/(m*s))
Air (i=1)	0,9759	28,9	1,76e-5
Propane (i=2)	0,0241	44	8,3e-6

Chart 8 – Viscosity calculation.

Calculating the Chapman Enskong coefficients (air, i=1; propane, i=2):

$\varphi_{11} = 1$
$\varphi_{12} = 1{,}8819$
$\varphi_{21} = 0{,}5829$
$\varphi_{22} = 1$

Solving the Chapman Enskong equation: $\boldsymbol{\mu_{mix} = 1{,}7156 * 10^{-5} \frac{kg}{m*s}}$

$\boldsymbol{Re = \frac{\rho * v * L}{\mu} = 60767 < 5 * 10^5}$ ➔ laminar flow

So I have got forced convection in a flat plate, with laminar flow. The equation which governs this convection regime is:

$$Nu = 0{,}664 * Re^{\frac{1}{2}} * Pr^{\frac{1}{3}} \qquad [Ec.64]$$

I need to calculate the Prandtl number for the gas mix.

$$Pr = \frac{\mu * C_p}{k} \qquad [Ec.65]$$

$\mu = dynamic\ viscosity = 1{,}7156 * 10^{-5}\ \frac{kg}{m*s}$
$Cp = specific\ heat\ at\ constant\ pressure$
$k = conductivity$

Conductivity

I use Chapman Enskong equiation:

$$k_{mix} = \sum_{i=1}^{n} \frac{X_i * k_i}{\sum_{j=1}^{n} X_j * \varphi_{ij}} \qquad [Ec.62]$$

$$\varphi_{ij} = \frac{1}{\sqrt{8}} * \left(1 + \frac{M_i}{M_j}\right)^{-\frac{1}{2}} * \left[1 + \left(\frac{k_i}{k_j}\right)^{1/2} * \left(\frac{M_j}{M_i}\right)^{1/4}\right]^2 ; \varphi_{ij} = 1\ if\ i = j \qquad [Ec.63]$$

Component	Xi	Mi (g/mol)	ki (W/(m*K))
Air (i=1)	0,9759	28,9	0,024
Propane (i=2)	0,0241	44	0,0152

Chart 9 – Conductivity calculation.

Calculating the Chapman Enskong coefficients (air, i=1; propane, i=2):

$\varphi_{11} = 1$
$\varphi_{12} = 1{,}5766$
$\varphi_{21} = 0{,}6558$
$\varphi_{22} = 1$

Solving the Chapman Enskong equation: $\boldsymbol{k_{mix} = 0{,}0237\ \frac{W}{m*K}}$

Specific heat

In a gas mix, the specific heat is calculated by:

$$Cp_{mix} = \sum_{i=1}^{n} X_i * Cp_i \qquad [Ec.66]$$

Component	Xi	Cpi (kJ/(mol*K))	Cpi (J/(kg*K))
Air	0,9759	0,029	1003,46
Propane	0,0241	0,075	1704,55

Chart 10 - Specific heat calculation.

$$\boldsymbol{Cp_{mix} = 1020,36\ \frac{J}{kg * K}}$$

Prandtl

$$Pr = \frac{\mu * C_p}{k} = 0,7386$$

Now I have got everything to calculate the convection coefficient:

$$Nu = 0,664 * Re^{\frac{1}{2}} * Pr^{\frac{1}{3}} = \frac{hi * Lc}{k}$$

$h_i = 11,35 \frac{W}{m^2 * K}$
$Ai = 0,080031\ m^2$

$$\boldsymbol{Rconv, i = \frac{1}{hi * Ai} = 1,1011\ \frac{K}{W}}$$

EXTERNAL CONVECTION

$$Rconv, e = \frac{1}{he * Ae} \qquad [Ec.59]$$

$$Ae = 445 * 445 = 0,198025\ m^2$$

Natural convection with air in a vertical flat plate. For calculating the convection coefficient, I relate it with Nusselt number:

$$\mathrm{Nu} = \mathrm{f}(\mathrm{Gr}, \mathrm{Pr}) = \frac{h * Lc}{k} \qquad [Ec.60]$$

For vertical plates:

$$Nu = \left\{ 0{,}825 + \frac{0{,}387 * Ra^{1/6}}{\left[1 + \left(\frac{0{,}492}{Pr}\right)^{9/16}\right]^{8/27}} \right\}^2 \qquad [Ec.67]$$

$$Ra = \frac{g * \beta * (Ts - T\infty) * Lc^3}{v^2} * Pr \qquad [Ec.68]$$

$g = gravity = 9{,}81\ \frac{m}{s^2}$
$Ts = Tsurface = 63{,}7\ °C$
$T\infty = Troom = 21{,}9\ °C$
$Tf = \frac{Ts+T\infty}{2} = 42{,}8\ °C = 315{,}8\ K$
$\beta = \frac{1}{Tf} = 3{,}1666 * 10^{-3}\ \frac{1}{K}$
$v = cinematic\ viscosity\ (at\ Tf.See\ table\ 1\ in\ annex) = 1{,}729 * 10^{-5}\ \frac{m^2}{s}$
$Lc = 0{,}445\ m$
$Pr = Prandtl\ (at\ Tf.See\ table\ 1) = 0{,}7247$
$Ra = 277387447{,}5$

$$Nu = \left\{ 0{,}825 + \frac{0{,}387 * Ra^{1/6}}{\left[1 + \left(\frac{0{,}492}{Pr}\right)^{9/16}\right]^{8/27}} \right\}^2 = 83{,}2218 = \frac{h * Lc}{k}$$

$K\ (at\ Tf.See\ table\ 1) = 0{,}02683\ \frac{W}{m*K}$

$h_e = 5{,}017 \frac{W}{m^2 * K}$

$$\boldsymbol{Rconv,e = \frac{1}{he * Ae} = 1{,}0065\ \frac{K}{W}}$$

CONDUCTION IN FIRE CLAY

$$Rfi.cl = \frac{L_{fi.cl}}{k_{fi.cl} * A_{fi.cl}} \qquad [Ec.56]$$

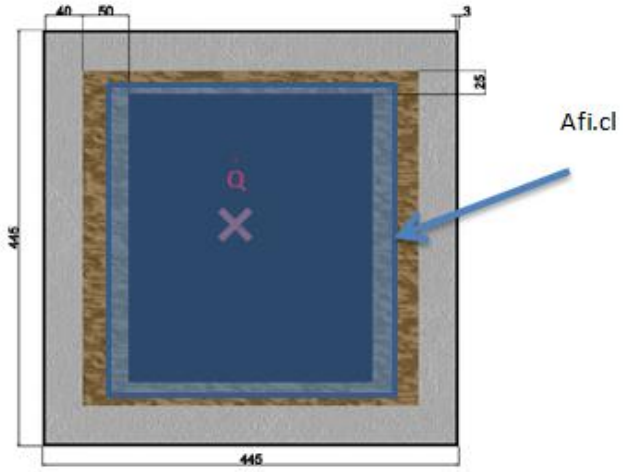

Image 48 - fire clay conduction area in front and behind walls.

$Lfi.cl = 0{,}025\ m$

$Afi.cl = (445 - 2 * 3 - 2 * 40 - 25) * (445 - 2 * 3 - 2 * 40 - 50) = 0{,}103206\ m^2$

$Kfi.cl = 0{,}46\ \frac{W}{m*K}$

$$\boldsymbol{Rfi.cl = 0,526595\ \frac{K}{W}}$$

CONDUCTION IN CALCIUM SILICATE

$$Rca.si = \frac{L_{ca.si}}{k_{ca.si} * A_{ca.si}} \qquad [Ec.57]$$

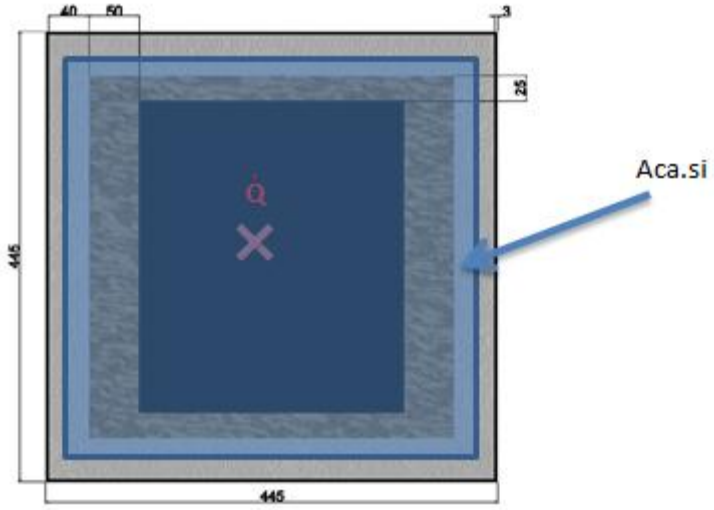

Image 49 - calcium silicate conduction area in front and behind walls.

$$Lca.si = 0{,}04\ m$$

$$Aca.si = (445 - 2 * 3 - 40) * (445 - 2 * 3 - 40) = 0{,}159201\ m^2$$

$$Kca.si = 0{,}09\ \frac{W}{m*K}$$

$$\boldsymbol{Rca.si = 2{,}791719\ \frac{K}{W}}$$

CONDUCTION IN STEEL

$$Rsteel = \frac{L_{steel}}{k_{steel} * A_{steel}} \qquad [Ec.58]$$

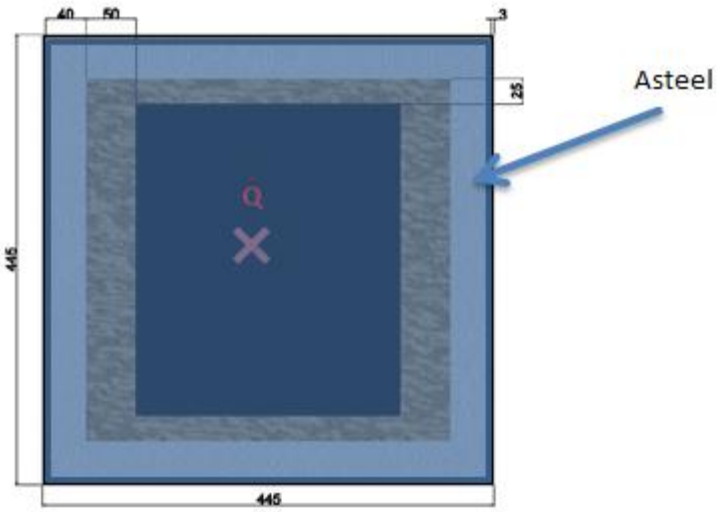

Image 50 - conduction area in front and behind walls.

$$Lsteel = 0{,}003\ m$$

$$Asteel = (445 - 3) * (445 - 3) = 0{,}195364\ m^2$$

$$Ksteel = 52{,}5\ \frac{W}{m*K}$$

$$\boldsymbol{Rsteel = 2{,}9249e - 4\ \frac{K}{W}}$$

TOTAL

$$Rtot = Rconv,i + Rfi.cl + Rca.si + Rsteel + Rconv,e = 5{,}4262\ \frac{K}{W}$$

$$Tint - Text = Q * Rtot$$

$$Tint = 574{,}5\ ℃$$
$$Text = 21{,}9\ ℃$$

$$\boldsymbol{Qfrontal = Qbehind = 101{,}84\ W}$$

4.2.1.2. LATERAL WALLS

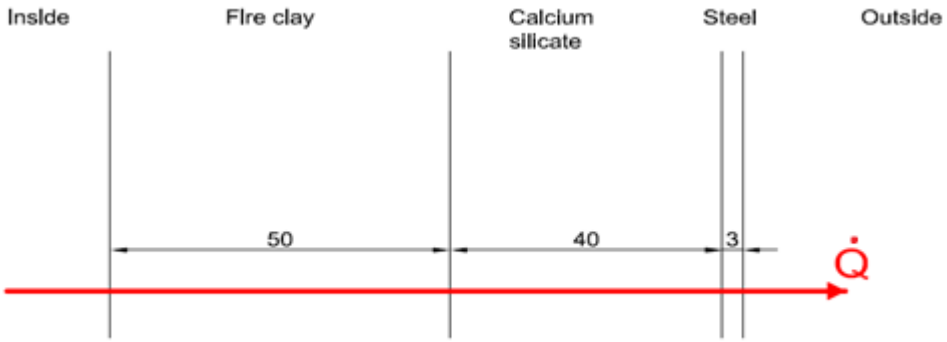

Image 51 - profile for lateral and behind walls.

For determinig the thermal properties in the convection, I use de characteristic length, Lc. For the lateral walls, Lc is the largest length:

Internal convection: $Lc = inner\ height = 445 - 2 * 3 - 2 * 40 - 2 * 25 = 0{,}309\ m$
External convection: $Lc = exterior\ height = 0{,}445\ m$

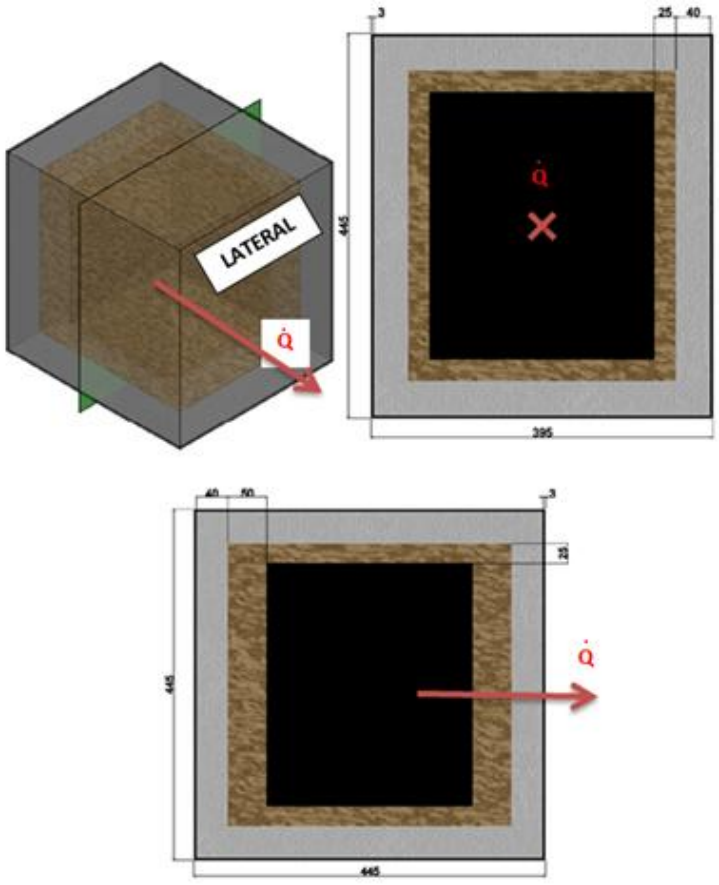

Image 52 - sections for lateral walls.

As the equations for the heat resistances are going to be the same, is not necessary to rewrite them again. The same for the schematics of the fire clay, calcium silicate and steel areas; these areas which are not the same, but are measured in the same way.

INTERNAL CONVECTION

$$Ai = (445 - 2 * 3 - 2 * 40 - 2 * 25) * (395 - 2 * 3 - 2 * 40 - 2 * 25) = 0{,}080031\ m^2$$

As I have got the same Lc, and the "room" is the same (same gas, same forced convection) as in internal convection in frontal and behind walls, the convection coefficient hi is going to be the same.

$h_i = 11{,}35 \frac{W}{m^2 * K}$
$Ai = 0{,}080031\ m^2$

$$\boldsymbol{Rconv, i = \frac{1}{hi * Ai} = 1{,}1009\ \frac{K}{W}}$$

EXTERNAL CONVECTION

$$Ae = 445 * 395 = 0{,}175775\ m^2$$

As I have got the same Lc, and the "environment" is the same (so same air and natural convection) as in external convection in frontal and behind walls, the convection coefficient he is going to be the same.

$h_e = 5{,}017 \frac{W}{m^2 * K}$

$$Rconv, e = \frac{1}{he * Ae} = 1{,}134 \frac{K}{W}$$

CONDUCTION IN FIRE CLAY

$Lfi.cl = 0{,}05\ m$

$$Afi.cl = (445 - 2 * 3 - 2 * 40 - 25) * (395 - 2 * 3 - 2 * 40 - 25) = 0{,}094856\ m^2$$

$Kfi.cl = 0{,}46\ \frac{W}{m * K}$

$$\boldsymbol{Rfi.cl = 1{,}145902\ \frac{K}{W}}$$

CONDUCTION IN CALCIUM SILICATE

$Lca.si = 0{,}04\ m$

$Aca.si = (445 - 2*3 - 40)*(395 - 2*3 - 40) = 0{,}139251\ m^2$

$Kca.si = 0{,}09\ \frac{W}{m*K}$

$$\boldsymbol{Rca.si = 3{,}19168\ \frac{K}{W}}$$

CONDUCTION IN STEEL

$Lsteel = 0{,}003\ m$

$Asteel = (445 - 3)*(395 - 3) = 0{,}173264\ m^2$

$Ksteel = 52{,}5\ \frac{W}{m*K}$

$$\boldsymbol{Rsteel = 3{,}298e\ -4\ \frac{K}{W}}$$

TOTAL

$$Rtot = Rconv,i + Rfi.cl + Rca.si + Rsteel + Rconv,e = 6{,}5728\frac{K}{W}$$

$$Tint - Text = Q * Rtot$$

$$Tint = 574{,}5\ ℃$$
$$Text = 21{,}9\ ℃$$

$$\boldsymbol{Qlateral,right = Qlateral,left = 84{,}07\ W}$$

4.2.1.3. TOP AND BOTTOM WALLS

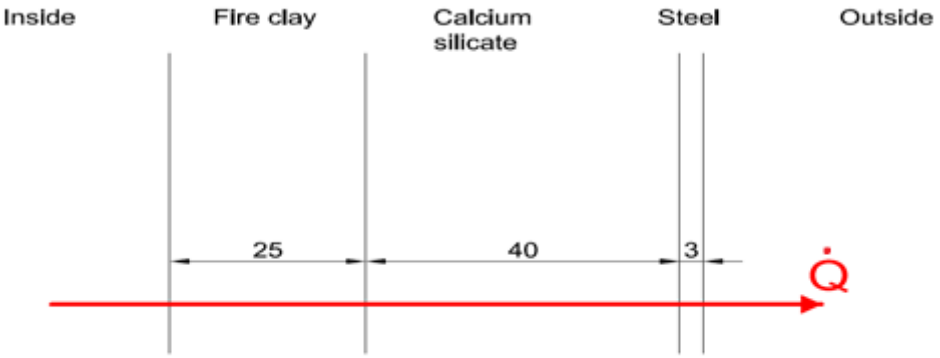

Image 53 - Profile for top and bottom walls.

For determinig the thermal properties in the convection, I use de characteristic length, Lc. For the top and bottom walls, Lc is the largest length:

Internal convection: $Lc = inner\ width = 445 - 2 * 3 - 2 * 40 - 2 * 50 = 0{,}259\ m$
External convection: $Lc = exterior\ width = 0{,}445\ m$

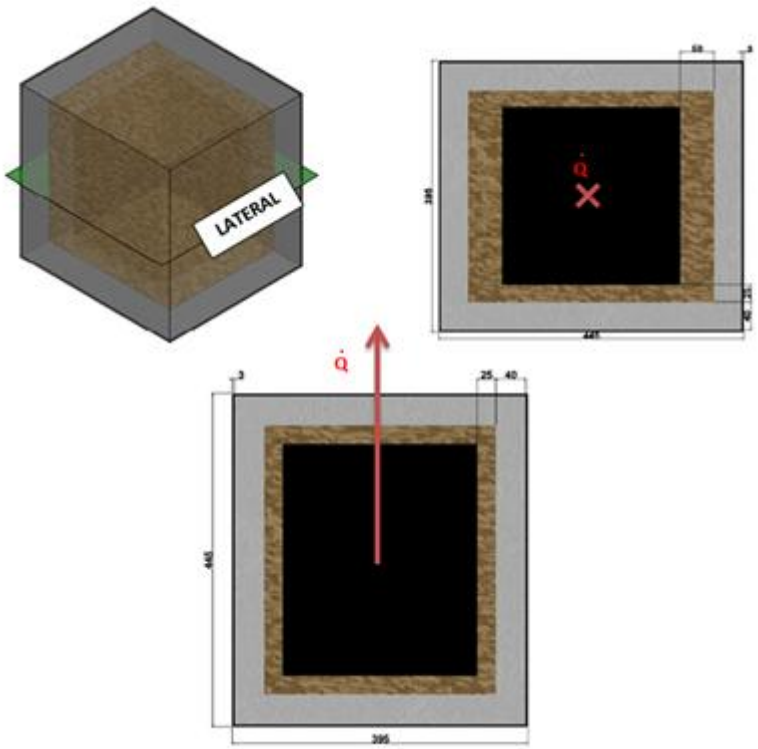

Image 54 - Sections for top and bottom walls.

As the equations for the heat resistances are going to be the same, is not necessary to rewrite them again. The same for the schematics of the fire clay, calcium silicate and steel areas; these areas which are not the same, but are measured in the same way.

INTERNAL CONVECTION

$$Ai = (445 - 2*3 - 2*40 - 2*50)*(395 - 2*3 - 2*40 - 2*25) = 0{,}067081\ m^2$$

As I have got the same gas mix as in the two previous analysis, the characteristic of this gas are the same (density, viscosity, convection speed…); however, the Lc is different for the internal convection (259 mm instead of 309), so Re is going to be different, and Nusselt as well.

$$Re = \frac{\rho * v * L}{\mu} \qquad [Ec.61]$$

$\rho_{air+propane} = 1{,}218\ \frac{kg}{m^3}$
$v = 2{,}77\ \frac{m}{s}$
$\mu_{mix} = 1{,}7156 * 10^{-5}\ \frac{kg}{m*s}$
$Lc = 0{,}259\ m$
$Re = 50934 < 5 * 10^5$ ➔ laminar flow

So I have got forced convection in a flat plate, with laminar flow. The equation which governs this convection regime is:

$$Nu = 0{,}664 * Re^{\frac{1}{2}} * Pr^{\frac{1}{3}} = \frac{hi * Lc}{k}$$

I have already calculated Pr and k for the gas mix:

$Pr_{mix} = 0{,}7438$
$k_{mix} = 0{,}0234\ \frac{W}{m*K}$

$$Nu = 135{,}78$$

$h_i = 12{,}27\ \frac{W}{m^2*K}$
$Ai = 0{,}067081\ m^2$

$$\boldsymbol{Rconv,i = \frac{1}{hi * Ai} = 1{,}2152\ \frac{K}{W}}$$

EXTERNAL CONVECTION

$$Ae = 445 * 395 = 0{,}175775\ m^2$$

As I have got the same Lc (Lc = 0,445 m), and the "environment" is the same (so same air and natural convection) as in external convection in lateral, frontal and behind walls, the convection coefficient he is going to be the same.

$h_e = 5{,}017 \frac{W}{m^2 * K}$

$$\boldsymbol{Rconv,e = \frac{1}{he * Ae} = 1{,}134 \frac{K}{W}}$$

CONDUCTION IN FIRE CLAY

$Lfi.cl = 0{,}025\ m$

$Afi.cl = (445 - 2 * 3 - 2 * 40 - 50) * (395 - 2 * 3 - 2 * 40 - 25) = 0{,}087756\ m^2$

$Kfi.cl = 0{,}46 \frac{W}{m*K}$

$$\boldsymbol{Rfi.c = 0{,}61931 \frac{K}{W}}$$

CONDUCTION IN CALCIUM SILICATE

$Lca.si = 0{,}04\ m$

$Aca.si = (445 - 2 * 3 - 40) * (395 - 2 * 3 - 40) = 0{,}139251\ m^2$

$Kca.si = 0{,}09 \frac{W}{m*K}$

$$\boldsymbol{Rca.si = 3{,}19168 \frac{K}{W}}$$

CONDUCTION IN STEEL

$Lsteel = 0{,}003\ m$

$Asteel = (445 - 3) * (395 - 3) = 0{,}173264\ m^2$

$Ksteel = 52{,}5 \frac{W}{m*K}$

$$\boldsymbol{Rsteel = 3{,}298e\ -4 \frac{K}{W}}$$

TOTAL

$$Rtot = Rconv,i + Rfi.cl + Rca.si + Rsteel + Rconv,e = 6{,}1605\,\frac{K}{W}$$

$$Tint - Text = Q * Rtot$$

$$Tint = 574{,}5\ ℃$$
$$Text = 21{,}9\ ℃$$

$$\boldsymbol{Qtop = Qbottom = 89{,}7\ W}$$

4.2.1.4. TOTAL LOSSES

$$Qtotal = Qtop + Qbottom + Qlateral,right + Qlateral,left + Qfrontal + Qbehind$$

$$\boldsymbol{Qtotal = 89{,}7 + 89{,}7 + 84{,}07 + 84{,}07 + 101{,}84 + 101{,}84 = 551{,}22\ W}$$

4.2.2. HEAT LOSS DUE TO THE SENSIBLE HEAT OF EXHAUST GASES, P_{sh}

The exhaust gases leave the burning room at very high temperature, so they sweep along a high amount of hot that therefore cannot be used for increasing the heater temperature.
This is, probably, the most important heat loss. It is produced due to the temperature and volume of the exhaust gases that goes out from the burning room: the higher temperature and volume of the gases, the lower efficiency. A too high temperature in these gases can be because of two reasons:

- The burner produces more heat than the necessary for the specific charge of the engine.
- The engine's heater does not work property and does not absorb enough heat to warm up the air inside the engine.
- Most of the heat that is not used to warm up the heater of the engine (and therefore, the air), is wasted in heating the exhaust gases. When the temperature of the fumes is higher than the room temperature, these fumes are transporting not-used energy.

$$P_{sh} = \dot{m}_{fumes} * C_{p,fumes} * \left(T_{fumes} - T_{\infty}\right)\ [W] \qquad [Ec.\,69]$$

Where

$\dot{m}_{fumes} = exhaust\ gases\ flow\ \left[\frac{kg}{s}\right]$

$C_{p,fumes} = specific\ heat\ of\ exhaust\ gases\ [\frac{J}{kg*ºC}]$

$T_{fumes} = temperature\ of\ the\ exhaust\ gases\ at\ the\ exit\ of\ the\ burning\ room$

$T_\infty = reference\ temperature$

In this case, the fumes do not go to the laboratory (whose temperature is defined by T_∞. The exhaust gases go to the outside of the laboratory. In this case, we take $T_\infty = 15\ ºC$.
As seen in Test 300513-7, $T_{fumes} = 452\ ºC$.

Using the chart 6 of the convection and conduction heat losses:

Component	mol/min	g/mol	$\frac{g}{min} = \frac{mol}{min} * \frac{g}{mol}$
CO_2	0,42	44	18,48
H_2O	0,56	18	10,08
N_2	2,63	28	73,64
Air	2,166	28,9	62,6

$$\dot{m}_{fumes} = (18{,}48 + 10{,}08 + 73{,}64 + 62{,}6)\frac{g}{min} * \frac{1min}{60s} * \frac{1kg}{1000g} = 2{,}7467 \cdot 10^{-3}\frac{kg}{s}$$

For calculating the specific heat of the gas mix, we have the following equation:

$$Cp_{mix} = \sum_{i=1}^{n} X_i * Cp_i \qquad [Ec.66]$$

Where Xi is the molar fraction of each component. This molar fractions are calculated in the following table; the Cp,i is calculated using the chart A3.1 in the annex, at temperature of 452 ºC.

Component	mol/min	$X_i = \frac{(mol/min)_i}{(mol/min)_{total}}$	Cpi (J/kg°C)
CO_2	0,42	0,0727	1134,9
H_2O	0,56	0,097	2102,9
N_2	2,63	0,455	1108
Air	2,166	0,375	1081,5

Chart 11 - Calculation of the specific heat of the fumes.

Therefore, $C_{p,fumes} = 1196{,}19\ \frac{J}{kg*ºC}$

$$P_{sh} = \dot{m}_{fumes} * C_{p,fumes} * (T_{fumes} - T_{\infty}) = 2,7467 \cdot 10^{-3} * 1196,19 * (452 - 15)$$
$$= 1435,8 \frac{J}{s} = 1435,8\ W$$

So, as we can see, this amount of heat lost is really high, higher even than the heat lost through the walls of the burning room.

4.2.3. HEAT LOSS DUE TO LATENT HEAT OF EXHAUST GASES, P_{lh}

In the combustion of the propane, one of the products is water vapor, due to the H_2 of the fuel that reacts with the O_2 of the air. Moreover, this air has a certain relative humidity, which means that also contains some water. By the chemical characteristics of the water, the greater part of its enthalpy is due to the latent heat of vaporization. In the combustion, this heat is used only if the temperature of the exhaust gases is below the condensation temperature of water at atmospheric pressure, i.e., at 100 ° C, which is not true in this case.

This loss is one of the most obvious; part of this overheated steam produced escapes through the porous layers of the burning room (fire clay and calcium silicate), and comes into contact with the inner surface of the steel layer, which is at a temperature below 100 °C; the consequence of this is the condensation of this vapor, which comes out the burning room as water, what we can see when the engine is running.

$$P_{lh} = \dot{m}_{H20} * h_{fg} \qquad [Ec.70]$$

Where

$\dot{m}_{H20} = steam\ flow\ produced\ in\ the\ combustion\ \left[\frac{kg}{s}\right]$

$h_{fg} = vaporization\ enthalpy\ at\ T = \frac{T_{fumes}+T_{\infty}}{2}\ \left[\frac{kJ}{kg}\right]$

$\dot{m}_{H20}$ can be seen in the chart 6:

$$\dot{m}_{H20} = 0{,}56\ \frac{mol}{min} * 18\ \frac{g}{mol} * \frac{1kg}{1000g} * \frac{1min}{60s} = 1{,}68 \cdot 10^{-4}\frac{kg}{s}$$

To calculate h_{fg} we use the table A3.3 in the annex:

$$T = \frac{T_{fumes} + T_{\infty}}{2} = \frac{452 + 15}{2} = 233{,}5\ ºC$$

$$h_{fg} = 1797{,}2\frac{kJ}{kg}$$

$$\boldsymbol{P_{lh} = \dot{m}_{H20} * h_{fg} = 1{,}68 \cdot 10^{-4} * 1797{,}2 = 0{,}3019\frac{kJ}{s} = 301{,}9\ W}$$

4.2.4. OTHER HEAT LOSSES IN THE BURNING ROOM

There are more losses that are difficult to calculate, because we do not have the necessary equipment for measuring some parameters.

One of those losses is the one due to the air excess. For the combustion of the propane, we need a stoichiometric amount of air, as we can see in the combustion of propane in Annex 1.

For security reasons, always is necessary to have an amount of air higher than the stoichiometric, to ensure that there is no incomplete combustion and therefore it is not produced carbon monoxide, a dangerous gas.

However, this excess of air is counterproductive in the efficiency of the combustion chamber. The heat released in the combustion of propane is independent of the amount of air used, provided that it is at least equal to the stoichiometric. However, the use of such heat is inversely proportional to the increase of excess air, as part of the combustion heat is used in heating the fumes, and these fumes increase its volume with increasing the excess of air (as this air does not contribute in the combustion and goes directly to join them), and consequently decreases the maximum attainable temperature in the burning room.

As we can see in the real combustion of propane, we have 5,5 mol/min of air, and in the combustion only takes part 3,33 mol/min. Therefore, we have the 165% of the needed air, or what is the same, an excess of air of the 65%.

Another heat loss is the one due to the leakage in the burning room, that causes that air from the outside comes into the burning room, reducing the temperature inside, and vice versa, air from the inside of the burning room goes out.

Another heat loss is because of radiation. The burning room is a higher temperature than the rest of elements in the laboratory, and therefore there is a heat exchange between all of them. Because of the big amount of objects in the laboratory, the presence of people (who are at different temperature also than the rest of things), the windows, central heating,… it results very difficult to calculate properly the heat losses because of radiation.

Finally, the last heat loss that is important to mention is the one due to the unburned fuel. As we have seen, there is an excess of air of 65%, so we can suppose that the combustion happens completely and therefore there is no unburned fuel.

4.2.5. TOTAL LOSSES AND EFFICIENCY OF THE BURNING ROOM

If we summarize the heat losses in the burning room, we have:

- Heat loss due to the conduction and convection through the walls, P_{cc} = 551,22 W.
- Heat loss due to the sensible heat of exhaust gases, P_{sh} = 1435,8 W.
- Heat loss due to the latent heat of exhaust gases, P_{lh} = 301,9 W.
- Other heat losses (due to air excess, leakage, radiation, unburned fuel, etc.; uncalculated).

In the test 300513-7, in which all of these study is based, we got a propane flow of 0,1 g/s. The net calorific value for propane is 11080 kcal/kg.

$$\dot{Q}_{propane} = 0{,}1\frac{g}{s} * \frac{1kg}{1000g} * 11080\frac{kcal}{kg} * \frac{0{,}00116222222kWh}{1kcal} * \frac{3600s}{1h} = 4{,}64\ kW$$

In total, heat losses:

$$\dot{Q}_{losses} = P_{cc} + P_{sh} + P_{lh} = 551{,}22 + 1435{,}8 + 301{,}9 = 2288{,}92\ W$$

$$\boldsymbol{\varepsilon_{burning\ room} = \frac{useful\ heat}{total\ heat} = \frac{\dot{Q}_{propane} - \dot{Q}_{losses}}{\dot{Q}_{propane}} = \frac{4640 - 2288{,}92}{4640} * 100 = 50{,}67\%}$$

Therefore, we can see that more than the half of the heat supplied by the propane is lost because of many different reasons. This entails negative economic consequences, because we are wasting 50% of the propane we use. It would be interesting from the point of view of efficiency decreasing these losses as much as possible:

- Have a better insulation
- Use less excess of air
- Ensure the best possible seal in the combustion chamber
- Use more efficient combustion gas than propane
- Recover part of the heat lost in the exhaust gases
- Use for the combustion air with the lowest possible moisture

4.3. EFFICIENCY OF THE ENGINE

Now that is known the efficiency of the burning room, is important to see where the rest of the losses of our engine happen.

Following is made an analysis of losses, as the one made for the burning room; to make this analysis, I am going to use the same data than for the analysis of burning room: the data got in the test of the engine of the 30th of May with a load pressure of 7 bars (Experiment 4, chapter 7).

In that test, we got a propane flow of 0,1 g/s. The net calorific value for propane is 11080 kcal/kg.

$$\dot{Q}_{propane} = \dot{Q}_{total} = 0{,}1\frac{g}{s} * \frac{1kg}{1000g} * 11080\frac{kcal}{kg} * \frac{0{,}00116222222kWh}{1kcal} * \frac{3600s}{1h}$$

$$\dot{Q}_{total} = 4{,}64\ kW$$

Therefore, if, as estimated, $\eta_b = 50\%$:

$$Q_{in} = Q_{total} - L_b = 4640 - 2288{,}92 = 2351{,}08\ W = Q_{reject} + L_i$$

The rejected heat, Q_{reject} is calculated using a specific heat of the cooling water, an inlet water temperature, T_{in}, an outlet water temperature, T_{out} and a water mass flow, $\dot{m}_w$.

$$Q_{reject} = C_{water} * \dot{m}_w * (T_{out} - T_{in}) \qquad [Ec.71]$$

$$C_{water} = 4187\ \frac{J}{kg \cdot K}$$

As seen in the experiment 4:

$$T_{out} = 303{,}4\ K$$

$$T_{in} = 298{,}6\ K$$

$$\dot{m}_w = 5{,}075\ \frac{L}{min} \cdot \frac{1kg}{1L} \cdot \frac{1min}{60s} = 0{,}084583\ \frac{kg}{s}$$

Therefore:

$$Q_{reject} = C_{water} * \dot{m}_w * (T_{out} - T_{in}) = 4187 * 0{,}084583 * (303{,}4 - 298{,}6)$$

$$\boldsymbol{Q_{reject} = 1699{,}9\ W}$$

As we see, this is a very high amount of heat; in fact, it is the 73% of the heat that goes inside the engine, and the 37% of the heat that provides the propane in the burning room. It is a huge heat spending, but necessary, because is very important to cold down air inside the engine, the more as possible.

$$L_i = Q_{in} - Q_{reject} = 2351{,}08 - 1699{,}9 = 651{,}18\ W = \ L_s + L_m$$

As we see in the results collected by DIAdem:

$$L_s = power\ output = 188{,}26\ W$$

Therefore

$$\boldsymbol{L_m = L_i - L_s = 620{,}1 - 188{,}26 = 462{,}92\ W}$$

These mechanical losses suppose the 19% of the power that goes inside the engine; so we can see that is not a very high value, compared with other losses of the system.

At the end, only the 4% of the total power supplied by the propane is converted into the output power. This is a very small amount, that can make think about if it is worth to spend so much propane for getting so less power, or not.

4.4. SUMMARY OF LOSSES

As we have seen, the half of the heat supplied by the propane is lost in the burning room; the other half enters the engine, but of course does not go directly to the power output; inside the engine, there are other losses, that make the efficiency of the engine to be so low. This losses are, mainly, because of friction, and because of the necessary of cooling part of the engine.
Below is shown the real Sankey diagram for the system engine + burning room in the laboratory.

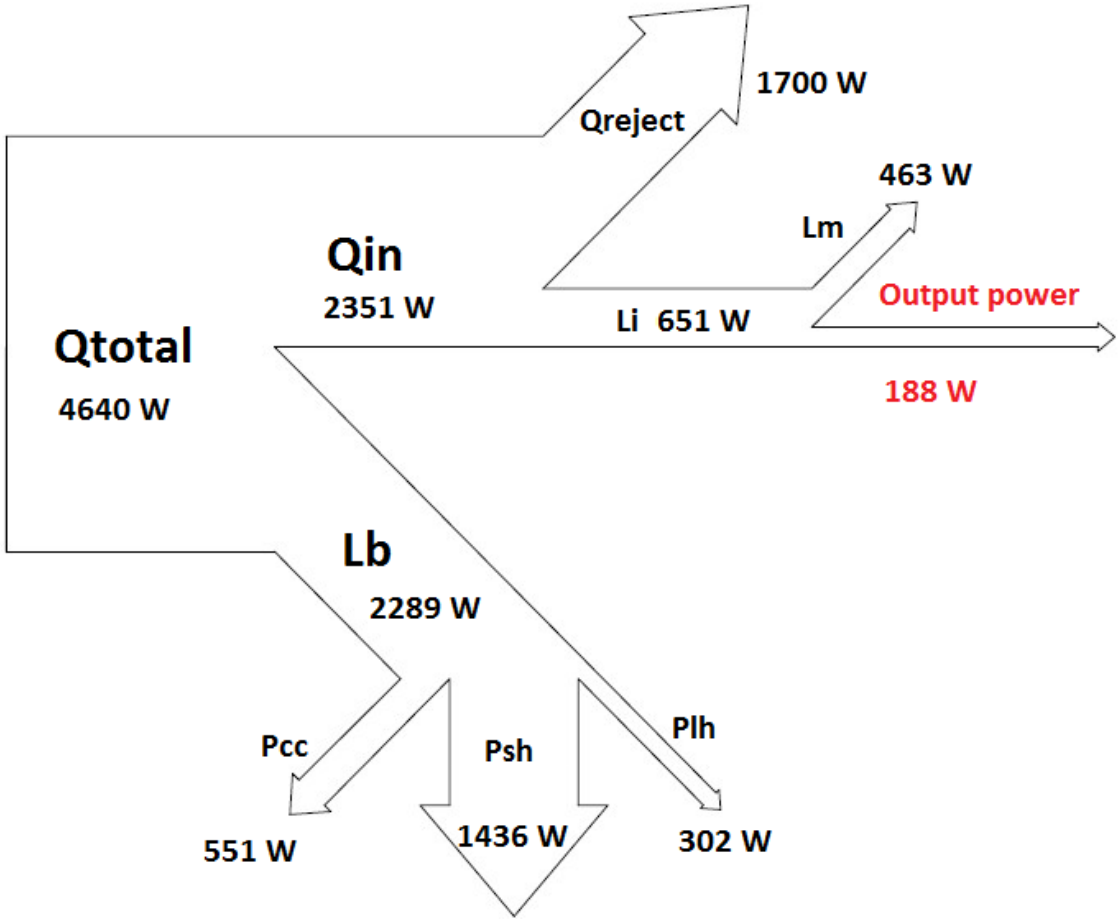

Image 55 - Sankey diagram for the engine in the laboratory.

5. STIRLING ENGINES WORKING WITH TWO-PHASE TWO-COMPONENT WORKING FLUIDS

5.1. INTRODUCTION

As we have mentioned in the chapter 3.4.3, one of the possible working fluids in Stirling engines is a compound working fluid. This kind of fluids, also named TPTC (two-phase two-component), consist basically in the incorporation of a phase-changing component in the normal working fluid, to enhance the power density of the engine.

In the TPTC working fluids, the carrier component remains gaseous during the whole cycle, while the another component changes its phase from liquid to vapor in moving from the cold space to the hot space through the regenerator (absorbing heat from the regenerator), and vice versa, it condensates when going again from the hot to the cold space (giving back the heat to the regenerator).

The great advantage of this type of working fluid is that, for the same same conditions of maximum and minimum temperatures (which determine the material and therefore cost), volume (which determines the size) and maximum pressure (which determines the weight), the area of the P-V diagram is increased, more the greater is the amount of condensing component. Therefore, in the same engine, with the same size, weight and cost, we could increase the power output. The explanation for this is simple: in the liquid-to-vapor phase change of the phase-changing component, it is caused an increase in the volume compression ratio of the cycle, with a consequent improvement in the pressure ratio and work output. This increase in the volume ratio causes an increase in the amplitude in the cyclic pressure excursion, i.e. in the area of the work diagram. We will analyze this following.

Throughout history, many authors have conducted various studies on Stirling engines working with TPTC working fluids.

Walker and Agbi (1973) and Metwally (1977) gave a solution using first-order methods, similar to the Schmidt analysis but with certain modifications. Years later, in 1981, Renfroe realized an adiabatic analysis using third-order equations. For reasons of computational cost, this project will approach the first order method developed by Walker and Agbi, being the model equations easily integrated without using numerical methods.

5.2. ISOTHERMAL ANALYSIS WITH TPTC WORKING FLUID

As in the case of using gaseous working fluid, the engine cycle can be split into various different processes. For this explanation, is considered the start point of the cycle as the compression process. The hot compressed gaseous mixture enters the regenerator and gives heat to the regenerator matrix material. At the low temperature end of the regenerator the condensable fluid changes its phase from vapor to liquid. During the expansion stroke, as the displacer moves away from the cold end, the suction occurs and simultaneously the pressure level continues to drop due to increasing volume of the expansion space. The condensed fluid is dragged by the carrier gas into the expansion space. Depending on the composition a certain quantity of the condensable fluid goes through the reverse phase change in the presence of the carrier gas till the saturation condition occurs.

Schmidt analysis, with some modifications, is suitable for two-phase two-component (TPTC) working fluids.

We assume that the composite working fluid consists of two components, one that works all the time as an ideal gas, and the other works as a liquid in the compression zone, at low temperature, and as an ideal gas in the expansion zone, at high temperature. The specific mass ratio, β, is assumed to remain constant in the system and is not affected by phase changes.

For our analysis, which will be put into practice in the laboratory, we will take as gaseous component air, and as phase-changing component water (liquid and vapor).

In the Schmidt conventional analysis, the regenerator temperature has a linear profile. For the engine working with TPTC working fluid, we assume that the dead space of the regenerator is divided into two zones, one at expansion temperature T_e and another at compression temperature T_c, so that the total mass of working fluid in the regenerator is divided equally between the two areas. At the interface, we assume that there is a jump in temperature accompanied by a phase change in one of the components of the working fluid; in addition, we assume that the interface moves so that there is equal mass of fluid work in the two areas at all times. There is no physical explanation for this assumption, simply it was taken to facilitate the calculus, and probably it will be needed to improve in future.

The total pressure p is the sum of the partial pressures of the two components, and is considered to be instantaneously constant throughout the system, namely:

$$p = p_{ae} + p_{we} = p_{ac} + p_{wc}$$

Where

p_{ae}: $partial\ pressure\ of\ air\ in\ the\ expansion\ space$
p_{we}: $partial\ pressure\ of\ water\ (vapor)\ in\ the\ expansion\ space$
p_{ac}: $partial\ pressure\ of\ air\ in\ the\ compression\ space$
p_{wc}: $partial\ pressure\ of\ water\ (liquid)\ in\ the\ compression\ space$

p_{wc} is considered zero at all times, and the liquid volume is considered negligible and therefore, in the compression zone, $p = p_{ac}$.

It should be clear that the assumption of a constant β is probably not applicable in reality, as the steam component will tend to move all the way from the hot zone to the cold zone expansion of compression; this should be compensated, for example with gravity, positioning the engine so that the compression zone is above the expansion one. For our engine, is positioned properly, as we can see in the next picture:

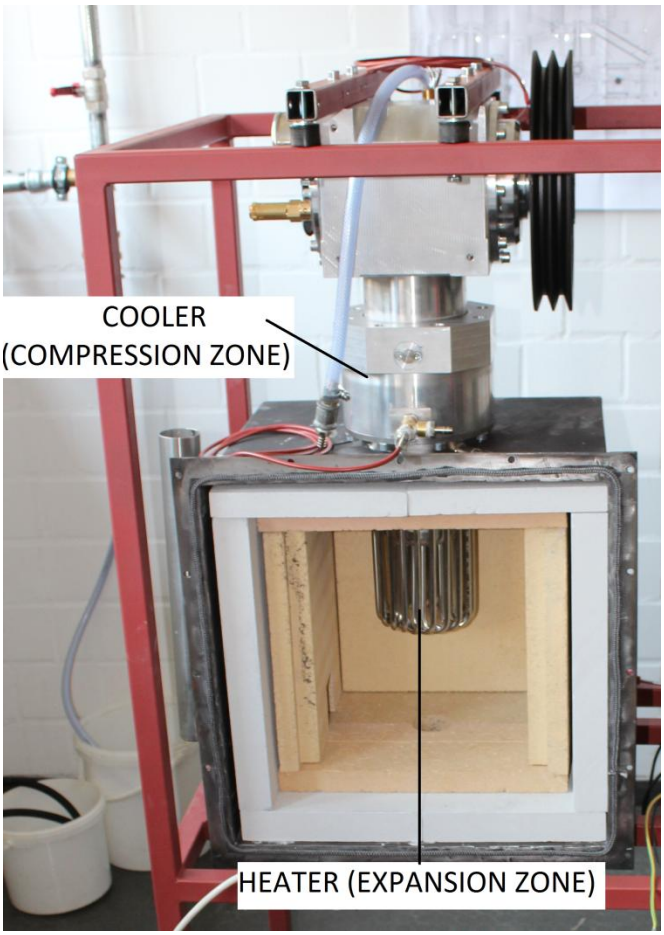

Image 56 - Arrangement of the compression zone above the expansion zone in the Stirling engine of our laboratory.

Walker and Agbi, in 1974, used the Schmidt isothermal analysis to test the effects of ß factor on the main parameters of the Stirling engine. With very simplifying assumptions that will be presented later, and assuming homogenous relationship ß throughout the volume, they reached the following conclusions:

- In the compression and heating, water evaporation supposes an increase in the number of moles in the gas phase, a fact that causes an additional increase of the maximum pressure of the cycle. Growing cycle area and consequently more power is obtained.

- Boiling and condensation increase the heat capacity of the working fluid, which improves heat transfer and makes the cycle closer to the isothermal. This also contributes to the increase in thermodynamic work.
- The effect of ß on power is not always the same. If ß grows, the power goes through a maximum and back down. Moreover, this positive effect of the presence of condensing fluid only happens when the heater temperature, T_{max}, is moderate. For high temperatures, growth of ß is detrimental, as seen in Fig.
- ß gain reduces the effect of variations of T_{max} and the dead volume of the engine in power. This provides greater ease of control and freedom of design of heat exchangers, respectively.

The working fluid tends to accumulate more in the compression chamber than in the expansion, which forces constructing the first smaller than the second, to compensate for the effect and maintain the power level. The mass increase in the compression chamber makes the flows faster and, therefore, there are more friction losses.

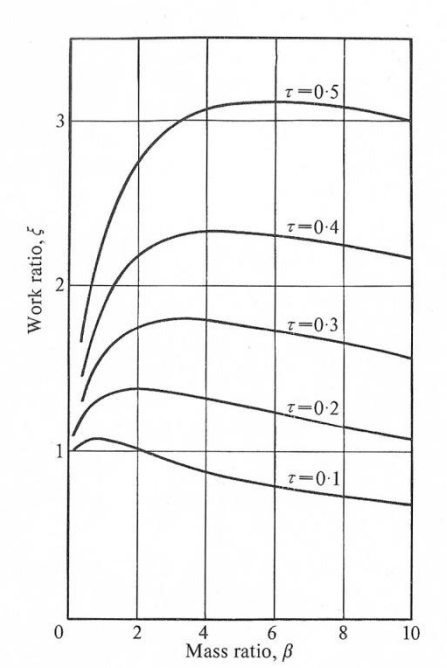

Image 57 - Effect of mass ratio of compound working fluids in output. Effect of temperatures.

Experimentation has identified the following advantages and disadvantages of compound working fluids in Stirling engines:

- The presence of fluid in the cylinder walls facilitates the seal and acts as a lubricant, extending the life of the shutters.
- The liquid tends to accumulate in the compression chamber, leaving out the cycle and reducing ß. It is necessary to design the motor so that the liquid falls by gravity to the regenerator, so that it is recirculated.

- If ß = 4, i.e. in the absence of carrier gas, the problem of nonhomogeneity disappears. Water and steam are not the best candidates for this option, but there are other fluids that can be self-supporting as the working fluids with phase change.

In view of the effects of the composite working fluid on the behavior of the motors we can sense their possible applications. In automotive engines they can reduce P_{max} (which results in a weight reduction) without loss of potency. It may also be useful in low ΔT Stirling engines (temperature difference), both motor and non-cryogenic refrigerators.

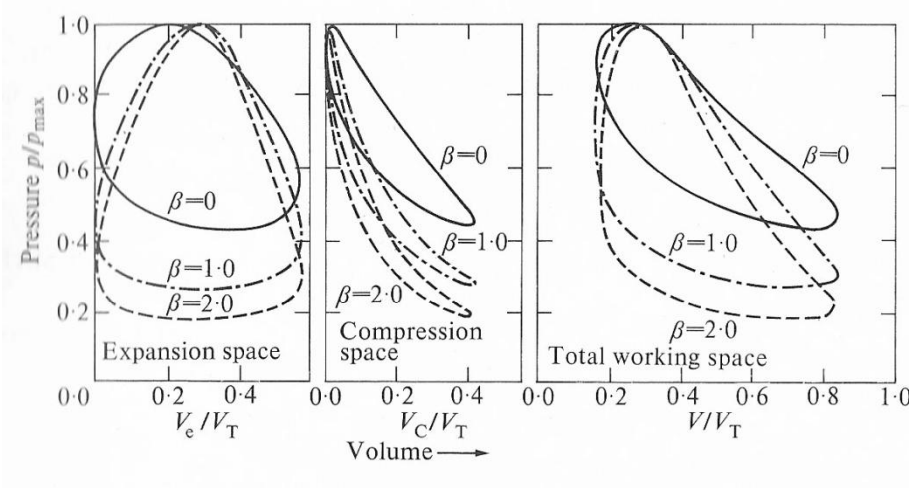

Image 58 - Work diagrams for Schmidt cycle system with compund working fluid.

5.2.1. ANALYTICAL ANALYSIS

Following we will carry out the analytical Schmidt analysis for Stirling engines working with TPTC fluids.

These are the main assumptions:

- Perfect regenerative process.
- Isothermal compression at T_c and expansion at T_e.
- Sinusoidal volume variations in compression and expansion spaces.
- Water in the liquid state at T_c exists with negligible volume and partial pressure.
- Water in the vapor state at T_e exists in the superheated vapor state and behaves as a perfect gas, according to the ideal gas equation, $p_w V = m_w R_w T$.
- Air behaves all the time as a perfect gas, according to the ideal gas equation, $p_a V = m_a R_a T$.
- Total mass of working fluid distributed between the compression, expansion and dead spaces remains constant.
- The ratio of mass of water to air, β, is constant and uniform throughout the system.
- The instantaneous total pressure of the working fluid is uniform throughout the system.

- The total mass of working fluid in the dead space is divided equally into two parts, one at T_c and the other at T_e. At the interface there is a phase change of water from superheated vapor to liquid.
- Constant rotational speed.
- Steady state conditions in the engine operation; therefore, volumes and pressure are subjected to cyclic variation, and exists equilibrium between components and phases all the time.

The development of the analysis is similar to the Schmidt analysis made in **chapter 2,** with light variations.

VOLUME

Expansion space

$$V_e = V_{cle} + \frac{1}{2}V_{swe}(1+\cos(\theta)) \qquad [Ec.20]$$

Compression space

$$V_c = V_{clc} + \frac{1}{2}V_{swc}(1+\cos(\theta-\alpha)) \qquad [Ec.19]$$

PRESSURE

Instantaneous pressure

$$\frac{p}{p_{max}} = \frac{1-\delta}{1+\delta\cos(\theta-\varphi)} \qquad [Ec.72]$$

Pressure ratio

$$\frac{p_{max}}{p_{min}} = \frac{1+\delta}{1-\delta} \qquad [Ec.73]$$

Where

$A = (K^2 + \kappa^2 + 2\kappa K\cos\alpha)^{1/2}$
$B = K + \kappa + 2S$
$\delta = \frac{A}{B}$
$S = \frac{2KX}{1+K}$
$K = \frac{\tau}{1+\beta N}$ $\qquad N = {}^{M_a}/_{M_w}$ $\qquad \varphi = \tan^{-1}\left(\frac{\kappa\sin\alpha}{K+\kappa\cos\alpha}\right)$

WORK DONE

Expansion space

$$\frac{P_e}{p_{max}V_T} = \frac{\pi}{2}\left(\frac{1}{1+\kappa}\right)\left(\frac{1-\delta}{1+\delta}\right)^{\frac{1}{2}}(\Delta\sin(\theta)) \qquad [Ec.74]$$

Compression space

$$\frac{P_c}{p_{max}V_T} = \frac{\pi}{2}\left(\frac{1}{1+\kappa}\right)\left(\frac{1-\delta}{1+\delta}\right)^{\frac{1}{2}}(\Delta\sin(\theta-\alpha)) \qquad [Ec.75]$$

Net cycle work

$$P = P_e + P_c = (1-K)P_e \qquad [Ec.76]$$

HEAT TRANSFERRED

There are no adequate expressions for the heat transfer. In the simple Schmidt analysis, the equality $dQ = \int pdV$ works because the fluid is considered a perfect gas, and the compression and expansion are assumed isothermal. With a TPTC working fluid the equality is not valid, because part of the fluid is not a perfect gas in the compression space. The heat transferred may best be estimated by consideration of the enthalpy or entropy changes for the unsteady flow two-fluid systems, represented by the expansion and compression spaces, considered separately. In this thesis, thanks to the various assumptions (particularly those of isothermal compression and expansion) we can consider a cycle efficiency equivalent to the Carnot value, as in the case of simple Schmidt analysis. In that case:

$$\eta = \frac{P}{Q_e} = 1 - \tau \qquad [Ec.27]$$

MASS DISTRIBUTION

Expansion space

$$\frac{m_e}{m^*} = (1+\beta)\frac{K}{2}\left[\frac{1-\delta}{1+\kappa}\right] * \left[\frac{1+\cos(\theta)}{1+\delta\cos(\theta-\varphi)}\right] \qquad [Ec.77]$$

And the mass velocity

$$\frac{d\left({}^{m_e}/_{m^*}\right)}{d\theta} = (1+\beta)\frac{K}{2}\left[\frac{1-\delta}{1+\kappa}\right] * \left[\frac{\delta\sin(\theta-\varphi) - \delta\sin(\varphi) - \sin(\theta)}{(1+\delta\cos(\theta-\varphi))^2}\right] \qquad [Ec.78]$$

Where the characteristic mass

$$m^* = \frac{p_{max} V_T}{R_a T_c}$$

Compression space

$$\frac{m_c}{m^*} = (1+\beta)^\kappa \frac{K}{2}\left[\frac{1-\delta}{1+\kappa}\right] * \left[\frac{1+\cos(\theta-\alpha)}{1+\delta\cos(\theta-\varphi)}\right] \qquad [Ec.79]$$

And the mass velocity

$$\frac{d\left({}^{m_e}/_{m^*}\right)}{d\theta} = (1+\beta)^\kappa \frac{K}{2}\left[\frac{1-\delta}{1+\kappa}\right] * \left[\frac{\delta\sin(\theta-\varphi)-\sin(\varphi-\alpha)-\sin(\theta-\alpha)}{(1+\delta\cos(\theta-\varphi))^2}\right] \qquad [Ec.80]$$

Dead space

$$\frac{m_{de}}{m^*} = XK\frac{(1+\beta)}{(1+\kappa)}\left(\frac{1-\delta}{1+K}\right) * \frac{1}{1+\delta\cos(\theta-\varphi)} \qquad [Ec.81]$$

Since

$$\frac{m_d}{m^*} = \frac{2m_{de}}{m^*}$$

The mass velocity

$$\frac{d\left({}^{m_d}/_{m^*}\right)}{d\theta} = 2\left(\frac{1+\beta}{1+\kappa}\right)\left(\frac{KX}{1+K}\right) * \left[\frac{(1-\delta)(-\delta\sin\theta-\varphi)}{(1+\delta\cos(\theta-\varphi))^2}\right] \qquad [Ec.82]$$

NOMENCLATURE

A, B, K: already defined
M_a, M_w: molecular weight of air, vapor (water)
m^*: characteristic mass, defined above
m_c: mass of working fluid in the compression space
m_e: mass of working fluid in the expansion space
m_d: mass of working fluid in the dead space
m_a: mass of air in the working space
m_w: mass of water in the working space
m_t: total mass of working fluid ($m_a + m_w$)
N: ratio of characteristic gas constants, defined above
P: engine output
P_c: engine output in the compression space
P_e: engine output in the expansion space
p: instantaneous cycle pressure
p_{ae}, p_{we}, p_{ac}, p_{wc}: defined above

Q_e: heat transferred in the expansion space
R_a, R_w: characteristic gas constant for air, water (vapor)
T_c: temperature of compression space
T_e: temperature of expansion space
t: time
V_{swc}, V_{swe}: swept volumes in compression, expansion spaces
V_c, V_e: instantaneous volumes of compression, expansion spaces
V_d: dead volume
V_t: combined swept volume of the working space $V_{swe} + V_{swc}$
X: dead volume ratio V_d/V_{swe}
α: phase angle between expansion and compression spaces
β: component mass ratio m_w/m_a
Δ: defined by $\frac{2}{\delta}\left[(1-\delta^2)^{\frac{1}{2}}-1\right]$
δ: defined above
η: thermal efficiency
φ: defined above
κ: swept volume ratio V_{swc}/V_{swe}
τ: temperature ratio T_c/T_e
θ: crank angle (ωt)
ω: angular speed

6. STIRLING ENGINE OF THE LABORATORY

6.1. DATA SUMMARY OF THE ENGINE IN THE LABORATORY

6.1.1. EXPANSION SPACE

Displacer piston:

- Stroke: $l_e = 75\ mm = 0{,}075\ m$
- Bore: $d_e = 96\ mm = 0{,}096\ m$
- Swept volume: $V_{swe} = \frac{\pi}{4} {d_e}^2 l_e = 542{,}87\ cc = 5{,}4287 \cdot 10^{-4}\ m^3$

6.1.2. COMPRESSION SPACE

Working piston:

- Stroke: $l_e = 75\ mm = 0{,}075\ m$
- Bore: $d_e = 85\ mm = 0{,}085\ m$
- Swept volume: $V_{swe} = \frac{\pi}{4} {d_e}^2 l_e = 425{,}59\ cc = 4{,}2559 \cdot 10^{-4}\ m^3$

We can find the data of strokes and bores of displacer and working piston in the preamble of the data sheets of the ST 05 G engine, given by the manufacturer (see Annex 4).

6.1.3. HEATER

- Number of pipes: n = 20
- Diameter of pipe: $d_h = 8\ mm = 0{,}008\ m$
- Length of pipe: $l_h = 326{,}5\ mm = 0{,}3265\ m$
- Volume: $V_h = n * \frac{\pi}{4} {d_h}^2 l_h = 328{,}23\ cc = 3{,}2823 \cdot 10^{-4}\ m^3$

6.1.4. COOLER

- Diameter: $d_k = 96\ mm = 0{,}096\ m$
- Length: $l_k = 84\ mm = 0{,}084\ m$
- Volume: $V_k = \frac{\pi}{4} {d_k}^2 l_k = 608{,}01\ cc = 6{,}0801 \cdot 10^{-4}\ m^3$

6.1.5. REGENERATOR

- Number of regenerators: n = 1
- Cover internal diameter: $d_{in} = 134\ mm = 0{,}134\ m$
- Matrix of regenerator internal diameter: $d_{imat} = 96\ mm = 0{,}096\ m$
- Height: $l_r = 57{,}5\ mm = 0{,}0575\ m$
- Regenerator matrix area: $a_{mat} = n * \frac{\pi}{4}\left({d_{in}}^2 - {d_{imat}}^2\right) = 68{,}64\ cm^2 = 6{,}864 \cdot 10^{-3}\ m^2$

$$porosity = \frac{A_{void}}{A_{total}} \qquad [Ec.135]$$

We take a square piece of mesh of 2x2 cm; if we count the number of wires in that 2x2 square, we get:

- Horizontally: 14 wires
- Vertically: 20 wires

De diameter of wire is 0,05 mm (given by the manufacturer). In this case, we get a void area of:

$$A_{void} = (20mm - 14 * 0{,}05mm) * (20mm - 20 * 0{,}05mm) = 366{,}7\ mm2$$

$$A_{total} = 20mm * 20mm = 400\ mm2$$

$$porosity = \frac{A_{void}}{A_{total}} = 0{,}917$$

- Volume: $V_r = porosity * a_{mat} * l_r = 360{,}88\ cc = 3{,}6088 \cdot 10^{-4}\ m^3$

6.1.6. DEAD VOLUME

Dead volume is all volume which does not take part in the expansion or compression, i. e., volumes of heat exchangers:

$V_d = V_k + V_r + V_h = 1297{,}12\ cc = 1{,}29712 \cdot 10^{-3}\ m^3$

6.2. CINEMATICS OF WORKING AND DISPLACER PISTONS

Following it is made an analysis of the movement of the pistons of the engine, which is supposed to be sinusoidal; it will be represented graphically with the help of Matlab.

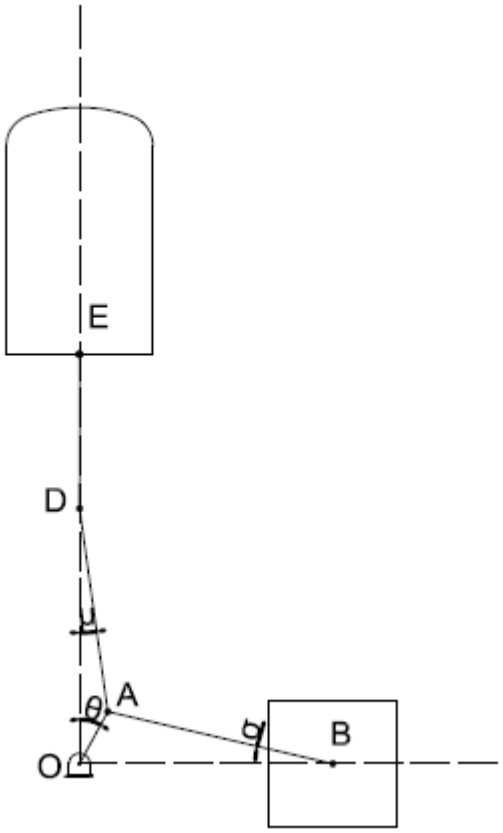

Image 59 - Schematic of the pistons.

6.2.1. WORKING PISTON

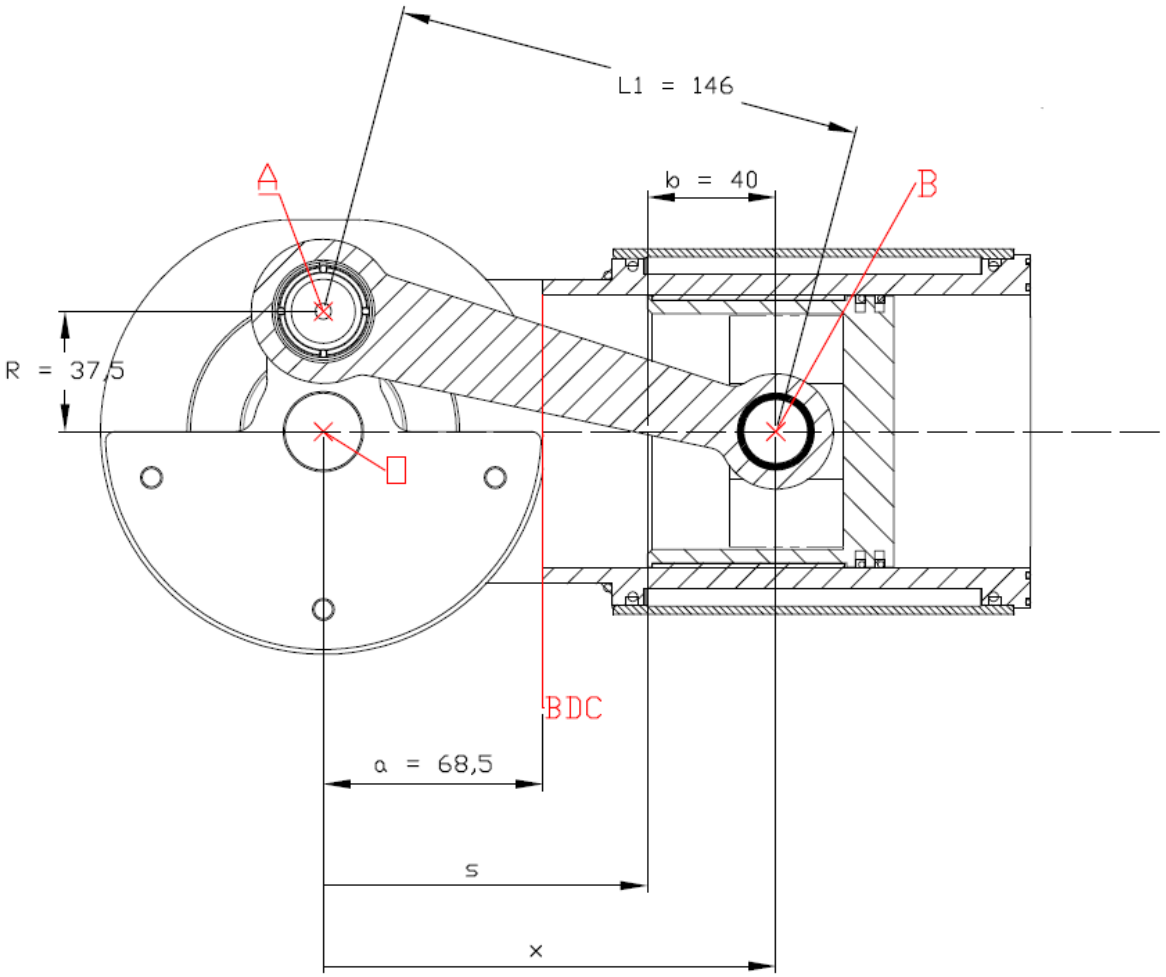

Image 60 - Working piston.

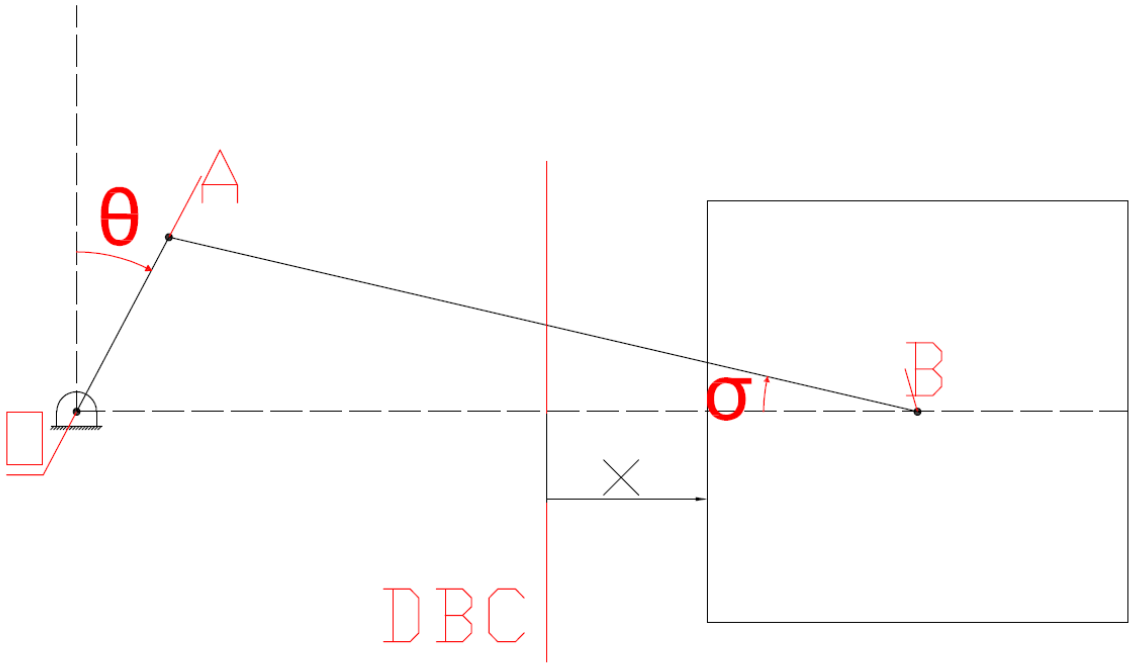

Image 61 - Parameters in working piston movement.

BOTTOM DEAD CENTRE (BDC): x = min = 0 (θ = 270°)
TOP DEAD CENTRE (TDC): x = max = stroke = 75 mm (θ = 90°)

$$\overrightarrow{OA} = (R\sin\theta\,, R\cos\theta)$$
$$\overrightarrow{AB} = (L_1\cos\sigma\,, -L_1\sin\sigma)$$

$$x = s - a, \qquad s = \overrightarrow{OA}_x + \overrightarrow{AB}_x - b$$
$$x = \overrightarrow{OA}_x + \overrightarrow{AB}_x - b - a = R\sin\theta + L_1\cos\sigma - b - a$$
$$a = s(when\ the\ working\ piston\ is\ in\ its\ bottom\ dead\ centre) = s(\theta = 270°)$$

We need a relationship to get the value of σ as a function of θ.

Points O and B are situated in the same altitude ➔ their component *y* is the same.

$$\overrightarrow{OA}_y = \overrightarrow{AB}_y \;\rightarrow\; R\cos\theta = -L_1\sin\sigma \;\rightarrow\; \sigma = \sin^{-1}\left(-\frac{R}{L_1}\cos\theta\right)$$

Now we can express the position of the working piston, referred to its bottom dead point, and as a function of crank angle, θ.

$$x = R\sin\theta + L_1\cos\left(\sin^{-1}\left(-\frac{R}{L_1}\cos\theta\right)\right) - b - a$$
$$a = s(\theta = 270°) = R\sin 270 + L_1\cos\left(\sin^{-1}\left(-\frac{R}{L_1}\cos 270\right)\right) - b = 68{,}5\ [mm]$$

$$x = 37{,}5 \sin\theta + 146 \cos\left(\sin^{-1}\left(-\frac{37{,}5}{146}\cos\theta\right)\right) - 40 - 68{,}5\ [mm] \qquad [Ec.\ 83]$$

6.2.2. DISPLACER PISTON

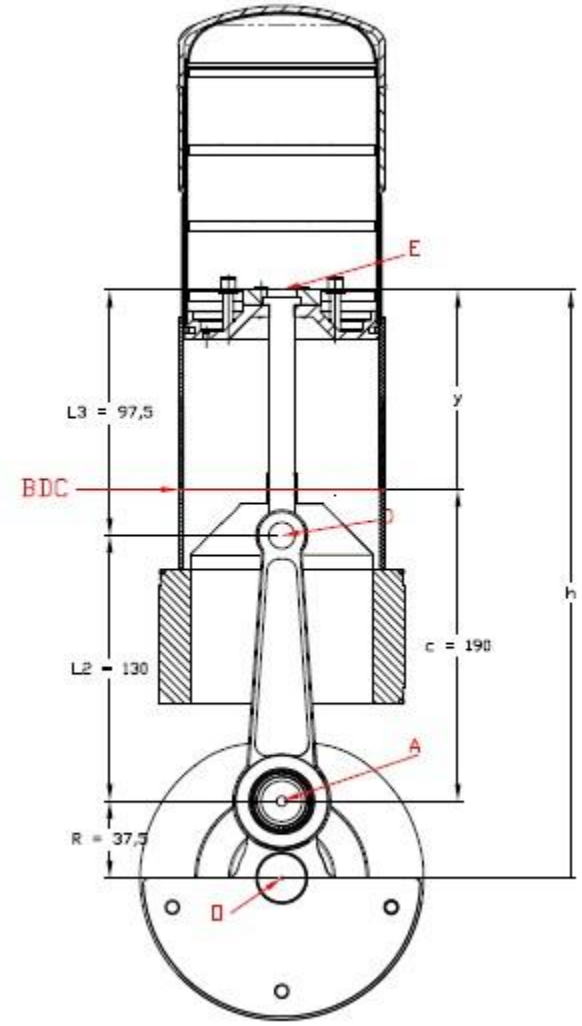

Image 62 - Displacer pistons.

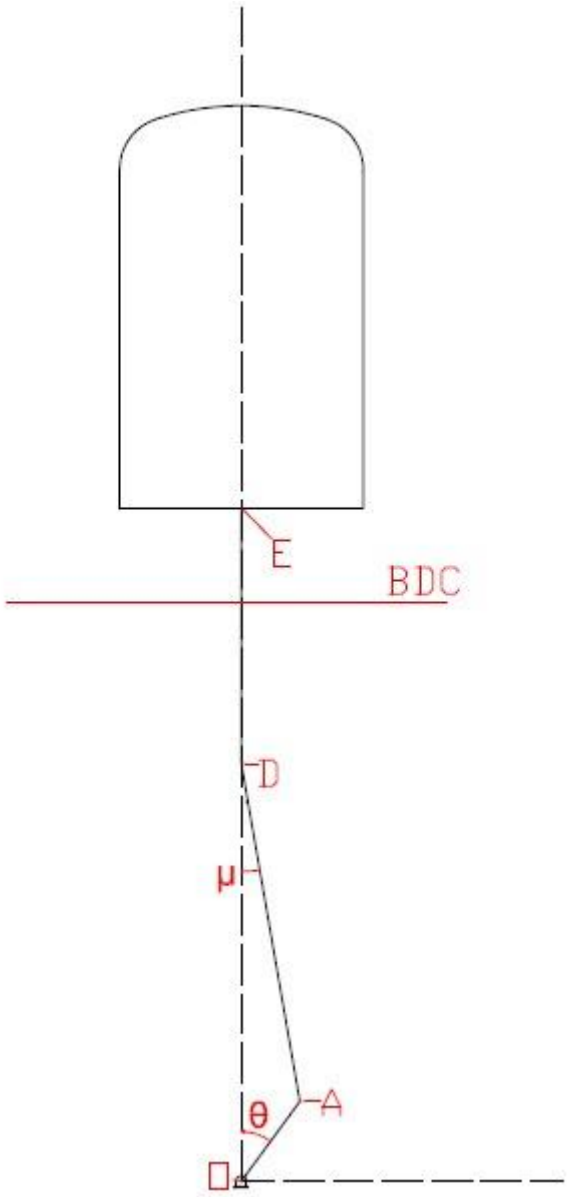

Image 63 - Parameters in displacer piston movement.

BOTTOM DEAD CENTRE (BDC): y = min = 0 (θ = 180°)
TOP DEAD CENTRE (TDC): y = max = stroke = 75 mm (θ = 0°)

$$\overrightarrow{OA} = (R\sin\theta\,, R\cos\theta)$$
$$\overrightarrow{AD} = (-L_2\sin\mu\,, L_2\cos\mu)$$
$$\overrightarrow{DE} = (0, L_3)$$

$$y = h - c, \qquad h = \overrightarrow{OA}_y + \overrightarrow{AD}_y + \overrightarrow{DE}_y$$
$$y = \overrightarrow{OA}_y + \overrightarrow{AD}_y + \overrightarrow{DE}_y - c = R\cos\theta + L_2\cos\mu + L_3 - c$$
$$c = h(when\ the\ displacer\ piston\ is\ in\ its\ bottom\ dead\ centre) = h(\theta = 180°)$$

We need a relationship to get the value of μ as a function of θ.

Points O and D are situated in the same vertical line ➔ their component *x* is the same.

$$\overrightarrow{OA}_x = \overrightarrow{AD}_x \rightarrow R\sin\theta = -L_2\sin\mu \rightarrow \mu = \sin^{-1}\left(-\frac{R}{L_2}\sin\theta\right)$$

Now we can express the position of the displacer piston, referred to its bottom dead point, and as a function of crank angle, θ.

$$y = R\cos\theta + L_2\cos\left(\sin^{-1}\left(-\frac{R}{L_2}\sin\theta\right)\right) + L_3 - c$$

$$c = h(\theta = 180°) = R\cos 180 + L_2\cos\left(\sin^{-1}\left(-\frac{R}{L_2}\sin 180\right)\right) + L_3 = 190\ [mm]$$

$$y = 37{,}5\cos\theta + 130\cos\left(\sin^{-1}\left(-\frac{37{,}5}{130}\sin\theta\right)\right) + 97{,}5 - 190\ [mm] \qquad [Ec.84]$$

Following, we will show the graphics of the movement of the pistons as a function of the crank angle; for it, we program a function in MATLAB, called "piston", which represents this movements, and also compares them with pure sinus and cosines functions, to see the deviation between real movement and theoretical.

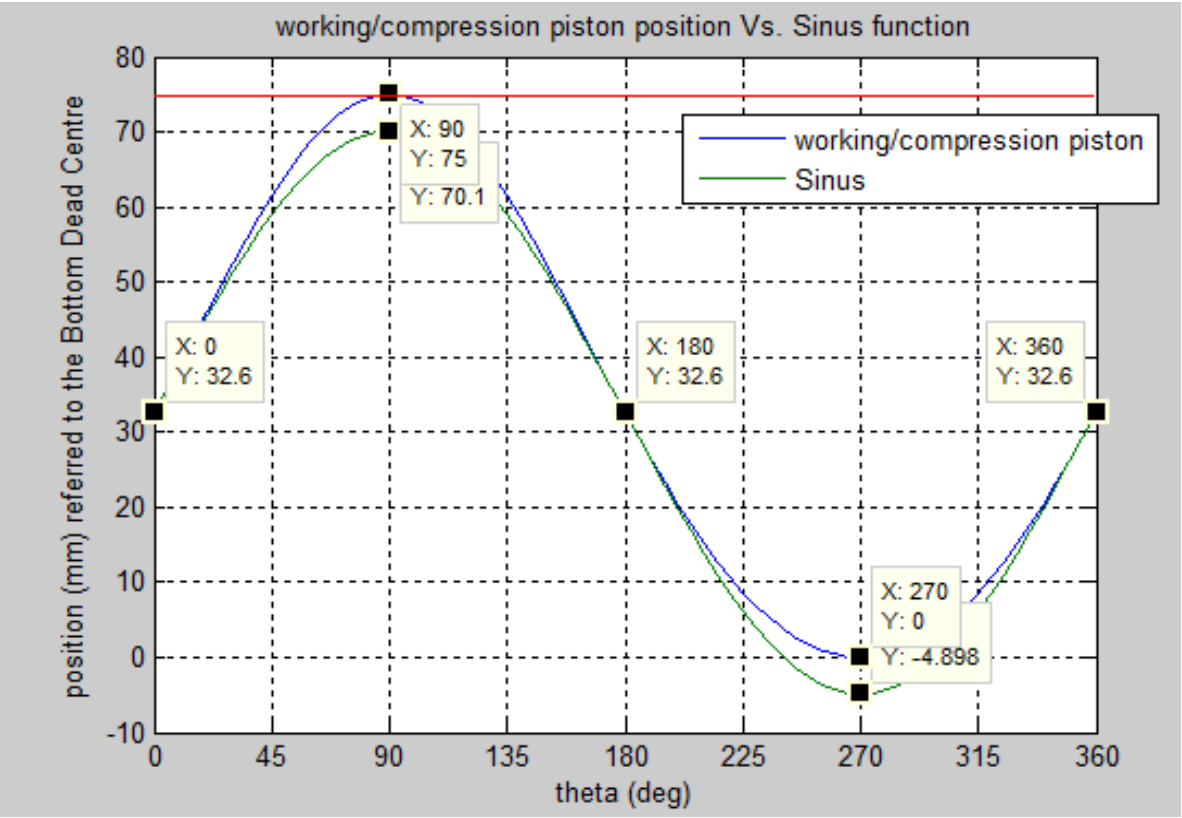

Image 64 - Working piston Vs. sinus function.

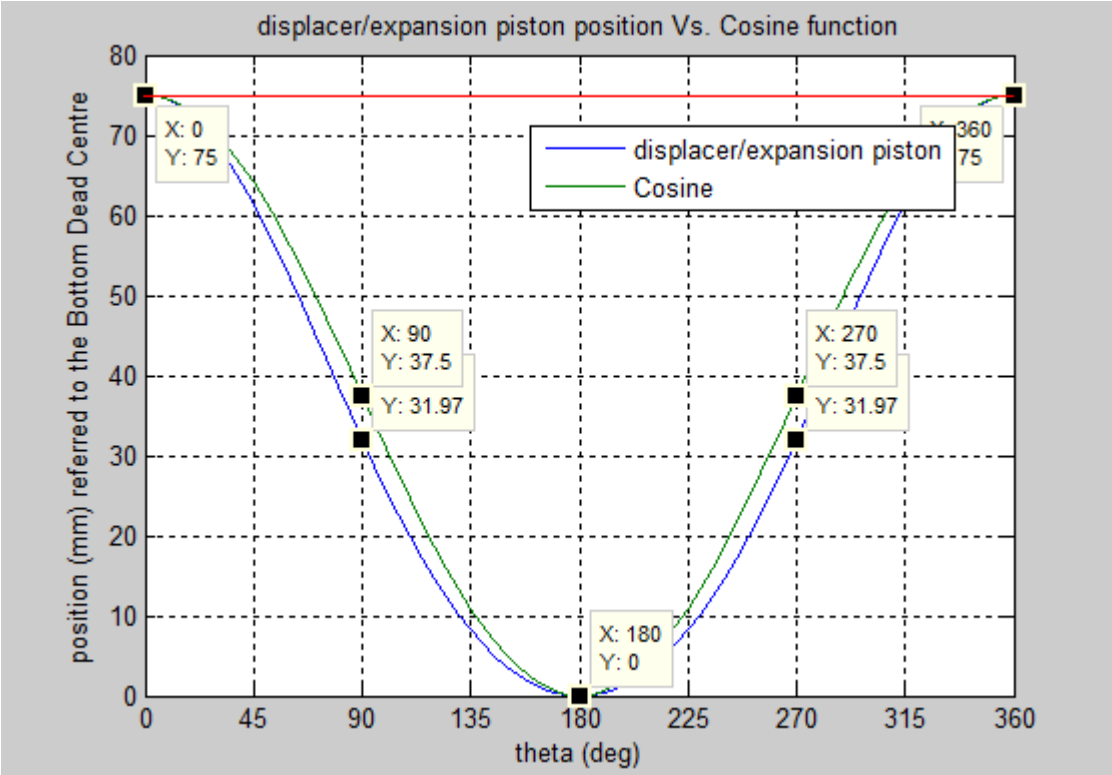

Image 65 - Displacer piston Vs. cosinus function.

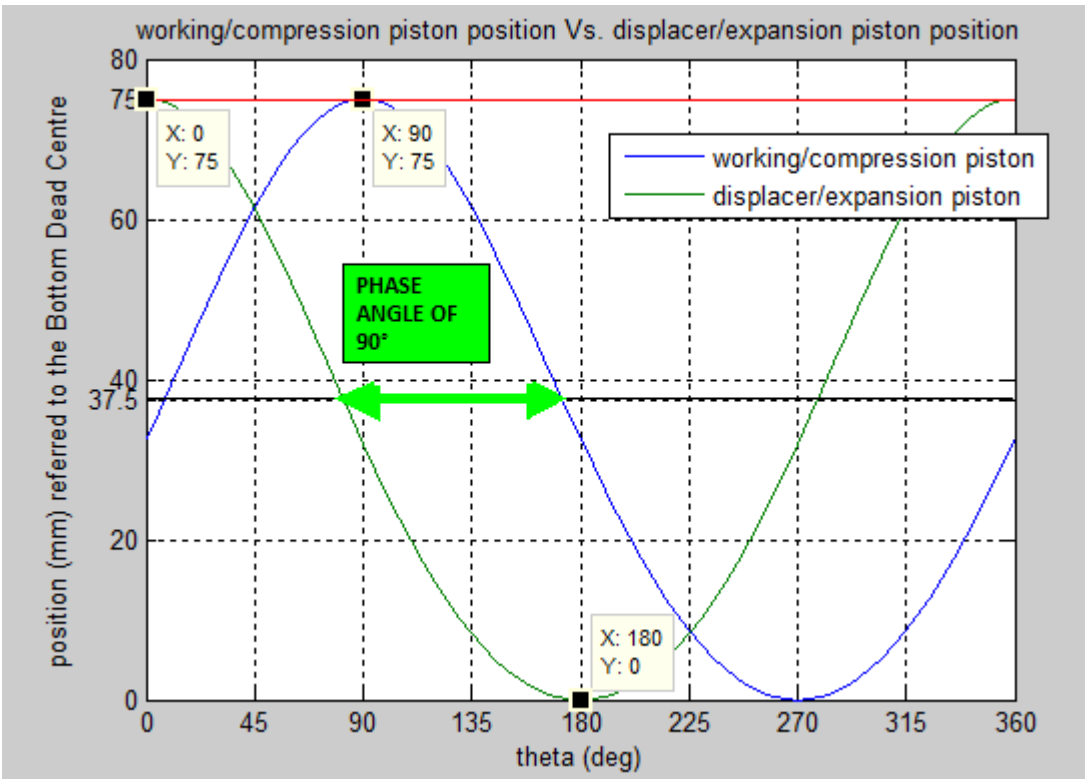

Image 66 - Working piston Vs. displacer piston.

6.3. ENGINE BRAKE

6.3.1. OPERATION OF THE BRAKE

The engine of the laboratory is connected to a electromagnetic brake that is responsible of transforming the mechanical energy into electricity.
Its operation is based on the electromagnetic currents that are induced when a metallic mass is placed in a varying magnetic field. These are called eddy currents (also named Foucault currents).

The two main parts of the brake are the stator and rotor. The stator comprises two solenoids connected in series and fed by a DC generator, to obtain a magnetic field of a given intensity.
The brake is coupled to the motor by a shaft, and said shaft serves as a rotor, which rotates together with the engine. Because of this movement, the rotor is crossed by a magnetic field flux in continuous variation, and electromotive forces are induced on it. These currents have a direction opposite to the movement of the rotor (and hence of the engine), therefore gives a braking effect which slows down the movement of the shaft, i.e., it causes engine braking.
The intensity of the effect increases the larger the magnetic field of the coils and the higher the speed of the shaft.

Thanks to this principle of operation it is achieved that, when the shaft is stationary, the braking action is null.

In the case of the brake in the laboratory, variation of the magnetic field of the coils, and hence the braking effect on the engine, is achieved by a driver circuit of which plane is shown on the following page. The main element of this circuit is a potentiometer, which of value can be manually changed: when the value of this is 0%, does not cause any modification, and thus the braking force exerted on the motor is negligible. By increasing the value of the potentiometer, increase the braking force exerted on the motor, thereby decreasing the rate of rotation of the latter but increasing the strength (and therefore power) that is obtained from the engine.

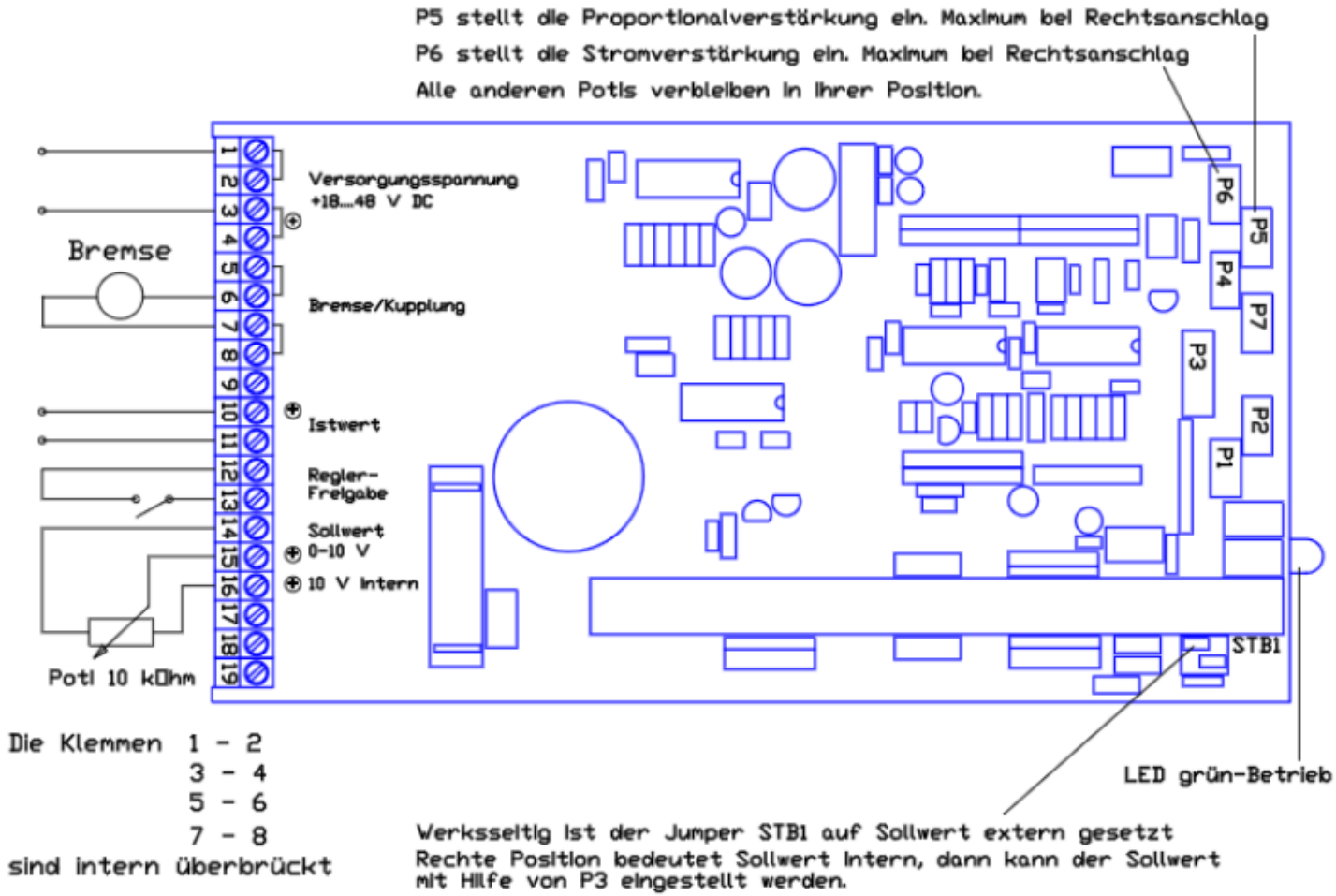

Nennstrom: 5 A
Spitzenstrom: 10 A

Platinenausführung IP 00
Steckkarte im Europaformat 100x160 (187) mm

7. ANALYSIS OF EXPERIMENTS

7.1. INTRODUCTION

Various experiments have been performed by varying some parameters of the engine, to compare these results with theoretical analysis, both isothermal (Schmidt) and adiabatic.
As we have seen in section 3.4, one of the parameters that affect the operation of the engine is the working fluid. Therefore, experiments were performed for two different fluids: air and air + water (compound working fluid).

In section 3.5.1.1, we analyze the different working variables of the engine:

- Rotation speed (n): in the case of our engine, for all other parameters kept constant, it is not possible to vary the engine speed. The only way to change it is by changing the brake potentiometer value, which also influences the strength, and therefore we cannot clearly see the influence of speed on power alone. The engine output power is directly proportional to the rate of rotation.
- Mean cycle pressure (P_{mean}): This is one of the parameters that we vary in our engine. As we can see in the specifications sheet (Annex 4) of the same, the maximum bearable pressure is 10 bar. In our case, experiments have been performed by varying the pressure from 4 to 9 bar (as this will increase due to heating of the working fluid during operation of the motor). With increasing pressure at constant volume is provoked an increase in the work output of the engine, as it increases the area of the P-V diagram.
- Heater temperature (T_h): by increasing the temperature of the heater, increases the temperature of the working fluid in the hot zone (and hence the temperature difference between it and the cold zone), which causes an increase in performance . The way to increase the temperature of the heater is increasing the propane flow entering the burning room.
- Cooler temperature (T_c): the way to vary the temperature of the cold zone in the engine is by varying the cooling water flow, since we are not able to vary its temperature because it is running water. A decrease in the cold zone temperature causes the same effect as the increase in heater temperature.

We shall see how it is affected the engine performance by varying the above parameters, and compare with theoretical studies, both isothermal analysis (Schmidt) and adiabatic.

7.2. DIFFERENCES BETWEEN THE VARIOUS THEORETICAL CYCLES AND THE REAL ONE

As we have seen above, throughout history there have been various theoretical studies of the Stirling engine cycle, some more idealized than others. Obviously, these theories are far from reality, because of the many assumptions made when developing them.

One of the assumptions that are made at all levels, and we have taken during the development of this project, is the steady state operation of the engine and the working speed constant. Also despise at all times the kinetic and potential working fluid.

Depending on the degree of simplicity or ideality, the first cycle we have seen is the ideal. Due to the enormous idealization of the cycle, this is only suitable for early estimates.

The main shortcoming of this cycle is the assumption that the total amount of the working fluid (which is supposed to behave like an ideal gas) is, at all times, under the same conditions, either in the expansion zone or the compression. This assumption implies that the void volume of the regenerator is zero, and requires that the pistons have a discontinuous movement.
Additionally, in this cycle is assumed that there are no leaks in the working fluid, then its mass remains constant at all times.

Other assumptions that makes this cycle are that the expansion and compression processes are isothermal, and that there is perfect regeneration. Furthermore, they are no taken into account the aerodynamic pressure losses, due to many factors.

The next cycle is the isothermal, and particularly the Schmidt cycle. Unlike the ideal cycle, Schmidt does not involve the discontinuous movement, but develops from the assumption of a sinusoidal motion of the pistons. Thus, the assumption that all the working fluid (assumed ideal gas) is instantaneously in the same condition disappears. The fact that the movement of the pistons (and with them, the variations in volume) is sinusoidal are considered because only with it, can be achieved closed-form solutions, otherwise it would be very difficult to find ways to describe this variation.

Moreover, isothermal analysis maintains the remaining assumptions: isothermal expansion and compression, perfect regeneration, no leakage of working fluid.

The fact that the expansion and compression processes are isotherm means that the heat exchanged between the walls of the cylinders and the working fluid is infinite. This means that the temperature of the heater is equal to the expansion zone, and always equal to the maximum temperature of the cycle, and in the same way, the temperature of the cooler is equal to the temperature in compression at all times and equal to the minimum cycle temperature. This means that the temperatures are kept constant in both the heat exchangers and in the cylinder wall, that is, there are no heat gradients. Also implies that the efficiency of all the heat exchangers (including the regenerator) is 100%, i.e., they are ideal exchangers.

The latter assumptions cause heat exchanged in the piston-cylinder, and this heat exchanged is equal to the work done, and no heat transfer in the exchangers, which is paradoxical. This deficiency is resolved in the adiabatic model.

The advantage of the isothermal model, that makes it very used despite the error made, is that the equations derived from it can be easily integrated.

Finally, we find the adiabatic analysis. Said analysis differs from the isothermal in that heat exchange does not occur between the walls of the cylinders and the working fluid; therefore, the air is not always kept to the minimum or maximum temperature of the cycle, but in the cylinders during expansion or compression, may be at temperatures below the maximum, or above the minimum. Therefore, in the adiabatic analysis, net heat transfer occurs in the heat exchangers.

In the adiabatic case, the thermal efficiency is not only a function of temperature, as in the ideal and isothermal, in which the efficiency matches with the Carnot one; in the adiabatic, it also depends on the ratio of swept volume, the phase angle and the ratio of dead volume. Therefore, the analysis takes into account adiabatic dead volumes existing in the engine.
For the same mass of gas, the non-isothermal analysis (adiabatic) does not result in significantly different performance than the isothermal analysis. However, the thermal efficiency will inevitably be lower than the Carnot, due to the irreversibility of the discontinuities introduced by temperature.

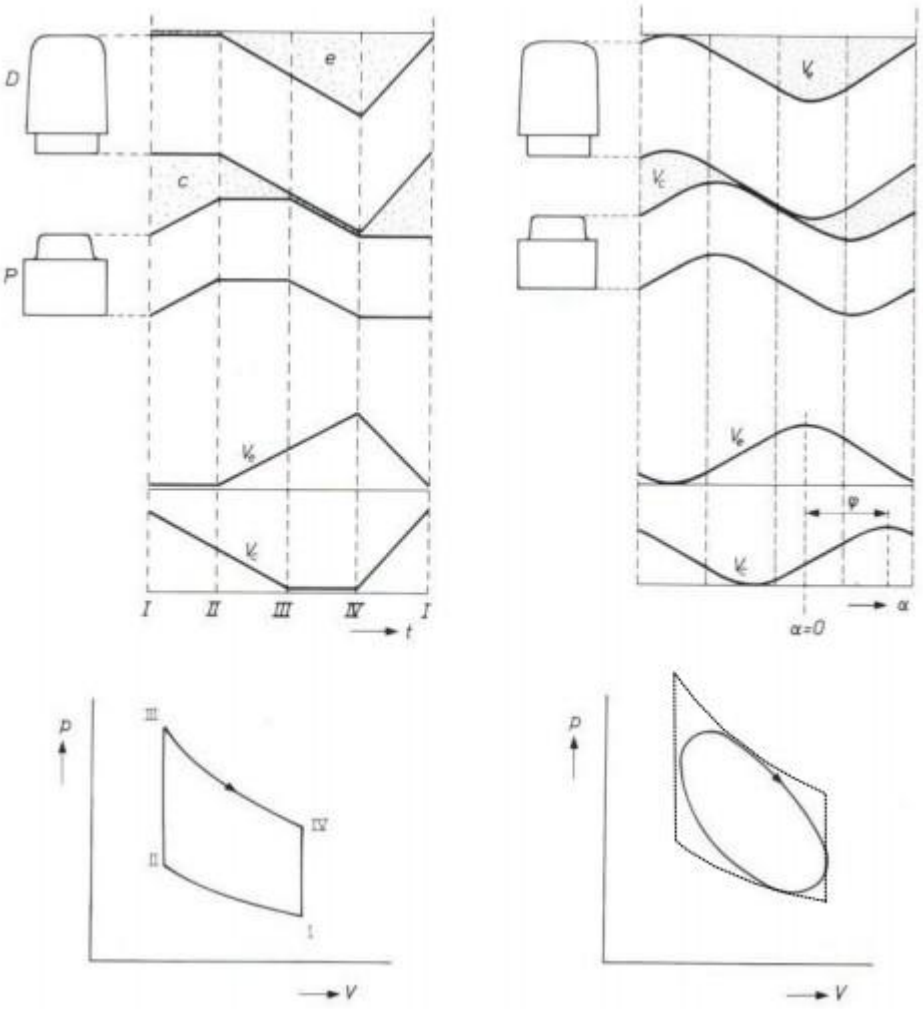

Image 67 - Piston and displacer motion, discontinuous (left) and sinusoidal (right) and resulting p-V diagrams

Due to the influences of dead space and sinusoidal piston motion, the p-V diagram is rounded and smaller than it should be. This means that less net work is produced per cycle as the area enclosed is smaller. Figure 67 shows what the ideal piston and displacer motion would look like. The ideal piston motion is quasi-sinusoidal, being a symmetrical waveform with equal time spent idle at the top and bottom of the range of motion. The displacer motion is somewhat different, and hard to quantify. We can see the real displacer and working piston motion in chapter 6.2.

7.3. RESULTS SUMMARY

7.3.1. EXPERIMENTS WITH AIR

They have been made a series of tests using air as working fluid for different inlet propane flow (which varies the temperature of the hot area of the engine), and at different load pressures. The values collected by the sensors are read into the computer using the software "DIAdem", with whom it has been implemented a data reader.

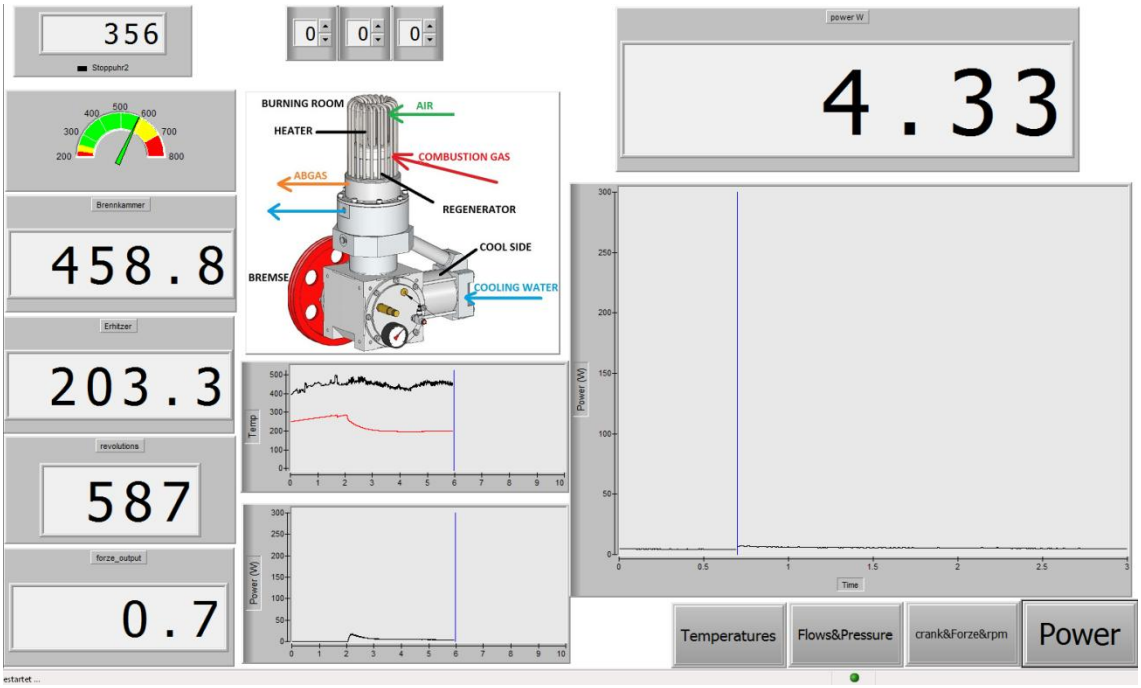

Image 68 - DIAdem data reader.

The program includes multiple engine parameters, some of which are important during the operation of this, but they are not relevant when analyzing the performance of the engine. Therefore, here are summarized only the most important data. The relevant parameters are listed below:

- Propane flow (g /s): to measure the propane flow there is a scale that can be connected to the computer; it gave problems because their response time was greater than the time of other sensors, and blocked the program DIAdem, impeding this program read normally the data collected from other sensors. To solve this problem, we proceeded to eliminate this parameter from the measurement program, and measure it manually.
- Mean pressure (bar): this parameter is determined by the amount of air with the engine is loaded before starting. As we can see in the engine specification sheet (Annex 4), the maximum bearable pressure is 10 bar.

- Cold temperature (K): this parameter is measured with the temperature in the engine cold source, which depends mainly on the cooling water flow.
- Hot Temperature (K): this parameter measures the maximum temperature of the engine, located in the heater. This temperature varies with the burning room temperature, which depends on the propane flow.
- Torque (N·m): this parameter, which is measured with a sensor attached to the brake, measures the angular momentum delivered from the motor shaft.
- Rotation speed (rpm): it measures the angular velocity of the motor.
- Output power (W): this is the most important parameter, which is obtained from the rotation speed and torque.

As is known, by varying the value of the potentiometer it is varied the braking power extracted from the engine. In the results shown below are reflected only the relative values obtained at maximum power for each experiment.
Below there are different tables summarizing the results obtained in the multiple tests, at different propane flow and pressure rates.

To calculate the real efficiency, we use the equations in chapter 4.

7.3.1.1. EXPERIMENTS WITH PROPANE FLOW 0,1 g/s

Experiment 1: Propane flow 0,1 g/s and mean pressure 4,87 bar

Propane flow (g/s)	Q_{in} (W)	Mean pressure (bar)	Cold temp. (K)	Hot temp. (K)	Max. Torque (N·m)	Rotation speed (rpm)	Output power (W)	Eff. (%)
0,1	2317,9	4,87	308	526	2,23	444	103,8	4,50

Chart 12 - Results of experiment 1.

Experiment 2: Propane flow 0,1 g/s and mean pressure 5,75 bar

Propane flow (g/s)	Q_{in} (W)	Mean pressure (bar)	Cold temp. (K)	Hot temp. (K)	Max. Torque (N·m)	Rotation speed (rpm)	Output power (W)	Eff. (%)
0,1	2317,9	5,75	309	552	3,80	391	155,4	6,70

Chart 13 - Results of experiment 2.

Experiment 3: Propane flow 0,1 g/s and mean pressure 6,60 bar

Propane flow (g/s)	Q_{in} (W)	Mean pressure (bar)	Cold temp. (K)	Hot temp. (K)	Max. Torque (N·m)	Rotation speed (rpm)	Output power (W)	Eff. (%)
0,1	2317,9	6,60	310	559	4,60	366	176,0	7,59

Chart 14 - Results of experiment 3.

Experiment 4: Propane flow 0,1 g/s and mean pressure 7,47 bar

Propane flow (g/s)	Q_{in} (W)	Mean pressure (bar)	Cold temp. (K)	Hot temp. (K)	Max. Torque (N·m)	Rotation speed (rpm)	Output power (W)	Eff. (%)
0,1	2317,9	7,47	312	541	4,57	393	188,3	8,12

Chart 15 - Results of experiment 4.

Experiment 5: Propane flow 0,1 g/s and mean pressure 8,98 bar

Propane flow (g/s)	Q_{in} (W)	Mean pressure (bar)	Cold temp. (K)	Hot temp. (K)	Max. Torque (N·m)	Rotation speed (rpm)	Output power (W)	Eff. (%)
0,1	2317,9	8,98	313	535	5,35	384	215,3	9,29

Chart 16 - Results of experiment 5.

7.3.1.2. EXPERIMENTS WITH PROPANE FLOW 0,163 g/s

Experiment 6: Propane flow 0,163 g/s and mean pressure 5,04 bar

Propane flow (g/s)	Q_{in} (W)	Mean pressure (bar)	Cold temp. (K)	Hot temp. (K)	Max. Torque (N·m)	Rotation speed (rpm)	Output power (W)	Eff. (%)
0,163	3778,1	5,04	313	651	4,58	494	237,0	6,27

Chart 17 - Results of experiment 6.

Experiment 7: Propane flow 0,163 g/s and mean pressure 5,63 bar

Propane flow (g/s)	Q_{in} (W)	Mean pressure (bar)	Cold temp. (K)	Hot temp. (K)	Max. Torque (N·m)	Rotation speed (rpm)	Output power (W)	Eff. (%)
0,163	3778,1	5,63	314	665	5,36	496	278,5	7,37

Chart 18 - Results of experiment 7.

Experiment 8: Propane flow 0,163 g/s and mean pressure 6,34 bar

Propane flow (g/s)	Q_{in} (W)	Mean pressure (bar)	Cold temp. (K)	Hot temp. (K)	Max. Torque (N·m)	Rotation speed (rpm)	Output power (W)	Eff. (%)
0,163	3778,1	6,34	315	680	6,57	461	317,3	8,40

Chart 19 - Results of experiment 8.

Experiment 9: Propane flow 0,163 g/s and mean pressure 7,90 bar

Propane flow (g/s)	Q_{in} (W)	Mean pressure (bar)	Cold temp. (K)	Hot temp. (K)	Max. Torque (N·m)	Rotation speed (rpm)	Output power (W)	Eff. (%)
0,163	3778,1	7,90	319	653	7,28	501	382,0	10,11

Chart 20 - Results of experiment 9.

Experiment 10: Propane flow 0,163 g/s and mean pressure 8,53 bar

Propane flow (g/s)	Q_{in} (W)	Mean pressure (bar)	Cold temp. (K)	Hot temp. (K)	Max. Torque (N·m)	Rotation speed (rpm)	Output power (W)	Eff. (%)
0,163	3778,1	8,53	319	656	8,05	479	404,0	10,69

Chart 21 - Results of experiment 10.

In view of the study of the above tables we have the following conclusions:

- The propane flow influences the hot area temperature. A higher propane flow rate means a higher heat input to the combustion chamber, and thus an increase in the temperature of the hot space.

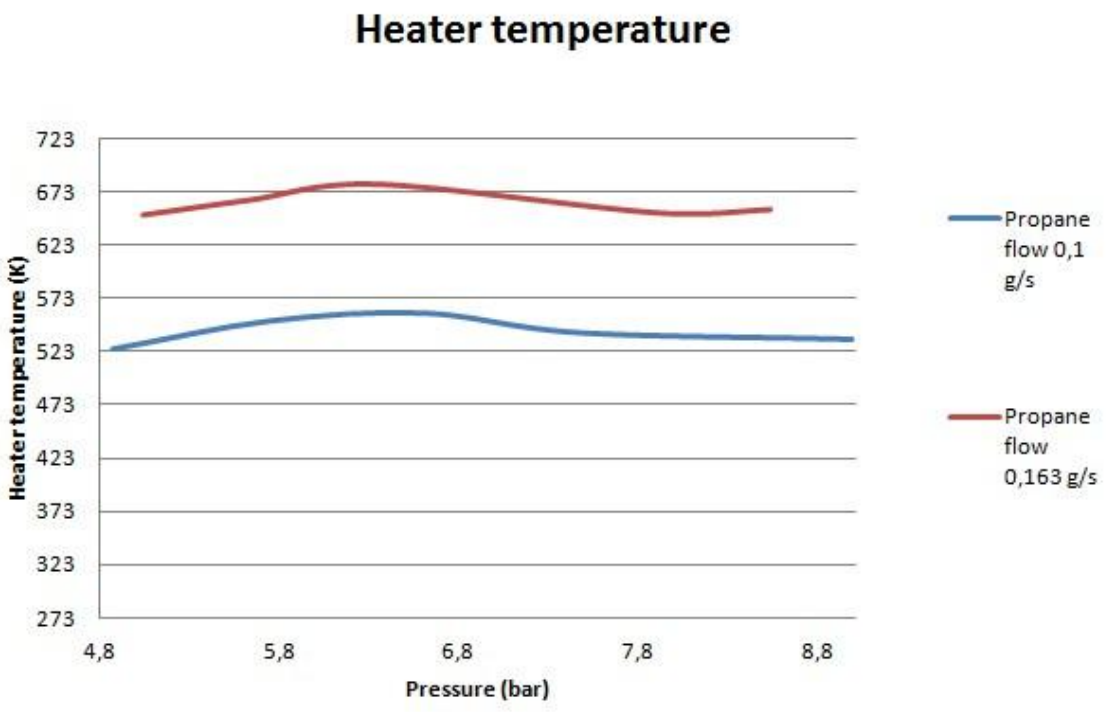

Image 69 - Influence of propane flow in heater temperature.

As we can see graphically the temperature is higher for higher flow rates of propane. However, we see that it is independent of pressure.

- The torque, and therefore power, increases by increasing pressure so as propane flow.

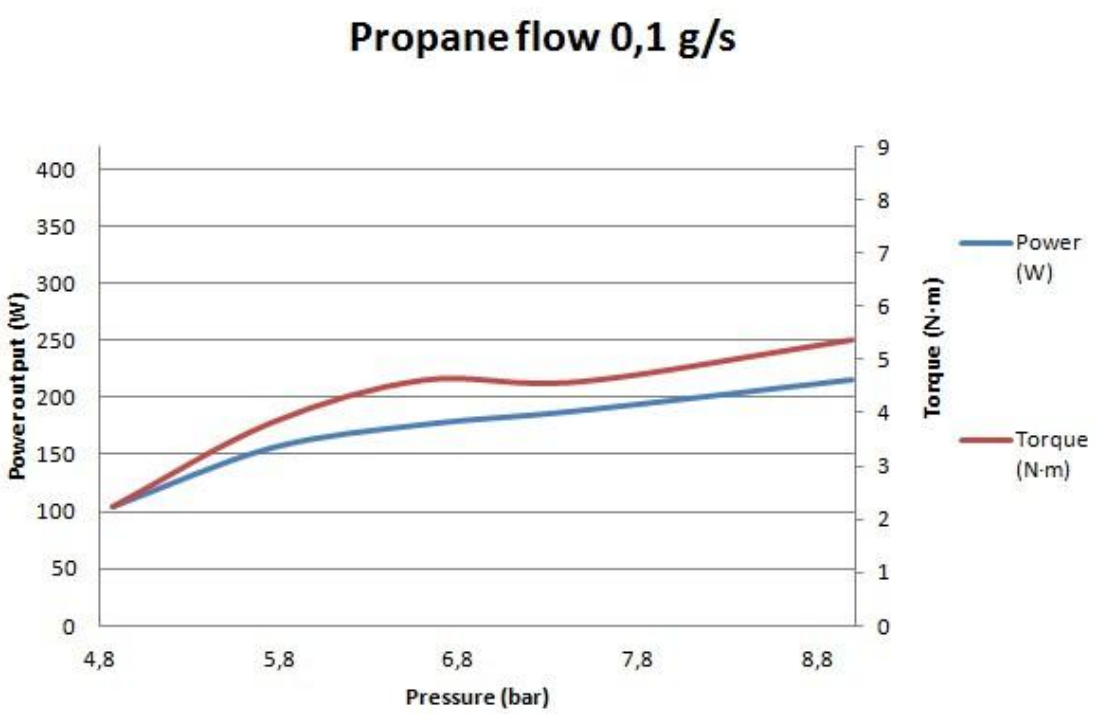

Image 70 - Power and torque as a function of pressure at 0,1 g/s of propane.

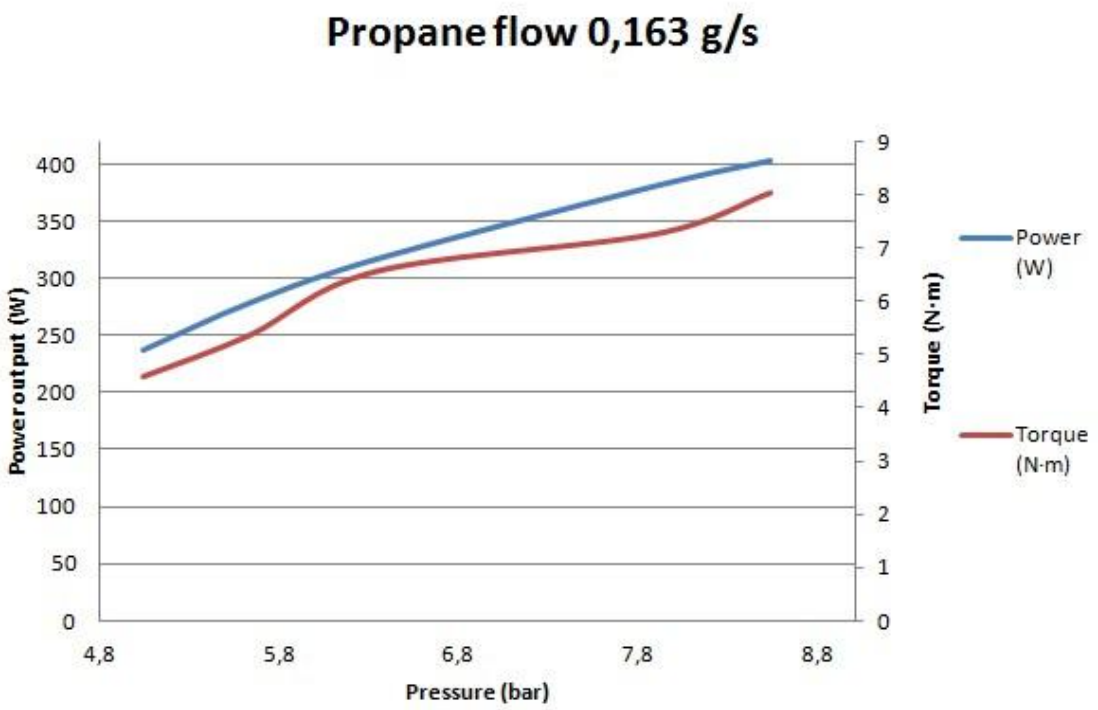

Image 71 - Power and torque as a function of pressure at 0,163 g/s of propane.

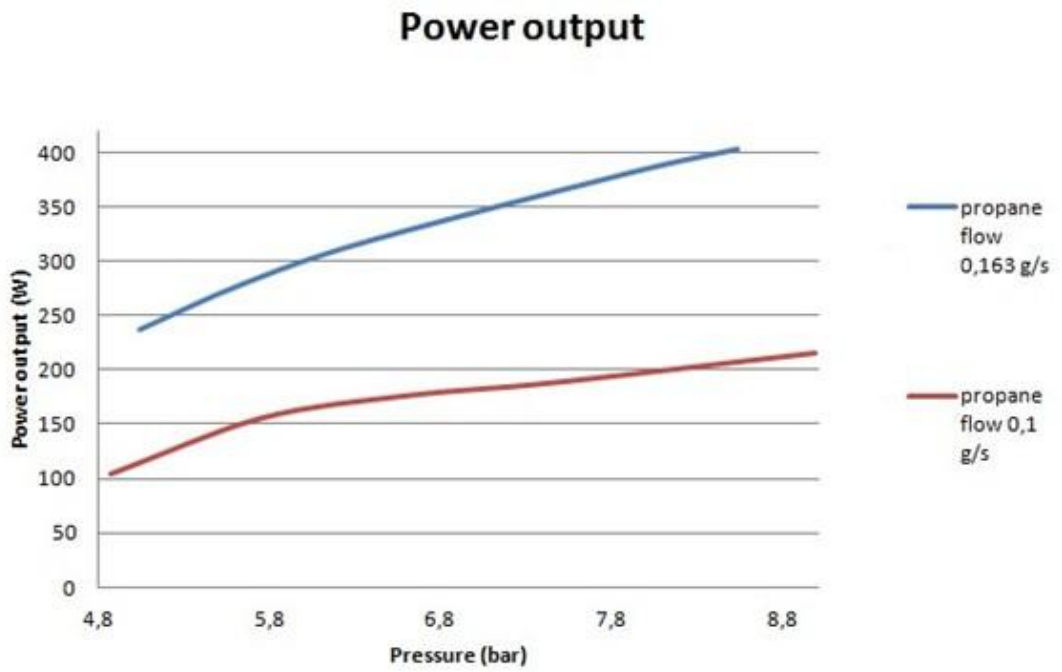

Image 72 - Power output as a function of pressure and propane flow.

The efficiency increases with the pressure, and also is a little bit higher for higher propane flows.

Image 73 - Efficiency as a function of pressure and propane flow.

7.3.1.3. EXPERIMENTS VARYING PROPANE FLOW

We proceed to carry out one test, varying the aperture of the propane valve, and therefore, the propane flow that comes into the burning room. The variation of this flow should vary the temperature in the heater, which ensures a higher output power.
Because of the problem explained later in chapter 7.3.2, it is impossible to keep the pressure constant during the whole experiment.

Valve aperture	Propane flow (g/s)	Q_{in} (W)	Mean pressure (bar)	Cold temp. (K)	Hot temp. (K)	Mean rotation speed (rpm)	Max. output power (W)	Eff. (%)
15º	0,135	3129,3	4,75	315	625	592	212,1	6,78
30º	0,142	3291,5	4,7	316	633	617	221,1	6,72
45º	0,145	3361,0	4,62	316	641	630	225,4	6,71
60º	0,147	3407,4	4,52	316	652	628	224,8	6,60
75º	0,155	3592,9	4,41	316	663	628	224,4	6,25
90º	0,159	3685,5	4,29	316	672	635	227,1	6,16

Chart 22 - Results of experiment varying propane flow.

In view of the previous table, the following conclusions are extracted:

- The temperature in the heater increases by increasing the propane flow; this is obvious, because by increasing the propane flow, we put into the burning room more calorific power, and therefore, its temperature is increased, and with it, the temperature in the heater.

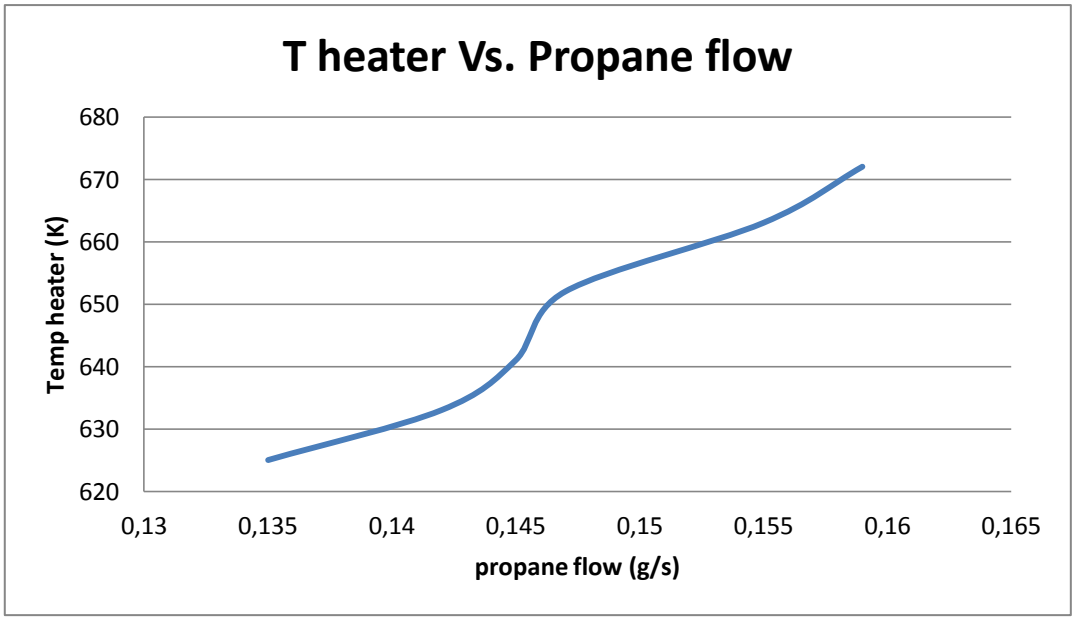

Image 74 - Heater temperature Vs. propane flow

- If we compare this results of power output with the results for another propane flows (0,1 and 0,163 g/s), in the same pressure range (we do not have experiments for that flows and pressures, but we extrapolate that results from the experiments made at that flows and higher pressures, as we can see in image 74) can be seen that the power output is higher than should be. There is no logical reason for it, but if we compare the working speed of experiments at 0,1 and 0,163 g/s, with working speed of the last experiments, we can see that is higher for the last ones. This can be the reason for getting higher power than expected. Another reason can be that, as mentioned, the power output for 0,1 and 0,163 g/s at low pressures is not a experimental result, but extrapolated, considering the power output as a linear function of pressure. This is an assumption that is not real, and can give room for mistakes.

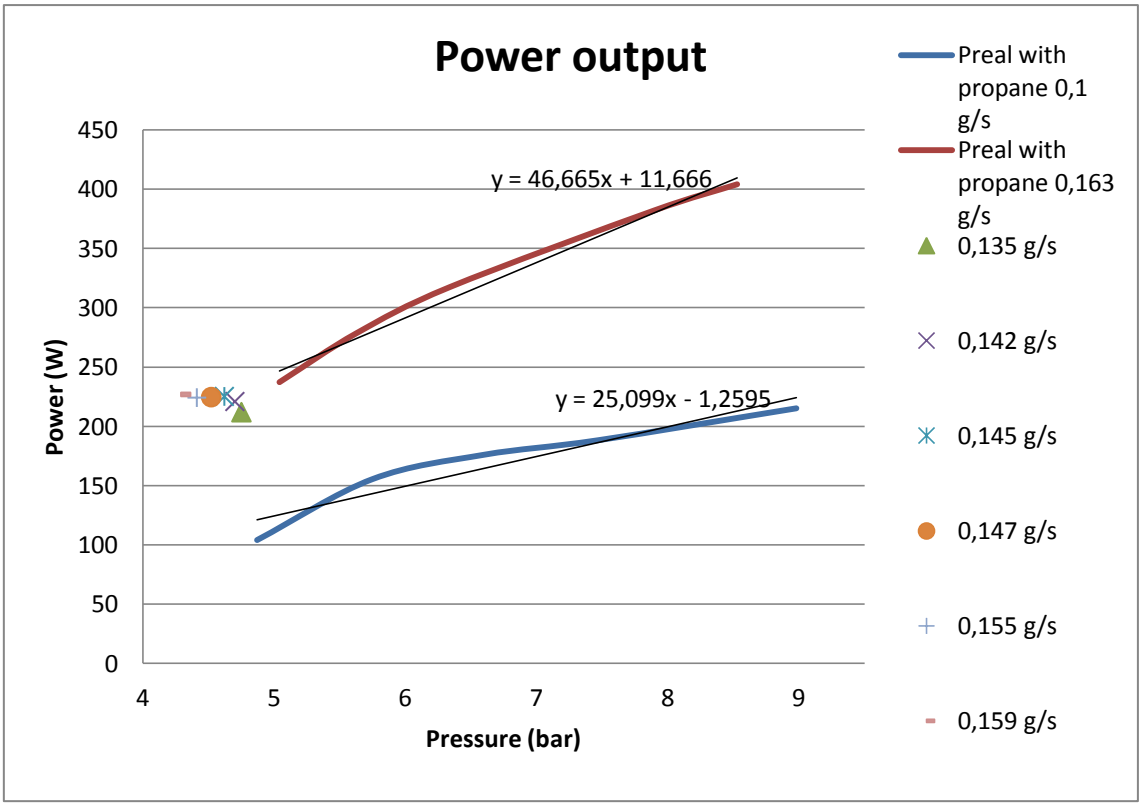

Image 75 - Power for different propane flows. Auxiliary graph.

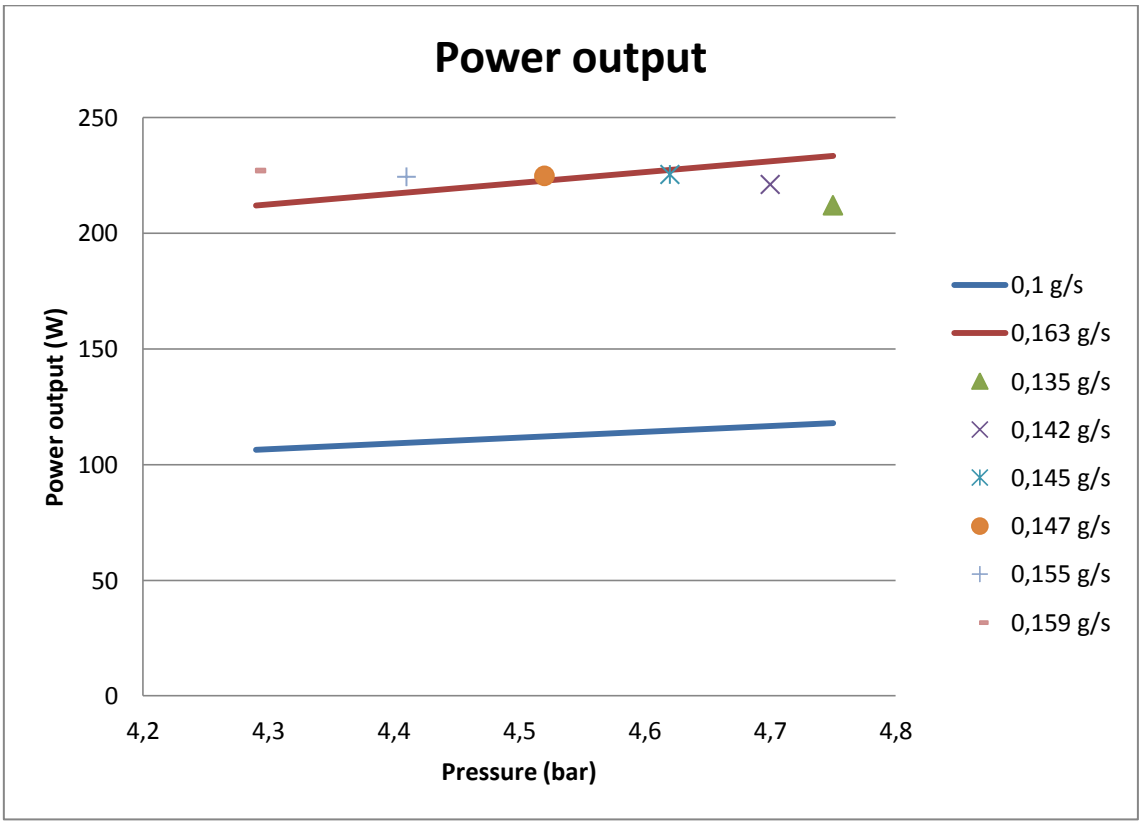

Image 76 - Power for different propane flows.

7.3.2. EXPERIMENTS WITH AIR + WATER

As seen before , by adding a small amount of water to the working fluid is significantly increased the area of the p-V diagram, i.e. the output power of the cycle, for the same conditions of pressure, temperature and velocity.
For this reason, and because one of the ultimate goals of this project is to improve the operation of the engine in the laboratory, we proceed to perform some simple experiments to see if actually happens the theoretically expected.

As we can see in the engine specification sheet (see Annex 4) fluids with which the engine can work are nitrogen, helium and dry air. Therefore, it is advisable to add only a small amount of water. Furthermore, by adding a small amount of water the pressure increases considerably: this is another motive for which is dangerous to add too much water.

Another important issue is how to introduce water in the engine. One option is to put it directly into the regenerator, but this possibility needs to disassemble large part of the engine, which is very laborious and therefore not feasible.

The first option which is considered done is to introduce the water through the conduit through which air is introduced under pressure to charge the engine, but this option is not fruitful, and added water comes back out.

The following idea is to introduce water through the conduit in which is housed the thermocouple that measures the temperature of the cold zone, because said conduit reaches inside the working piston cylinder. In this case, the water goes into the engine properly.

However, when conducting the experiments, we have a problem: the pressure inside the motor falls very quickly, which means that there is an air leak. The motive may be the high temperatures reached inside the burning room during the previous experiments, which have been able to exceed the maximum allowable temperature for the material of a motor component (aluminum, or some rubber seal), which has caused that some piece has melted or cracked, and thus, gives rise to a leak.

Nevertheless, given the impossibility of performing a further series of experiments, are performed a couple of them with different amounts of water in the working fluid, and during which it is not possible to have a constant pressure. Therefore, the comparison of these experiments with reality supposes a complication.
For reasons of time, it is impossible to detect and fix the air leak, since this requires removing and disassembling almost the entire engine and this means days or weeks of job.

Experiment 11: 4 grams of water

Propane flow (g/s)	Q_{in} (W)	Mean pressure (bar)	Cold temp. (K)	Hot temp. (K)	Mean rotation speed (rpm)	Max. output power (W)	Eff. (%)
0,151	3500,1	6,24	313	646	636	340,5	9,73

Chart 23 - Results of experiment 11.

Experiment 12: 8 grams of water

Propane flow (g/s)	Q_{in} (W)	Mean pressure (bar)	Cold temp. (K)	Hot temp. (K)	Mean rotation speed (rpm)	Max. output power (W)	Eff. (%)
0,151	3500,1	3,81	310	675	616	245,1	7,00

Chart 24 - Results of experiment 12.

Following we compare in a graphic the power output as a function of both pressure and propane flow, for experiments with and without air (see next page).

As we can see, dots corresponding to experiments with water are higher than should be if the experiments were with only air as a propane flow (what means higher output power). Red line means 0,163 g/s of propane flow, and blue line, 0,1 g/s. Experiments with water are with 0,151 g/s of propane flow, so the dots should be between that lines. However, they are above line corresponding to 0,163 g/s.

The green line is the estimation of the power Vs. pressure line, corresponding to 0,151 g/s of propane. As we can see, for the pressure corresponding to 4 grams of water (6,24 bar), if it would be with air as a working fluid, it should give a output power of 275 W approximately; however, it gives 340,5 W, i.e., almost the 25% more.

If we do the same analysis for 8 grams of water, if it were only with air, it should give a power of 180 W approx., and it really gives 245,1, i.e., 36% more.

Although we could not have performed more experiments with air+water as a working fluid, it is in view, with the few results we have, that using TPTC working fluid provokes an increase in engine output power, for the same working conditions.

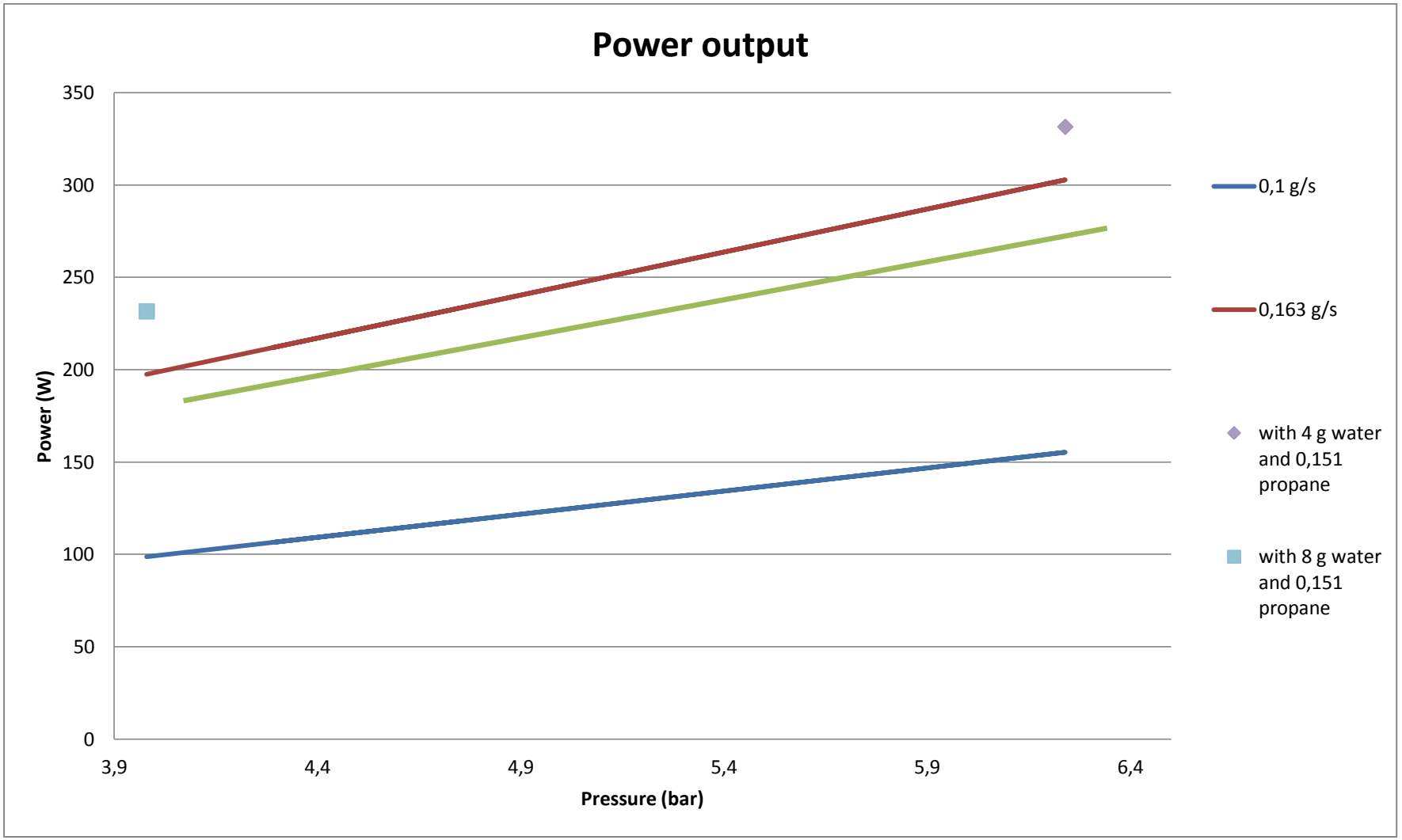

Image 77 - Output power for TPTC working fluids.

7.4. COMPARISON BETWEEN EXPERIMENTS AND THEORETICAL CYCLE

In the previous section we have seen a summary of the experimental results of each experiment.

Then we will determine for the values of pressure, temperature and speed of these experiments, i.e., for these conditions, isothermal values (with analysis Schmidt) and adiabatic. Simulations based on the analysis of Schmidt are made using a simulation with Matlab (see annex 2).This simulation is based on the analysis of theoretical Schmidt cycle explained in chapter 2.

On the other hand, as we have seen in chapter 2, theoretical analysis for the adiabatic cycle, it is studied by a system of nonlinear differential equations, which is only possible to solve using numerical methods . The programming of this resolution with Matlab is too complex and is beyond the scope of this project. For the analysis of the adiabatic cycle, we proceed to use software available online on a website (see bibliography, webpages, reference /2/) which from the input data yields a pdf file that contains the important output parameters of the study.

Following there is a comparison between the real performance with both theoretical cycles, for each of the experiments.

EXPERIMENT 1:

Gas type	Propaneflow	Mean pressure	Temp. cold	Temp. hot	Frequency
Air	0,1 g/s	4,87 bar	308 K	526 K	444 rpm

Chart 25 - Data input of experiment 1.

Schmidt analysis:

- Mass of gas inside the engine: 7,3 g
- Output power (P): 208,5 W
- Heat exchanged in compression space (Q_c): -39,7 J
- Heat exchanged in expansion space (Q_e): 67,9 J
- Efficiency (Carnot): 41,5%

Adiabatic analysis:

- Mass of gas inside the engine: 7,87 g
- Output power (P): 163,1 W
- Heat exchanged in cooler (Q_k): -40,6 J
- Heat exchanged in regenerator (Q_r): 266,5 J
- Heat exchanged in heater (Q_h): 63,9 J
- Work exchanged in compression space (W_c): -40,6 J
- Work exchanged in expansion space (W_e): 63,9 J
- Efficiency: 36,5%

Real results:

- Output power (P): 103,8 W
- Efficiency: 4,50%

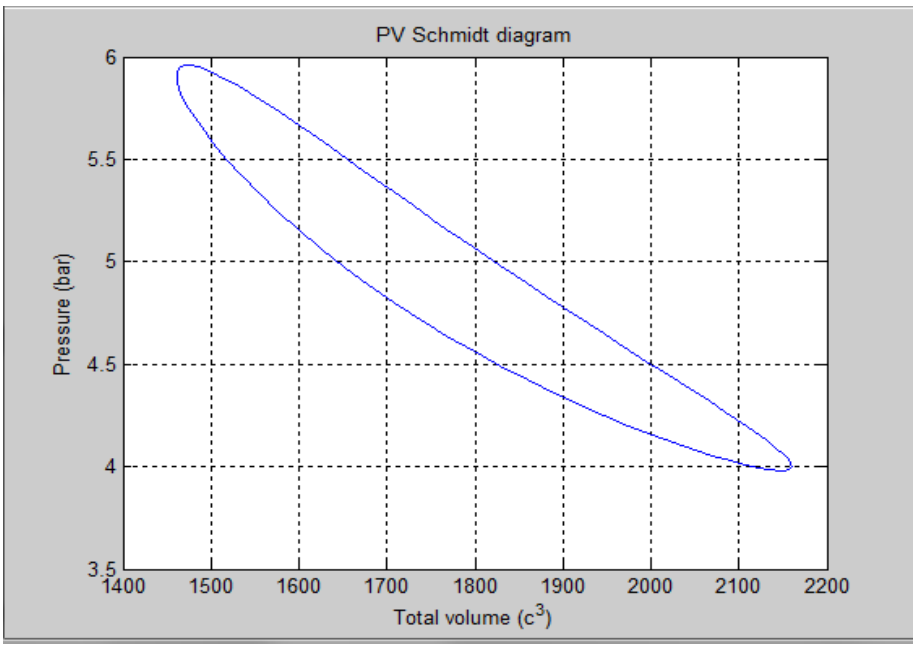

Image 78 - Experiment 1. p-V diagram

EXPERIMENT 2:

Gas type	Propaneflow	Mean pressure	Temp. cold	Temp. hot	Frequency
Air	0,1 g/s	5,75 bar	309 K	552 K	391 rpm

Chart 26 - Data input of experiment 2

Schmidt analysis:

- Mass of gas inside the engine: 8,37 g
- Output power (P): 235,8 W
- Heat exchanged in compression space (Q_c): -46 J
- Heat exchanged in expansion space (Q_e): 82,2 J
- Efficiency (Carnot): 44%

Adiabatic analysis:

- Mass of gas inside the engine: 9,13 g
- Output power (P): 180 W
- Heat exchanged in cooler (Q_k): -46,6 J
- Heat exchanged in regenerator (Q_r): 342,2 J
- Heat exchanged in heater (Q_h): 76,6 J
- Work exchanged in compression space (W_c): -46,6 J
- Work exchanged in expansion space (W_e): 76,6 J
- Efficiency: 39,2%

Real results:

- Output power (P): 155,4 W
- Efficiency: 6,70%

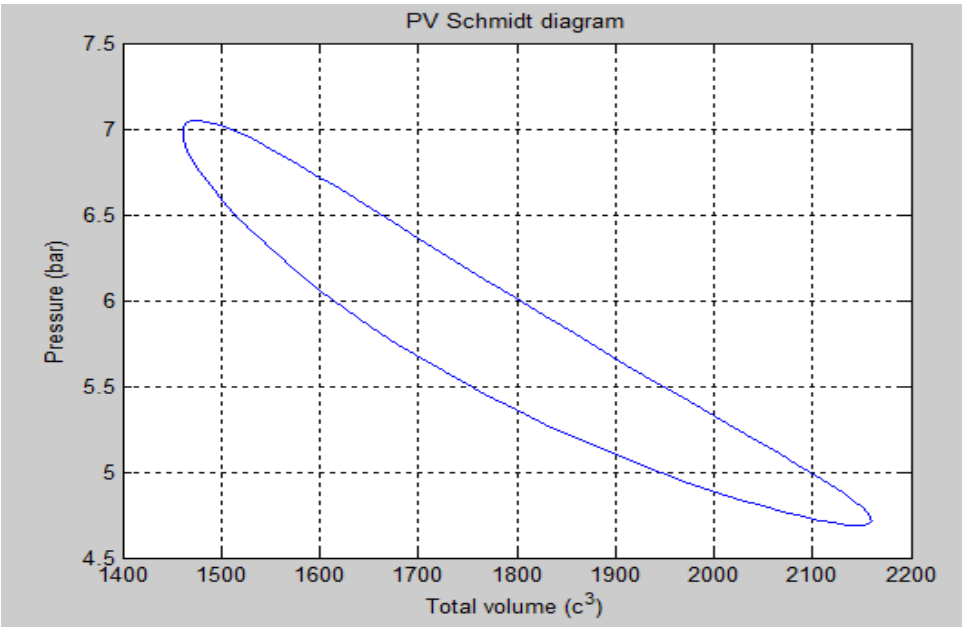

Image 79 - Experiment 2. p-V diagram

EXPERIMENT 3:

Gas type	Propaneflow	Mean pressure	Temp. cold	Temp. hot	Frequency
Air	0,1 g/s	6,60 bar	310 K	559 K	366 rpm

Chart 27 - Data input of experiment 3

Schmidt analysis:

- Mass of gas inside the engine: 9,52 g
- Output power (P): 258,5 W
- Heat exchanged in compression space (Q_c): -52,6 J
- Heat exchanged in expansion space (Q_e): 95 J
- Efficiency (Carnot): 44,6%

Adiabatic analysis:

- Mass of gas inside the engine: 10,4 g
- Output power (P): 211,1 W
- Heat exchanged in cooler (Q_k): -53,1 J
- Heat exchanged in regenerator (Q_r): 400,9 J
- Heat exchanged in heater (Q_h): 88,3 J
- Work exchanged in compression space (W_c): -53,1 J
- Work exchanged in expansion space (W_e): 88,3J
- Efficiency: 39,9%

Real results:

- Output power (P): 176 W
- Efficiency: 7,59%

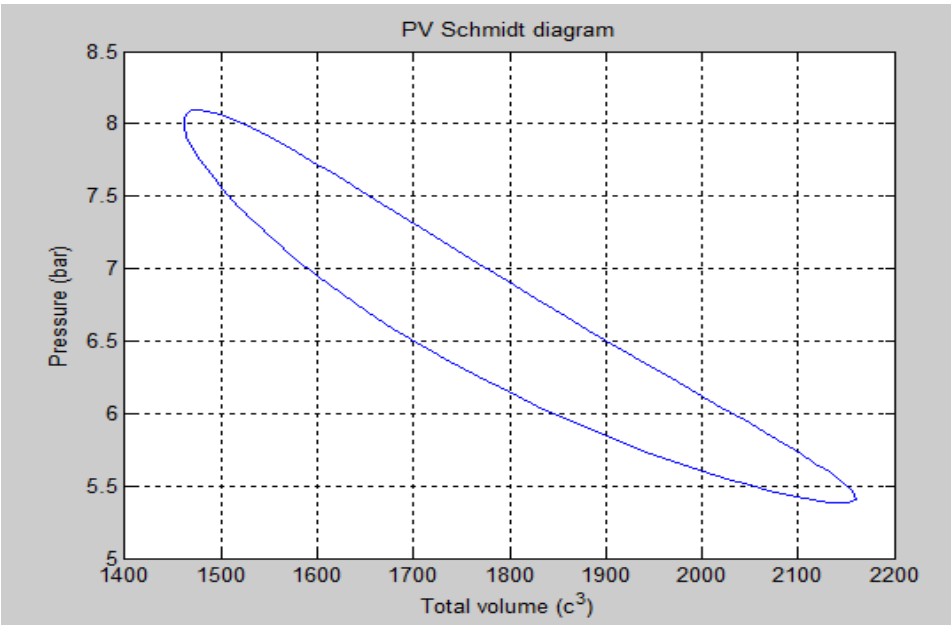

Image 80 - Experiment 3. p-V diagram

EXPERIMENT 4:

Gas type	Propaneflow	Mean pressure	Temp. cold	Temp. hot	Frequency
Air	0,1 g/s	7,47 bar	312 K	541 K	393 rpm

Chart 28 - Data input of experiment 4

Schmidt analysis:

- Mass of gas inside the engine: 10,96 g
- Output power (P): 291,6 W
- Heat exchanged in compression space (Q_c): -60,5 J
- Heat exchanged in expansion space (Q_e): 105 J
- Efficiency (Carnot): 42,4%

Adiabatic analysis:

- Mass of gas inside the engine: 11,9 g
- Output power (P): 220,5 W
- Heat exchanged in cooler (Q_k): -61,7 J
- Heat exchanged in regenerator (Q_r): 419,9 J
- Heat exchanged in heater (Q_h): 98,4 J
- Work exchanged in compression space (W_c): -61,7 J
- Work exchanged in expansion space (W_e): 98,4 J
- Efficiency: 37,3%

Real results:

- Output power (P): 188,3 W
- Efficiency: 8,12%

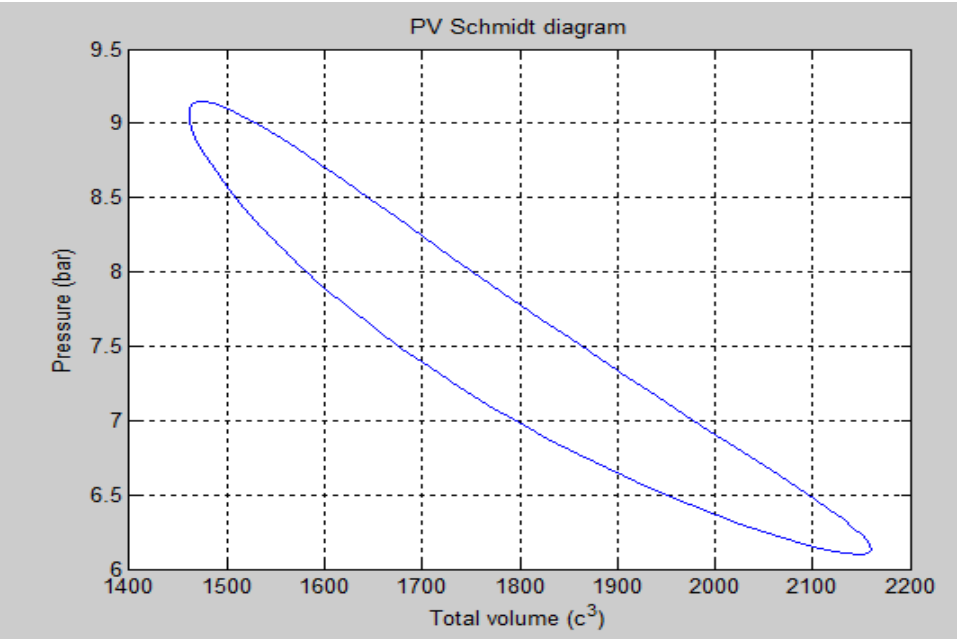

Image 81 - Experiment 4. p-V diagram.

EXPERIMENT 5:

Gas type	Propaneflow	Mean pressure	Temp. cold	Temp. hot	Frequency
Air	0,1 g/s	8,98 bar	313 K	535 K	384 rpm

Chart 29 - Data input of experiment 5

Schmidt analysis:

- Mass of gas inside the engine: 13,22 g
- Output power (P): 331,4 W
- Heat exchanged in compression space (Q_c): -73,2 J
- Heat exchanged in expansion space (Q_e): 125 J
- Efficiency (Carnot): 41,4%

Adiabatic analysis:

- Mass of gas inside the engine: 14,2 g
- Output power (P): 256,5 W
- Heat exchanged in cooler (Q_k): -74,9 J
- Heat exchanged in regenerator (Q_r): 489 J
- Heat exchanged in heater (Q_h): 117,6 J
- Work exchanged in compression space (W_c): -74,9 J
- Work exchanged in expansion space (W_e): 117,6 J
- Efficiency: 36,3%

Real results:

- Output power (P): 215,3 W
- Efficiency: 9,29%

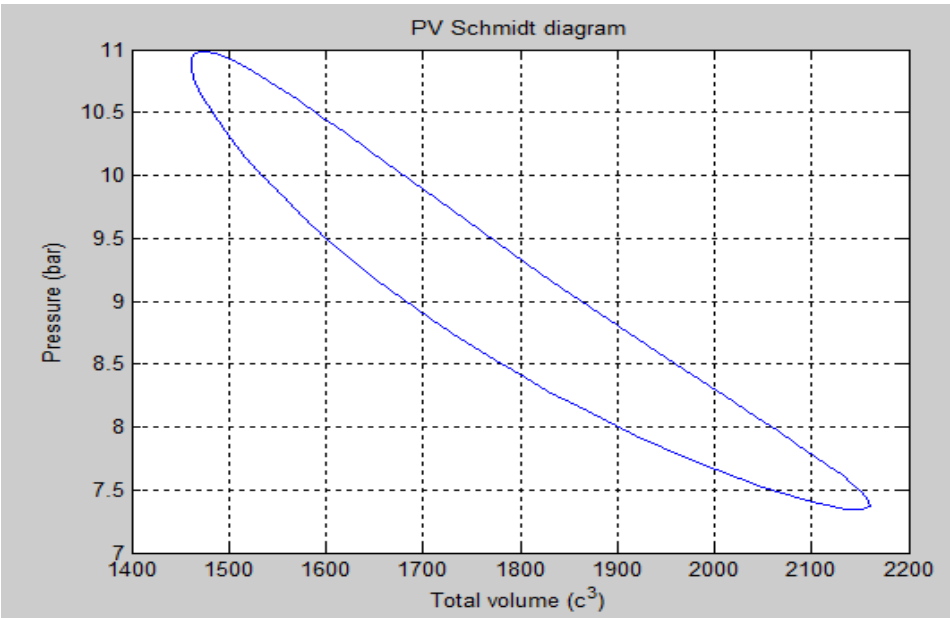

Image 82 - Experiment 5. p-V diagram.

The previous 5 experiments were for air as a working fluid, and a propane flow of 0,1 g/s. Following it is represented the different output powers and efficiencies, for the 3 cycles (isotherm, adiabatic and real) as a function of the mean pressure.

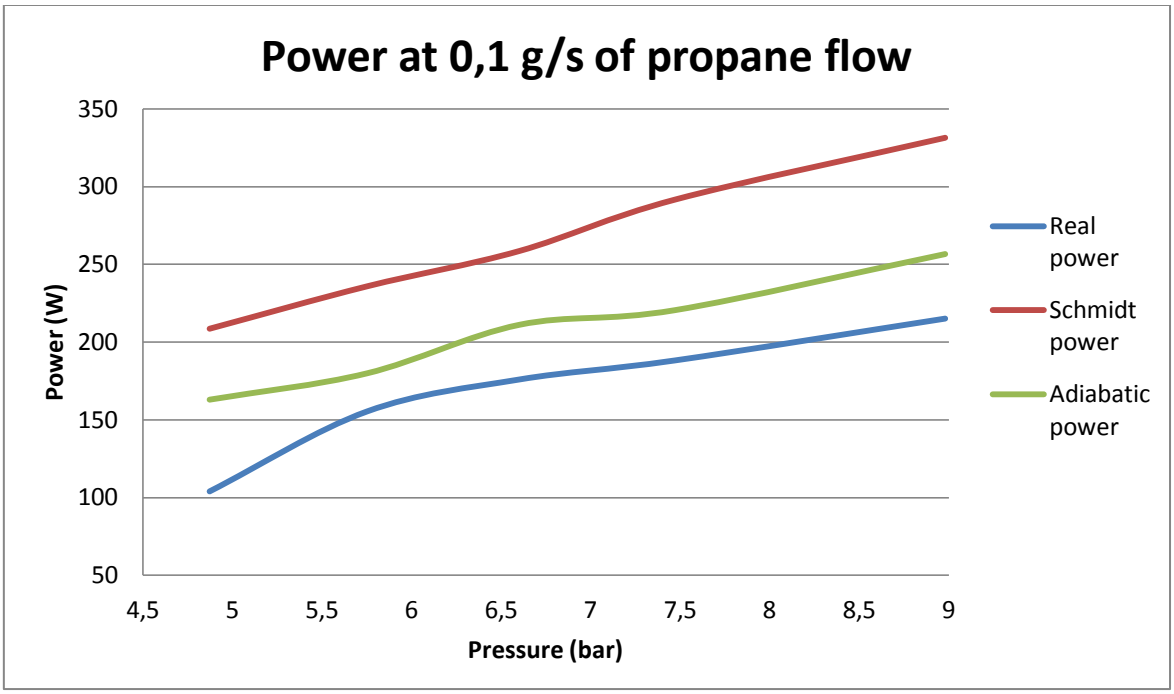

Image 83 - Real, isotherm and adiabatic power for 0,1 g/s of propane.

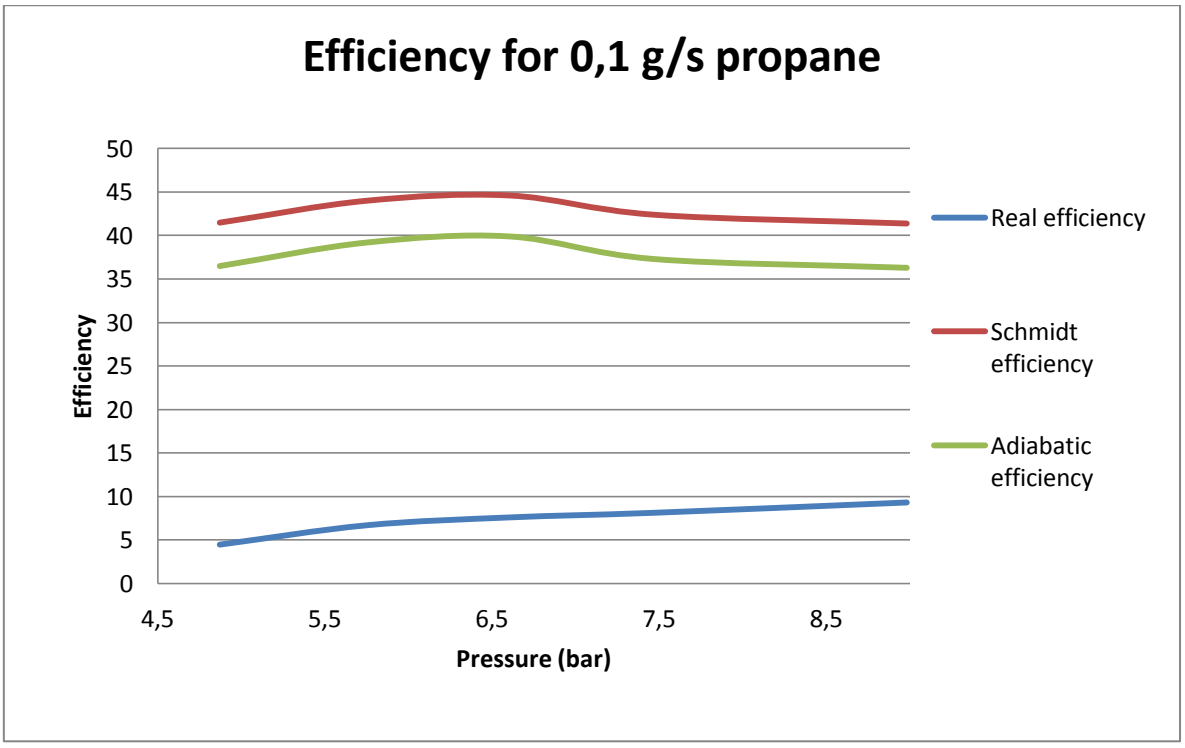

Image 84 - Real, isotherm and adiabatic efficiency for 0,1 g/s of propane.

EXPERIMENT 6:

Gas type	Propaneflow	Mean pressure	Temp. cold	Temp. hot	Frequency
Air	0,163 g/s	5,04 bar	313 K	651 K	494 rpm

Image 85 - Data input of experiment 6.

Schmidt analysis:

- Mass of gas inside the engine: 6,61 g
- Output power (P): 336,9 W
- Heat exchanged in compression space (Q_c): -37,7 J
- Heat exchanged in expansion space (Q_e): 78,8 J
- Efficiency (Carnot): 51,9%

Adiabatic analysis:

- Mass of gas inside the engine: 7,5 g
- Output power (P): 269,7 W
- Heat exchanged in cooler (Q_k): -37 J
- Heat exchanged in regenerator (Q_r): 381,8 J
- Heat exchanged in heater (Q_h): 70,7 J
- Work exchanged in compression space (W_c): -37 J
- Work exchanged in expansion space (W_e): 70,7 J
- Efficiency: 47,7%

Real results:

- Output power (P): 237 W
- Efficiency: 6,27%

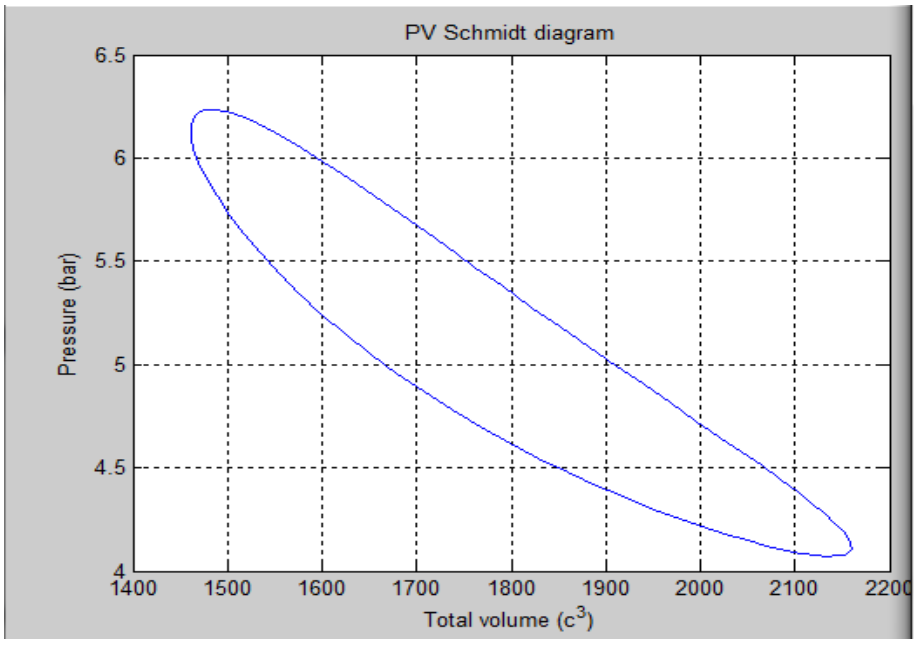

Image 86 - Experiment 6. p-V diagram.

EXPERIMENT 7:

Gas type	Propaneflow	Mean pressure	Temp. cold	Temp. hot	Frequency
Air	0,163 g/s	5,63 bar	314 K	665 K	496 rpm

Image 87 - Data input of experiment 7.

Schmidt analysis:

- Mass of gas inside the engine: 7,28 g
- Output power (P): 388,4 W
- Heat exchanged in compression space (Q_c): -42 J
- Heat exchanged in expansion space (Q_e): 89 J
- Efficiency (Carnot): 52,8%

Adiabatic analysis:

- Mass of gas inside the engine: 8,3 g
- Output power (P): 309 W
- Heat exchanged in cooler (Q_k): -40,9 J
- Heat exchanged in regenerator (Q_r): 473,2 J
- Heat exchanged in heater (Q_h): 79,5 J
- Work exchanged in compression space (W_c): -40,9 J
- Work exchanged in expansion space (W_e): 79,5 J
- Efficiency: 48,6%

Real results:

- Output power (P): 278,5 W
- Efficiency: 7,37%

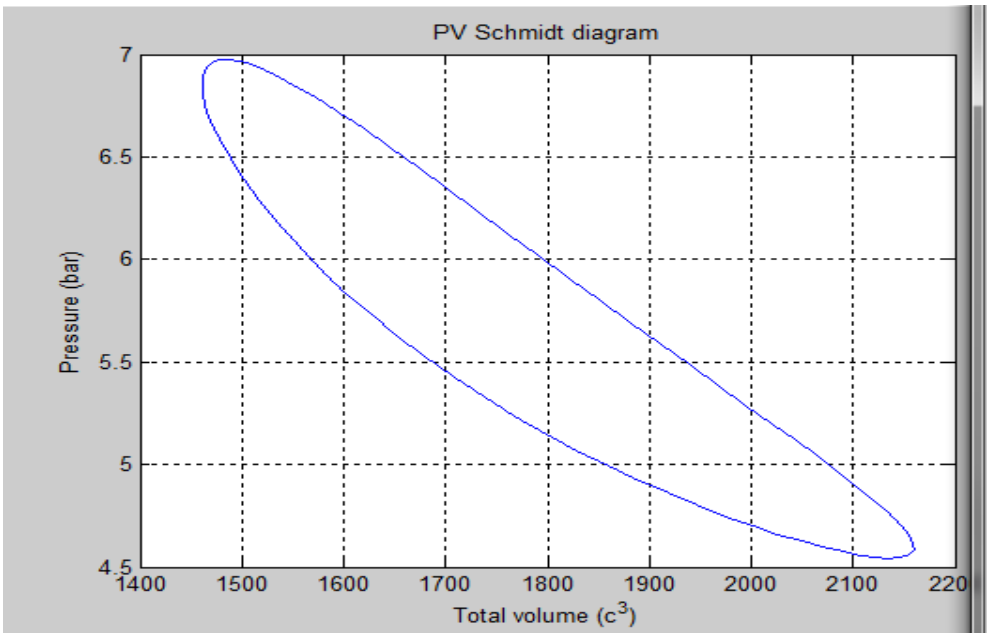

Image 88 - Experiment 7. p-V diagram.

EXPERIMENT 8:

Gas type	Propaneflow	Mean pressure	Temp. cold	Temp. hot	Frequency
Air	0,163 g/s	6,34 bar	315 K	680 K	461 rpm

Image 89 - Data input of experiment 8.

Schmidt analysis:

- Mass of gas inside the engine: 8,08 g
- Output power (P): 418,1 W
- Heat exchanged in compression space (Q_c): -47 J
- Heat exchanged in expansion space (Q_e): 101,4 J
- Efficiency (Carnot): 53,7%

Adiabatic analysis:

- Mass of gas inside the engine: 9,26 g
- Output power (P): 312,5 W
- Heat exchanged in cooler (Q_k): -45,4 J
- Heat exchanged in regenerator (Q_r): 505 J
- Heat exchanged in heater (Q_h): 90,1 J
- Work exchanged in compression space (W_c): -45,4 J
- Work exchanged in expansion space (W_e): 90,1 J
- Efficiency: 49,6%

Real results:

- Output power (P): 317,3 W
- Efficiency: 8,4%

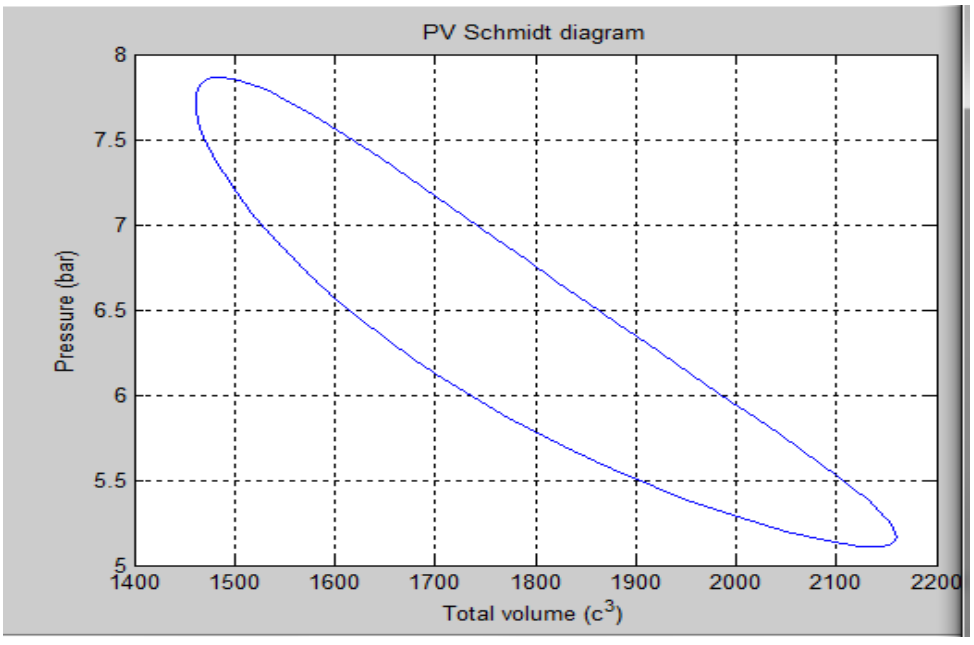

Image 90 - Experiment 8. p-V diagram.

EXPERIMENT 9:

Gas type	Propaneflow	Mean pressure	Temp. cold	Temp. hot	Frequency
Air	0,163 g/s	7,90 bar	319 K	653 K	501 rpm

Image 91 - Data input of experiment 9.

Schmidt analysis:

- Mass of gas inside the engine: 10,26 g
- Output power (P): 522,7 W
- Heat exchanged in compression space (Q_c): -59,8 J
- Heat exchanged in expansion space (Q_e): 122,4 J
- Efficiency (Carnot): 51,2%

Adiabatic analysis:

- Mass of gas inside the engine: 11,6 g
- Output power (P): 413,1 W
- Heat exchanged in cooler (Q_k): -58,6 J
- Heat exchanged in regenerator (Q_r): 585,2 J
- Heat exchanged in heater (Q_h): 110,3 J
- Work exchanged in compression space (W_c): -58,6 J
- Work exchanged in expansion space (W_e): 110,3 J
- Efficiency: 46,8%

Real results:

- Output power (P): 382 W
- Efficiency: 10,11%

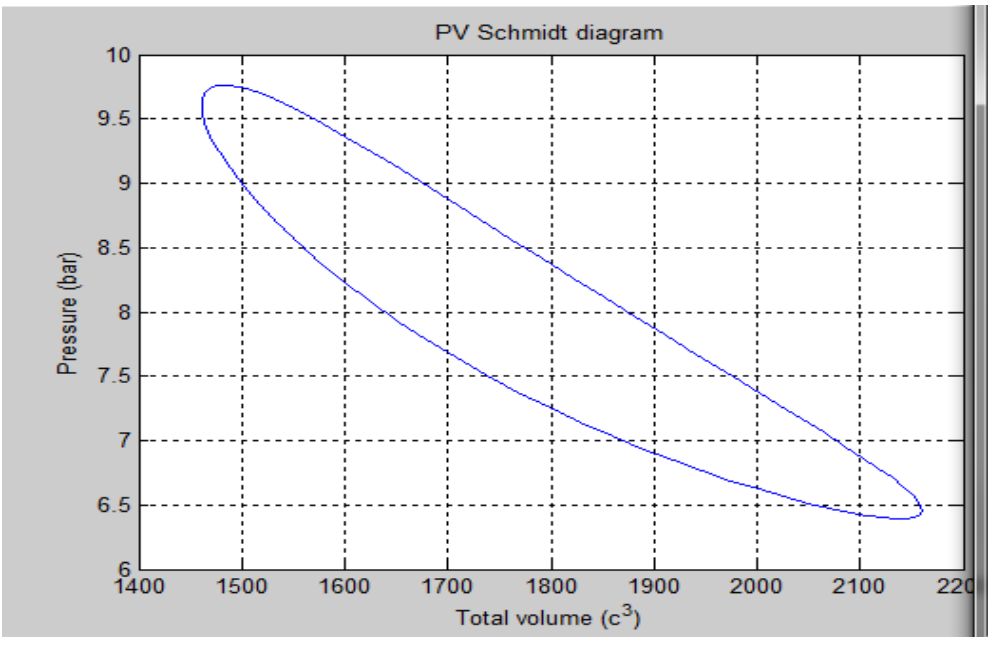

Image 92 - Experiment 9. p-V diagram.

EXPERIMENT 10:

Gas type	Propaneflow	Mean pressure	Temp. cold	Temp. hot	Frequency
Air	0,163 g/s	8,53 bar	319 K	656 K	479 rpm

Image 93 - Data input of experiment 10.

Schmidt analysis:

- Mass of gas inside the engine: 11,05 g
- Output power (P): 543,4 W
- Heat exchanged in compression space (Q_c): -64,4 J
- Heat exchanged in expansion space (Q_e): 132,5 J
- Efficiency (Carnot): 51,4%

Adiabatic analysis:

- Mass of gas inside the engine: 12,49 g
- Output power (P): 449 W
- Heat exchanged in cooler (Q_k): -63,1 J
- Heat exchanged in regenerator (Q_r): 636 J
- Heat exchanged in heater (Q_h): 119,2 J
- Work exchanged in compression space (W_c): -63,1 J
- Work exchanged in expansion space (W_e): 119,2 J
- Efficiency: 47,1%

Real results:

- Output power (P): 404 W
- Efficiency: 10,69%

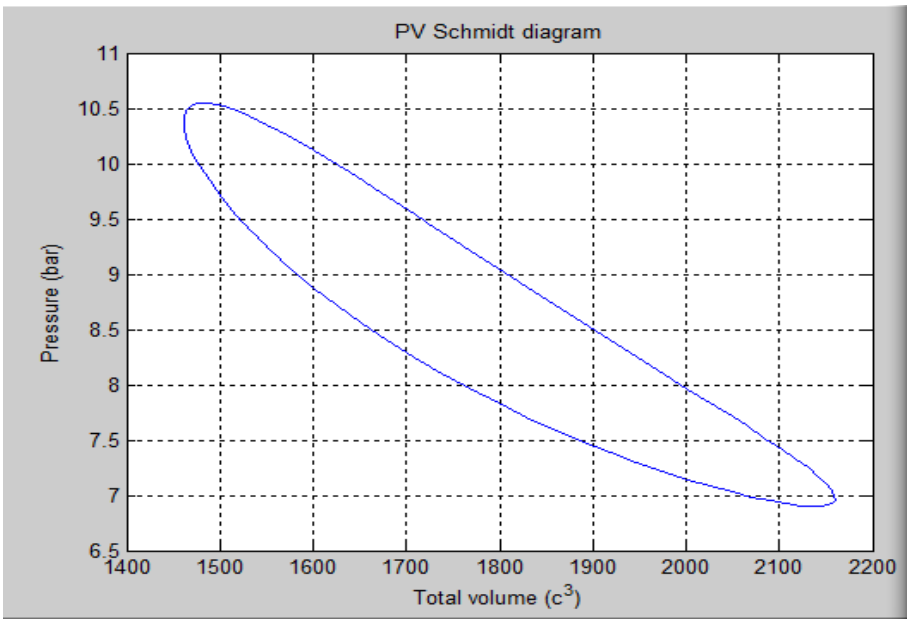

Image 94 - Experiment 10. p-V diagram.

The previous 5 experiments were for air as a working fluid, and a propane flow of 0,163 g/s. Following it is represented the different output powers and efficiencies, for the 3 cycles (isotherm, adiabatic and real) as a function of the mean pressure.

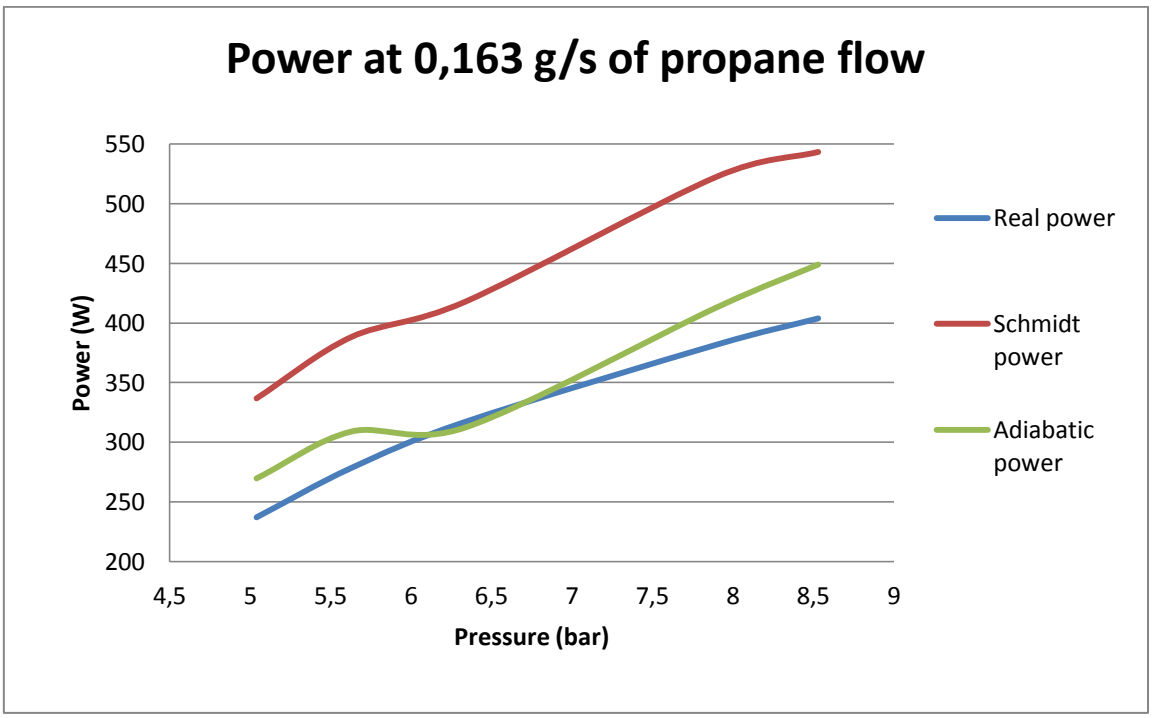

Image 95 - Real, isotherm and adiabatic power for 0,163 g/s of propane.

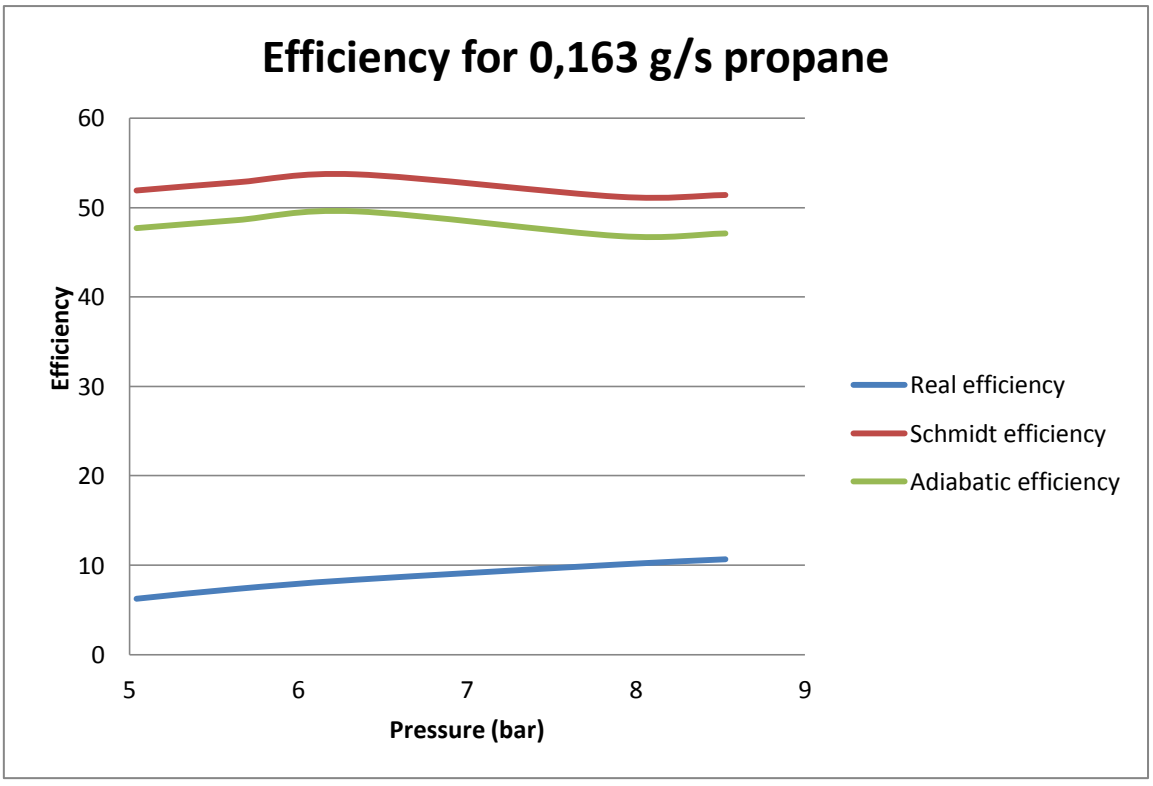

Image 96 - Real, isotherm and adiabatic efficiency for 0,163 g/s of propane.

As we can see, and obviously, the maximum power for each value of pressure is the one related to the isotherm analysis. This is because, as mentioned in chapter 2 the isotherm analysis is very ideal, and does not take in account most of the losses that happen during the working of the engine. Therefore, the isotherm efficiency matches the Carnot efficiency.
On the other hand, we can see that the adiabatic power is more similar to the real one; this is because this analysis is more realistic than the isotherm; while the isotherm assumes discontinuous movement of the pistons, perfect regeneration and not dead volume, the adiabatic is closer to the reality in these aspects: it assumes sinusoidal movement, imperfect regeneration and existence of dead volume in both expansion and compression areas.

Finally, we can see that the real performance of the engine is less than in the ideal cycles; this is because, in the real working, occur some facts that are not taken into account in the ideal analysis:

- The working gas (air) is not a perfect gas
- There is flow resistance inside the engine, and therefore, the pressure is not constant at every moment in the whole engine
- The regeneration is imperfect; there is heat losses in the regenerator
- There are heat losses because of conduction, convection and radiation from the engine to the environs
- The expansion and compression are neither adiabatic nor isotherm, there is heat drop across the heat exchangers surfaces
- The variation of compression and expansion volumes is neither discontinuous nor perfectly sinusoidal
- There is mechanical friction
- There are dead volumes

The ideal (isotherm and adiabatic) analysis make some of the previous assumptions, and for that reason, are far from the real performance; the isothermal one makes more unrealistic assumptions than the adiabatic, and it is therefore farer from the reality.

Other conclusion we can draw is that, as expected, the isothermal efficiency (or Carnot efficiency) is greater than the adiabatic, and both are much higher than the real. This is due, firstly, that in both theoretical analyzes many losses are not taken into account (as we have already mentioned above). In addition, losses of the combustion chamber, which could not be 100% calculated but estimated, also have very important influence on the efficiency of the motor.

As we can see in the figures of efficiencies, for Carnot and adiabatic efficiencies the pressure is not a factor in which they depend on. This is not true, and is because Carnot efficiency only depends on hot and cold temperature, and adiabatic efficiency on temperatures, dead volumes and swept volume ratio. However, in real efficiency we can see that it depends on pressure, and it is obvious, because heat input is the same (for constant propane flow), but power output depends on pressure (higher with higher pressures); therefore, efficiency must be higher at higher pressures, for the same propane flow.

EXPERIMENT 11:

Gas type	Amount of water	ß	Propaneflow	Mean pressure	Temp. cold	Temp. hot	Frequency
TPTC	4 g	0,49	0,151 g/s	6,24 bar	313 K	646 K	636 rpm

Chart 30 - Data input of experiment 11.

Schmidt analysis if it would have only air as a working fluid:

- Mass of gas inside the engine: 8,22 g
- Output power (P): 530,9 W
- Heat exchanged in compression space (Q_c): -47,1 J
- Heat exchanged in expansion space (Q_e): 97,1 J
- Efficiency (Carnot): 51,6%

Schmidt analysis for TPTC working fluid:

- Output power: 1203,2 W
- Output work: 113,5 J
- Real efficiency: 9,73 %

See graphics in next page.

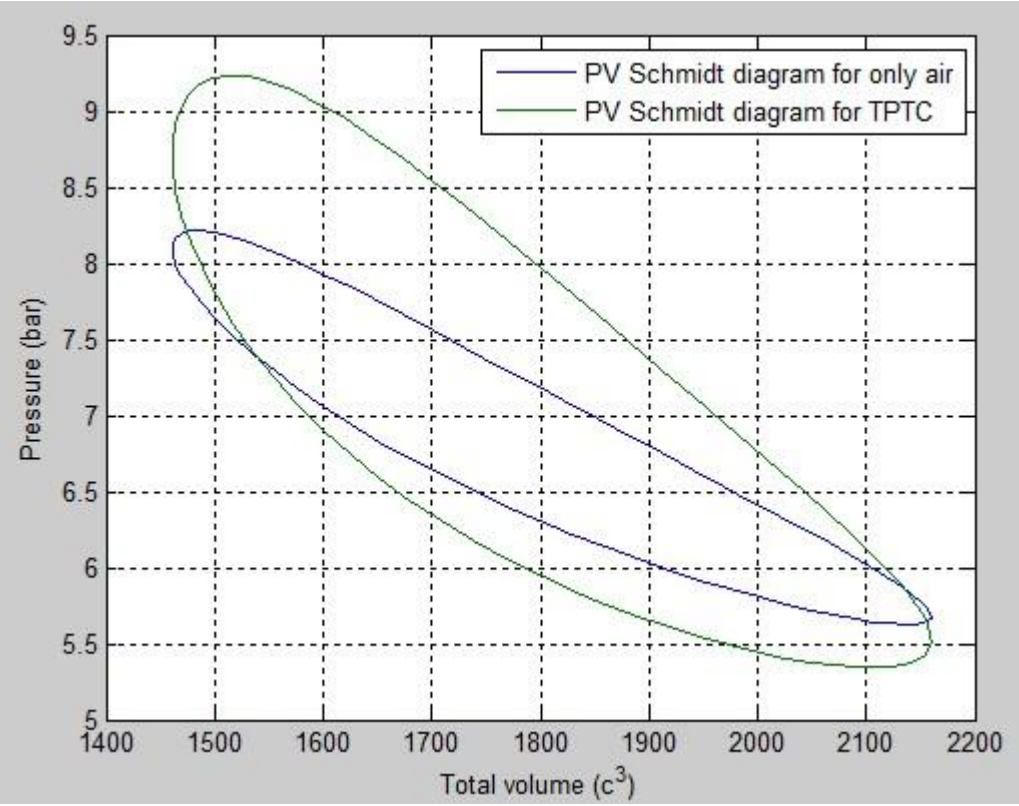

Image 97 - Experiment 11. p-V diagram.

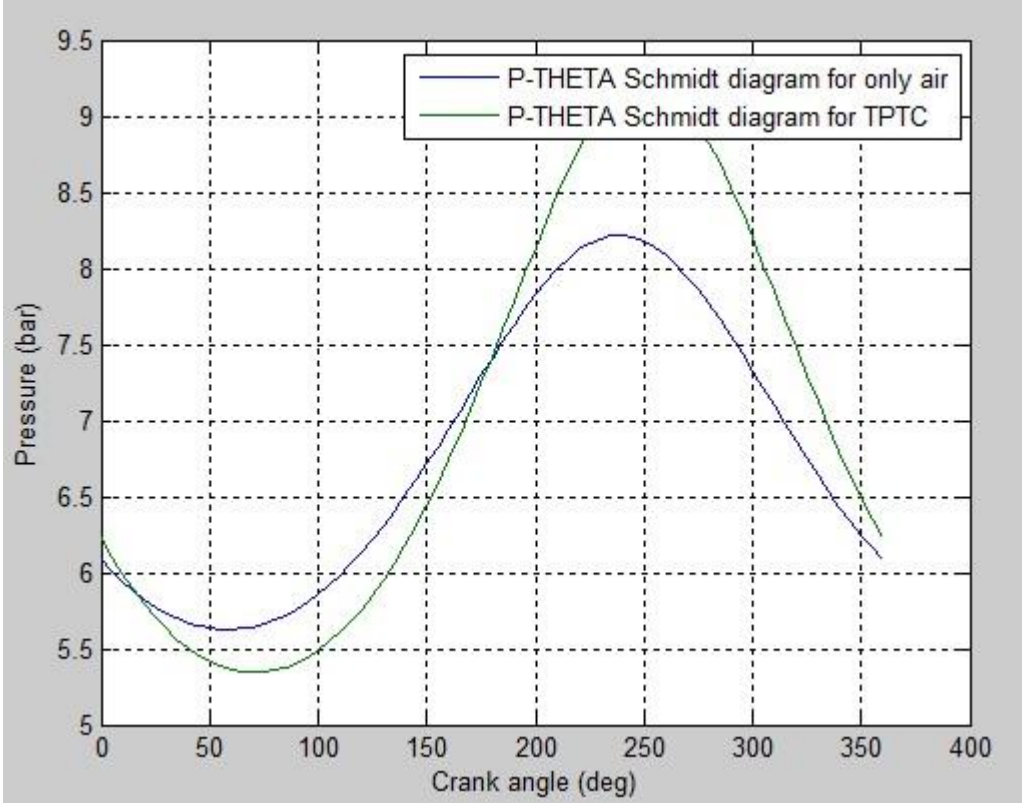

Image 98 - Experiment 11. p-theta diagram.

EXPERIMENT 12:

Gas type	Amount of water	ß	Propaneflow	Mean pressure	Temp. cold	Temp. hot	Frequency
TPTC	8 g	1,63	0,151 g/s	3,81 bar	310 K	675 K	616 rpm

Chart 31 - Data input of experiment 12.

Schmidt analysis if it would have only air as a working fluid:

- Mass of gas inside the engine: 4,91 g
- Output power (P): 340 W
- Heat exchanged in compression space (Q_c): -28,1 J
- Heat exchanged in expansion space (Q_e): 61,2 J
- Efficiency (Carnot): 54,1%

Schmidt analysis for TPTC working fluid:

- Output power: 1433,1 W
- Output work: 139,6 J
- Real efficiency: 7,00 %

See graphics in next page.

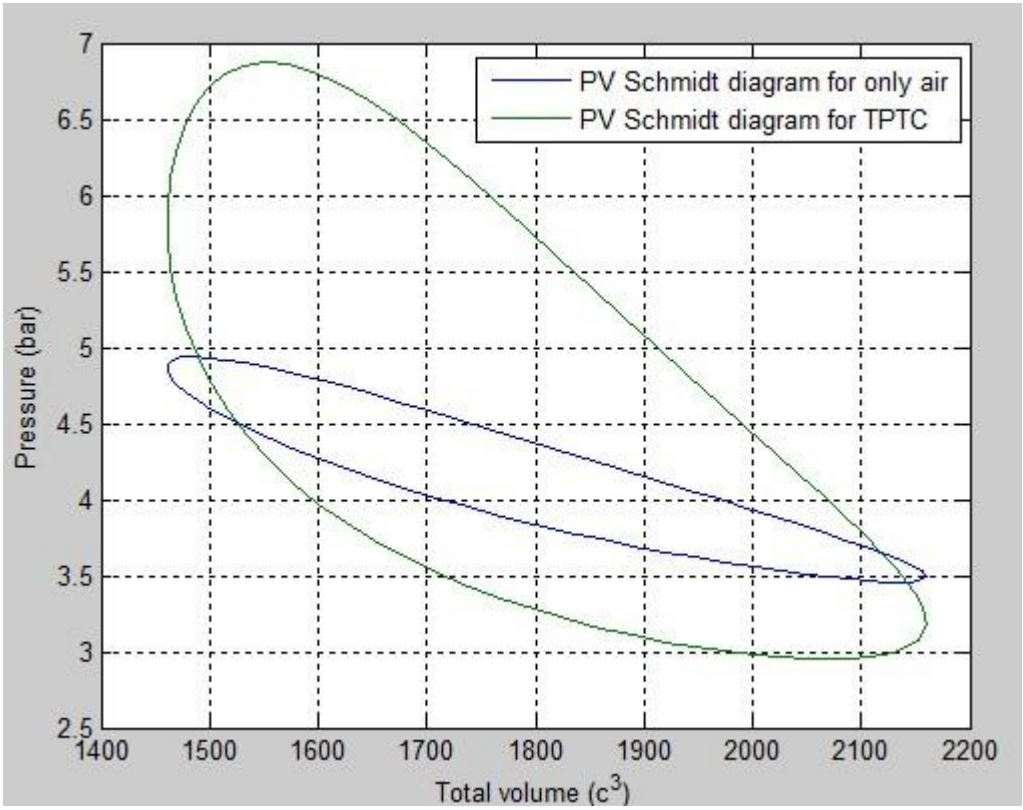

Image 99 - Experiment 12. p-V diagram.

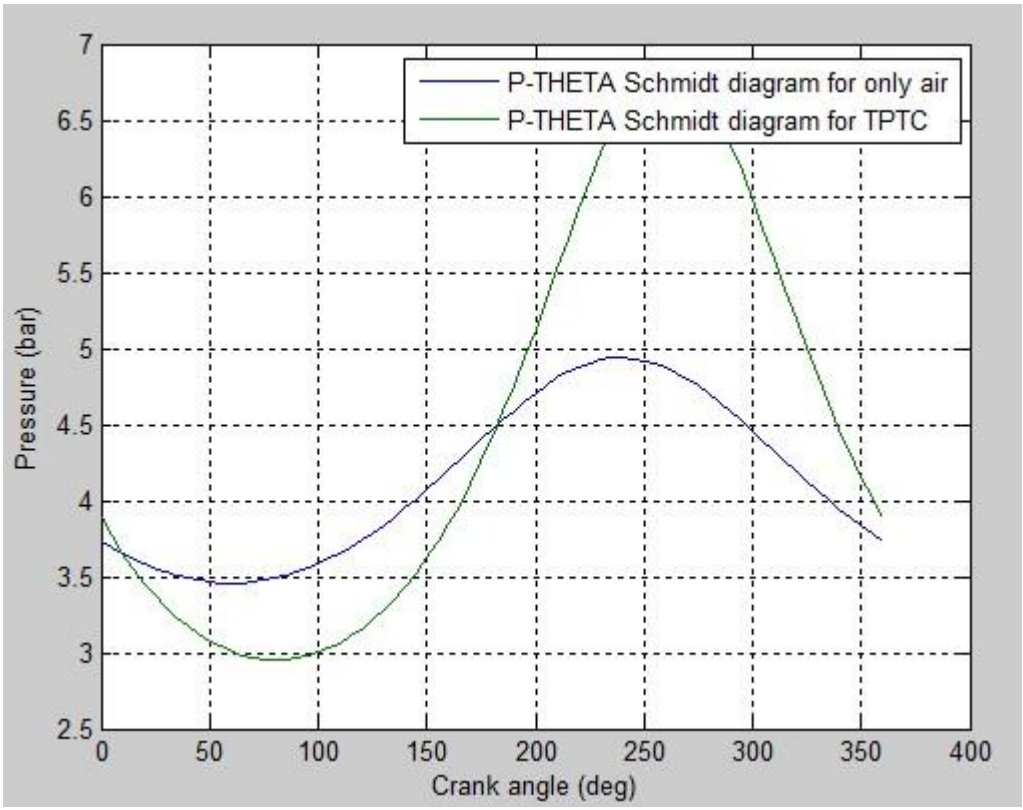

Image 100 - Experiment 12. p-theta diagram.

As we can see, and obviously, the power related to the isothermal analysis is much higher than the real power. This is because, as mentioned in chapter 2, the isotherm analysis is very ideal, and does not take in account most of the losses that happen during the working of the engine. Therefore, the isotherm efficiency matches the Carnot efficiency.

CONCLUSSIONS AND OUTLOOK OF THE THESIS

This Thesis allows learning many things about the working of engines. And not only the things concerning the engine by itself: it also allows learning about programming with Matlab, about using DIAdem, and about solving problems when they arise in the workplace.

Before this work, there were many problems with the engine in the laboratory: there were some sensors uninstalled, there were nothing programming for calculating efficiencies and powers, and for comparing with theoretic, and, in short, there was only a engine but nothing else.

Now, the engine is ready for working with it; furthermore, there is a DIAdem program for displaying and calculating many parameters, and a Matlab program that makes many comparisons.

As we have seen, the variation of various parameters affects engine performance, both in theory and in practice.

It has been shown that by increasing the load pressure of the engine, increases the efficiency thereof.

Also that performance is improved by increasing the temperature of the hot zone, which in turn is done by increasing the flow of propane.

Finally, it has become clear what it was supposed at the beginning of the thesis: adding a phase change component to the gaseous working fluid, improves significantly the engine performance, for the same conditions.

Some improvements could be performed in order to improve the performance of the engine. The major disadvantage has been found in this motor is the large number of losses in it is, above all, the losses by the exhaust gases, which could be minimized if built into the engine a recirculation of said gas , whose heat could be used to preheat the air entering the combustion chamber.

Finally, this Thesis has been the perfect addition to the degree courses of Industrial Engineering. In the last ten semesters (this is what the degree lasts in Spain), not many aspects about programming were studied, but basic aspects of this. And the same for many things related to Stirling engines. Many things were new and therefore had to be learnt from the beginning. Even so, with enthusiasm and effort, everyone can learn what is needed to achieve the required objectives.

SUMMARY OF EQUATIONS

Ec. 1: Heat transferred in the isothermal compression in ideal Stirling cycle.

$$Q = W = p_1 V_1 \ln\left(\frac{1}{r_v}\right) = mRT_1 \ln\left(\frac{1}{r_v}\right) \qquad [Ec.1]$$

Ec. 2: Entropy difference in the isothermal compression in ideal Stirling cycle.

$$s_2 - s_1 = R \ln\left(\frac{1}{r_v}\right) \qquad [Ec.2]$$

Ec. 3: Heat transferred in the heating in ideal Stirling cycle.

$$Q(heat\ transferred) = C_v(T_3 - T_2) \qquad [Ec.3]$$

Ec. 4: Entropy difference in the heating in ideal Stirling cycle.

$$s_3 - s_2 = C_v \ln\left(\frac{1}{\tau}\right) \qquad [Ec.4]$$

Ec. 5: Heat transferred in the isothermal expansion in ideal Stirling cycle.

$$Q = W = P_3 V_3 \ln(r_v) = mRT_3 \ln(r_v) \qquad [Ec.5]$$

Ec. 6: Entropy difference in the isothermal expansion in ideal Stirling cycle.

$$s_3 - s_4 = R \ln(r_v) \qquad [Ec.6]$$

Ec. 7: Heat transferred in the cooling in ideal Stirling cycle.

$$Q(heat\ transferred) = C_v(T_1 - T_4) \qquad [Ec.7]$$

Ec. 8: Entropy difference in the cooling in ideal Stirling cycle.

$$s_1 - s_4 = C_v \ln(\tau) \qquad [Ec.8]$$

Ec. 9: Efficiency of the ideal Stirling cycle.

$$\eta = \frac{W_{output}}{Q_{input}} = 1 - \tau \qquad [Ec.9]$$

Ec. 10: Ideal gas equation.

$$pV = mRT \qquad [Ec.10]$$

Ec. 11: Mass of working fluid in isotherm model.

$$M = \frac{p}{R}\left(\frac{V_c}{T_k} + \frac{V_k}{T_k} + \frac{V_r}{T_r} + \frac{V_h}{T_h} + \frac{V_e}{T_h}\right) \qquad [Ec.11]$$

Ec. 12: Temperature distribution in regenerator.

$$T(x) = (T_h - T_k)\frac{x}{L_r} + T_k \qquad [Ec.12]$$

Ec. 13: Mass of gas in regenerator.

$$m_r = \frac{V_r \cdot p}{R} \cdot \frac{\ln\left({}^{T_h}/_{T_k}\right)}{(T_h - T_k)} \qquad [Ec.13]$$

Ec. 14: Temperature in regenerator.

$$T_r = \frac{T_h - T_k}{\ln {}^{T_h}/_{T_k}} \qquad [Ec.14]$$

Ec. 15: Pressure of the cycle of isotherm analysis.

$$p = M \cdot R \cdot \left(\frac{V_c}{T_k} + \frac{V_k}{T_k} + \frac{V_r \ln\left({}^{T_h}/_{T_k}\right)}{(T_h - T_k)} + \frac{V_h}{T_h} + \frac{V_e}{T_h} \right)^{-1} \qquad [Ec.15]$$

Ec. 16: Total performed work in isotherm analysis.

$$W = \oint p \left(\frac{dV_c}{d\theta} + \frac{dV_e}{d\theta} \right) d\theta \,,\ where\ \theta = crank\ angle \qquad [Ec.16]$$

Ec. 17: Equation of energy for the working fluid inside a cell.

$$\frac{dQ}{d\theta} + \left(C_p T_i m_i' - C_p T_o m_o' \right) = \frac{dW_d}{d\theta} + C_v \frac{d(mT)}{d\theta} \qquad [Ec.17]$$

Ec. 18: Net heat transferred to the working gas during the cycle in the isothermal model.

$$Q = \oint \frac{dQ}{d\theta} = RT \oint \frac{dm}{d\theta} + \oint \frac{dW_d}{d\theta} \qquad [Ec.18]$$

Ec. 19: Volume variation in compression space.

$$V_c = V_{clc} + \frac{V_{swc}}{2}(1 + \cos\theta) \qquad [Ec.19]$$

Ec. 20: Volume variation in expansion space.

$$V_e = V_{cle} + \frac{V_{swe}}{2}(1 + \cos(\theta + \alpha)) \qquad [Ec.20]$$

Ec. 21: Pressure of isotherm analysis as a function of crank angle.

$$p = M \cdot R \cdot \left(s + \left(\frac{V_{swe} \cdot \cos\alpha}{2T_h} + \frac{V_{swc}}{2T_k} \right) \cos\theta - \left(\frac{V_{swe}}{2T_h} \sin\alpha \right) \sin\theta \right)^{-1} \qquad [Ec.21]$$

Ec. 22: Maximum pressure in isothermal analysis.

$$p_{max} = \frac{MR}{s(1-b)} \qquad [Ec.22]$$

Ec. 23: Minimum pressure in isothermal analysis.

$$p_{min} = \frac{MR}{s(1+b)} \qquad [Ec.23]$$

Ec. 24: Mean pressure in isothermal analysis.

$$p_{mean} = \frac{MR}{s\sqrt{(1-b^2)}} \qquad [Ec.24]$$

Ec. 25: Work of the compression space in isothermal analysis.

$$W_c = \pi V_{swc} p_{mean} \sin\beta \frac{\left(\sqrt{1-b^2}-1\right)}{b} \qquad [Ec.25]$$

Ec. 26: Work of the expansion space in isothermal analysis.

$$W_e = \pi V_{swe} p_{mean} \sin(\beta - \alpha) \frac{(\sqrt{1-b^2}-1)}{b} \qquad [Ec.26]$$

Ec. 27: Carnot efficiency.

$$\eta = 1 - \frac{T_k}{T_h} \qquad [Ec.27]$$

Ec. 28: Specific heats.

$$C_p = \frac{\gamma R}{\gamma - 1}; \quad C_v = \frac{R}{\gamma - 1}; \quad where\ \gamma = {}^{C_p}\!/_{C_v}\ , R = C_p - C_v \qquad [Ec.28]$$

Ec. 29: Differential compression zone mass in adiabatic model.

$$\frac{dm_c}{d\theta} = \left(p \cdot \frac{dV_c}{d\theta} + \frac{V_c}{\gamma} \cdot \frac{dp}{d\theta}\right) \cdot \frac{1}{RT_{ck}} \qquad [Ec.29]$$

Ec. 30: Differential expansion zone mass in adiabatic model.

$$\frac{dm_e}{d\theta} = \left(p \cdot \frac{dV_e}{d\theta} + \frac{V_e}{\gamma} \cdot \frac{dp}{d\theta}\right) \cdot \frac{1}{RT_{he}} \qquad [Ec.30]$$

Ec. 31: Differential pressure in adiabatic model.

$$\frac{dp}{d\theta} = \frac{-p \cdot \gamma \cdot \left(\frac{1}{T_{ck}} \frac{dV_c}{d\theta} + \frac{1}{T_{he}} \frac{dV_e}{d\theta}\right)}{\frac{V_c}{T_{ck}} + \frac{V_e}{T_{he}} + \gamma \cdot \left(\frac{V_k}{T_k} + \frac{V_r}{T_r} + \frac{V_h}{T_h}\right)} \qquad [Ec.29]$$

Ec. 32: Mass flows in adiabatic model.

$$m'_{ck} = -\frac{dm_c}{d\theta},\ m'_{kr} = m'_{ck} - \frac{dm_k}{d\theta},\ m'_{rh} = m'_{kr} - \frac{dm_r}{d\theta},\ m'_{he} = m'_{rh} - \frac{dm_h}{d\theta},\ m'_{he} = \frac{dm_e}{d\theta} \qquad [Ec.32]$$

Ec. 33: Differential work in adiabatic model.

$$\frac{dW}{d\theta} = p \cdot \frac{dV_c}{d\theta} + p \cdot \frac{dV_e}{d\theta} \qquad [Ec.33]$$

Ec. 34: Differential heat transferred in cooler in adiabatic model.

$$Cooler: \frac{dQ_k}{d\theta} = \left(\frac{C_v V_k}{R} \cdot \frac{dp}{d\theta}\right) - C_p(T_{ck} m'_{ck} - T_{kr} m'_{kr}) \qquad [Ec.34]$$

Ec. 35: Differential heat transferred in regenerator in adiabatic model.

$$Regenerator: \frac{dQ_r}{d\theta} = \left(\frac{C_v V_r}{R} \cdot \frac{dp}{d\theta}\right) - C_p(T_{kr} m'_{kr} - T_{rh} m'_{rh}) \qquad [Ec.35]$$

Ec. 36: Differential heat transferred in heater in adiabatic model.

$$Heater: \frac{dQ_h}{d\theta} = \left(\frac{C_v V_h}{R} \cdot \frac{dp}{d\theta}\right) - C_p(T_{rh} m'_{rh} - T_{he} m'_{he}) \qquad [Ec.36]$$

Ec. 37: Differential compression space temperature in adiabatic model.

$$\frac{dT_c}{d\theta} = T_c \left(\frac{dp}{d\theta} \cdot \frac{1}{p} + \frac{dV_c}{d\theta} \cdot \frac{1}{V_c} - \frac{dm_c}{d\theta} \cdot \frac{1}{m_c}\right) \qquad [Ec.37]$$

Ec. 38: Differential expansion space temperature in adiabatic model.

$$\frac{dT_e}{d\theta} = T_e \left(\frac{dp}{d\theta} \cdot \frac{1}{p} + \frac{dV_e}{d\theta} \cdot \frac{1}{V_e} - \frac{dm_e}{d\theta} \cdot \frac{1}{m_e}\right) \qquad [Ec.38]$$

Ec. 39: Differential work of expansion space in adiabatic model.

$$\frac{dW_e}{d\theta} = p\frac{dV_e}{d\theta} \qquad [Ec.39]$$

Ec. 40: Differential work of compression space in adiabatic model.

$$\frac{dW_c}{d\theta} = p\frac{dV_c}{d\theta} \qquad [Ec.40]$$

Ec. 41: Heat transfer in heater.

$$Q_h = h_h A_h \Delta T_h \qquad [Ec.41]$$

Ec. 42: Nusselt number for a cylinder of diameter D.

$$Nu = \frac{h \cdot D}{k} \qquad [Ec.42]$$

Ec. 43: Total heat transfer coefficient of cooler.

$$h_t = \frac{h_w}{(1+0{,}882h_w)} \qquad [Ec.43]$$

Ec. 44: Heat transfer coefficient of the water film in the cooler.

$$h_w = 0{,}35Re^{0{,}55}Pr^{0{,}33}k_w d_o \qquad [Ec.44]$$

Ec. 45: Heat transfer in regenerator.

$$h_{bulk} \cdot A \cdot (T_M - T_F) = m_f \cdot C_{PF} \cdot L_R \cdot \frac{dT_f}{dx} + M_{FR} \cdot C_P \cdot \frac{dT_f}{dt} \qquad [Ec.45]$$

Ec. 46: Temperature of matrix of regenerator.

$$\Delta T_M \approx \frac{m_f \cdot C_{PF} \cdot \Delta T_F}{C_R} \qquad [Ec.46]$$

Ec. 47: Efficiency of the regenerator.

$$\varepsilon_R = \frac{Real\ heat\ transferred}{Available\ heat\ for\ transference} = \frac{T_2 - T_1}{T_3 - T_1} \qquad [Ec.47]$$

Ec. 48: Capacity factor of a working fluid.

$$Capacity\ factor = \frac{Thermal\ conductivity}{Specific\ heat \cdot density} \qquad [Ec.48]$$

Ec. 49: Approximation of output power using Beale number.

$$P = B_N \cdot p_{mean} \cdot N \cdot V_{swe} \qquad [Ec.49]$$

Ec. 50: Relationship between Stirling engine and Carnot efficiencies.

$$\eta_{STIRLING} \approx 0{,}5 \cdot \eta_{CARNOT} = 0{,}5 \cdot \left(1 - \frac{T_{min}}{T_{max}}\right) \qquad [Ec.50]$$

Ec. 51: Beale number.

$$B_N = \frac{P}{p_{mean} \cdot V_{swe} \cdot N} \qquad [Ec.51]$$

Ec. 52: West number.

$$W_S = \frac{P}{p_{mean} \cdot V_{swe} \cdot N \frac{(T_e - T_c)}{(T_e + T_c)}} \qquad [Ec.52]$$

Ec. 53: Total efficiency.

$$\eta_{total} = \eta_b * \eta_i * \eta_m \qquad [Ec.53]$$

Ec. 54: Input heat into the engine.

$$Q_{in} = \eta_b * Q_{total} = \eta_b * \dot{m}_{propane} * LHV \qquad [Ec.54]$$

Ec. 55: External convection resistance.

$$Rconv, i = \frac{1}{hi * Ai} \qquad [Ec.55]$$

Ec. 56: Fire clay conduction resistance.

$$Rfi.cl = \frac{L_{fi.cl}}{k_{fi.cl} * A_{fi.cl}} \qquad [Ec.56]$$

Ec. 57: Calcium silicate conduction resistance.

$$Rca.si = \frac{L_{ca.si}}{k_{ca.si} * A_{ca.si}} \qquad [Ec.57]$$

Ec. 58: Steel conduction resistance.

$$Rsteel = \frac{L_{steel}}{k_{steel} * A_{steel}} \qquad [Ec.58]$$

Ec. 59: Internal convection resistance.

$$Rconv, e = \frac{1}{he * Ae} \qquad [Ec.59]$$

Ec. 60: Nusselt number.

$$Nu = f(Re, \Pr) = \frac{h * L_c}{k} \qquad [Ec.60]$$

Ec. 61: Reynolds number.

$$Re = \frac{\rho * v * L}{\mu} \qquad [Ec.61]$$

Ec. 62: Chapman Enskong equation for parameters of a fluid mix (where α_i is the parameter α of the component i).

$$\alpha_{mix} = \sum_{i=1}^{n} \frac{X_i * \alpha_i}{\sum_{j=1}^{n} X_j * \varphi_{ij}} \qquad [Ec.62]$$

Ec. 63: Coefficients of Chapman Enskong equation.

$$\varphi_{ij} = \frac{1}{\sqrt{8}} * \left(1 + \frac{M_i}{M_j}\right)^{-\frac{1}{2}} * \left[1 + \left(\frac{\alpha_i}{\alpha_j}\right)^{1/2} * \left(\frac{M_j}{M_i}\right)^{1/4}\right]^2 ; \varphi_{ij} = 1 \; if \; i = j \qquad [Ec.63]$$

Ec. 64: Nusselt number in convection in a flat plate with laminar flow.

$$Nu = 0{,}664 * Re^{\frac{1}{2}} * Pr^{\frac{1}{3}} \qquad [Ec.64]$$

Ec. 65: Prandtl number.

$$Pr = \frac{\mu * C_p}{k} \qquad [Ec.65]$$

Ec. 66: Specific heat for a fluid mix.

$$Cp_{mix} = \sum_{i=1}^{n} X_i * Cp_i \qquad [Ec.66]$$

Ec. 67: Nusselt number for a vertical plate.

$$Nu = \left\{ 0{,}825 + \frac{0{,}387 * Ra^{1/6}}{\left[1+\left(\frac{0{,}492}{Pr}\right)^{9/16}\right]^{8/27}} \right\}^2 \qquad [Ec.67]$$

Ec. 68: Rayleigh number for a vertical plate.

$$Ra = \frac{g*\beta*(Ts-T\infty)*Lc^3}{v^2} * Pr \qquad [Ec.68]$$

Ec. 69: Heat loss due to exhaust gases.

$$P_{sh} = \dot{m}_{fumes} * C_{p,fumes} * \left(T_{fumes} - T_{\infty}\right)[W] \qquad [Ec.69]$$

Ec. 70: Heat loss due to latent heat.

$$P_{lh} = \dot{m}_{H20} * h_{fg} \qquad [Ec.70]$$

Ec. 71: Heat rejected while cooling.

$$Q_{reject} = C_{water} * \dot{m}_w * (T_{out} - T_{in}) \qquad [Ec.71]$$

Ec. 72: Instantaneous pressure in TPTC analysis.

$$\frac{p}{p_{max}} = \frac{1-\delta}{1+\delta\cos(\theta-\varphi)} \qquad [Ec.72]$$

Ec. 73: Pressure ratio in TPTC analysis.

$$\frac{p_{max}}{p_{min}} = \frac{1+\delta}{1-\delta} \qquad [Ec.73]$$

Ec. 74: Work done in expansion space in TPTC analysis.

$$\frac{P_e}{p_{max}V_T} = \frac{\pi}{2}\left(\frac{1}{1+\kappa}\right)\left(\frac{1-\delta}{1+\delta}\right)^{\frac{1}{2}}(\Delta\sin(\theta)) \qquad [Ec.74]$$

Ec. 75: Work done in compression space in TPTC analysis.

$$\frac{P_c}{p_{max}V_T} = \frac{\pi}{2}\left(\frac{1}{1+\kappa}\right)\left(\frac{1-\delta}{1+\delta}\right)^{\frac{1}{2}}(\Delta\sin(\theta-\alpha)) \qquad [Ec.75]$$

Ec. 76: Net work in TPTC analysis.

$$P = P_e + P_c = (1-K)P_e \qquad [Ec.76]$$

Ec. 77: Expansion space mass in TPTC analysis.

$$\frac{m_e}{m^*} = (1+\beta)\frac{K}{2}\left[\frac{1-\delta}{1+\kappa}\right] * \left[\frac{1+\cos(\theta)}{1+\delta\cos(\theta-\varphi)}\right] \qquad [Ec.77]$$

Ec. 78: mass velocity in expansion space in TPTC analysis.

$$\frac{d\left({}^{m_e}/_{m^*}\right)}{d\theta} = (1+\beta)\frac{K}{2}\left[\frac{1-\delta}{1+\kappa}\right] * \left[\frac{\delta\sin(\theta-\varphi)-\delta\sin(\varphi)-\sin(\theta)}{(1+\delta\cos(\theta-\varphi))^2}\right] \qquad [Ec.78]$$

Ec. 79: Compression space mass in TPTC analysis.

$$\frac{m_c}{m^*} = (1+\beta)^{\kappa}\frac{K}{2}\left[\frac{1-\delta}{1+\kappa}\right] * \left[\frac{1+\cos(\theta-\alpha)}{1+\delta\cos(\theta-\varphi)}\right] \qquad [Ec.79]$$

Ec. 80: mass velocity in expansion space in TPTC analysis.

$$\frac{d\left({}^{m_e}/_{m^*}\right)}{d\theta} = (1+\beta)^{\kappa}\frac{K}{2}\left[\frac{1-\delta}{1+\kappa}\right] * \left[\frac{\delta\sin(\theta-\varphi)-\sin(\varphi-\alpha)-\sin(\theta-\alpha)}{(1+\delta\cos(\theta-\varphi))^2}\right] \qquad [Ec.80]$$

Ec. 81: Dead space mass in TPTC analysis.

$$\frac{m_{de}}{m^*} = XK\frac{(1+\beta)}{(1+\kappa)}\left(\frac{1-\delta}{1+K}\right) * \frac{1}{1+\delta\cos(\theta-\varphi)} \qquad [Ec.81]$$

Ec. 82: mass velocity in dead space in TPTC analysis.

$$\frac{d\left({}^{m_d}/_{m^*}\right)}{d\theta} = 2\left(\frac{1+\beta}{1+\kappa}\right)\left(\frac{KX}{1+K}\right) * \left[\frac{(1-\delta)(-\delta\sin\theta-\varphi)}{(1+\delta\cos(\theta-\varphi))^2}\right] \qquad [Ec.82]$$

Ec. 83: Position of working piston.

$$x = 37{,}5\sin\theta + 146\cos\left(\sin^{-1}\left(-\frac{37{,}5}{146}\cos\theta\right)\right) - 40 - 68{,}5\ [mm] \qquad [Ec.83]$$

Ec. 84: Position of displacer piston.

$$y = 37{,}5\cos\theta + 130\cos\left(\sin^{-1}\left(-\frac{37{,}5}{130}\sin\theta\right)\right) + 97{,}5 - 190\ [mm] \qquad [Ec.84]$$

REFERENCES

BOOKS AND JOURNALS

/1/ G. Walker: STIRLING ENGINES. Claredon Press. Oxford 1980.

/2/ Israel Urieli, David M. Berchowitz: STIRLING CYCLE ENGINE ANALYSIS. Adam Hilger Ltd. Bristol 1984.

/3/ Unknown author: BRIEF HISTORY OF STIRLING MACHINES.

/4/ Unknown author: MOTOR STIRLING. DISPOSITIVO TERMODINÁMICO REGENERATIVO (Stirling engine. Thermodynamic regenerative device).

/5/ D. G. Thombare and S. K. Verma: TECHNOLOGICAL DEVELOPMENT IN THE STIRLING CYCLE ENGINES. Renewable and Sustainable Energy Reviews 12 (2008) 1-38

/6/ Rallis CJ: A NEW CONSTANT VOLUME EXTERNAL HEAT SUPPLY REGENERATIVE CYCLE. Proceeding of the 12th IECEC, September 1977. P. 1534-37.

/7/ Berchowitz DM: A NEW MATHEMATICAL MODEL FOR STIRLING CYCLE MACHINE. Proceedings of the 12th IECEC, September 1977. P. 1522-27.

/8/ K. Mahkamov and D.B. Ingham: ANALYSIS OF THE WORKING PROCESS AND MECHANICAL LOSSES IN A STIRLING ENGINE FOR A SOLAR POWER UNIT. Journal of solar energy engineering, 1999, 121 (2): p. 121-127.

/9/ A. J. Organ: THERMODYNAMICS AND GAS DYNAMICS OF STIRLING CYCLE MACHINES. Cambridge University Press, Cambridge 1992.

/10/ J. R. Senft: THEORICAL LIMITS ON THE PERFORMANCE OF STIRLING ENGINES. Int. Journal Energy Res 22 (1998), p. 991-1000.

/11/ P.C.T. de Boer: MAXIMUM OBTAINABLE PERFORMANCE OF STIRLING ENGINE AND REFRIGERATORS. ASME Journal, Heat transfer 125 (2003), p. 911-915.

/12/ Koichi Hirata: SCHMIDT THEORY FOR STIRLING ENGINES. 1997.

/13/ G. Reader and C. Hooper: STIRLING ENGINES. University Press (1983).

/14/ J. A. Alvarez Flórez and I. Callejón Agramunt. MAQUINAS TERMICAS MOTORAS (Thermal machines). Ediciones UPC 2002

/15/ D. A. Renfroe, M. Counts. MODEL OF TPTC STIRLING ENGINE WITH ADIABATIC WORKING SPACES. J. Eng. Gas Turbines Power 110(4), 658-663 (Oct 01, 1988)

WEB

/1/ STIRLING ENGINE: http://www.robertstirlingengine.com/gamma_uk.php

/2/ DAS ST05G STIRLINGMOTOR PROJEKT: http://www.ve-ingenieure.de/projekt_st05g_cnc.html

/3/ STIRLING CYCLE MACHINE ANALYSIS. OHIO UNIVERSITY: http://www.ohio.edu/mechanical/stirling/me422.html

/4/ UNIVERSITY OF NEW HAVEN STIRLING ENGINE PROJECT MECHANICAL ENGINEERING: http://stirlingengineunh.weebly.com/

/5/ MOTORES DE CICLO STIRLING (STIRLING CYCLE ENGINES): http://personales.able.es/jgros

/6/ IDEAL ADIABATIC SIMULATION OF STIRLING ENGINES: http://mac6.ma.psu.edu/stirling/simulations/IdealAdiabatic/

ANNEX 1: COMBUSTIONS

A1.1. PROPANE COMPLETE COMBUSTION

$$C_3H_8 + a(O_2 + 3{,}76N_2) \rightarrow bCO_2 + cH_2O + dN_2$$

C) 3 = b
H) 8 = 2*c ➔ c = 4
O) 2*a = 2*b + c ➔ a = 5
N) 3,76*a = d ➔ d = 18,8

Air demand: 1 mol of propane needs 4,76*a = 23,8 mol of air
1 m^3 of propane needs 4,76*a = 23,8 m^3 of air

Calorific value: $\sum H_r^o = \sum(n_i * \Delta h_{fi}^o)_{products} - \sum(n_i * \Delta h_{fi}^o)_{reagents}$

$$\sum H_r^o = 3 * (-393{,}52) + 4 * (-285{,}84) - 1 * (-103{,}85) = -2220{,}07 \frac{kJ}{mol\ propane}$$

-2220,07 kJ/mol = 27,53 kWh/m^3 (1 mol = 22,4 L)

Burning performance of propane: maximum 7 kW

Theoretical volumetric flow of propane: $\dot{V} = \frac{7\ kW}{27{,}53 kWh/m3} = 0{,}00424 \frac{m^3}{min}$

⇨ We need 4,24 L/min of propane and 4,24*23,8 = 100,86 L/min of air

A1.2. NATURAL GAS COMPLETE COMBUSTION

$$(0{,}0024CO_2 + 0{,}1083N_2 + 0{,}8811CH_4 + 0{,}0075C_2H_6 + 0{,}0005C_3H_8 + 0{,}0002C_4H_{10}) + a(O_2 + 3{,}76N_2) \rightarrow bCO_2 + cH_2O + dN_2$$

C) 0,0024 + 0,8811 + 2*0,0075 + 3*0,0005 + 4*0,0002 = b ➔ b = 0,9008
H) 4*0,8811 + 6*0,0075 + 8*0,0005 + 10*0,0002 = 2c ➔ c = 1,7877
O) 2*0,0024 + 2*a = 2*b + c ➔ a = 1,7923
N) 2*0,1083 + 2*3,76*a = 2*d ➔ d = 6,8473

Air demand: 1 mol of natural gas needs 4,76*a = 8,53 mol of air
1 m^3 of natural gas needs 4,76*a = 8,53 m^3 of air

Calorific value: $\sum H_r^o = \sum(n_i * \Delta h_{fi}^o)_{products} - \sum(n_i * \Delta h_{fi}^o)_{reagents}$

$$\sum H_r^o = 0{,}9008 * (-393{,}52) + 1{,}7877 * (-285{,}84) - 0{,}0024 * (-393{,}52) - 0{,}8811 * (-74{,}87) - 0{,}0075 * (-84{,}64) - 0{,}0005 * (-103{,}85) - 0{,}0002 * (-124{,}73) = -795{,}85 \frac{kJ}{mol\ natural\ gas}$$

-795,85 kJ/mol = 9,87 kWh/m^3 (1 mol = 22,4 L)

Burning performance of natural gas: maximum 5 kW

Theoretical volumetric flow of natural gas: $\dot{V} = \frac{5\ kW}{9{,}87 kWh/m3} = 0{,}00844 \frac{m^3}{min}$

⇨ We need 8,44 L/min of natural gas and 8,44*8,53 = 72,02 L/min of air

A1.3. ENTALPIES OF FORMATION

$$\Delta h^o_{f,CO2} = -393{,}52\,\frac{kJ}{mol}$$

$$\Delta h^o_{fH2O} = -285{,}84\,\frac{kJ}{mol}$$

$$\Delta h^o_{fCH4} = -74{,}87\,\frac{kJ}{mol}$$

$$\Delta h^o_{fC2H6} = -84{,}68\,\frac{kJ}{mol}$$

$$\Delta h^o_{fC3H8} = -103{,}85\,\frac{kJ}{mol}$$

$$\Delta h^o_{fC4H10} = -124{,}73\,\frac{kJ}{mol}$$

$$\Delta h^o_{fO2} = 0$$

$$\Delta h^o_{fN2} = 0$$

ANNEX 2: MATLAB PROGRAMS

A2.1. POSITION OF PISTONS

```
function piston

theta = 0:5:360;

x = 37.5*sind(theta) + 146*cosd(asind(-37.5*cosd(theta)/146)) - 68.5 - 40;
x0 = 37.5*sind(0) + 146*cosd(asind(-37.5*cosd(0)/146)) - 68.5 - 40;
y = 37.5*cosd(theta) + 130*cosd(asind(-37.5*sind(theta)/130)) + 97.5 - 190;
y0 = 37.5*cosd(0) + 130*cosd(asind(-37.5*sind(0)/130)) + 97.5 - 190;

figure
plot(theta,x,theta,37.5*sind(theta)+x0)
grid on;
hold on;
title('working/compression piston position Vs. Sinus function')
xlabel('theta (deg)')
ylabel('position (mm) referred to the Bottom Dead Centre')
legend('working/compression piston','Sinus')

figure
plot(theta,y,theta,37.5*cosd(theta)+y0/2)
grid on;
hold on;
title('displacer/expansion piston position Vs. Cosine function')
xlabel('theta (deg)')
ylabel('position (mm) referred to the Bottom Dead Centre')
legend('displacer/expansion piston','Cosine')

figure
plot(theta,x,theta,y)
grid on;
hold on;
title('working/compression piston position Vs. displacer/expansion piston
position')
xlabel('theta (deg)')
ylabel('position (mm) referred to the Bottom Dead Centre')
legend('working/compression piston','displacer/expansion piston')

figure
plot(theta,x,theta,37.5*sind(theta)+x0,theta,y,theta,37.5*cosd(theta)+y0/2)
grid on;
hold on;
title('summary')
xlabel('theta (deg)')
ylabel('position (mm) referred to the Bottom Dead Centre')
legend('working/compression piston','Sinus','displacer/expansion
piston','Cosine')
```

A2.2. SCHMIDT ANALYSIS

```
function stirling

isoterm;


function isoterm
define;
%isoterm (Schmidt) analysis

disp('Isoterm (Schmidt) analysis');
disp('');
disp('');

heater;
cooler;
regen;

global pmean pmax pmin %mean, maximal, minimal charge pressure (Pa)
global tk tr th %refrigerator, cooler, heater temperatures (K)
global freq freqh omega %cycle frequency (rpm), (herz), (rad/s)
global vswc vswe %swept volumes in compression and expansion spaces (m^3)
global alpha %phase angle that is moving the expansion space (rad)
global vk vr vh %volume of cooler, regenerator, heater (m^3)
global tau kappa X S delta B K phi


pmean = input('Introduce mean charge pressure (Pa): ');
tk = input('Introduce cool temperature (K): ');
th = input('Introduce hot temperature (K): ');
freq = input('Introduce cycle frequency (rpm): ');
disp('');
disp('');

tau=tk/th;
kappa=vswc/vswe;
X=(vk+vr+vh)/vswe;
S=2*X*tau/(tau+1);
delta=(sqrt(tau^2+kappa^2+2*tau*kappa*cos(alpha)))/(tau+kappa+2*S);
pmax=pmean/(sqrt((1-delta)/(1+delta)));
pmin=pmax*(1-delta)/(1+delta);
B=tau+kappa+2*S;
K=pmax*B*(1-delta);
phi=atan((kappa*sin(alpha))/(tau+kappa*cos(alpha)));


tr = (th-tk)/log(th/tk);
omega = 2*pi*freq/60;
freqh = freq/60;
disp('Working parameters');
disp('Mean pressure (bar): ');
disp(pmean*1e-5);
disp('Maximal pressure (bar): ');
disp(pmax*1e-5);
disp('Minimal pressure (bar): ');
disp(pmin*1e-5);
disp('Cold temperature (K): ');
disp(tk);
```

```
disp('Hot temperature (K): ');
disp(th);
disp('Regenerator effective temperature (K): ');
disp(tr);
disp('Working frequency (rpm): ');
disp(freq);
disp('');
disp('');

Schmidt;
%=========================================================================
function Schmidt
%Schmidt analysis

global mgas %total mass of gas inside the engine (kg)
global pmean %mean charge pressure (Pa)
global tk %refrigerator temperature (K)
global freqh %cycle frequency (rpm), (herz), (rad/s)
global vswe %swept volumes in expansion space (m^3)
global alpha %phase angle that is moving the expansion space (rad)
global rgas %gas constraint (J/kg*K)
global kappa delta K phi
%*************************************************************************

%total mass of working gas in engine

mgas = K*vswe/(2*rgas*tk);
disp('Total mass of gas (g): ');
disp(mgas*1e3);
disp('');
disp('');

%obtained work

we = pi*pmean*vswe*delta*sin(phi)/(1+sqrt(1-delta^2));
wc = pi*pmean*vswe*kappa*delta*sin(phi-alpha)/(1+sqrt(1-delta^2));
w = we+wc;
power = w*freqh;
eff = w/we; %qe=we

%printout Schmidt analysis results
disp('');
disp('');

disp('========= SCHMIDT ANALYSIS =========')
disp('');

disp(' Work(Jules): ');
disp(w);
disp(' Power(Watts): ');
disp(power);
disp(' Qexp(Jules): ');
disp(we);
disp(' Qcom(Jules): ');
disp(wc);
disp(' Indicated efficiency: ');
disp(eff);
disp('');

disp('====================================')
```

```
%Schmidt analysis representation, P-V and P-THETA diagrams
disp('Schmidt analysis diagrams?');
choice = input('s)i or n)o: ','s');
if(strncmp(choice,'s',1))
    plotpv
    tptcbeta
end

disp('End of simulation')



function define

%Define the engine configuration and geometric mechanism parameters

global vclc vcle %free volumes in compression and expansion spaces (m^3)
global vswc vswe %swept volumes in compression and expansion spaces (m^3)
global alpha %phase angle between pistons (rad)
global dcomp dexp %diameter of compression and expansion pistons (m)
global acomp aexp %area of compression and expansion pistons (m^2)


disp('Geometrical data of the Gamma Stirling Motor')

vclc = 0;
vcle = 0;
dcomp = 0.085;%m
lcomp = 0.076;%m
dexp = 0.096;%m
lexp = 0.076;%m
alpha = pi/2;%rad


acomp = pi*dcomp^2/4; %(m2)
aexp = pi*dexp^2/4;%(m2)


vswc = acomp*lcomp;%m3
vswe = aexp*lexp;%m3


disp('');
disp('');
disp('');
disp('Compression piston diameter(mm)');
disp(dcomp*1e3);
disp('Expansion piston diameter (mm)');
disp(dexp*1e3);
disp('Death volume in compression (cm^3)');
disp(vclc*1e6);
disp('Swept volume in compression (cm^3)');
disp(vswc*1e6);
disp('Death volume in expansion (cm^3)');
disp(vcle*1e6);
disp('Swept volume in expansion (cm^3)');
disp(vswe*1e6);
disp('Phase angle between displacer/expansion and working/compression
piston, alpha(degrees)');
```

```
disp(alpha*180/pi);

gas;



function gas
 %define the working gas properties

global rgas %gas constraint (J/kg*K)
global cp %specific heat at constant pressure (J/kg*K)
global cv %specific heat at constant volume (J/kg*K)
global gama %ratio: cp/cv
global mu0 %dynamic viscosity at reference temperature t0 (kg*m/s)
global t0 %reference temperature (K)
global prandtl %prandtl number. Dimensionless number proportional to the
quotient between viscosity and thermal diffusivity

disp('Gas type: AIR');
gama = 1.4;
rgas = 287.0;
mu0 = 17.08e-6;
cv = rgas/(gama - 1);
cp = gama*cv;
t0 = 273;
prandtl = 0.71;


function heater
%Define geometric parameters of heater

global vh %Volume inside heater (m^3)
global ah %internal flow area heater (m^2)
global dh %hidraulic diameter heater (m)
global lh %effective length heater (m)

disp('DEFINE HEATER')

n = 20; %number of pipes
dh = 0.008;%m
lh = 0.18 + 0.0948 + pi*0.01645;%m
ah = pi*dh^2/4;%m2
vh = n*ah*lh;%m3

disp('Heater data summary:');
disp('Number of pipes');
disp(n);
disp('Heater effective length of each pipe (mm)');
disp(lh*1e3);
disp('Diameter of pipe (mm)');
disp(dh*1e3);
disp('Internal flow area of each pipe (mm^2)');
disp(ah*1e6);
disp('Internal total volume (cm^3)');
disp(vh*1e6);


function cooler
%Define geometric parameters of cooler
```

```
global vk %Volume inside cooler (m^3)
global ak %internal flow area cooler (m^2)
global dk %hidraulic diameter cooler (m)
global lk %effective length cooler (m)

disp('DEFINE COOLER:')

dk = 0.096;%m
lk = 0.084;%m

ak = pi*dk^2/4;%m2
vk = ak*lk;%m3
disp('Cooler data summary:');
disp('Cooler length (mm)');
disp(lk*1e3);
disp('Hidraulic diameter (mm)');
disp(dk*1e3);
disp('Internal flow area (mm^2)');
disp(ak*1e6);
disp('Internal volume (cm^3)');
disp(vk*1e6);


function regen
%Define geometric parameters of regenerator

global vr %Volume inside regenerator (m^3)
global ar %internal flow area regenerator (m^2)
global drext drint %hidraulic diameter regenerator (m)
global lr %effective length regenerator (m)
global porosity %

disp('DEFINE REGENERATOR:\n')

drext = 0.13385;%m
drint = 0.096;%m
lr = 0.0575;%m
porosity = 0.916;

ar = pi*(drext^2-drint^2)/4;%m2
vr = porosity*ar*lr;%m3

disp('Regenerator data summary:');
disp('Regenerator length (mm)');
disp(lr*1e3);
disp('Internal flow area (mm^2)');
disp(ar*1e6);
disp('Internal volume (cm^3)');
disp(vr*1e6);

function plotpv
%Diagrams P-V and P-THETA for Schmidt analysis

global vclc vcle %free volumes in compression and expansion spaces (m^3)
global vswc vswe %swept volumes in compression and expansion spaces (m^3,
swept volumes ratio)
global alpha %phase angle that is moving the expansion space (rad)
global vk %volume cooler (m^3)
global vh %volume heater (m^3)
```

```
global vr %volume regenerator (m^3)
global pmean %mean pressure (Pa)
global K B delta phi

%*************************************************************************
%PV DIAGRAM

theta = 0:5:360;

p=1e-5*K./(B*(1+delta*cos(theta*pi/180-phi))); %bar
vc=vclc+0.5*vswc*(1+cos(theta*pi/180-alpha));
ve=vcle+0.5*vswe*(1+cos(theta*pi/180));
vtot=(vc+ve+vh+vr+vk)*1e6; %c3

figure
plot(vtot,p)
grid on
xlabel('Total volume (c^3)')
ylabel('Pressure (bar)')
title('PV Schmidt diagram')
figure
plot(theta,p)
grid on
hold on
x = [0,360];
y = [pmean*1e-5, pmean*1e-5];
plot(x,y)
xlabel('Crank angle (deg)')
ylabel('Pressure (bar)')
title('P-THETA Schmidt diagram (air)')


function tptcbeta

global bt %vector of values of beta (mass ratio)
global K A S B delta phi tr wcbt wbt pbt
global pmax %maximum pressure of cycle (calculated in Schmidt analysis)
(Pa)
global kappa %swept volume ratio
global Ma Mw %molar mass of air and water (g/mol
global N %molar mass ratio
global X %dead volume ratio
global tau; %temperatures ratio
global vswc vswe vclc vcle vk vr vh vtot alpha freqh pmean mwater mgas

disp('')
disp('TPTC working fluid')
Ma=28.9; Mw=18; N=Ma/Mw;
bt0=0;
mwater=input('Introduce mass of water (g): ');
bt=mwater/(mgas*1e3);

K=tau/(1+N*bt);
A=sqrt(K^2+kappa^2+2*K*kappa*cos(alpha));
S=2*K*X/(1+K);
B=K+kappa+2*S;
delta=A/B;
phi=atan(kappa*sin(alpha)/(K+kappa*cos(alpha)));
tr=2/delta*(sqrt(1-delta^2)-1);
pmax=pmean/(sqrt((1-delta))/(1+delta));
K0=tau/(1+N*bt0);
```

```
A0=sqrt(K0^2+kappa^2+2*K0*kappa*cos(alpha));
S0=2*K0*X/(1+K);
B0=K0+kappa+2*S0;
delta0=A0/B0;
phi0=atan(kappa*sin(alpha)/(K0+kappa*cos(alpha)));
tr0=2/delta0*(sqrt(1-delta0^2)-1);
pmax0=pmean/(sqrt((1-delta0))/(1+delta0));


disp('========= SCHMIDT ANALYSIS FOR TPTC =========')

    wcbt=pmax*(vswe+vswc)*0.5*pi*kappa/(1+kappa)*sqrt((1-
delta)/(1+delta))*tr*sin(phi-alpha);
    wbt=wcbt*(1/K-1);
    pbt=wbt*freqh;

    disp('');
    disp('beta: ');
    disp(bt);
    disp(' Work(Jules): ');
    disp(wbt);
    disp(' Power(Watts): ');
    disp(pbt);
    disp('====================================')



theta = 0:5:360;

c0=(1-delta0)./(1+delta0*cos(theta*pi/180-phi0));
pb0=pmax0*1e-5*c0;
c=(1-delta)./(1+delta*cos(theta*pi/180-phi));
pbt=pmax*1e-5*c; %bar


vc=vclc+0.5*vswc*(1+cos(theta*pi/180-alpha));
ve=vcle+0.5*vswe*(1+cos(theta*pi/180));
vtot=(vc+ve+vh+vr+vk)*1e6; %cr

figure
plot(vtot,pb0,vtot,pbt)
grid on
xlabel('Total volume (c^3)')
ylabel('Pressure (bar)')
legend('PV Schmidt diagram for only air','PV Schmidt diagram for TPTC')
figure
plot(theta,pb0,theta,pbt)
grid on
hold on
xlabel('Crank angle (deg)')
ylabel('Pressure (bar)')
legend('P-THETA Schmidt diagram for only air','P-THETA Schmidt diagram for
TPTC')
```

ANNEX 3: TABLES

A3.1. GAS PROPERTIES AT 1 ATM.

Temp.	Density	Spec. Heat	Conductivity	Diffusivity	Dyn. Viscosity	Cin. Viscosity	Prandtl
50	1.6597	866.6	0.01858	1.291×10^{-5}	1.612×10^{-5}	9.714×10^{-6}	0.7520
100	1.4373	914.8	0.02257	1.716×10^{-5}	1.841×10^{-5}	1.281×10^{-5}	0.7464
150	1.2675	957.4	0.02652	2.186×10^{-5}	2.063×10^{-5}	1.627×10^{-5}	0.7445
200	1.1336	995.2	0.03044	2.698×10^{-5}	2.276×10^{-5}	2.008×10^{-5}	0.7442
300	0.9358	1 060	0.03814	3.847×10^{-5}	2.682×10^{-5}	2.866×10^{-5}	0.7450
400	0.7968	1 112	0.04565	5.151×10^{-5}	3.061×10^{-5}	3.842×10^{-5}	0.7458
500	0.6937	1 156	0.05293	6.600×10^{-5}	3.416×10^{-5}	4.924×10^{-5}	0.7460
1 000	0.4213	1 292	0.08491	1.560×10^{-4}	4.898×10^{-5}	1.162×10^{-4}	0.7455
1 500	0.3025	1 356	0.10688	2.606×10^{-4}	6.106×10^{-5}	2.019×10^{-4}	0.7745
2 000	0.2359	1 387	0.11522	3.521×10^{-4}	7.322×10^{-5}	3.103×10^{-4}	0.8815
				Nitrógeno, N_2			
−50	1.5299	957.3	0.02001	1.366×10^{-5}	1.390×10^{-5}	9.091×10^{-6}	0.6655
0	1.2498	1 035	0.02384	1.843×10^{-5}	1.640×10^{-5}	1.312×10^{-5}	0.7121
50	1.0564	1 042	0.02746	2.494×10^{-5}	1.874×10^{-5}	1.774×10^{-5}	0.7114
100	0.9149	1 041	0.03090	3.244×10^{-5}	2.094×10^{-5}	2.289×10^{-5}	0.7056
150	0.8068	1 043	0.03416	4.058×10^{-5}	2.300×10^{-5}	2.851×10^{-5}	0.7025
200	0.7215	1 050	0.03727	4.921×10^{-5}	2.494×10^{-5}	3.457×10^{-5}	0.7025
300	0.5956	1 070	0.04309	6.758×10^{-5}	2.849×10^{-5}	4.783×10^{-5}	0.7078
400	0.5072	1 095	0.04848	8.727×10^{-5}	3.166×10^{-5}	6.242×10^{-5}	0.7153
500	0.4416	1 120	0.05358	1.083×10^{-4}	3.451×10^{-5}	7.816×10^{-5}	0.7215
1 000	0.2681	1 213	0.07938	2.440×10^{-4}	4.594×10^{-5}	1.713×10^{-4}	0.7022
1 500	0.1925	1 266	0.11793	4.839×10^{-4}	5.562×10^{-5}	2.889×10^{-4}	0.5969
2 000	0.1502	1 297	0.18590	9.543×10^{-4}	6.426×10^{-5}	4.278×10^{-4}	0.4483
				Vapor de agua, H_2O			
−50	0.9839	1 892	0.01353	7.271×10^{-6}	7.187×10^{-6}	7.305×10^{-6}	1.0047
0	0.8038	1 874	0.01673	1.110×10^{-5}	8.956×10^{-6}	1.114×10^{-5}	1.0033
50	0.6794	1 874	0.02032	1.596×10^{-5}	1.078×10^{-5}	1.587×10^{-5}	0.9944
100	0.5884	1 887	0.02429	2.187×10^{-5}	1.265×10^{-5}	2.150×10^{-5}	0.9830
150	0.5189	1 908	0.02861	2.890×10^{-5}	1.456×10^{-5}	2.806×10^{-5}	0.9712
200	0.4640	1 935	0.03326	3.705×10^{-5}	1.650×10^{-5}	3.556×10^{-5}	0.9599
300	0.3831	1 997	0.04345	5.680×10^{-5}	2.045×10^{-5}	5.340×10^{-5}	0.9401
400	0.3262	2 066	0.05467	8.114×10^{-5}	2.446×10^{-5}	7.498×10^{-5}	0.9240
500	0.2840	2 137	0.06677	1.100×10^{-4}	2.847×10^{-5}	1.002×10^{-4}	0.9108
1 000	0.1725	2 471	0.13623	3.196×10^{-4}	4.762×10^{-5}	2.761×10^{-4}	0.8639
1 500	0.1238	2 736	0.21301	6.288×10^{-4}	6.411×10^{-5}	5.177×10^{-4}	0.8233
2 000	0.0966	2 928	0.29183	1.032×10^{-3}	7.808×10^{-5}	8.084×10^{-4}	0.7833

A3.2. AIR PROPERTIES AT 1 ATM

Temp. T, °C	Density ρ, kg/m^3	Spec. Heat C_p, J/kg · °C	Conductivity k, W/m · °C	Diffusivity α, m^2/s	Dyn. Viscosity μ, kg/m · s	Cin. Viscosity ν, m^2/s	Prandtl Pr
−150	2.866	983	0.01171	4.158×10^{-6}	8.636×10^{-6}	3.013×10^{-6}	0.7246
−100	2.038	966	0.01582	8.036×10^{-6}	1.189×10^{-6}	5.837×10^{-6}	0.7263
−50	1.582	999	0.01979	1.252×10^{-5}	1.474×10^{-5}	9.319×10^{-6}	0.7440
−40	1.514	1 002	0.02057	1.356×10^{-5}	1.527×10^{-5}	1.008×10^{-5}	0.7436
−30	1.451	1 004	0.02134	1.465×10^{-5}	1.579×10^{-5}	1.087×10^{-5}	0.7425
−20	1.394	1 005	0.02211	1.578×10^{-5}	1.630×10^{-5}	1.169×10^{-5}	0.7408
−10	1.341	1 006	0.02288	1.696×10^{-5}	1.680×10^{-5}	1.252×10^{-5}	0.7387
0	1.292	1 006	0.02364	1.818×10^{-5}	1.729×10^{-5}	1.338×10^{-5}	0.7362
5	1.269	1 006	0.02401	1.880×10^{-5}	1.754×10^{-5}	1.382×10^{-5}	0.7350
10	1.246	1 006	0.02439	1.944×10^{-5}	1.778×10^{-5}	1.426×10^{-5}	0.7336
15	1.225	1 007	0.02476	2.009×10^{-5}	1.802×10^{-5}	1.470×10^{-5}	0.7323
20	1.204	1 007	0.02514	2.074×10^{-5}	1.825×10^{-5}	1.516×10^{-5}	0.7309
25	1.184	1 007	0.02551	2.141×10^{-5}	1.849×10^{-5}	1.562×10^{-5}	0.7296
30	1.164	1 007	0.02588	2.208×10^{-5}	1.872×10^{-5}	1.608×10^{-5}	0.7282
35	1.145	1 007	0.02625	2.277×10^{-5}	1.895×10^{-5}	1.655×10^{-5}	0.7268
40	1.127	1 007	0.02662	2.346×10^{-5}	1.918×10^{-5}	1.702×10^{-5}	0.7255
45	1.109	1 007	0.02699	2.416×10^{-5}	1.941×10^{-5}	1.750×10^{-5}	0.7241
50	1.092	1 007	0.02735	2.487×10^{-5}	1.963×10^{-5}	1.798×10^{-5}	0.7228
60	1.059	1 007	0.02808	2.632×10^{-5}	2.008×10^{-5}	1.896×10^{-5}	0.7202
70	1.028	1 007	0.02881	2.780×10^{-5}	2.052×10^{-5}	1.995×10^{-5}	0.7177
80	0.9994	1 008	0.02953	2.931×10^{-5}	2.096×10^{-5}	2.097×10^{-5}	0.7154
90	0.9718	1 008	0.03024	3.086×10^{-5}	2.139×10^{-5}	2.201×10^{-5}	0.7132
100	0.9458	1 009	0.03095	3.243×10^{-5}	2.181×10^{-5}	2.306×10^{-5}	0.7111
120	0.8977	1 011	0.03235	3.565×10^{-5}	2.264×10^{-5}	2.522×10^{-5}	0.7073
140	0.8542	1 013	0.03374	3.898×10^{-5}	2.345×10^{-5}	2.745×10^{-5}	0.7041
160	0.8148	1 016	0.03511	4.241×10^{-5}	2.420×10^{-5}	2.975×10^{-5}	0.7014
180	0.7788	1 019	0.03646	4.593×10^{-5}	2.504×10^{-5}	3.212×10^{-5}	0.6992
200	0.7459	1 023	0.03779	4.954×10^{-5}	2.577×10^{-5}	3.455×10^{-5}	0.6974
250	0.6746	1 033	0.04104	5.890×10^{-5}	2.760×10^{-5}	4.091×10^{-5}	0.6946
300	0.6158	1 044	0.04418	6.871×10^{-5}	2.934×10^{-5}	4.765×10^{-5}	0.6935
350	0.5664	1 056	0.04721	7.892×10^{-5}	3.101×10^{-5}	5.475×10^{-5}	0.6937
400	0.5243	1 069	0.05015	8.951×10^{-5}	3.261×10^{-5}	6.219×10^{-5}	0.6948
450	0.4880	1 081	0.05298	1.004×10^{-4}	3.415×10^{-5}	6.997×10^{-5}	0.6965
500	0.4565	1 093	0.05572	1.117×10^{-4}	3.563×10^{-5}	7.806×10^{-5}	0.6986
600	0.4042	1 115	0.06093	1.352×10^{-4}	3.846×10^{-5}	9.515×10^{-5}	0.7037
700	0.3627	1 135	0.06581	1.598×10^{-4}	4.111×10^{-5}	1.133×10^{-4}	0.7092
800	0.3289	1 153	0.07037	1.855×10^{-4}	4.362×10^{-5}	1.326×10^{-4}	0.7149
900	0.3008	1 169	0.07465	2.122×10^{-4}	4.600×10^{-5}	1.529×10^{-4}	0.7206
1 000	0.2772	1 184	0.07868	2.398×10^{-4}	4.826×10^{-5}	1.741×10^{-4}	0.7260
1 500	0.1990	1 234	0.09599	3.908×10^{-4}	5.817×10^{-5}	2.922×10^{-4}	0.7478
2 000	0.1553	1 264	0.11113	5.664×10^{-4}	6.630×10^{-5}	4.270×10^{-4}	0.7539

A3.3. PROPERTIES OF SATURATED WATER

Temp. °C	Presión bar	Volumen específico m³/kg		Energía interna kJ/kg		Entalpía kJ/kg			Entropía kJ/kg · K		Temp. °C
		Líquido sat. $v_f \times 10^3$	Vapor sat. v_g	Líquido sat. u_f	Vapor sat. u_g	Líquido sat. h_f	Vaporización h_{fg}	Vapor sat. h_g	Líquido sat. s_f	Vapor sat. s_g	
,01	0,00611	1,0002	206,136	0,00	2375,3	0,01	2501,3	2501,4	0,0000	9,1562	,01
4	0,00813	1,0001	157,232	16,77	2380,9	16,78	2491,9	2508,7	0,0610	9,0514	4
5	0,00872	1,0001	147,120	20,97	2382,3	20,98	2489,6	2510,6	0,0761	9,0257	5
6	0,00935	1,0001	137,734	25,19	2383,6	25,20	2487,2	2512,4	0,0912	9,0003	6
8	0,01072	1,0002	120,917	33,59	2386,4	33,60	2482,5	2516,1	0,1212	8,9501	8
10	0,01228	1,0004	106,379	42,00	2389,2	42,01	2477,7	2519,8	0,1510	8,9008	10
11	0,01312	1,0004	99,857	46,20	2390,5	46,20	2475,4	2521,6	0,1658	8,8765	11
12	0,01402	1,0005	93,784	50,41	2391,9	50,41	2473,0	2523,4	0,1806	8,8524	12
13	0,01497	1,0007	88,124	54,60	2393,3	54,60	2470,7	2525,3	0,1953	8,8285	13
14	0,01598	1,0008	82,848	58,79	2394,7	58,80	2468,3	2527,1	0,2099	8,8048	14
15	0,01705	1,0009	77,926	62,99	2396,1	62,99	2465,9	2528,9	0,2245	8,7814	15
16	0,01818	1,0011	73,333	67,18	2397,4	67,19	2463,6	2530,8	0,2390	8,7582	16
17	0,01938	1,0012	69,044	71,38	2398,8	71,38	2461,2	2532,6	0,2535	8,7351	17
18	0,02064	1,0014	65,038	75,57	2400,2	75,58	2458,8	2534,4	0,2679	8,7123	18
19	0,02198	1,0016	61,293	79,76	2401,6	79,77	2456,5	2536,2	0,2823	8,6897	19
20	0,02339	1,0018	57,791	83,95	2402,9	83,96	2454,1	2538,1	0,2966	8,6672	20
21	0,02487	1,0020	54,514	88,14	2404,3	88,14	2451,8	2539,9	0,3109	8,6450	21
22	0,02645	1,0022	51,447	92,32	2405,7	92,33	2449,4	2541,7	0,3251	8,6229	22
23	0,02810	1,0024	48,574	96,51	2407,0	96,52	2447,0	2543,5	0,3393	8,6011	23
24	0,02985	1,0027	45,883	100,70	2408,4	100,70	2444,7	2545,4	0,3534	8,5794	24
25	0,03169	1,0029	43,360	104,88	2409,8	104,89	2442,3	2547,2	0,3674	8,5580	25
26	0,03363	1,0032	40,994	109,06	2411,1	109,07	2439,9	2549,0	0,3814	8,5367	26
27	0,03567	1,0035	38,774	113,25	2412,5	113,25	2437,6	2550,8	0,3954	8,5156	27
28	0,03782	1,0037	36,690	117,42	2413,9	117,43	2435,2	2552,6	0,4093	8,4946	28
29	0,04008	1,0040	34,733	121,60	2415,2	121,61	2432,8	2554,5	0,4231	8,4739	29
30	0,04246	1,0043	32,894	125,78	2416,6	125,79	2430,5	2556,3	0,4369	8,4533	30
31	0,04496	1,0046	31,165	129,96	2418,0	129,97	2428,1	2558,1	0,4507	8,4329	31
32	0,04759	1,0050	29,540	134,14	2419,3	134,15	2425,7	2559,9	0,4644	8,4127	32
33	0,05034	1,0053	28,011	138,32	2420,7	138,33	2423,4	2561,7	0,4781	8,3927	33
34	0,05324	1,0056	26,571	142,50	2422,0	142,50	2421,0	2563,5	0,4917	8,3728	34
35	0,05628	1,0060	25,216	146,67	2423,4	146,68	2418,6	2565,3	0,5053	8,3531	35
36	0,05947	1,0063	23,940	150,85	2424,7	150,86	2416,2	2567,1	0,5188	8,3336	36
38	0,06632	1,0071	21,602	159,20	2427,4	159,21	2411,5	2570,7	0,5458	8,2950	38
40	0,07384	1,0078	19,523	167,56	2430,1	167,57	2406,7	2574,3	0,5725	8,2570	40
45	0,09593	1,0099	15,258	188,44	2436,8	188,45	2394,8	2583,2	0,6387	8,1648	45

Temp. °C	Presión bar	Volumen específico m^3/kg		Energía interna kJ/kg		Entalpía kJ/kg			Entropía kJ/kg · K		Temp. °C
		Líquido sat. $v_f \times 10^3$	Vapor sat. v_g	Líquido sat. u_f	Vapor sat. u_g	Líquido sat. h_f	Vaporización h_{fg}	Vapor sat. h_g	Líquido sat. s_f	Vapor sat. s_g	
50	,1235	1,0121	12,032	209,32	2443,5	209,33	2382,7	2592,1	,7038	8,0763	50
55	,1576	1,0146	9,568	230,21	2450,1	230,23	2370,7	2600,9	,7679	7,9913	55
60	,1994	1,0172	7,671	251,11	2456,6	251,13	2358,5	2609,6	,8312	7,9096	60
65	,2503	1,0199	6,197	272,02	2463,1	272,06	2346,2	2618,3	,8935	7,8310	65
70	,3119	1,0228	5,042	292,95	2469,6	292,98	2333,8	2626,8	,9549	7,7553	70
75	,3858	1,0259	4,131	313,90	2475,9	313,93	2321,4	2635,3	1,0155	7,6824	75
80	,4739	1,0291	3,407	334,86	2482,2	334,91	2308,8	2643,7	1,0753	7,6122	80
85	,5783	1,0325	2,828	355,84	2488,4	355,90	2296,0	2651,9	1,1343	7,5445	85
90	,7014	1,0360	2,361	376,85	2494,5	376,92	2283,2	2660,1	1,1925	7,4791	90
95	,8455	1,0397	1,982	397,88	2500,6	397,96	2270,2	2668,1	1,2500	7,4159	95
100	1,014	1,0435	1,673	418,94	2506,5	419,04	2257,0	2676,1	1,3069	7,3549	100
110	1,433	1,0516	1,210	461,14	2518,1	461,30	2230,2	2691,5	1,4185	7,2387	110
120	1,985	1,0603	0,8919	503,50	2529,3	503,71	2202,6	2706,3	1,5276	7,1296	120
130	2,701	1,0697	0,6685	546,02	2539,9	546,31	2174,2	2720,5	1,6344	7,0269	130
140	3,613	1,0797	0,5089	588,74	2550,0	589,13	2144,7	2733,9	1,7391	6,9299	140
150	4,758	1,0905	0,3928	631,68	2559,5	632,20	2114,3	2746,5	1,8418	6,8379	150
160	6,178	1,1020	0,3071	674,86	2568,4	675,55	2082,6	2758,1	1,9427	6,7502	160
170	7,917	1,1143	0,2428	718,33	2576,5	719,21	2049,5	2768,7	2,0419	6,6663	170
180	10,02	1,1274	0,1941	762,09	2583,7	763,22	2015,0	2778,2	2,1396	6,5857	180
190	12,54	1,1414	0,1565	806,19	2590,0	807,62	1978,8	2786,4	2,2359	6,5079	190
200	15,54	1,1565	0,1274	850,65	2595,3	852,45	1940,7	2793,2	2,3309	6,4323	200
210	19,06	1,1726	0,1044	895,53	2599,5	897,76	1900,7	2798,5	2,4248	6,3585	210
220	23,18	1,1900	0,08619	940,87	2602,4	943,62	1858,5	2802,1	2,5178	6,2861	220
230	27,95	1,2088	0,07158	986,74	2603,9	990,12	1813,8	2804,0	2,6099	6,2146	230
240	33,44	1,2291	0,05976	1033,2	2604,0	1037,3	1766,5	2803,8	2,7015	6,1437	240
250	39,73	1,2512	0,05013	1080,4	2602,4	1085,4	1716,2	2801,5	2,7927	6,0730	250
260	46,88	1,2755	0,04221	1128,4	2599,0	1134,4	1662,5	2796,6	2,8838	6,0019	260
270	54,99	1,3023	0,03564	1177,4	2593,7	1184,5	1605,2	2789,7	2,9751	5,9301	270
280	64,12	1,3321	0,03017	1227,5	2586,1	1236,0	1543,6	2779,6	3,0668	5,8571	280
290	74,36	1,3656	0,02557	1278,9	2576,0	1289,1	1477,1	2766,2	3,1594	5,7821	290
300	85,81	1,4036	0,02167	1332,0	2563,0	1344,0	1404,9	2749,0	3,2534	5,7045	300
320	112,7	1,4988	0,01549	1444,6	2525,5	1461,5	1238,6	2700,1	3,4480	5,5362	320
340	145,9	1,6379	0,01080	1570,3	2464,6	1594,2	1027,9	2622,0	3,6594	5,3357	340
360	186,5	1,8925	0,006945	1725,2	2351,5	1760,5	720,5	2481,0	3,9147	5,0526	360
374,14	220,9	3,155	0,003155	2029,6	2029,6	2099,3	0	2099,3	4,4298	4,4298	374,14

Fuente: Las tablas A-2 a A-5 se han extraído de J. H. Keenan, F. G. Keyes, P. G. Hill y J. G. Moore, *Steam Tables*, Wiley, New York, 1969.

ANNEX 4: DATA SHEET OF THE ENGINE

ANNEX 5: PLANS

Design Data:
-mech. performance: 500 W at 500 1/min, max. engine speed: 750 1/min
-max. heater-head temperature: 550°C (material heater-head: 1.4571)
-working gas pressure: 10 bar, limited by sealed pressure-relieve valve 11 bar
-working gas: Nitrogen, conditionally dry, oil-free compressed air. other gases might cause damages by corrosion or excess rotation speed
-cooling water: max. 45° C at intake, min. 1,5 l/min, max. 3 bar
-stroke: 75 mm, bore displacer: 96 mm, bore working piston: 85 mm
-main dimensions: approx. 410×375×780 mm, total weight: 33,5 kg

Assembly Precautions:
The engine is designed for oil-free operation. Oil that gets onto the hot heater walls during operation could ignite, the engine might explode. Dust or any kind of particles will jam the regenerator or accumulate in the dry bearings and destroy them. Thoroughly clean all parts prior to assembly, do not use oil at assembly and keep the engine free of any particles. Only apply oil sparingly to piston-pin and piston-rod. Fill some ball bearing grease into the space between outer crankshaft-bearing and the shaft sealing ring according to the directions of the seal manufacturer.
Use a throttle to limit pressure changes to max. 2 bar/min. during filling the engine or when blowing off filling gas. This avoids grease beeing driven out of the ball bearings or deformation of the displacer dome.

Security Advice:
All constructional sketches for the ST05G-CNC stirling engine were developed with best knowledge and diligence. When bringing the engine or parts of it into circulation all necessary proof, ex. strength, safety, etc., have to bee supplied. Test and operation only by adept operators. Any kind of liability or warranty is excluded.

Copyright:
Purchase of this plans authorizes to build the stirling engine ST05G-CNC. It is only allowed to copy this plans or CAD-data for personal use. Passing them on to third parties is interdicted. Copyright: VE-Ingenieure. Any commercial use is subject to approval.

There is an extended copyright according to http://creativecommons.org/licenses/by-nc-sa/3.0 for the engine itself. It allows to share, distribute or adapt any ST05G-CNC engine for non-commercial use. The engine or its modifikations have to be named "ST05G-CNC, cc: www.ve-ingenieure.de". Passing on the engine to thirds has to happen under the same license.

VE-Ingenieure, January 15th 2009

Auslegungsdaten:
-mechanische Leistung: 500 W bei 500 1/min, Maximaldrehzahl: 750 1/min
-max. Erhitzertemperatur: 550°C (Erhitzerwerkstoff 1.4571)
-Arbeitsgasdruck: 10 bar, durch fest eingebautes, verplombtes Überdruckventil 11bar begrenzt
-Arbeitsgas: Stickstoff oder bedingt auch getrocknete, ölfreie Druckluft;
andere Medien können zur Beschädigung (Überdrehzahl, Korrosion) des Motors führen
-Kühlwassereintritt: max. 45° C, Durchsatz min. 1,5 l/min, max. 3 bar
-Hub: 75 mm, Verdrängerdurchmesser: 96 mm, Arbeitskolbendurchmesser: 85 mm
-Grundabmessungen: ca. 410×375×780 mm, Gesamtmasse: 33,5 kg

Montagehinweise:
Der Motor wurde für ölfreien Betrieb ausgelegt. Öl im Motorinneren könnte sich im Betrieb an den heißen Erhitzerwänden entzünden, der Motor somit explodieren. Schmutzpartikel im Motor sammeln sich im Regenerator an oder setzen sich in den Gleitbelägen fest und schädigen diese. Bei der Montage müssen deshalb alle Bauteile gründlich gereinigt werden und sind dann staub- und ölfrei zu montieren. Lediglich Verdrängerstange und Kolbenbolzen sollten mit einem leichten Ölfilm versehen werden. Zwischen dem äußeren Kurbelwellenlager und dem Wellendichtring bei Montage entsprechend den Anweisungen des Dichtringherstellers etwas Kugellagerfett einfüllen.
Das Befüllen und Ablassen von Arbeitsgases sollte immer über ein Drosselventil mit max. 2 bar/min. erfolgen, damit sich ein gleichmäßiges Druckniveau im inneren des Motors einstellen kann. Bei zu schnellen Druckänderung könnte der Verdränger implodieren/bersten und Fett aus den Kugellagern und Dichtungen gedrückt werden.

Sicherheitshinweise:
Dieser Konstruktionsentwurf für den Stirlingmotor ST05G-CNC wurde nach bestem Wissen und mit Sorgfalt angefertigt. Bei Inverkehrbringen des Motors oder von Teilen davon sind vom Betreiber entsprechende Nachweise über Festigkeit und Betriebssicherheit zu erbringen. Inbetriebnahme und Betrieb darf nur durch entsprechend qualifiziertes Personal erfolgen. Eine Haftung jeglicher Art ist ausgeschlossen.

VE-Ingenieure, 15.1.2009

Schutzvermerk ISO 16016 beachten.
Refer to protection notice ISO 16016.

ST05G-CNC				Zul. Abweichung DIN ISO 2768 fH		Oberfläche	Maßstab XXX		Gewicht
							Material	XXXXXX	
					Datum	Name	Benennung	Präambel *Preamble*	
				Bearb.	15.1.2009	Eckl			
				Gepr.	15.1.2009	SV			
				Norm					
Zust.	Änderung	Datum	Name	ve//ingenieure			Zg. Nr.	01.99	Blatt 1
				ve//ingenieure GmbH					1 Bl.
				Bergsiedlung 19, 83059 Kolbermoor			Ersatz für:		Ersatz durch:

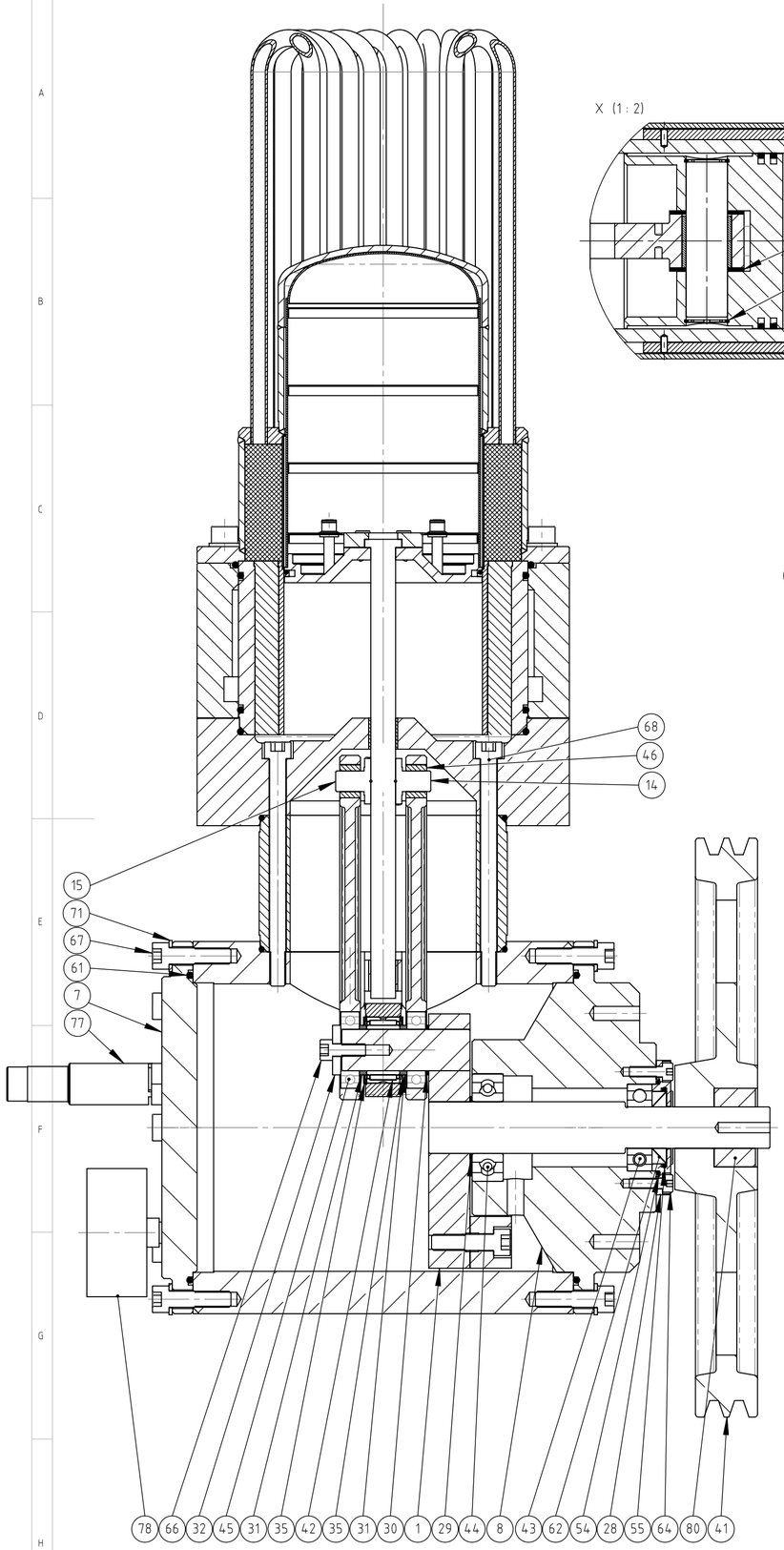

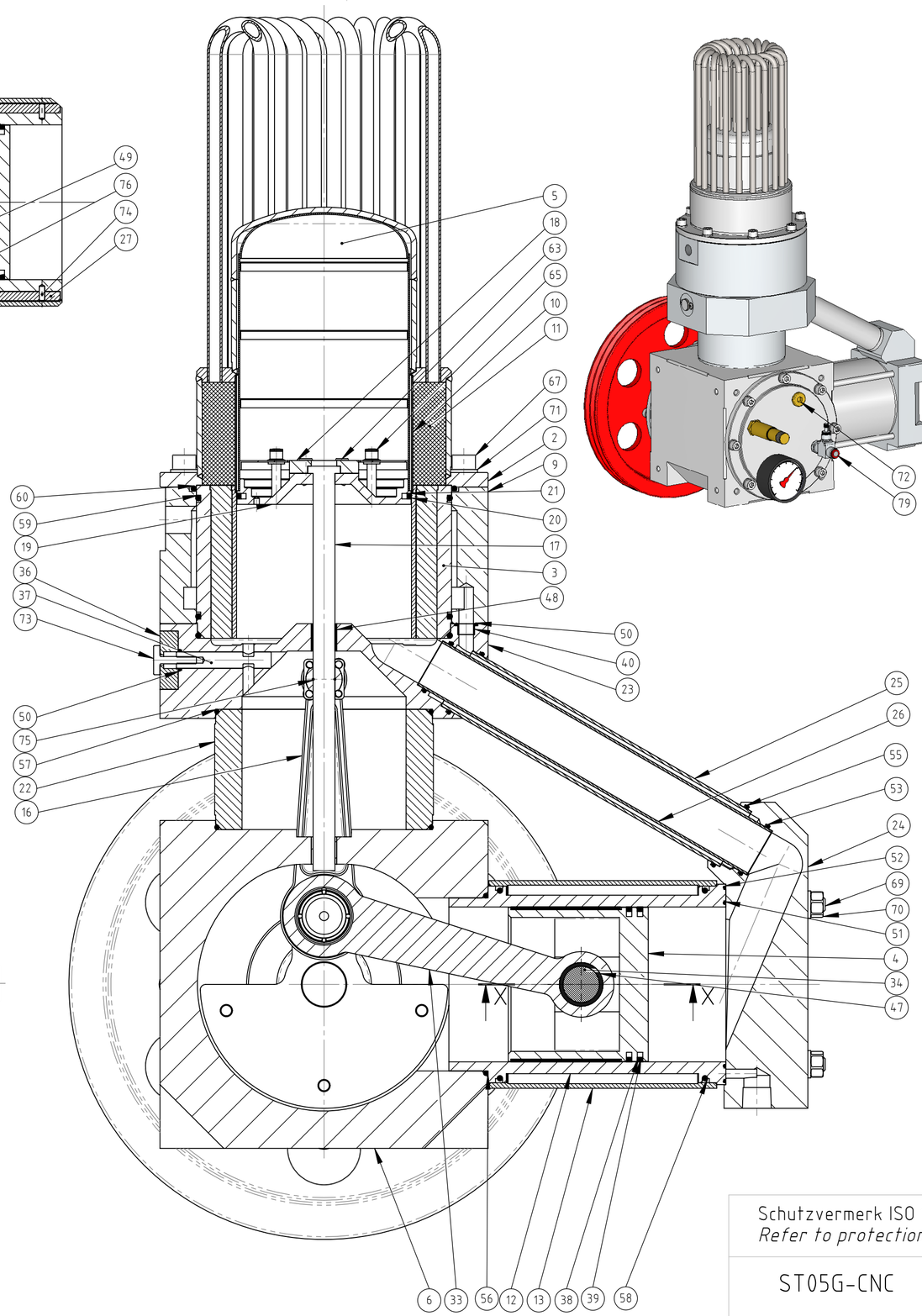

POS-NR.	MENGE	Zg.Nr.	BENENNUNG	BESCHREIBUNG
	1	01.99	Präambel	Preamble
1	1	01.01	Kurbelwelle kpl.	
2	1	01.06	Erhitzer	
3	1	01.13	Kühler kpl.	
4	1	01.17	Arbeitskolben kpl.	
5	1	01.20	Verdränger kpl.	
6	1	01.25	Kurbelgehäuse	
7	1	01.27	Gehäusedeckel	
8	1	01.26	Hauptlagereinsatz	
9	1	01.28	Kühlermantel	
10	1	01.37	Erhitzerinnenrohr	
11	1	01.38	Regenerator	
12	1	01.32	Zylinderbuchse	
13	1	01.33	Kühlwassermantel	
14	1	01.47	Kreuzkopf links	
15	1	01.48	Kreuzkopf rechts	
16	2	01.40	Verdrängerpleuel	
17	1	01.49	Verdrängerstange	
18	1	01.46	Verdrängerstangenklemmring	
19	1	01.45	Verdrängerboden	
20	1	01.42	Verdrängerkolbenring	
21	1	01.44	Spiralfeder 96mm	
22	1	01.30	Fuss	
23	1	01.29	Verdrängerlager	
24	1	01.31	Zylinderkopf	
25	1	01.36	Verbindungsrohr Kühlwasser	
26	1	01.35	Verbindungsrohr	
27	2	01.34	Dichtleiste	
28	1	01.55	Dichtringaufnahme	
29	1	01.51	Distanzscheibe 115	
30	1	01.52.	Distanzscheibe 116	
31	2	01.53	Distanzscheibe 117	
32	1	01.54	Distanzscheibe 118	
33	1	01.39	Arbeitskolbenpleuel	
34	1	01.60	Kolbenbolzen	
35	2	01.50	Deckscheibe	
36	1	01.56	Bypassplatte	
37	1	01.57	Bypassschieber	
38	2	01.41	Kolbenring Arbeitskolben	
39	2	01.43	Spiralfeder 85mm	
40	1	01.58	Stützring	
41	1	01.59	Schwungrad bearbeitet	
42	1	01.79	Nadellager NKI 20/16A 20x32x16	needle bearing
43	1	01.76	Rillenkugellager 6004 2Z 20x42x12	ball bearing
44	1	01.77	Rillenkugellager 6205 2Z 25x52x15	ball bearing
45	2	01.78	Rillenkugellager 61904 2Z 20x37x9	
46	2	01.82	Sinterbronzebuchse 10x16x10	sintered bronze bushing
47	1	01.83	Sinterbronzebuchse 20x24x25	sintered bronze bushing
48	2	01.80	Iglidur WSM-1214-15	bushing
49	2	01.81	Iglidur WTM-2036-015	bushing
50	2	01.85	O-Ring 9x1,5	o-ring seal
51	1	01.89	O-Ring 88x1,5	o-ring seal
52	1	01.92	O-Ring 105x1,5	o-ring seal
53	2	01.86	O-Ring 28x2	o-ring seal
54	1	01.88	O-Ring 42x2	o-ring seal
55	3	01.87	O-Ring 35x2	o-ring seal
56	1	01.90	O-Ring 95x2,5	o-ring seal
57	2	01.93	O-Ring 115x2,5	o-ring seal
58	2	01.91	O-Ring 100x3	o-ring seal
59	3	01.94	O-Ring 135x3	o-ring seal
60	1	01.95	O-Ring 140x3	o-ring seal
61	2	01.96	O-Ring 144,5x3	o-ring seal
62	1	01.84	Wellendichtring B2PT 20-35-7	shaft sealing ring
63	8	01.62	DIN 912 – M4x10 8.8	
64	8	01.63	DIN 912 – M5x16 8.8	
65	4	01.61	DIN 7991 – M5x30 8.8	
66	1	01.64	DIN 912 – M6x16 8.8	
67	35	01.66	DIN 912 – M8x30 8.8	
68	6	01.65	DIN 912 – M8x110 8.8	
69	4	01.69	Gewindestange M8x200 8.8	thread rod
70	4	01.73	Mutter M8 DIN ISO 4032-A2	nut
71	36	01.71	Scheibe DIN 433, M8	washer
72	1	01.68	Verschlussschraube R3/8"	lock screw
73	1	01.67	Rändelschraube DIN 653 – M4x20	knurled screw
74	4	01.74	Zylinderstift DIN 6325 3x8	parallel pin
75	1	01.70	DIN 7993-A12 Federdrahtsprengring 12x1	
76	2	01.72	Sicherungsring DIN 472-20x1	retaining ring
77	1	01.98	Sicherheitsventil 0-16 bar	safety valve 0-16 atm
78	1	01.99	Manometer 0-16 bar, R1/4"	manometer
79	1	01.100	Druckluftkupplung mit Absperrventil, R1/4"	shut off valve
80	1	01.97	Spannsatz (bsp BAR 20mm)	clamping set

Schutzvermerk ISO 16016 beachten.
Refer to protection notice ISO 16016.

ST05G-CNC

Zul. Abweichung DIN ISO 2768 fH

Oberfläche

Maßstab 1:2

Gewicht

Material XXXXXX

	Datum	Name
Bearb.	16.12.2008	Eckl
Gepr.	9.1.2009	SV
Norm		

Benennung

Zusammenstellung
Assembly

Zg. Nr. 01.00

Blatt 1

1 Bl.

ve//ingenieure

ve//ingenieure GmbH
Bergsiedlung 19, 83059 Kolbermoor

Zust. Änderung Datum Name

Ersatz für:

Ersatz durch:

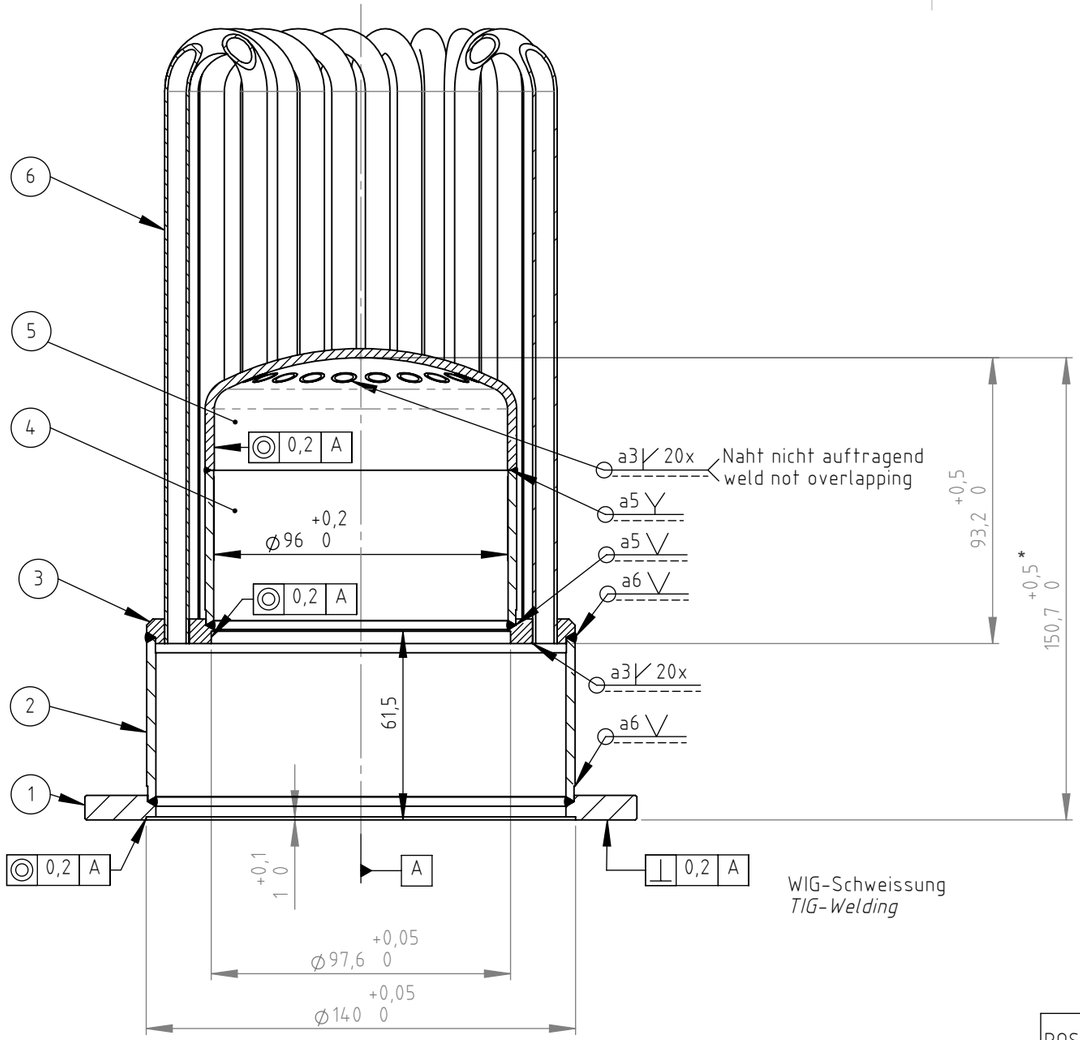

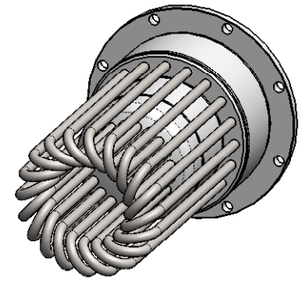

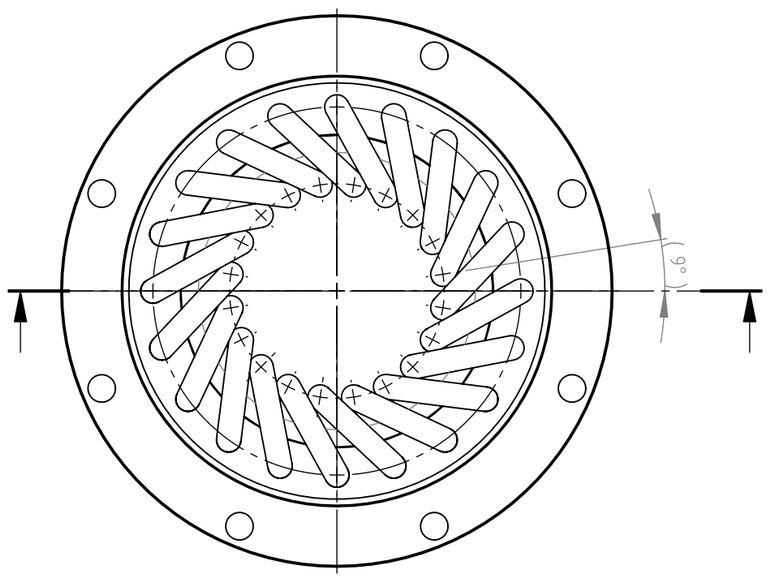

* ungeschweißt ca. 155
** before welding approx. 155*

POS-NR.	MENGE	SN	BENENNUNG	BESCHREIBUNG
1	1	01.07	Erhitzerflansch	
2	1	01.08	Erhitzeraussenrohr	
3	1	01.09	Erhitzer-Zwischenflansch	
4	1	01.10	Erhitzer-Zwischenrohr	
5	1	01.11	Erhitzerhaube	
6	20	01.12	Erhitzerrohrbogen	

Schutzvermerk ISO 16016 beachten.
Refer to protection notice ISO 16016.

					Zul. Abweichung DIN ISO 2768 fH	Oberfläche
	diverse Änderunen	4.3.2008	Eckl		Datum	Name
				Bearb.	8.12.2008	Eckl
				Gepr.	9.1.2009	SV
				Norm		
a	Nachbearbeitung	12.04.11	Vie			
Zust.	Änderung	Datum	Name			

ve//ingenieure
ve//ingenieure GmbH
Bergsiedlung 19, 83059 Kolbermoor

Maßstab 2:1 | Gewicht
Material

Benennung
Erhitzer
Heater Head

Zg. Nr. 01.06 | Blatt 1 | 1 Bl.

Ersatz für: | Ersatz durch:

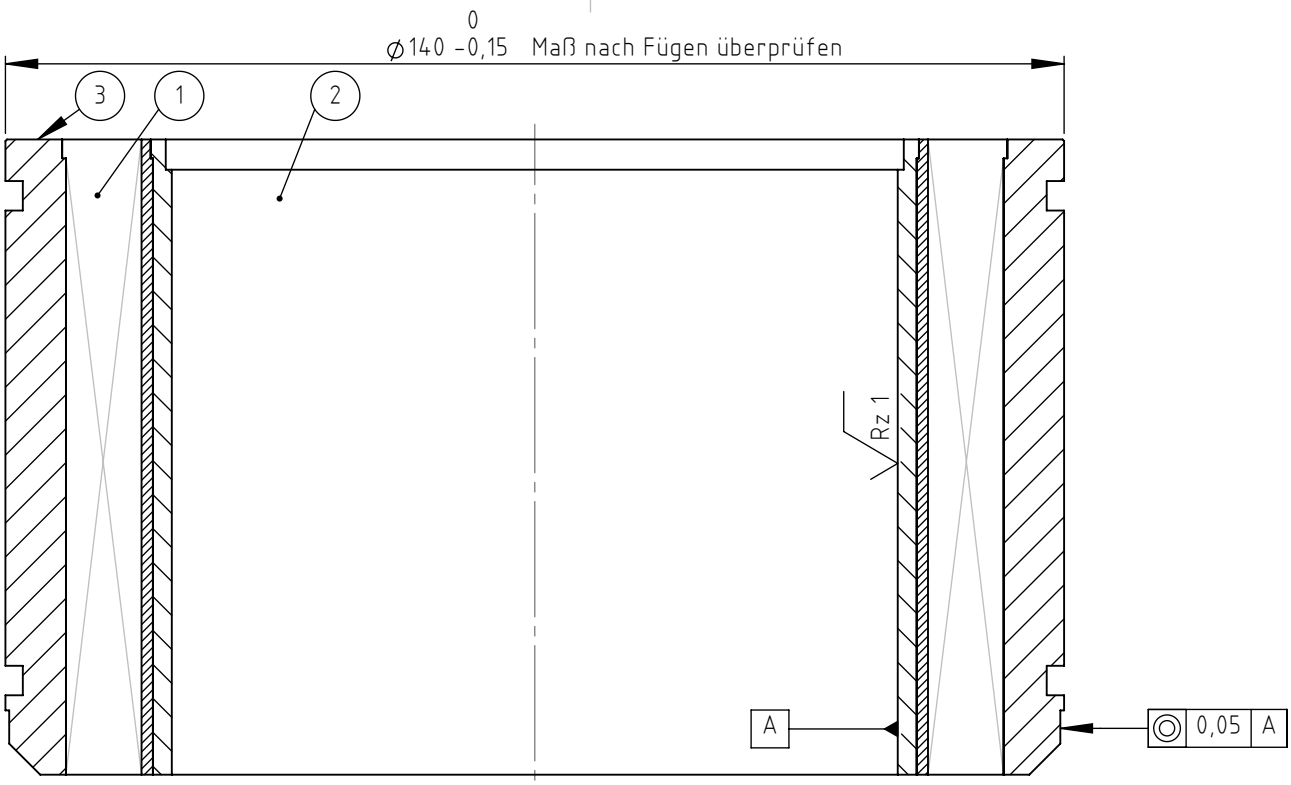

Montage:

1. Alle Bauteile reinigen, Fügeflächen entfetten.
2. Fügefläche von Teil 2 mit Loctite 620 bestreichen, dann das auf 250°C erwärmte Rohteil 1 einschrumpfen. Optional können die beiden Bauteile auch verlötet werden.
3. Kühllamellen im Kühlereinsatz 1 gem. Zeichnung fertig bearbeiten.
4. Die gefügten Teile nun auf -20°C abkühlen und ohne Klebstoff in das auf 250°C erwärmte Teil 3 einschrumpfen.
5. Abgekühltes Bauteil ggf. nach Zeichnung auf Endmaß bearbeiten.

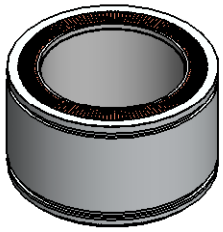

Mounting:

1. *Clean and degrease joining area.*
2. *Heat-up raw part 1 to 250°C, coat joint surface of part 2 with Loctite 620, then shrink fit parts. Optionally solder parts.*
3. *Finish cooling fins of part 1 as shown in drawing "Cooling Cartridge".*
4. *Cool-down joint parts to -20°C, heat-up part 3 to 250°C, then shrink fit parts without the use of adhesive.*
5. *If necessary, finish part to final dimensions after cooldown.*

POS-NR.	MENGE	Zg.Nr.	BENENNUNG	BESCHREIBUNG
1	1	01.15	Kühlereinsatz	
2	1	01.16	Verdrängerlaufbuchse	
3	1	01.14	Kühlerbuchse	

Schutzvermerk ISO 16016 beachten.
Refer to protection notice ISO 16016.

ST05G-CNC

Zul. Abweichung DIN ISO 2768 fH

Oberfläche

Maßstab 1:1

Gewicht

Material

	Datum	Name
Bearb.	24.11.2008	Eckl
Gepr.	9.1.2009	SV
Norm		

Benennung

Kühler kompl.
Cooler Assy

Zust.	Änderung	Datum	Name
a	Maß ⌀140	12.04.11	Vie

ve//ingenieure
ve//ingenieure GmbH
Bergsiedlung 19, 83059 Kolbermoor

Zg. Nr. 01.13

Blatt 1
1 Bl.

Ersatz für:

Ersatz durch:

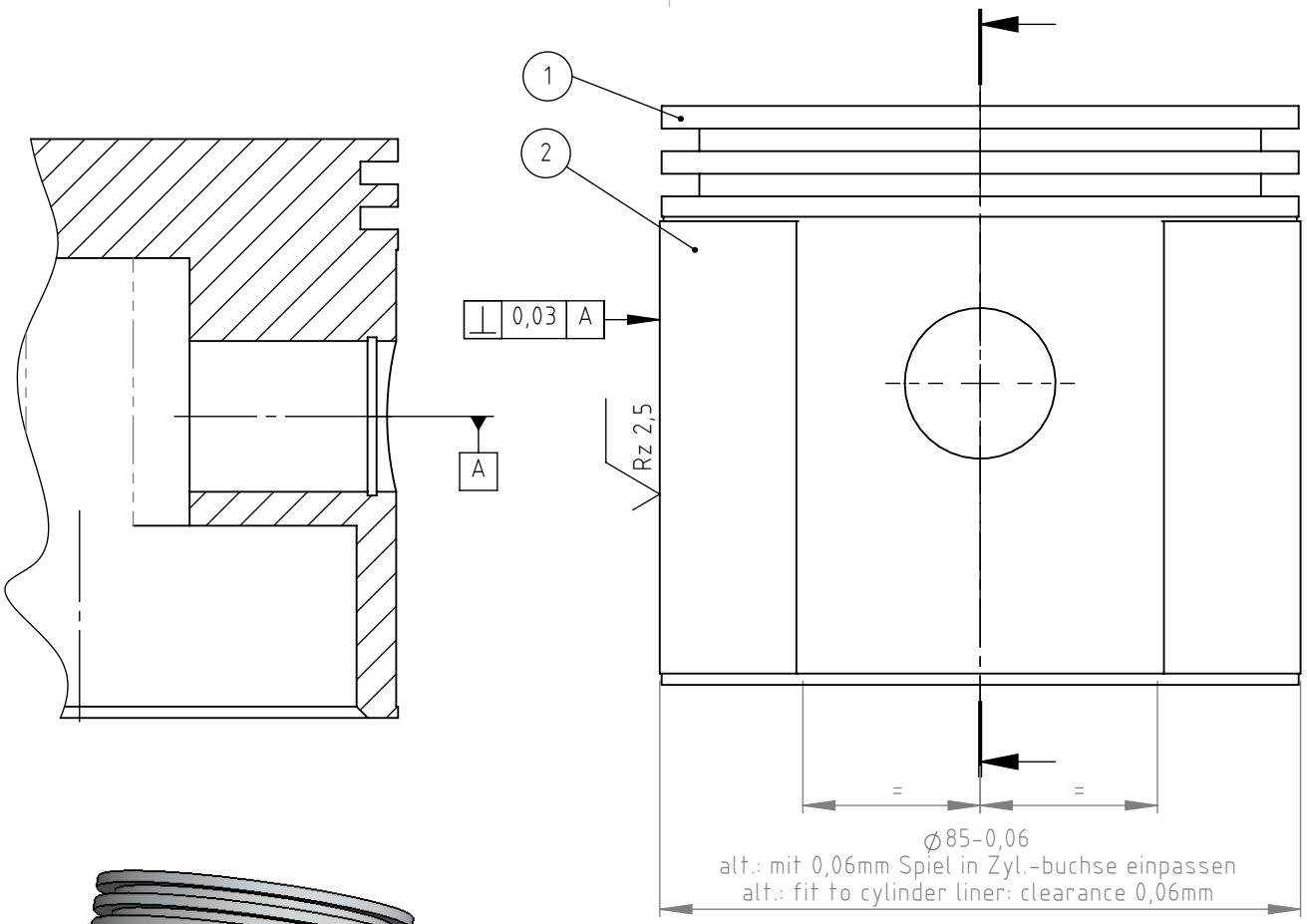

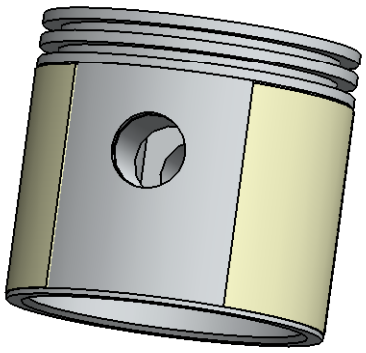

1. Klebeflächen beidseitig fein sandstrahlen (alternativ beflämmen).
   Slightly sandblast both adherends (alt. prepare by flame treatment).
2. Gleitbelag mit Zweikomponenten Epoxydharz (Araldit 2011 oder vergleichbar) aufkleben.
   Glue-on linings with two-component epoxy resin (Araldit 2011 or similar).
3. Kleber bei 80°C aushärten.
   Harden glue at 80°C.

POS-NR.	MENGE	Zg. Nr.	BENENNUNG	BESCHREIBUNG
1	1	01.18	Arbeitskolben	
2	2	01.19	Gleitbelag Arbeitskolben	

Schutzvermerk ISO 16016 beachten.
Refer to protection notice ISO 16016.

ST05G-CNC

Zul. Abweichung DIN ISO 2768 fH

Oberfläche

Maßstab 1:1

Gewicht

Material XXXXXX

	Datum	Name
Bearb.	21.10.2008	Eckl
Gepr.	9.1.2009	SV
Norm		

Benennung

Arbeitskolben komplett

Power Piston Assy

ve//ingenieure

ve//ingenieure GmbH
Bergsiedlung 19, 83059 Kolbermoor

Zg. Nr. 01.17

Blatt 1

1 Bl.

Zust. Änderung | Datum | Name

Ersatz für:

Ersatz durch:

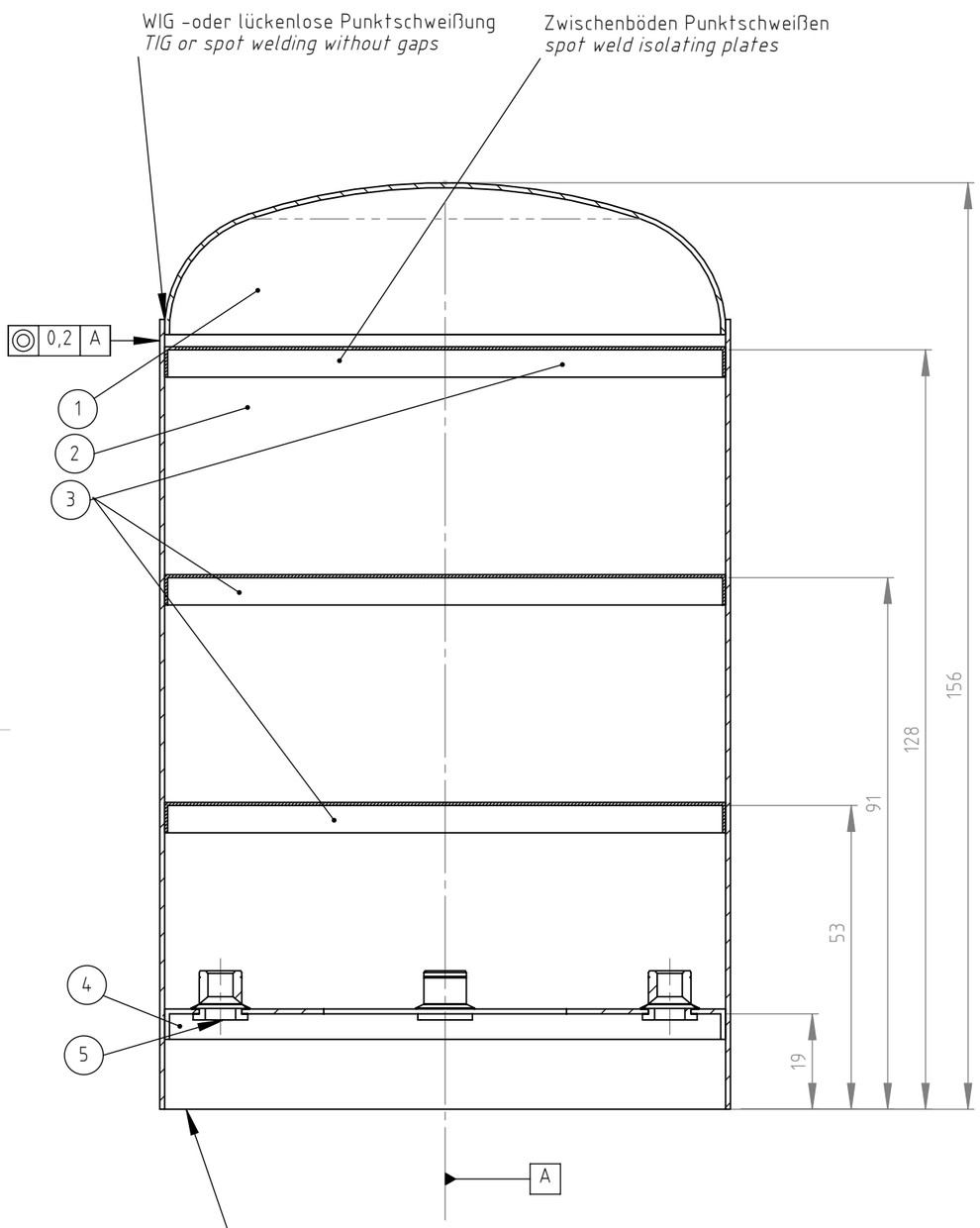

Höhe ggf. bei Montage auf Erhitzerinnenmaß abstimmen
adjust to length of heater head on assembly

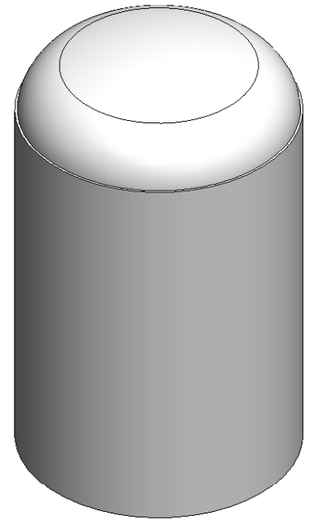

POS-NR.	MENGE	Zg. Nr.	BENENNUNG	BESCHREIBUNG
1	1	01.21	Verdrängerhaube	
2	1	01.22	Verdrängermantel	
3	3	01.23	Verdrängerzwischenboden	
4	1	01.24	Verdrängermontageboden	
5	4	01.75	Blindnietmutter M5 / *Pop Rivet Nut M5*	blind rivet nut

Schutzvermerk ISO 16016 beachten.
Refer to protection notice ISO 16016.

ST05G-CNC

Zul. Abweichung DIN ISO 2768 fH

Oberfläche

Maßstab 1:1

Gewicht

Material

	Datum	Name
Bearb.	27.2.2008	Eckl
Gepr.	9.1.2009	SV
Norm		

Benennung

Verdränger kpl.
Displacer Piston Assy.

ve//ingenieure
ve//ingenieure GmbH
Bergsiedlung 19, 83059 Kolbermoor

Zg. Nr. 01.20

Blatt 1
1 Bl.

Ersatz für:

Ersatz durch:

Zust. | Änderung | Datum | Name

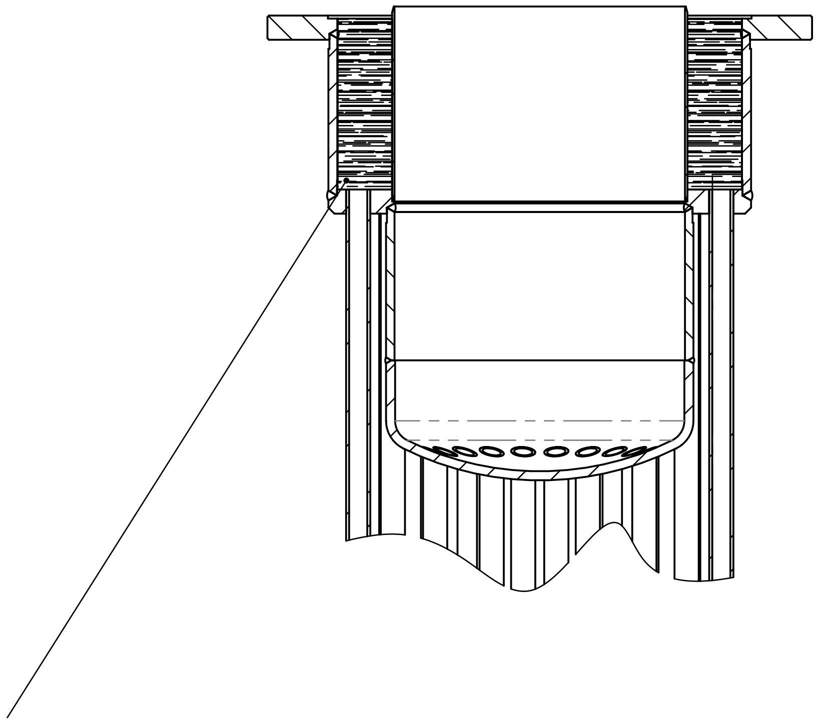

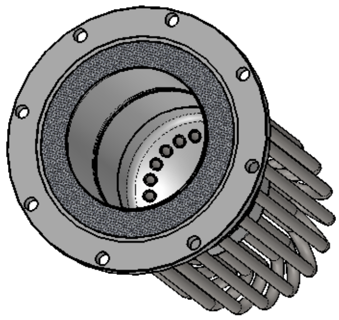

Regeneratorvolumen im Erhitzer mit 250g Gestrick aus Edelstahldraht Ø0,05-0,06mm stopfen.
Mit dieser Menge an Gestrick wird ein Regenerator-Füllfaktor von ca. 0,1 erreicht. Das Regeneratormaterial muss vor dem Einfüllen auf 330°C aufgeheizt werden, um herstellungsbedingte Ölreste vom Material zu entfernen. Evtl. anhaftende sonstige Verunreinigungen mit Druckluft abblasen. Beim Stopfen darauf achten, dass der Regeneratorraum gleichmäßig dicht gefüllt wird und dass keine Verunreinigungen oder Drahtpartikel in den Erhitzer gelangen.

Bezugsquelle des Drahtgestricks:
z.B. Rhodius GmbH, www.rhodius.com

Stuff regenerator space with 250gr. of Knitted Stainless Steel Wire Mesh Ø0,05-0,06mm. This yields a filling faktor of 0,1. In order to remove oil residues from the wire, heat-up the material to 330°C before stuffing, then blow off any particles with compressed air. Take care to stuff the mesh equally into the regenerator space and keep the heater head free from impurities or wire particles.

Supplier for wire mesh:
e.g. Rhodius GmbH, www.rhodius.com

Schutzvermerk ISO 16016 beachten.
Refer to protection notice ISO 16016.

ST05G-CNC

Zul. Abweichung DIN ISO 2768 fH

Oberfläche

Maßstab 1:2

Gewicht

Material Edelstahl-Drahtgestrick Ø0,05-0,06mm, 250g
stainless steel wire mesh Ø0,05-0,06mm, 250gr.

	Datum	Name
Bearb.	10.12.2008	Eckl
Gepr.	9.1.2009	SV
Norm		

Benennung
Regenerator
Regenerator

ve//ingenieure

ve//ingenieure GmbH
Bergsiedlung 19, 83059 Kolbermoor

Zg. Nr. 01.38

Blatt 1
1 Bl.

Zust. Änderung | Datum | Name

Ersatz für: | Ersatz durch: